Engineering composite particles to overcome the poor pharmaceutical performance of paracetamol

By

AYUK AGBOR ROSE (BSc, MSc)

A thesis submitted in partial fulfilment of the requirements of the University of Wolverhampton for the degree of Doctor of Philosophy

Faculty of Science and Engineering,

University of Wolverhampton, Wolverhampton

United Kingdom

April 2019

DECLARATION

This work or any part thereof has not previously been presented in any form to the University or any other body whether for assessment, publication or for any other purpose (unless otherwise indicated). Save for any express acknowledgements, references and/or bibliographies cited in the work, I confirm that the intellectual content of the work is the result of my own efforts and of no other person.

The right of Ayuk, Agbor Rose to be identified as the author of this work is asserted in accordance with ss.77 and 78 of the Copyright, Designs and Patents Act 1988. At this date, copyright is owned by the author,

Ayuk, Agbor Rose

Date……..

Thesis Summary

Tablets are the most common solid dosage forms because of their several advantages including the ease of administration, precise dosing, ease of manufacturing, good product stability in comparison to liquids, and tamper–proofness in comparison to capsules. Direct compression is the favoured smart choice for tablet manufacturing. The advantages of direct compression: include simplicity, reduced time and the final cost of the product due to fewer processing stages, continuous nature, and elimination of heat and moisture effects, making direct compression an appropriate process for hygroscopic and thermo–sensitive materials. However, it is unfortunate that only less than ~20% of pharmaceutical powders can be compressed into tablets by direct compression due to their inherent poor functional properties required for direct compression.

The situation is particularly severe when a high dose of a poorly compactible drug such as paracetamol must be used. Paracetamol is a widely used analgesic drug. The monoclinic form is usually selected in the pharmaceutical industry and is the commercially available form because it is thermodynamically stable at room temperature and pressure. However, the monoclinic form of paracetamol is notorious for exhibiting poor tableting properties by direct compression, reduced plastic deformation during compression, commonly resulting in fragile tablets with a high propensity to cap.

This work commences by providing insights into how, current and innovative processing techniques, parameters (milling time, temperature and solvents), and the combination of drugs and/or excipient impact the mechanical properties of paracetamol. The mechanical properties were investigated by applying blending, freeze drying, milling, batch cooling crystallisation, solvent evaporation and cocrystals formation, while, modifying the physicochemical structure of paracetamol crystals to improve tabletability was the rationale.

The modified particles, with the desired behaviour acquired, were characterised using FT−IR, PXRD, laser diffraction, SEM, DSC, TGA, Water absorption profile, flowability, stability, content uniformity, dissolution and tabletability.

Tabletabilty data demonstrated an immerse enhancement in the drug's tensile strength upon processing using different blending energy (~8 folds) and preparation techniques (~11 folds), various freezing temperatures (~12 folds) with the polymer polyvinylpyrrolidone using various drugs such as Ibuprofen (~5 folds), aspirin and caffeine (~9 folds), Curcumin (~9 folds) chondroitin sulphate A (~11 folds) and cocrystals with the coformer 5–Nitroisophthalic acid (~12 folds). Regardless, of the co–processing techniques applied with paracetamol in the presence of other drugs and excipient, there was an improvement of the tablettabililty of paracetamol in comparison to the drug alone.

In conclusion, the co–engineering of poorly compactable model drug chosen paracetamol with other drugs and excipient influenced the mechanical properties of paracetamol without changes in crystallinity and polymorphic structure.

Keywords: Direct compression; Crystal size; crystal habit; Electrostatic interaction; Interactive mixtures; Hydrogen bonding; Mechanical properties; Physicochemical properties; Tableting.

Acknowledgement

I want to thank Dr Kaialy Waseem (director of study) for his supervision, guidance, kindness, encouragement, accessibility and support from the early phases of this research and the freedom he gave me to decide on the next step in relative to my research work. I am grateful to Prof Stephen Britland, Dr Amr Edshear, Prof Craig D Williams, Mr David Townrow, Dr Angela Williams, Diane, Karen, Dr Keith Jones and Mr Keith Holding for their kindness and technical support throughout my research.

It is an utmost pleasure to thank my laboratory mates at the University of Wolverhampton who made the atmosphere conducive during my research.

Dedication

I dedicate this work to God Almighty, who has been my protector and guardian throughout my life. I am very grateful to my family, special gratitude to my grandmother Ayuk Comfort Amenko for being my everything/*hero*/role model and mother Miss Rabiatou Mohammed for her support throughout my studies. My supervisor Dr Waseem Kaialy, Miss Asie Marie Ayuk, Mr Mbah Peter, My aunties Chantal Ebangha, Civil Nanfack and my cousins Atemkeng Paul and Agbor Matelot. My friends, Lucia Bateosoh, Dr Aisha Wali, Dr Babiaka Smith, William Chittey and Hamisu Hamisu for their emotional, physical and psychological support.

Table of contents

List of tables

List of figures

Abbreviation list

APIs, Active pharmaceutical ingredients ; ANOVA, Analysis of variance; APIs, Active pharmaceutical ingredients; ATR, Attenuated total reflectance; BCC, Batch cooling crystallisation; BCS, Biopharmaceutical classification system; Db, Bulk density; CI, Carr's index; CHONS, Chondroitin sulphate sodium salt C; ASP, Commercial aspirin; CAF, Commercial caffeine; CUR, Commercial curcumin; IBU, Commercial ibuprofen; 5NIP, Commercial 5–Nitroiphthalic acid; PA, Commercial paracetamol; PVP, Commercial polyvinylpyrrolidone; ºC, Degree Celsius; DHS, Dry high shear; DSC, Differential Scanning Calorimetry; DC, Direct compression; pKa, Dissociation constant; DE, Dissolution efficiency; FT–IR, FDA, Food and Drug Administration; Fourier Transform Infrared; FD, Freeze drying; GRAS, Generally recognised as safe; g, Gram; HSH, High–speed homogenization; h, Hour; Kg, Kilogram; L, Litre; Log, Logarithm; LS, Low Shear; MDR, Mean dissolution rate; MDT, Mean dissolution time; MS, Medium shear; MPa, Megapascal; mg, Milligram; ML, Milling; MLA, Milling with acetone; MLB, Milling with butanol; MLE, Milling with ethanol; MLM, Milling with methanol; min, Minutes; MW, Molecular weight; D10%, Particle diameter at 10% volume distribution; D50%, Particle diameter at 50% volume distribution (median diameter); D90%, Particle diameter at 90% volume distribution; %, Percentage; PM, Physical mixture; PSD, Particle size distribution; PVP, Polyvinylpyrrolidone; PXRD, Powder X–ray powder diffraction; Rh Relative humidity; SEM, Scanning electron microscope; SCM, Slow cooling crystallisation with methanol; SCW, Slow cooling crystallisation with water; SE, Solvent evaporation; *f*2, Similarity factor; SD, Standard deviation; Dt or ρt, Tapped density; TS, Tensile strength; TGA, Thermogravimetric analysis; VMD, Volume mean diameter; WE, Water evaporation; WHS, Wet high shear.

1 CHAPTER 1: INTRODUCTION

1.1. History of paracetamol

Cahn and Hepp (1886) applied the name Antifebrin into the medical practice of representing the first aniline derivative known as acetanilide which was serendipitously found to have analgesic and antipyretic characteristics. The quest for less toxic aniline derivatives was impelled due to acetanilide's undesirable toxic effects and the most severe being cyanosis due to methemoglobinemia. Although acetanilide and phenacetin have fallen into abandonment, paracetamol (PA) has become the most widely used analgesic–antipyretic drug in the world, due to the absence of some imperilling attributes including its high risk benefit ratio and weak potential for harmful drug interactions at standard doses (Bannwarth & Pehourcq, 2003). According to Bertolini *et al*. (2006), paracetamol which is part of the class of drug recognised as aniline analgesics is the only drug still in use currently.

Paracetamol, N–acetyl–para–aminophenol (Figure 1) is being used under a synonymous name in other countries (United States, Canada, and Hong Kong) as acetaminophen.

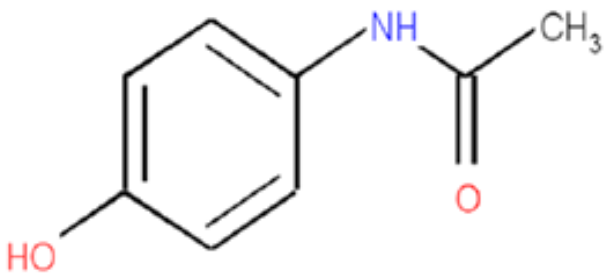

Figure 1. Chemical structure of paracetamol.

1.2. Physiochemical properties of paracetamol

PA possesses five polymorphic forms (*I*, *II*, *III*, *IV* and *V*) (Di Martino *et al*., 1996; Al–Zoubi *et al*., 2002; Smith *et al*., 2014). Only forms (*I* to *III*) are well studied and documented. The form *I*, *II* and *III* of paracetamol are well defined with respect to the crystal structures, stability and the vibrational spectra (Table 1).

The thermodynamically stable Form *I* (monoclinic, *P21/a*), metastable Form *II* (orthorhombic, *Pcab*), and Form *III* (orthorhombic, *Pca21*) that are stable only under strict geometric constraints (Burley *et al*., 2007; Di Martino *et al*., 1997; Zimmermann and Baranovic, 2011; Bustamante *et al*., 2004; Gaisford *et al*., 2010). Nevertheless, the polymorphic form *I* (monoclinic PA) which is the marketed form, is of primary interest and it is well used in the pharmaceutical companies regardless of its shortcomings such as, very poor compressibility, wettability and cohesive mode (Bucar *et al*., 2015; Larson *et al*., 2016).

Paracetamol		**Reference (s)**
Molecular formula	C_8 H_9NO_2	
Molecular weight (M.W) (g.mol^{-1})	151.16	
LogK_{ow}	0.49	(Machatha and Yalkowsky,2004)
LogP_{oct}	0.3	(Siissalo *et al*.,2010)
solubility(g/dm^3) (37 °C) in water	27.33 ± 2.97	(Mota *et al*., 2009)
BCS class	*I*	(Wu and Benet,2005)
pKa	9.5	(Kalantzi *et al*., 2006)
Glass transition temperature (T_g)	• 21 °C • 23.9 °C	(Martínez *et al*., 2014) (Sakata *et al*., 2007)

Crystal polymorphic form/habits	• **Form *I*/** Prism, plates; **Form *II*/** Prism, elongated; • **Form *III***/needle	(Nichols and Framptom, 1998; Türk and Bolten, 2016)
Melting point(°C)/Enthalpy (J g^{-1}	• Form *I*: Onset (170 °C) • 169 °C • 171 °C /186 J g^{-1}. • Form *II*: (onset): 122 °C/2 J.g^{-1}). • (157 °C/ 1 Jg^{-1}; 169 °C/185 J g^{-1}) • Form *III*: 155.5 °C	Rossi *et al*., (2003); Gharaibeh & Chick Al-Ard 2011a; Nichols and Frampton (1998). (Nichols and Frampton, 1998) Qi *et al.* (2008)
Diagnostic PXRD angles (2*θ*)	• **Form *I***: 12.1°, 15.5°, 16.7°, and 26.5°; **Form *II***: 10.35°, 14.7°, 16.7°, 17.2°, 21.5°, 21.85°, 24.03°, 27.4°, 28.4° and 29.8°; **Form *III***: (Not observed)	(Khanmohammadi *et al*.,2010) (Di Martino *et al*., 1996; Nichols and Frampton,1998)

FT−IR (bands)	• **Form *I*** (3325 cm^{-1}, N–H stretching vibration), (3163 cm^{-1}, hydrogen–bonded O–H stretching, vibration plus other combination bands), (1653 cm^{-1} C=O stretching vibration), (1564 cm^{-1}: N–H in–plane bending), (1610, cm^{-1} 1506 cm^{-1} and 1441 cm^{-1}: Aromatic ring mode), (1327 cm^{-1}: O–H bending vibration), (1259—1227 cm^{-1}: C–O and/or C–N stretching), (804 cm^{-1}: –C6H4–); **Form *II*** (3338 cm^{-1}, N–H stretching), (1651 cm^{-1}, C=O stretching), (1550 cm^{-1} N–H bending) and at 1319 cm^{-1} assigned to O–H bending shifting to 3334, 1660, 1558 and 1323 cm^{-1});**Form *III*** (3334 cm^{-1}: N–H stretching), (1660 cm^{-1}, C=O stretching), (1550 cm^{-1}, N–H bending), (1319 cm^{-1}, assigned to O–H bending shifting to 3334, 1660, 1558 and 1323 cm^{-1}).	(Wang *et al.*,2002; Zhao *et al.*, 2018)

Table 1. Physicochemical properties of paracetamol.

Tabletability may be defined as the ability of a powder to be transformed into a tablet of specified strength under the effect of compaction pressure (Joiris *et al*., 1998). Poor mechanical properties of the active pharmaceutical ingredients (APIs) is one of the numerous issue caused by the deficiency in physicochemical properties, which becomes an austere hindrance particularly for a high dosed administered drug like PA in the successful development of tablet formulation (Tjandrawinata *et al*., 2016).

Tableting problems caused by poor mechanical properties of the APIs are being traditionally dealt with by, using excipients to correct their deficiencies. The marketed PA tablets which consist of the poorly compactable monoclinic form *I* are generally formulated using up to 25 wt % of excipients to reduce the occurrence of defective tablets caused by capping (the separation of the bottom or top of the tablets), lamination (fracture of the tablet in layers parallel to the compact face or chip) (Garr and Rubinstein 1991; Santos and Sousa, 2008). However, this approach is not always practical when the tablet contains more than 20% APIs that are poorly compressible. Additionally, the use of a large number of excipients may also lead to unexpected drug instability, larger tablet size, and increased manufacturing costs (Shi and Sun 2010).

1.3.0. Particle engineering to enhance the physicochemical and mechanical properties of paracetamol

Particle engineering has emerged as a promising approach in pharmaceutics to modify, physicochemical, micrometrics and

biopharmaceutical properties of the poorly compressible drugs. Amid different methods for tableting enhancement, physical modifications of drug products including, reducing the particle size and modifying crystal habits are common approaches to increase drug hardness. These review emphases the various particle engineering techniques from bottom–up to top–down approaches that can be used to improve PA tableting properties.

1.3.1. Cooling Crystallisation

The crystallisation process is a critical step in the pharmaceutical industry and is essential for separation and purification. It accounts for over 90% of all active pharmaceutical ingredients (Acevedo *et al*., 2016; Seki and Su, 2015). The most common crystallisation approach is cooling crystallization, in which supersaturation is generated by decreasing the temperature and, the rate in which the temperature is decreased further influences the level of supersaturation and can be used as a control variable to achieve desired solid–state properties (Nagy *et al*., 2008; McNamara *et al*., 2006).

Cooling crystallisation possesses benefits such as, the temperature, which is a single process variable that is reduced to drive crystallisation. No additional raw material is needed, which could create additional problems in the product's purity and increase operating and capital cost (Griffin *et al.,* 2017; Nagy *et al*., 2008). However, it has limitations like, it is known to be slow and, a high supersaturation is vital at encouraging crystal

growth which attributes to the large width of the metastable zone. Also the sudden occurrence of early nucleation of crystals creates many crystals which eventually restrict the maximum crystal size that can be attained. Furthermore, the crystal product of a batch might not show all the wanted properties even, when the temperature is successfully controlled (Kaialy *et al.,* 2014; King *et al.,* 2015; Forgione *et al.,* 2015). Various researchers over the years have applied the method above to improve the poor mechanical performance of paracetamol. Di Martino *et al*. (1996) applied cooling crystallisation to obtain paracetamol form *II,* grown in a nonoxidizing atmosphere as polycrystalline material from the fused form *I*. The resultant orthorhombic form *II* paracetamol demonstrated good compression ability in comparison to the monoclinic paracetamol. Also, Nichols and Frampton, (1998) produced orthorhombic polymorph (form *II*) of paracetamol from a laboratory–scale using cooling crystallisation technique by nucleation of a supersaturated solution of industrial methylated spirit. The obtained orthorhombic form *II* showed improved compaction properties to that of form *I*. Fachaux *et al*. (1995) used cooling crystallisation technique from a dioxane solution or suspension to obtain pure paracetamol. The engineered paracetamol crystals exhibited a sintered like crystal structure and dramatically improved tabletability, plasticity, disintegration, and dissolution properties in comparison to the commercial paracetamol.

Joiris *et al*. (1998) applied fast cooling after melting of monoclinic paracetamol (Form *I*) to obtain the orthorhombic paracetamol (Form *II*).

The obtained Form *II* showed far better tabletability, reduced elastic recovery and absence of capping tendency in comparison to the monoclinic form *I* at the compression pressure range between 50 MPa and 350 MPa.

Patra *et al*. (2015) applied cooling crystallisation approach to prepare directly compressible paracetamol, with improved compressibility and lower elastic recovery was observed with higher compaction pressure demonstrated better dissolution rate than conventional granules of paracetamol. Garekani *et al*. (1999) applied cooling crystallisation technique to prepare prismatic polyhedral crystals of paracetamol from a saturated aqueous solution of paracetamol. The compressibility using the Heckel–plot of different crystal forms (polyhedral and thin plate–like crystals) of paracetamol was compared. Differences in compressibility were found as the polyhedral crystals exhibited the higher slope in the Heckel–plot than the plate–like crystals. Garekani *et al*. (2000) used cooling crystallisation procedure and investigated the elastic recovery, elastic energy and elastic energy/plastic energy ratio of untreated paracetamol powder and crystallised paracetamol in the presence of PVP. The investigation demonstrated that particles crystallised in the presence of PVP displayed reduced elastic behaviour under pressure and increased in tabletability in comparison to untreated paracetamol particles.

Bucar *et al*. (2015) made a mixture of nano and micrometre–sized crystals of the monoclinic form of paracetamol through sonocrystallisation

method in which the powder(nanosized) obtained demonstrated higher elastic moduli bulk cohesions (increased cohesion) leading improved tabletability behaviour compare to the micrometre–sized crystals of the monoclinic paracetamol (Form I).

1.3.2. Formation of Salt

Perumalla *et al.* (2012) prepared paracetamol salt (PA hydrochloride monohydrate) from high concentrated hydrochloric acid (Con.HCl) by slow cooling crystallisation approach. The formation of PA salt demonstrated superior compaction properties than PA form I. The tensile strength (TS) of the tablet of PA hydrochloride monohydrate increases with increasing pressure and reaches an impressive TS of 2.04 MPa at 200 Mpa. Before slightly decreasing at higher pressures whereas, the PA form I could not form tablets of appreciable strength at pressures up to 350 Mpa.

1.3.3. Antisolvent crystallisation

In this technique, a secondary solvent identified as precipitant or antisolvent is included to the solution resulting in the reduction of the solubility of the solute in the original solvent and subsequently producing a supersaturation driving force (Nowee *et al.,* 2008).

The advantages of the antisolvent crystallisation include the significant changes in the solvent activity; thus, it can have a more deep effect on the polymorphic form or the crystal morphology. Additionally, the core benefit of antisolvent crystallisation is its use of low operating temperature, which is important for thermally sensitive products (Nagy *et*

al., 2008). The disadvantages of this method include high local supersaturation at antisolvent induction zones which leads to excess primary nucleation subsequently resulting in fine crystal particle formation that effortlessly tend to agglomerate and its high-dependence on mixing for instance, where poor mixing regimes exist (Takiyama et al., 1998).

Kaialy *et al*. (2014a) used various additives such as (PVA), Avicel PH 102 (microcrystalline cellulose), Brij 58, methylcellulose (MC) and polyethene glycol to change the crystal habit of PA by applying antisolvent crystallisation technique. The engineered paracetamol crystals showed improved tabletability compared to the PA. As the compaction force changed from 50 MPa to 100 MPa, the TS of the tablets produced with untreated PA could not be measured (zero) at all compression pressures. Whereas, that of the tablets produced with the physical mixture with the corresponding 0.5% Brij 58 and crystallised PA increased from 0.2 MPa to 0.9 MPa and 0.3 MPa to 1.5 MPa correspondingly. PAs crystallised in the presence of Avicel (or physically mixed with Avicel), Brij 58 and PEG 6000 demonstrated the best compactibility over a range of compaction pressures.

FT−IR and DSC analyses indicated that 0.5% Brij 58−crystallised PA did not undergo structural conversions compared to untreated monoclinic PA, implying that the crystallisation process induced no polymorphic transformation. The technological and biopharmaceutical properties of paracetamol, the physical stability like the flow and polymorphic

transformation crystallinity of paracetamol could be influenced by the type, the grade and the concentration of additives used.

1.3.4. The formation of Eutectic mixture

The eutectic mixture (EM) is a mixture of two components that are immiscible in the solid state but miscible in the liquid state.

Jain *et al*. (2014) used the solvent evaporation technique, to formulate a eutectic mixture (EM) of aspirin−paracetamol (ASP−PA) (53:47%, *w/w*). The mixture exhibited an increase in compressibility, tabletability and plastic deformation compared to the physical mixing, affirmed using Heckel analysis which displayed lower (46.9 MPa) with EM as compared to PM (222.8 MPa). The greater compressibility and plastic deformation of EM in comparison to PM were attributed to its layered microstructure.

1.4.0. Ultrasound−assisted compaction

Ultrasound−assisted(US) compaction of pharmaceutical powders extends only over the last eight years; it is an innovative technique (Levina, and Rubinstein, 2000). Ultrasonic processing offers a net advantage in term of productivity, yield, selectivity, better processing time, enhanced quality, reduced chemical and physical hazards and environmentally friendly (Patist and Bates, 2008; Chemat and Khan, 2011).

(Levina and Rubinstein, 2000) Used fillers like microcrystalline cellulose (MCC) and dicalcium phosphate (DCP) and the binder polyvinylpyrrolidone (PVP) to increase the hardness of PA tablets by applying ultrasonic assisted compaction method for each formulation (PA/PVP; PA/DCP and

PA/MCC) at a compression pressure range of 24−32 MPa. When paracetamol was mixed with dicalcium phosphate dihydrate and microcrystalline cellulose, stronger compacts were prepared by the US–assisted compaction compared to the tablets containing no filler. An increase in binder PVP concentration and/or US time resulted in a significant increase in the hardness of paracetamol tablets produced with the US in comparison to the commercial paracetamol.

1.4. Hot melt extrusion

Hot melt extrusion (HME) is the process of converting raw material into a product of uniform shape and density by forcing it through a die under controlled conditions (Breitenbach, 2002). HME offers numerous advantages over traditional pharmaceutical processing techniques, including, the continuous operation, the possibility of the formation of solid dispersions, few processing steps, the absence of solvents/water and improved bioavailability (Crowley *et al.,* 2007). Through the short duration of the heating process, all components must be thermally stable at the processing temperature. Also, this technique necessitates a pharmaceutical grade polymer that can be processed at relatively minimal temperatures due to the thermal sensitivity of many drugs (Crowley *et al.,* 2007). The main disadvantage of extrusion is high shear forces and temperatures (Sauceau *et al.,* 2011).

The direct moulding of isomalt co−extruded with the PA demonstrated to be an appropriate method to yield tablets with outstanding physical

characteristics. Improved tableting of PA/isomalt tablets was obtained using co−extrusion technique before compression and demonstrated enhanced tabletabilty in comparison to physical mixture, with the highest tensile strength of 2.10 ± 0.16 MPa at 150°C with a compression pressure of 25 kN (Ndindayino *et al*., 2002).

1.5. Spray drying

Spray−drying is a technique based on the transformation of a fluid into a dry powder by atomization in a hot drying gas stream that is generally air. This method is unique and essential due to the production of dried particles from a liquid feed in a single processing step (Rattes and Oliveira, 2007). It possesses advantages such as the ease in scaling up, less dependence on the properties of drug and polymer. This method is fast, convenient and easily performed in mild conditions (Wang and Wang, 2002). However, this approach due to the rapid solvent evaporation it is recognised to yield amorphous material (Sebhatu *et al*., 1994), also with laboratory scale spray−dryers, processing variables must be meticulously controlled to avoid difficulties, for example, sticking, high moisture content or low yields which are frequently present (Masters, 1991). Nonetheless, (Vanhoorne *et al*., 2016) applied spray drying technique and used, 25% β−mannitol and 75% PA coating achieved ~0.2 MPa at the compaction force of 260 MPa) compared to physical mixing over the compaction force range of 50 to 275 MPa. With the composition being 5% PVP K30, 20% δ−mannitol and 75% PA coating

achieved ~ two−fold increase in tablet TS compared to physical mixing over the compaction force range of 50 to 275 MPa, with the TS increasing from 0.8 to 2.1 MPa at 260 MPa. The effect of 5% PVP and 5% β−mannitol are comparable, surface coating of PA with 20% δ−mannitol is ~21−fold more effective in enhancing the tabletability of PA than physically blending with 20% β mannitol, with the crystal form and surface coating contributing 8−fold and 2.6−fold enhancement correspondingly (Vanhoorne *et al*., 2016).

(Gonnissen and Vervaet, 2007) co−processed paracetamol with water−soluble carbohydrates including Erythritol, lactose, maltodextrin, and mannitol using spray−drying to enhance the co−processed mixtures with an increased in tensile strength from 0.38 ± 0.14 MPa with the spray dried paracetamol (absence of carbohydrates) to 2.39 ± 0.52 MPa for the mixture of paracetamol/maltodextrin at compression pressure of 74 Mpa. Though, the high residual moisture content of 7.10% found in the latter mixture could be the reason for the high tensile strength.

Sadeghi *et al*. (2013) studied the effect of particle engineering via spray drying of the hydro−alcoholic solution in the presence of various percentages of PVP K30 (0, 1.25, 2.5 and 5% *w/w*). Also, the co−processed particles exhibited a noticeable improvement in tabletability. The tablets produced with physical mixtures containing 2.5% PVP were very fragile with no measurable crushing force, and those containing 5% PVP showed the maximum crushing force of 6 N (Table 2).

Micronised paracetamol (d_{90} <10 µm, the PA form *I* was coated with 1%–10% of hydroxypropyl cellulose (HPC) by applying the spray drying technique. The obtained PA tablets demonstrated an increase in tensile strength as discussed in (Table 2)(Shi and Sun, 2011).

Vanhoorne *et al*. (2014) also applied Crystal coating via spray drying to increase the flowability and tabletability of agglomerate individual paracetamol particles. The tensile strength of 1.9 MPa obtained from the formulation comprises of, 75% paracetamol, 20% amorphous lactose and, 5% PVP at a compression pressure of 288 MPa, the excellent tabletability of this formulation which was ~5.3 fold higher than that yielded by the corresponding physical mixture, with the friability of tablets compacted at 188 MPa decreased by 36 times to only 0.6% was attributed to the coating of paracetamol crystals with amorphous lactose and PVP through co−processing.

1.6. Freeze drying

Freeze drying (FD) or lyophilisation is an alternative drying technology and, it is broadly used in the pharmaceutical industry to provide products with enhanced stability and/or desired physicochemical properties, like bioavailability or enhanced dissolution rates. Also, this technique involves the elimination of frozen water via sublimation (Kaialy *et al.,* 2016). Freeze drying is accomplished at relatively low temperatures, and the different heat−sensitive biological compounds are not damaged, which prolongs stability and circumvent particle aggregation in order to convert

the lipid dispersion to a solid state (Krokida and Philippopoulos 2006; Varshosaz *et al*. 2012). However, this approach generates various stresses during freezing and drying steps (Abdelwahed *et al*. 2006). A recent investigation demonstrated the formation of a spongy monoclinic PA form *I* prepared on quench−cooling of PA solutions in water–acetone mixtures sprayed into a vessel with liquid nitrogen followed by removal of solvents by freeze−drying. The obtained microcrystals of PA form *I* demonstrated enhanced compaction properties at a compression pressure of 350 MPa which yielded a tensile strength of 1.27 ± 0.27 MPa in comparison to the commercial PA with TS value of 0.225 ± 0.03 MPa (Ogienko *et al*., 2011).

In the last few decades, the pharmaceutical industry has achieved significant progress in its search for new drug compounds by, applying combinatorial approaches and high throughput in vivo screening. Henceforth, generating highly compactable drug compounds by using innovative techniques is now becoming one of the most critical tasks.

Polymorphs, solvates, salts, amorphous solids are the unique solid forms at which a variety of APIs exists. Also, each form shows distinctive physicochemical characteristics that can remarkably influence the purification, stability, performance properties, bioavailability and manufacturability of the drug (Morissette *et al.,* 2004).

1.7. The cocrystal route

Cocrystallisation is renowned as an overall approach of increasing the number of solid forms available to an active pharmaceutical ingredient (API), and it is a novel technique in pharmaceutical materials science (Shan and Zaworotko,2008; Srirambhatla *et al*., 2014). Also, cocrystals are not molecular mixtures of two components or physical mixtures (Chieng *et al*., 2009), as they contain two discrete neutral molecular reactants or more components (solids under ambient temperature) existing in a definite stoichiometric ratio and are structurally homogeneous crystalline materials (Shan and Zaworotko, 2008); by definition, these components are organised into three repeated dimensional order because they are crystals and each of the components has unique positions in the unit cell (Pal *et al*., 2014). In nature, between the components, hydrogen bonding or van der Waals, non–covalent and non–ionic interactions are the primary modes of interaction between the components.

The overall drive for investigating pharmaceutical cocrystals as an alternative way during drug development is to change the physicochemical properties (e.g. Solubility (Zhou *et al*., 2016), enhance the overall stability and efficacy of a dosage form (Blagden *et al*., 2008), mechanical properties (Karki *et al*., 2009). Nevertheless, for cocrystals to occur, it requires some partner molecule that enhances its biological, physical, chemical properties and, should be safe to use for human

consumption without impeding the pharmaceutical activity of the API, this is termed the cocrystal former or coformer (Vishweshwar *et al*., 2006; Qiao *et al*.,2011; Mohammad *et al*., 2011). Coformer selection for designing a cocrystal is the vital step for designing a cocrystal, and the primary request is for a coformer to be pharmaceutically acceptable for example, pharmaceutical excipients and compounds categorised as generally as safe (GRAS) for use as food additives (Qiao *et al*.,2011).

Solid form screening is being applied to exploit the physicochemical property advantage and to achieve regulatory necessities as, it is a routine activity in the pharmaceutical industry (Mohammad *et al*., 2011). However, one of the major restrictions of current screening methods is that they need large amount of materials, which further often leads to crystallisation of individual components; also, it is time-consuming and is not transferable to larger scale cocrystal formation (Kuminek *et al*., 2016).

Nonetheless, after the identification of supramolecular synthons for the design of new cocrystals (Friščić and jones, 2010), there are two sequential phases involved in the screening procedure of choosing pharmaceutical cocrystals with preset properties which are, cocrystal formation and thermodynamic stability (Manin *et al*., 2014).

1.7.1. The various routes of cocrystals formation

1.7.1.1. Solution cocrystallisation

This technique is based on the subsequent two approaches (Childs *et al*., 2008): (*a*) use of non–equivalent reactant concentrations in order to achieve the cocrystal stability region in noncongruently saturating solvents, which can be exemplified by isothermal ternary phase diagrams (TPDs) or (*b*) the usage of solvents or solvent mixtures where the cocrystal consistently saturates and hence the components have comparable solubility (Ainouz *et al*., 2009; Blagden *et al*., 2008; Miroshnyk *et al*.,2009). However, with solution−based the scale-up of this process is also tricky and, this technique habitually needs large quantity of solvents and experimental conditions to be tested and can suffer from the risk of crystallising the single component phases (Dhumal *et al*., 2010). Nonetheless, Hiendrawan *et al*. (2016) successfully prepared a pure cocrystal of PA and 5NIP of 1:1 ratio via the application of rapid solvent evaporation technique. The results obtained showed an increased tabletability of paracetamol using 29.4 KN compaction pressure, tablets of PA−5NIP showed tensile strength value of 2.78 Mpa

1.7.1.2 Milling

It is exceedingly hard to relate particles bulk behaviour with its processing routes because flow properties of micronised powders in comparison to the non–micronised are shown to be poor, which was ascribed to the

increase in surface energy (Shah *et al*., 2017). Also, powders are broadly work toughened during the ball milling process (Afshari, and Ghambari, 2016). Nonetheless, the benefits of this technique include, low processing−temperature, low−cost, the potential for easy industrial scaling−up (Cai *et al*., 2010).

1.7.1.2.1. Ball Milling

The material to be ground is partially filled in the ball mill device which is customarily, a cylindrical crushing device being utilised for grinding of pharmaceutical powders, by rotation around a horizontal axis and the grinding medium regularly contains stainless steel balls or flint pebbles or ceramic balls (Khadka *et al*., 2014) (Figure 7).

There are two different methods for cocrystal formation via grinding or milling. Neat grinding, also known as dry grinding, this approach entails one or both reactants displaying significant vapour pressures in the solid state. Neat grinding operates mechanically, using a ball mill or a vibratory mill or manually using a mortar and pestle to mix the stoichiometric cocrystal components (Friščić and Jones, 2009). To date, neat grinding has been used to meritoriously prepare many varieties of pharmaceutical cocrystals (Jayasankar *et al*., 2006; Lu and Rohani, 2009; Myz *et al*., 2009). Maeno *et al*. (2009) prepared cocrystals with PA using coformers like oxalic acid (OXA) and trimethylglycine (TMG) in 1:1 molar ratio) although, the compression and dissolution properties of APAP–TMG were

like that of the APAP–OXA cocrystal. Both cocrystals demonstrated enhanced tabletabilty compared to PA.

Grinding (liquid–assisted) or wet co–grinding (also referred to as kneading, solvent drop) works by adding small amounts of an appropriate solvent during grinding, significant enhancements in the kinetics of cocrystal formation can be attained, moreover, the nature of solvents used in grinding may have a profound impact on the process of the mechano–chemical reaction. The choice of solvent used in grinding is significant, and a straightforward prerequisite is that the solvent chosen should be capable of dissolving at least part of the original components (Shan *et al.*, 2002). According to the Q3C guideline, solvents are distributed into four classes (Class 1 possesses environmental hazards, and human carcinogens. Class 2 represents possible causative agents of irreversible toxicity like neurotoxicity or teratogenicity or non–genotoxic animal carcinogens solvents. Class 3 have an acceptable daily exposure of up to 50 mg and are commonly used in the chemical and pharmaceutical industry. Thus, for toxicological reasons manufacturers are increasingly required to reduce the number of solvents used in drug production (Grogowska and Parzcewski, 2010).

Karki *et al*.(2009) applied liquid–assisted technique in the formation of PA cocrystal using theophylline (THP) and naphthalene (NAP) phenazine(Phe2) and oxalic acid (OXA) as coformers, which showed improved tabletability (Figure 2) also, the enhanced mechanical

properties were attributed to differences in crystal packing, the obtained cocrystals exhibited a layered structure in comparison to monoclinic PA (corrugated structure)(Figure 3).

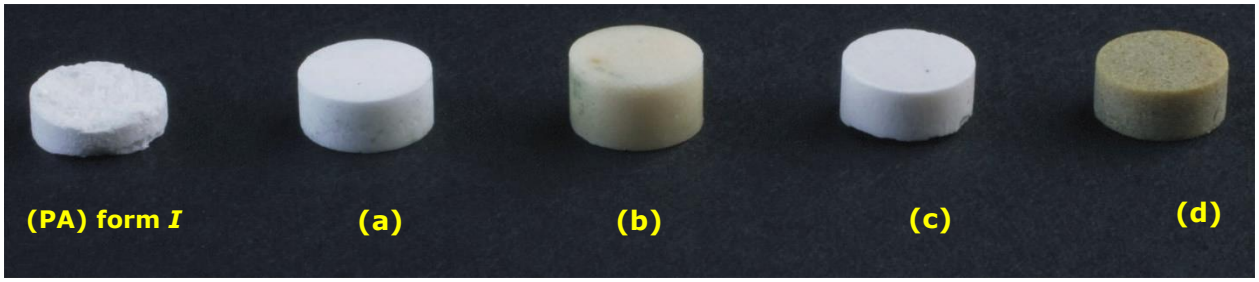

Figure 2. Tableting results of paracetamol form *I*. (a) Cocrystal with theophylline; (b) cocrystal with naphthalene; (c) cocrystal with oxalic acid; (d) cocrystal with phenazine. Adapted from (Karki *et al.*, 2009).

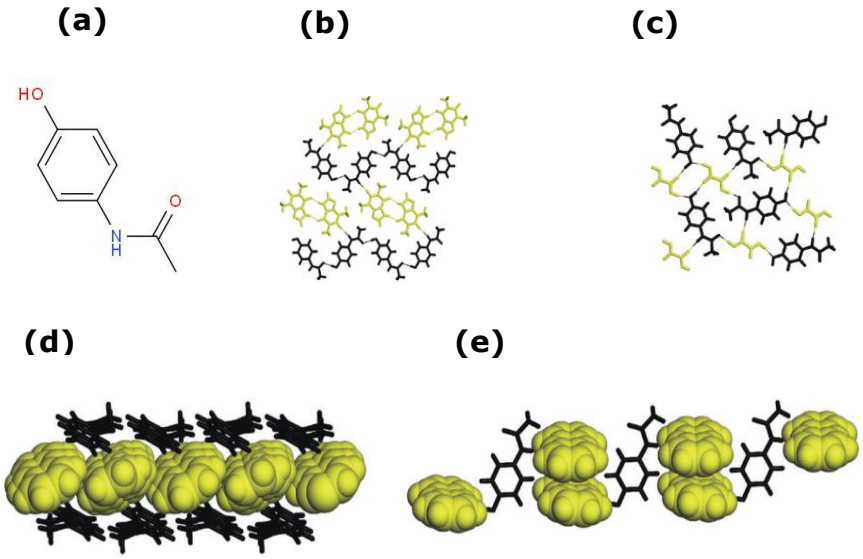

Figure 3. Paracetamol and its cocrystals (a) Molecular diagram of paracetamol; single hydrogen-bonded sheet in the cocrystal of paracetamol(yellow) with (b) oxalic acid, (c) theophylline, (d) naphthalene and (e) a single hydrogen-bonded and p-stacked chain in the cocrystal of paracetamol and phenazine. Adapted from(Karki *et al.*, 2009). Cocrystal formers are shown in black.

1.7.1.3. Supercritical fluid technology

Over the last years, the interest in the use of supercritical fluids mainly supercritical CO_2 for particle engineering has received consideration from the pharmaceutical industry. The method can be carried out at near-ambient temperatures consequently avoiding the thermal degradation of the substance in addition, carbon dioxide has comparatively, low toxicity, low critical temperature (31.1 °C) and low cost thus, makes it by far the most vital processing medium (Martín and Cocero, 2008; Shekunov *et al.*, 2001). However, the drawback of this technique is the obvious routes to commercial scale–up because of the high cost of large pressure vessels and, many of the supercritical researches have been carried out on batch reactions in sealed autoclaves (Han and Poliakoff, 2012).

Hiendrawan *et al.* (2016) successfully employed the above technique to obtain pure PA−DPA cocrystal with enhanced tableting and dissolution properties than commercial paracetamol at a compression pressure range of 4.9 kN−29.4KN.

Zhao *et al*. (2018) produced a cocrystal PA–TMG using the Supercritical CO_2 anti-Solvent (SAS) and ball milling (BM) techniques. For the cocrystal obtained with SAS, various operating parameters such as volume ratio (Vr), solution flow (Fl), the precipitation pressure (P) and temperature of precipitation (T^o) be employed. The optimal PA–TMG cocrystals presented a much larger tensile strength (with DC = 61.17 ± 1.82 %) and TS = 11.13 ± 0.46 MPa) over a compression pressure of 20kN to 80kN. Higher

drug content of PA and smaller particle size, which provides a larger total area for bonding and higher bonding strength than larger particles (Sun and Grant, 2001). In contrast to the BM sample, which recorded a TS of 20 kN (1.9 MPa) and 80kN at 5MPa (Zhao *et al*., 2018). Regardless of the techniques employed in the study, the tensile strengths were far better than that of the commercial Paracetamol.

1.8.0 The use of functional excipients

Excipient characterisation efforts have become more established because excipients in pharmaceutical dosage forms are immensely seen as vital contributors to the general characteristics of the dosage (Wasylaschuk *et al*., 2006). Notwithstanding, the physicomechanical properties of excipients which encompass good flowability, compressibility, low or no moisture sensitivity, low lubricant sensitivity, and good machineability even in high–speed tableting machinery with reduced dwell times (Chowdary *et al.,* 2012). Also, excipients provide an enhanced tablet binding, disintegration and better active pharmaceutical ingredients bioavailability, also processability of different active pharmaceutical ingredients into dosage forms due to their wide variety of functionalities (Eraga *et al*.,2015).

Formulation development offers a route to prepare a robust dosage form to resist post–compaction handling and transportation that includes choosing the suitable excipients to disguise or compensate lacks that are intrinsic to an API (Sun, 2009; Okoye *et al*., 2010).

A cellulose powder coated with 2% colloidal silica, known as Vitacel M80K is a newly developed direct compressible vehicle (DCV) and other known DCVs such as Elcema (P050+2% Aerosil 200) and AVICEL PH 101 were blended with paracetamol separately, further compressed using two compression forces at 10kN and 20kN. Paracetamol, M80K, Elcema P050+2% Aerosil 200 and AVICEL PH 101 resulted in the production of tablets with enhanced hardness, reduced disintegrating time and friability. The effect of increasing the applied compression force from 5 to 35 kN on the hardness and friability of paracetamol tablets formulated with the various DCVs, it was apparent that the increase in tablet hardness as a function of compression force was higher for M80K and ELC^{+} tablets than for Avicel tablets. Nonetheless, M80K−paracetamol tablets showed minimum friability values and the highest hardness sensitivity towards the increase of the applied compression force between 5 and 35 kN than the commercial paracetamol alone (Nada and Graf, 1998).

Obeidat *et al.* (2015) applied physical mixing of paracetamol with two polymers, Carbopol®971P NF and Eudragit®E100 of different sieved sizes to improve the crushing strength of PA tablets using different compression pressure (245 MPa, 490 MPa and 735 MPa) and, the obtained formulations sustained the release of PA. However, the compression pressures applied for each formulation were deemed extremely high. Nonetheless, the crushing strengths of the formulations were better than the paracetamol alone.

Enhanced processing methods	Additives	Coformers	Compaction pressure	Outcomes	Reference(s)
Spray drying	PVPk30 (0, 1.25%, 2.5% and 5%)	-	15kN	(25, 50, 75 and 110) N	Sadeghi *et al*. (2013)
PM	PVPK30 (2.5% and 5%)	-		(0 and 6N)	
Spray drying	HPC (1%, 2.5%, 5%, 10%)	-	100Mpa	(1.51, 1.95, 2.84 and 3.57) Mpa	(Sun and Shi, 2011)
PM	HPC (40%)	-	200Mpa	(0)N	
Dry grinding	-	Trimethylglycine	0.8 t/cm^2	(11.6 ± 1.5) kg	(Maeno *et al*., 2014)
		Oxalic acid		13.0 ± 1.4(kg)	

Table 2. Summary of enhancement in tabletability of paracetamol particles via co−processing methods.

1.9.0. Factors influencing compaction properties

Mechanisms for inter–particle interaction can be categorised as two broad classes, chemical and physical interactions. Physical interaction is due to intermolecular forces, for example, hydrogen bonding and van der–Waals. While, chemical interaction entails mostly metallic or electrostatic bonds, ionic and covalent. Inter–particle interaction is argued to be controlled by the material surface properties (Kendall, 1994). Also, the physical properties of pharmaceuticals are linked to one other, due to the modification of one of the properties, it can immensely affect the performance and processing of the solid dosage forms as well as, their compressibility (Sun, 2011).

1.9.1. Surface properties

The rise of the free surface energy of solid plays a pivotal role in interparticulate interaction, because ions or atoms located at a surface have a different distribution of intramolecular and intermolecular bonding forces than those existing within a particle, which is due to the unsatisfied attractive molecular forces that spread out to some small distance beyond the solid surface. So, surface properties of a powder material have a crucial impact on their flow and intermolecular attraction (Booth and Newton, 1987). Particulate attractive forces comprise of those called adhesion, which is between un−like particles and, conversely between like particles called cohesion (Otsuka, 1998). The attractive forces' resistance to relative movement of particles consists of, the adsorbed moisture,

residual solvent and electrostatic forces on the surface of solid particles, whereas, the other type resists the differential movement of constituent particles when exposed to an external force (Marshall, 1986).

1.9.2. Compression

The powder bed undergoes severe densification and the powder particles move collectively to form aggregates with significant, cohesive strength due to, mechanical interlocking, formation of solid bridges and Van der Waals forces; following the movement of the upper punch towards the bottom punch (Alderborn and Nystrom, 1996; Shah *et al*., 2017)(Figure 4,5 & 6).

1.9.3. Decompression

The compaction pressure falls rapidly as the distance between the two punches rises, and some of the elastic strain induced during compression will recuperate, this takes place once the upper punch starts to move away from the lower punch, a subsequent decrease in the relative density during this process afterwards follows an increase in the volume of the powder bed. Defects, like fracture of powder compacts and cracks, are more likely to be induced by a quicker elastic recovery, or spring–back, during decompression. So, controlling the elastic recovery rate is vital in the processing of powder compacts (Wu *et al*., 2005). There is a rise in the amount of particle surface area capable of forming interparticulate bonds as fine particles enter the voids between the larger ones and give a closer packing arrangement in this process also the energy is evolved

because of interparticulate friction (Marshall, 1986). Furthermore, the extent of volume reduction will be contingent upon the type of volume reduction mechanisms involved that pharmaceutical powder beds will undergo, and the mechanical characteristics of the powder, for example, plastic substances which undergo an irreversible process during deformation and leads to a lasting change in particles shape. Whereas for the elastic substance, the process is reversible, and its particles shape returns to its initial after undergoing deformation (Sun and Grant, 2001). Brittle materials that suffer extensive fragmentation produces tablets with a comparatively high porosity which halt further volume reduction, because of many bonding points that are being formed. On the other hand, for a ductile material because of the high degree of plastic deformation that occurs, it enables the particles to move to proximity to one another which frequently leads in tablets with reduced porosity. Also, different crystal habits possess different tendencies to pack in a closed structure, for example, spherical, cubical, and acicular (Booth and Newton, 1987; Joiris *et al*., 1998).

1.9.4. Other factors influencing compaction properties.

Particle size, size distribution (Vanhoorne *et al*., 2016 ;Sun and Grant, 2001; Sun and Himmelspach, 2005); crystal habit (Garekani *et al*., 2000;Kaialy *et al*., 2014), temperature (Olusanm *et al*.,2010), crystallinity (Kaialy *et al*., 2016), polymorphism (Al–zoubi *et al*., 2000; Di Martino *et al*., 2000), amorphism (Sadeghi *et al*., 2000), inter–planar d–

spacing (Shariare *et al.,* 2012), Moisture Content (Alderborn and Ahlneck,1991; Joiris *et al*., 1998; Gupta *et al*., 2005; Sun,2008), surface energy (Heng *et al*., 2006), molecular packing in crystal lattices, plasticity (Chattoraj *et al*.,2010; Karki *et al*., 2009; Jain *et al.,*2014), energy of mixing (Agbor Rose and Kaialy, 2019) are among the most common elements that can change the compression properties, because they play a crucial role in enhancing the tensile strength of the powder bed and decreasing the density variation within the tablet during interparticulate bond formation (Doelker and Massuelle, 2004).

The development of oral formulations that can explicitly release the medicament for optimal therapeutic benefits was facilitated due to its variable and versatile physiological conditions (Jindal *et al*., 2016).

Materials and methods that lead to the production of compressed tablets at a comparatively reduced cost, high speed, and containing a precise quantity of an active pharmaceutical ingredient (API) have been developed over the past decades by tablet manufacturers (Gohel and Jogani, 2005). In order to, circumvent the production of weak tablets with surface damage by chipping, which cannot only alter content uniformity but is unappealing and disagreeable. These tablets can result in waste that no longer meets required product specifications since they are frequently susceptible to breakage via production transportation and end use (Hare *et al*., 2018; Sun, 2011). Tablet product design guiding; (***i***)

rational excipient selection (***ii***) appropriate selection of the manufacturing process (***iii***) reliable determination of critical process parameters.

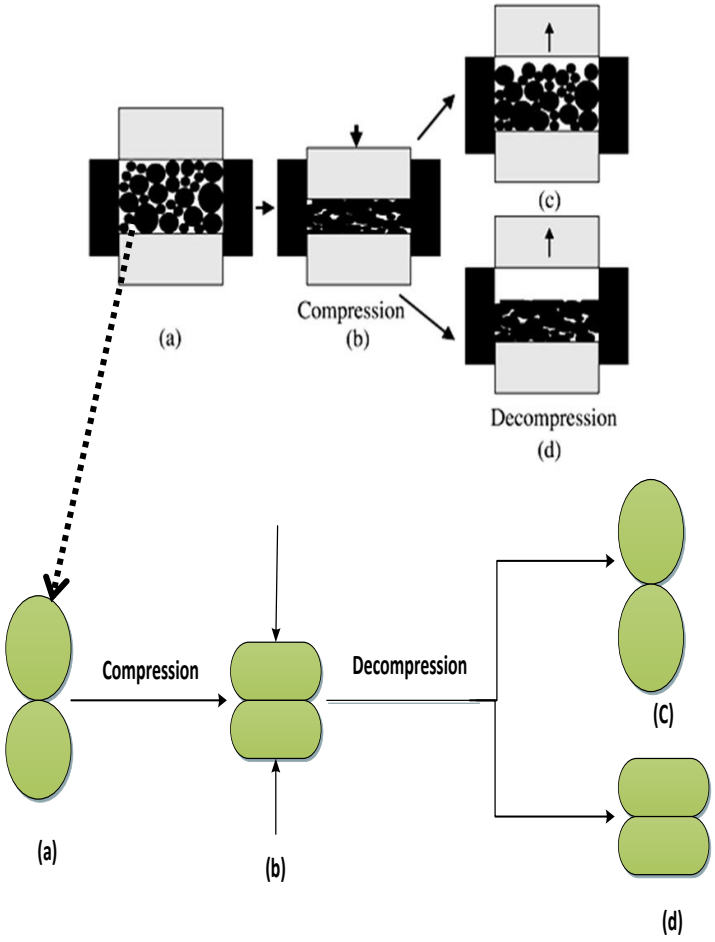

Figure 4. Phases observed during powder compaction. (*a*) particles packed in the die before compaction; (*b*) particles are deformed under maximum compaction pressure at the end of compression phase; (*c*) a porous tablet formed with an extensive recovery of elastic particles during decompression phase;(*d*) a dense tablet of plastic particles is formed after decompression. Adapted from (Sun, 2011; Sun, 2009).

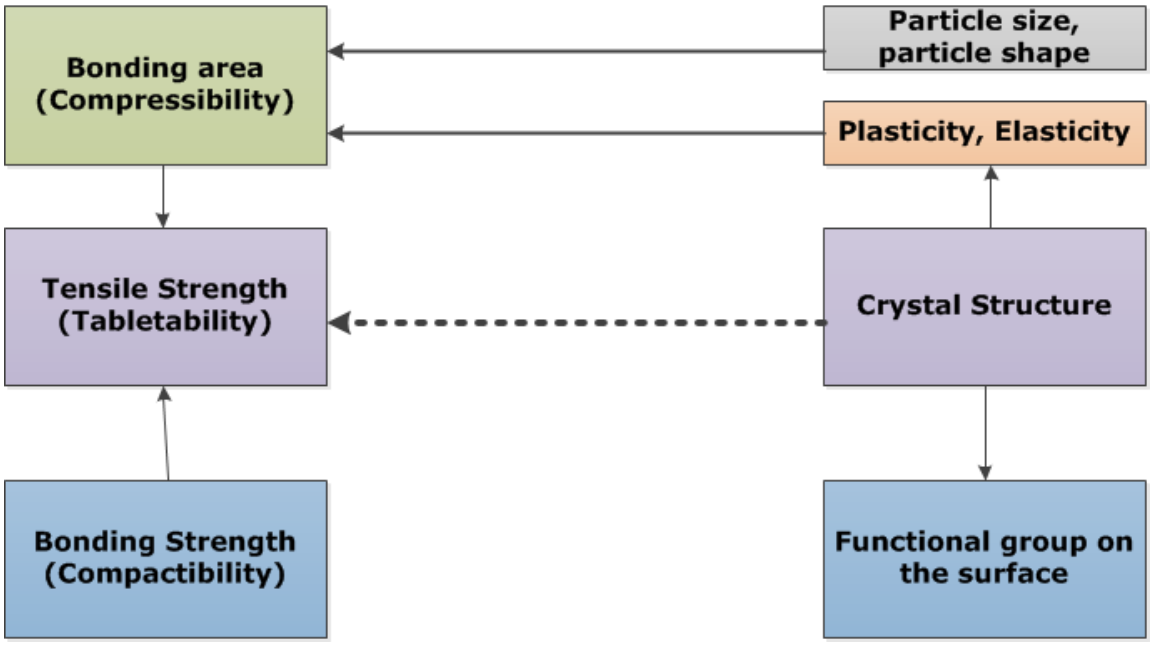

Figure 5. The relationship between crystal structure and powder tabletability. Modified from (Sun, 2009).

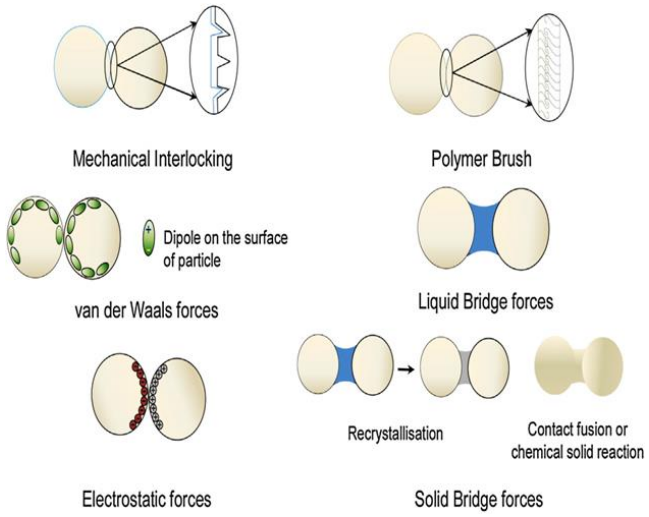

Figure 6. Different interparticle interaction mechanisms. Adapted from (Shah *et al.*, 2017).

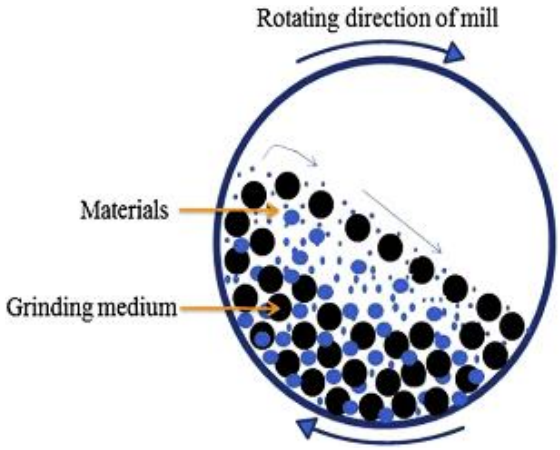

Figure 7. Schematic diagram of a Ball mill. Adapted from (Khadka *et al*., 2014).

1.10. AIMS AND OBJECTIVES

Tablets remain the best form of oral drug delivery. However, due to the poor pharmaceutical properties such as, poor tableting properties, amorphorcity, polymorphism and inadequate stability which many drugs possess nowadays, leads to the decrease of their bioavailability. Although many pharmaceutical industries and research scientists are yet to formulate and acquire paracetamol crystals with improved physicomechanical properties while maintaining the thermodynamically stable form. So, the aim of this research is to apply various co–processing techniques which can influence paracetamol crystals in the presence of functional excipient/drugs like; excipient polyvinylpyrrolidone (plastically deforming), ibuprofen (plastically deforming upon milling), Chondroitin sulphate, aspirin, caffeine (plastically deforming) and curcumin that own favourable mechanical properties due to the functional groups that they possess and could be the potential resolution to enhance the poor pharmaceutical properties of paracetamol crystals.

The objectives of the thesis comprise of:

1. Effect of preparation methods, mixing conditions and freezing temperatures on paracetamol and polyvinylpyrrolidone mixtures in order to evaluate their impact on the mechanical properties of paracetamol in comparison to the commercial paracetamol

2. Engineering of binary mixtures of paracetamol/ibuprofen, paracetamol/curcumin and paracetamol/chondroitin sulphate A and ternary mixtures of paracetamol/aspirin/caffeine on the tabletability of paracetamol

3. A successful preparation of paracetamol–5-Nitroisophthalic acid cocrystals via the applicability of engineering methods to increase the tensile strength of paracetamol crystals.

This research is explicitly based on the tabletability/compaction process. We focus on an approach where; the powder is compressed by the upper punch only while keeping the lower punch stationary: Single–ended compaction (SEC).

2 CHAPTER 2: MATERIALS AND METHOD

2.1. Materials

Paracetamol (PA,4-hydroxyacetanilide; acetaminophen; 4-acetamidophenol, >98.0%), polyvinylpyrrolidone K30 (PVP K30, average molecular weight: 40,000), ibuprofen (IBU, 2−(4−isobutyl phenyl)propionic acid, >98.0%), caffeine (CAF, $C_8H_{10}N_40_2$, >98%), aspirin (ASP, Acetylsalicylic acid, >98%), 5-nitroisophthalic acid (5NIP, $C_8H_5NO_6$), curcumin (CUR, *E*,*E* –1,7–Bis (4−hydroxy-3-methoxyphenyl) –1,6–heptadiene–3,5-dione (Natural) and chondroitin sulphate c sodium salt from bovine trachea (CHONS, $C_{13}H_{21}NO_{15}S$ > 98%, MW: 58,000 g/mol) were purchased from Tokyo chemical industry (Tokyo, Japan); 95% butanol, acetone, methanol, 100% absolute ethanol used in the content uniformity test, APC pure *n*–hexane (Cheshire, UK) and sodium chloride used for water absorption analysis were all purchased from Fisher Scientific (Gillingham, UK); BOC liquid nitrogen (Dudley, UK) and distilled water respectively.

2.2. Methods

2.2.1. General techniques employed for the preparation of formulations

2.2.1.1 Physical mixing (PM) or low shear mixing

A calculated quantity of various powders under investigation was mixed using a V–shaped powder mixer (GHP72, Zhejiang Wisely Machinery, Jiangsu, China; 50cm × 22cm × 22cm, L×W×H). Mixing was performed

at a rotation speed of 50 rpm (ten rotations clockwise followed by ten rotations anticlockwise repetitively) for 30 min under laboratory conditions (22 °C, 50% relative humidity (RH).

2.2.1.2. High shear mixing

A calculated amount of various powders under study was blended using a powerful motorised high shear mixer (Tefal, Berkshire, UK). It operated by rotation of two double–edged blades (6.5 cm×1.5 cm) at ~500 rpm in a 186–cm^3 bowl at different time intervals.

2.2.1.3. High–speed homogenization mixing

A calculated amount of various powders under study was mixed in a high–speed homogeniser (HSH, Silverson L5M, Massachusetts, USA) at 4000 rpm for 10 min. The resultant suspension was filtered (< 0.45 µm, cellulose filter paper, Fisher Scientific, UK) and then left to dry in an oven (Memmer, Durham, UK) at 50 °C for 12 h.

2.2.1.4. Batch cooling crystallisation (BCC) technique

Supersaturated aqueous solutions containing PA mixtures under study were prepared by dissolving in different amounts in each solvent under constant stirring of 200 rpm at a specific temperature. After being wholly dissolved all solutions were removed from heating and allowed to settle and cool (uncovered) at ambient conditions (22ºC, 50% RH) for some specific days until no apparent water could be observed in crystallisation

media of any samples. Then, each powder under study was harvested then left to dry in an oven (Memmer, Durham, UK) at 40 ºC.

2.2.1.5. Solvent evaporation (SE) preparation

A calculated amount of different powders under analysis was dissolved in different quantities of each respective solvent. The resultant solution of each mixture was stirred at 200 rpm using *Stuart* heat–stirrer at a constant temperature of 70 ºC until all the solvents present evaporated. The precipitated crystals in beakers were left to dry in an oven (Memmer, Durham, UK) at 40 ºC until no apparent water could be observed in crystallisation media of the sample.

2.2.1.6. Freeze drying (FD) technique

Freeze dried of various components under investigation were prepared accordingly, each solution was obtained by introducing into a 500 mL round–bottomed flasks (Shotts DURAN) and subsequently freeze–dried by applying a protocol as entails. The flasks encompassing the frozen formulations of PA solutions were rapidly placed on the shelves of a Christ Beta 1–8 LD Freeze Dryer (Martin Christ Gefriertrocknungsanlagen GmbH, Osterode am Harz, Germany) using manifolds. The primary drying was performed at a shelf temperature of −40 ^{o}C vacuum pressure of 0.500 Mbar and a safety pressure of 0.770 Mbar while the final drying was performed at a shelf temperature of –25 ºC, the vacuum pressure of 0.370 and a safety pressure of 0.633 Mbar). The freeze-dried

formulations were collected after 72h after which, they were transferred into sealed glass vials over silica gel until used.

2.2.1.7. Milling (ML) technique

Various formulations under investigation were milled into a hardened stainless steel jar vial (80 mL) using a Fritsch Pulverisette 6 (Fritsch GmbH Pulverisette 5, Idar−Oberstein, Germany), a planetary ball mill equipped with 18 balls (diameter ≈10 mm) at a constant speed of 400 rpm using different time intervals with no repetitions and the powder and further stored in a sealed glass vials at room temperature until required.

All mixtures prepared were stored in sealed glass vials for at least seven days at the laboratory conditions (22 ºC, RH = 50%). Preparations were performed at least in triplicate using an identical protocol to ensure reproducibility.

2.3. Sieving

Each mixture of PA formulation was poured onto the top of 500 µm sieve (Retsch® Gmbh Test Sieve, Germany) which was placed above another 1000 µm sieve. The sieve shaker (Retsch® Gmbh Test Sieve, Germany) was operated for 15 min. After sieving, the required size fraction (<500 µm) was collected. All engineered samples were stored in sealed glass vials for at least seven days under laboratory conditions (22°C, 50% RH) before further investigation to allow any possible charge

relaxation to occur (Kaialy, 2016a). The mixtures were prepared in triplicate (or better) using an identical protocol to ensure reproducibility.

2.4. Content uniformity

Five samples were selected randomly from different spots of each PA–PVP mixture to determine the quantity of PA in the mixture. Each sample weighed 526.3 mg ± 0.5 mg (corresponding to 500 mg unit dose of PA) and was dissolved in a fixed amount of solvent (hydro–alcoholic solution, 25% ethanol/water *v/v*). Each solution was analyzed for PA content using an ultraviolet spectrophotometer (Biochrom WPA Biowave *II* UV/visible, Cambridge, UK) at a wavelength of 250 nm. A calibration curve for the concentration of PA was constructed with a coefficient of determination of 0.9996. The samples were diluted for the drug concentrations to fall within the range covered by the calibration curve. For each mixture, the PA content uniformity was calculated as the percent amount of paracetamol in the nominal dose (500 mg). The degree of paracetamol content homogeneity was evaluated using the percent coefficient of variation (%CV: ratio of the standard deviation of drug content to the average drug content in the sample expressed as a percentage). A higher %CV value indicates a decrease in drug content homogeneity. A mixture is considered homogeneous when the content uniformity of the drug content is between 90% and 110%, and the CV is below 6%, according to the FDA guidelines (Williams, Adams, Poochikian, & Hauck, 2002).

2.5. Laser diffraction analysis

Volume-weighted particle size analyses of various powders under investigation were conducted using a Malvern Mastersizer 2000 (Malvern Instruments, Germany) laser diffraction particle size analyzer equipped with a dry sampling system (Aero S, Malvern Instruments, UK). The particle size range covered by the laser diffractometer was 0.1–3500 μm. Before measurement, a background reading was taken. The dispersion air pressure was adjusted to 2.0 bars, and the feed rate was adjusted to 30%. The measurement time was 5 s. The particle sizes at 10% ($d_{10\%}$), 50% ($d_{50\%}$, median diameter), and 90% ($d_{90\%}$) of the volume distribution, and the volume mean diameter (VMD, the average diameter based on the unit volume of a particle) were calculated automatically using the Malvern software (version 2.20). The span (calculated using Eq. (1)) of the volume distribution was used as a measure of the width of the distribution of size relative to the median diameter. Three samples were measured for each product and results were averaged.

$$\text{Span} = \frac{d_{90\%} - d_{10\%}}{d_{50\%}}. \quad (1)$$

2.6. Scanning electron microscopy

A representative specimen of each sample was gently mounted on an aluminium stub (G301, Agar Scientific, Essex, UK) with double-sided adhesive carbon tabs (G3347N, Agar Scientific). To increase the electrical conductivity on the surface of the samples, a sputter coater (Emscope

SC500, Quorum Technologies, Laughton, UK) was used to coat the samples with gold (15 nm layer thickness) in an argon atmosphere before observation. The morphological properties of the various powders under study were examined using a field-emission scanning electron microscope (SEM, Zeiss EVO050, Germany) with an acceleration voltage of 10 kV and a beam current of 10 μA. The powders were handled with care during preparation.

2.7. Bulk properties

An accurately weighed amount of each powder was gently poured into a 10-mL glass measuring cylinder using a glass funnel. The bulk volume was recorded, and then the cylinder was tapped (Tapped Density Tester, Copley Scientific, UK) under laboratory conditions (22 °C, 50% RH) for 500 taps. The volume was recorded after every 50 taps. The experiments showed that 500 taps were adequate to reach the maximum reduction in volume of the powder beds. The bulk density (or apparent density, D_b), tap density (or drop density, D_t), and Carr index (CI, Eq. (2)) of each powder were calculated.

$$CI = \left(\frac{D_t - D_b}{D_t}\right) \times 100. \quad (2)$$

Based on the calculated *CI* values, powder flowability was described as excellent (*CI* < 10%), fair (*CI* 16%–23%), or extremely poor (*CI* > 38%).

The packability was determined from the tapped density, according to Kawakita and Lüdde's equation (Eq. (3)) (Kawakita & Lüdde, 1971).

$$\frac{n}{C} = \frac{1}{ab} + \frac{n}{a}, \quad (3)$$

$$C = \frac{V_0 - V_n}{V_0}, \quad (4)$$

Where n is the tap number, C denotes the volume reduction (Eq. (4)), and V_0 and V_n are the powder bed volumes at the initial and n^{th} tapped state, respectively. The plot of n/C versus n is linear. The cohesivity is a constant related to cohesion, represented by $1/b$, and is obtained from the intercept of the plot through the modified Kawakita and Lüdde's equation. Three different samples were analyzed for each product.

2.8. Powder X–ray diffraction

To monitor the phase purity of PA co–processed under different conditions, powder X–ray diffraction (PXRD) structural patterns of all the various powders under investigation were recorded using a Panalytical Empyrean diffractometer (PANanalyical, Almelo, The Netherlands) with Cu Kα radiation (1.54056 Å) operated under laboratory conditions (22 °C, 50% RH). Each sample was placed in a sample holder, surface-smoothed with a glass slide, and scanned between 2θ values of 5° and 40° with a step-by-step increase of 0.01°/s. The sample stage was spun at 30 rpm. The instrument was calibrated using a silicon standard. The reproducibility of the PXRD patterns was verified by collecting multiple patterns of three different specimens of each sample.

2.8.1. Determination of the percentage of crystallinity (Alternative technique)

Following the technique employed in (Section 2.8.0) the background of the diffractogram of some specific samples were determined, followed by a scan list. Also, the scan statistic of the diffractogram of each sample was expanded. Also, the constant background which was initially set at minus one was changed to minus 241 in order to correct the crystallinity value as shown in (Table 21).

2.9. Fourier transforms infrared spectroscopy

The molecular structure of the starting materials and all the mixtures were analysed using an Alpha Platinum–ATR Fourier transform infrared (FT–IR) spectrometer (Bruker, USA) to investigate whether PA was chemically altered or whether any interaction with PA at the molecular level occurred during the preparation of different mixtures. A few milligrams of each powder was placed in the middle of the sample stage and were compressed by clicking the top of the arm of the sample stage. The samples were scanned under laboratory conditions (22 °C, 50% RH) over a wavenumber range of 400–4000 cm^{-1} with a 1 cm^{-1} resolution. Before each measurement, a background spectrum of air was acquired under the same instrumental conditions. The spectrum produced for each sample was the average of 15 scans. The acquired spectra were processed using Opus software (version 7.5.18, Massachusetts, USA)

2.10. Thermogravimetric analysis (TGA)

An accurately weighed sample of the starting materials and all the mixtures was placed in an open pan and analysed using a thermogravimetric analyser (Perkin–Elmer Thermal Analysis Series 7, Norwalk, USA). Mass calibration was performed with a 100–mg calibration weight. Each sample was heated from room temperature to 600 °C at a heating rate of 10 °C/min. The internal atmosphere was maintained by purging nitrogen as a purge gas at a flow rate of 20 mL/min. The reduction in the mass of the samples was measured.

2.11. Differential scanning calorimetry (DSC)

Differential scanning calorimeter (DSC Q2000 DSC (TA Instruments, Hertfordshire, UK) was used to examine the various samples. The commercial PA, commercial 5NIP, and the cocrystals powders (2.0 mg ± 0.5 mg) were heated individually, from 50 to 300 ºC at a scanning rate of 10 ºC/min, in hermetically sealed T zero aluminium pans. A purge gas of nitrogen was passed over the pans with a flow rate of 50 mL/min. The instrument was calibrated using indium (> 99.999%, DE, USA). Indium standard was used to calibrating the cell constant (enthalpy) and temperature, conducted at a heating rate of 10°C/min. A calibration check was made, before experimentation, using the indium standard (Onset=156.6 °C ± 0.2 °C, Peak Area=28.45 J/g ± 0.5 J/g). All the peak and onset temperatures and their enthalpies were calculated using TA TRIOS Software V4.3.1.

2.12. Karl Fischer titration

The (residual) moisture content of both the commercial materials and the engineered powders were determined by the Karl–Fisher method (Metter Toledo, C20 Coulometric KF Titrator, Switzerland). The Fischer reagent solution was Hydranal1 Coulomat AF (Sigma-Aldrich, USA). Following the calibration of the instrument, samples were rapidly added into the titrator vessel at the laboratory temperature (22 ºC), and the titration of each sample was repeated three times.

2.13. Water absorption

An accurately weighed sample of some of the powders under study was stored in a desiccator containing a saturated solution of pure sodium chloride, which gives a relative humidity of 75% at 25 °C (Richardson & Malthus, 1955). The mass of each stored sample was recorded at a time interval of 1, 3, 6, 12 months. The final mass (W_f) was noted when there was no further change in the sample mass. The percent moisture content was calculated by using Eq. (5), in which W_0 is the initial mass.

$$\% \text{ Moisture content} = \frac{W_0 - W_f}{W_f} \times 100 \qquad (5)$$

2.14. Preparation of tablets

Compression of the various powders under processing was carried out using a manual single punch Specac press (KBR 25.011; Gemini BV, The Netherlands) fitted with 13-mm-diameter flat-faced punches to produce round tablets with a target mass corresponding to a 500–mg unit dose of

PA. Before compression, the compaction surfaces were lubricated with 1% (*w/v*) magnesium stearate (Acrõs Organics, New Jersey, USA) in acetone (Fisher Scientific, UK) to reduce the friction between the die and the tablet, and to prevent the tablets from sticking to the die walls and punch faces. Tablets were compressed at increasing compression pressures of 37, 74, 111, 148, 185, and 222 MPa under load for 10 ± 1 s dwell time. Tablet diameter and thickness were measured using a digital micrometer (Fisher Scientific, UK) immediately after ejection and 24 h after ejection to allow for elastic recovery and possible hardening of tablets. Tablets were stored in screw-capped glass vials (22 °C, 50% RH). The results were generated as the mean and standard deviation (SD) of three determinations.

2.15. Crushing strength and capping tendency

The crushing strength was determined from the force required to fracture the tablet by diametral compression on a motorised Vankel Tablet Hardness Tester (Benchsaver VK 200, USA). The tensile strength (TS) of each compact was calculated using Eq. (6) (Fell & Newton, 1970).

$$TS = \frac{2F}{\pi Dt} \quad (6)$$

Where D and t are the diameter and thickness (mm) of the compact, respectively, and F is the force exerted to fracture the compact. Tests were carried out 24 h after ejection. Five tablets were selected for crushing strength measurements.

2.16. Friability test

Ten tablets compressed at a specific compression pressure of some of the samples were selected randomly, and the tablets were accurately weighed (initial weight). The tablets were placed in a friability tester and rotated at a constant speed of 25 rpm for 4 min in Erweka friabilator. The tablets were cleaned from loose dust and reweighed (final weight) and the weight loss % (friability) calculated.

$$\% \text{ Friability} = \frac{w1-w2}{w1} \times 100 \quad (7)$$

Where: W_1 = collective weight of tablets before testing. W_2 = collective weight of tablets after testing.

2.17. UV calibration curve of PA in aqueous media

A stock solution of PA reference standard was prepared by transferring 10 mg of the drug into a 100 ml of volumetric flask and diluting with distilled water. From this stock solution, seven various concentrations (0.001, 0.002, 0.003, 0.004, 0.005, 0.1 and 0.2 mg/ml) of each solution were transferred to 100 ml volumetric flasks and diluted with distilled water. The UV absorbance reading of this solution was measured at 250 nm for PA using UV/Visible spectrophotometer (UV–160, Shimadzu, Japan). Distilled water was used as a reference. Then, the absorbance versus concentration of solutions was plotted to obtain the calibration curve, which resulted in a very good R–square value (Figure 8).

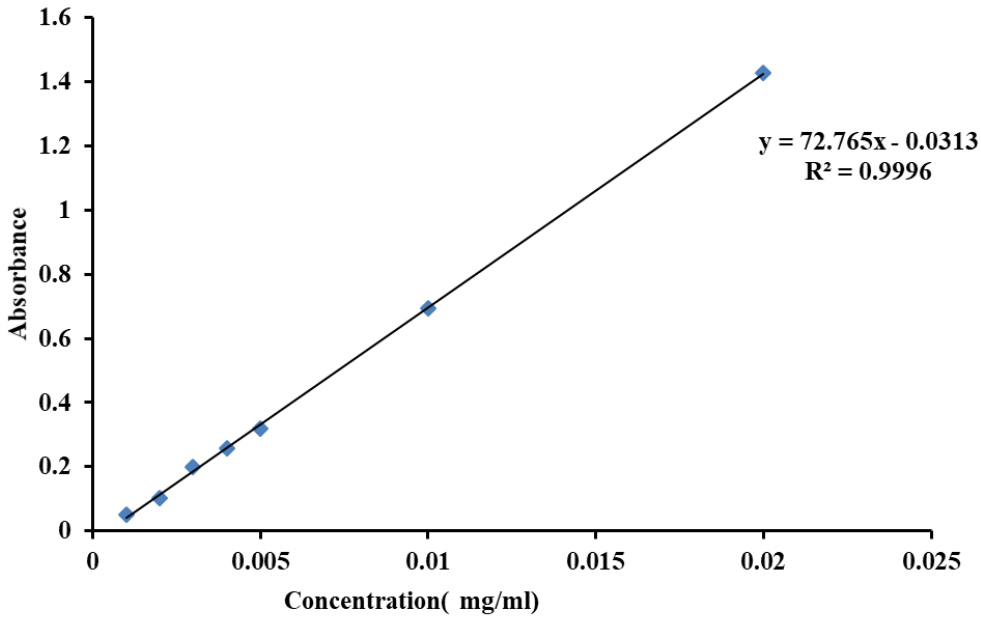

Figure 8. UV absorption calibration curve of PA reference standard in aqueous media at 250 nm.

2.18. *In–vitro* dissolution studies

This dissolution test was carried out to obtain the release profiles PA, the engineered mixtures to evaluate the inherent dissolution properties of different crystals. The dissolution profiles of paracetamol powders were evaluated using USP dissolution apparatus 2 (paddle method). Three tablets were tested for each formulation. The dissolution medium (900 mL of distilled water) was equilibrated to 37 ± 0.5 ºC at 50 rpm using the rotating paddle. Samples were withdrawn at pre-determined time intervals (5, 10, 15, 20, 25, 30, 40, 50 60, 75, 90, 105, 120, 140, 160 and 180 min). The amount of the paracetamol dissolved in the dissolution media was properly diluted and assayed spectrophotometrically at 250 nm max using a spectrophotometer (UV-160; Shimadzu, Kyoto, Japan). All determinations were carried out in triplicate.

2.18.1. Dissolution parameters

The percentage of paracetamol dissolved was calculated, and a minimum of three determinations was carried out for each sample (mean ± SD, n = 3). The dissolution efficiency (DE, Equation 7) (Khan, 1975) and the mean dissolution time (MDT, Equation 8), such mathematical analyses enable statistical comparisons between the various formulations. The DE is the area under the dissolution curve produced up to a certain time, t, expressed as a percentage of the area of the rectangle.

Where *t* is the total time of drug release, *y* is the percentage of drug release at time *t* and Y_{100} is a 100% drug release. The MDT is a model-independent method that is suitable for dosage forms having different mechanisms of drug release.

The MDT is the time at which 50% of the drug is dissolved from its solid state under dissolution conditions (Equation 8).

Where *j* is the sample number, *n* is the number of dissolution samples, Δt or t_j is the time at the mid – point between *t* and *t* – 1 (which can be calculated using (*t* + (*t* –1))/2) and ΔMj is the additional amount of drug dissolved between *t* and *t* – 1.

$$DE_t = \frac{\int_0^t y \times dt}{Y100 \times t} \quad (7)$$

$$MDT = \frac{\sum_{j=1}^{n} tj\Delta Mj}{\sum_{j=1}^{n} tj\Delta Mj} \quad (8)$$

2.18.2. Comparison of release profiles

The dissolution behavior of PA and the formulations tablets in deionised water were analysed. The drug release characteristics for the two formulations (PM (FDPA–FDCHONS)) and FD (PA–CHONS) and variables (PA and FDPA) under investigation were compared, by calculating the difference (*f*1) and similarity (*f*2) factors which were used to study the dissolution profile.

$$\boldsymbol{f1} = \frac{\sum_{j=1}^{n} |Rj - Tj|}{\sum_{j=1}^{n} Rj} \times 100 \text{.....} \quad (9)$$

$$\boldsymbol{f2} = 50 \text{ x log } \left\{ \left[1 + \frac{1}{n} \sum_{j=1}^{n} |R_j - T_j|^2 \right]^{-0.5} X\ 100 \right\} \text{.....} \quad (10)$$

Where, R_j and T_j are the cumulative percentage dissolved at each of the selected n time points of the commercial particles (reference) and freeze–dried mixtures (test product), respectively. In general, the dissolution profiles were taken as similar with *f*1 value lower than 15 and *f*2 value higher than 50.

2.19. Statistical analysis

One-way analysis of variance (ANOVA) test was employed to statistically compare mean results in this study, considering statistical probability (*P*) values less than 0.05 as indicative of significant difference. When ANOVA indicated a significant difference, Tukey's Honestly Significant Difference (HSD) post hoc test was performed. Data were expressed as the mean ± SD).

3 CHAPTER 3: IMPROVED TABLETING BEHAVIOUR OF PARACETAMOL IN THE PRESENCE OF POLYVINYLPYRROLIDONE ADDITIVE

3.1.0. Effect of mixing conditions

3.1.1. Introduction

Tablets are the most popular solid dosage forms because of their several advantages, including ease of administration, precise dosing, ease of manufacture, good product stability in comparison with liquids, and lower vulnerability to tampering than capsules, and most desired in comparison to capsules followed by powders and fines granules (Sunada and Bi, 2002; Brniak *et al*., 2015; Morissette *et al*. 2004; Gohel & Jogani, 2005). Direct compression (DC) is the favoured modern choice for tablet manufacturing. The advantages of DC include simplicity, reduced time and final cost of the product because of fewer processing stages, continuous nature, and elimination of heat and moisture effects. These latter attributes make DC suitable for processing hygroscopic and thermo–sensitive materials (Jivraj, Martini, & Thomson, 2000). However, it is unfortunate that less than ~20% of pharmaceutical powders can be compressed into tablets by DC because of their inherent poor functional properties required for DC (Armstrong, 2007). The situation is particularly severe when the formulation requires a high dose of a poorly compactible drug such as paracetamol (PA). PA is a widely used analgesic drug. The monoclinic form is usually selected in the pharmaceutical industry and is commercially available because it is the most thermodynamically stable form at room temperature and pressure. However, the monoclinic form of PA is notorious for exhibiting poor tableting properties by DC, reduced

plastic deformation during compression, and poor flowability. These flaws commonly result in fragile tablets with a high propensity to cap. Such poor mechanical properties have been explained in terms of the monoclinic crystal structure of PA (Beyer, Day, & Price, 2001). Crystallization has been extensively investigated as a particle engineering technique to improve the functional properties of poorly compactible drugs via the formation of an amorphous state (Berggren, Frenning, & Alderborn, 2004), a modified polymorphic form (Di Martino Guyot-Hermann, Conflant, Drache, & Guyot, 1996), and/or particle shape (Kaialy, Larhrib, Chikwanha, Shojaee, & Nokhodchi, 2014). However, studies on the effects of secondary manufacturing processes, such as mixing, on the tableting performance of poorly compactible drugs have been limited (Sallam & Orr, 1985). Mixing has evolved from being an empirical process to be a meticulously controlled process, therefore, optimum mixing is crucial for the manufacture of nearly all solid dosage forms (Kaialy, 2016b).

This work is aimed to study the influence of mixing conditions on the tableting properties of PA processed in the presence of polyvinylpyrrolidone (PVP), which is a plastically deforming binder under compaction. Because PVP contains carbonyl groups, it has the potential to interact via hydrogen bonding with drugs that contain amine groups, such as PA (Garekani, Ford, Rubinstein, & Rajabi-Siahboomi, 2000). A PVP concentration of only 5% (w/w) was used in this investigation because PA

requires high doses (300–1000 mg) for its analgesic and antipyretic actions. This means that a minimal amount of excipient(s) should be added to the formulation to minimise the mass of the final dosage form. The effects of various dry and wet mixing conditions on the physicochemical and mechanical properties of PA–PVP mixtures were studied.

3.2. Engineering of PA–PVP formulations

3.2.1. Low energy dry mixing

Tumble mixing is known to produce low shear forces, whereas hand mixing produces medium shear forces (Kaialy, 2016b).

3.2.1.1. Low shear (LS) or physical mixing (PM)

PA and PVP (95:5 *w/w*) powders were mixed using the technique in (Section 2.2.1.1).

3.2.1.2. Medium shear (MS) mixing

PA and PVP (95:5 *w/w*) powders were hand mixed by vigorous shaking in a plastic bag sample container for 10 min under laboratory conditions (22 °C, 50% RH).

3.2.2. High energy mixing

3.2.2.1. Dry high shear (DHS) mixing

PA (15g, *w/w*), PA and PVP (95:5 w/w) powders were blended using the high shear mixing technique as described in (Section 2.2.1.2).

3.2.2.2. Wet high shear (WHS) mixing

PA and PVP (95:5*, w/w*) powders were suspended in *n*-hexane (50 mL), using the technique in (Section 2.2.1.2) mixed above for 3 min. After mixing, the resultant suspension was filtered (< 0.45 µm, cellulose filter paper, Fisher Scientific, UK) and then left to dry in an oven (Memmer, Durham, UK) at 50 °C for 12 h.

3.2.2.3. High–speed homogenization mixing

PA and PVP powders (95:5, *w/w*) powders were suspended in 200 mL of *n*-hexane and then mixed in a high-speed homogeniser by applying the technique in (Section 2.2.1.3).

3.2.2.4. Tablet preparation

Each tablet weighs 526.3 ± 0.5 mg for the various formulations and 500 mg ± 0.5 mg for PA compressed using the method described in (Section 2.14).

3.3. Results and discussion

3.3.1. Content uniformity

The percent drug content uniformity obtained from all PA–PVP mixtures was acceptable (LS, 100.6% ± 5.9%; MS 100.7% ± 2.8%; DHS, 100.7% ± 1.2%; WHS, 108.5 % ± 2.9% and HSH, 101.9% ± 5.4%). The %CV of

PA content varied with (LS, 5.8%; MS, 3.5%; DHS, 5.8%; WHS, 2.9% and HSH, 5.4%) satisfying the acceptance level and indicating adequately homogeneous PA content in all mixtures, as well as accurate and reproducible processes of mixing, sampling, and analysis.

3.3.2. Particle size and shape distributions

PA–PVP mixtures prepared using low energy (LS and MS) mixing conditions showed slightly reduced VMDs and slightly increased span values compared with commercial PA (Table 3). This was caused by the VMD value of the PVP particles, which was lower than that of commercial PA (Table 3), as confirmed by SEM micrographs. The PA–PVP mixtures prepared using low energy (LS and MS) conditions showed statistically similar particle size distributions (PSDs). This agreed with SEM observations, which showed no striking differences in the structures of mixtures prepared at low energy conditions (Figure 9). A trend of lower VMD could nevertheless be observed with the increase in shear introduced during physical mixing (i.e., LS > MS > DHS) (Table 3). For example, the VMDs of PA–PVP mixtures prepared using LS, MS, and DHS conditions were 521 ± 24 µm, 504 ± 13 µm, and 80 ± 4 µm, respectively (Table 3). The mixtures prepared using high energy conditions (DHS, WHS, and HSH) showed smaller and broader VMDs (VMDs ranging from 52.3 ± 4 µm to 80 ± 4 µm, span values ranging 3.5 ± 0.2 to 6 ± 0.2) compared with the mixtures prepared using low energy (LS and MS) conditions (VMDs ranging from 504 ± 13 µm to 521 ± 24 µm, span values ranging

from 1.5 ± 0 to 1.7 ± 0) (Table 3). The shift towards lower VMDs for the mixtures prepared using high energy conditions was caused by the *in-situ* generation of intrinsic fine particulates (as evidenced by the lower $d_{10\%}$ values, Table 3) from particle collisions and attrition/fracturing during dry high energy mixing. This was confirmed when PA samples processed using high shear mixing in the absence of PVP showed considerably smaller VMD than commercial PA (Table 3). The generation of such fine particulates will have a significant influence on powder bulk properties (i.e., compactibility, cohesivity, bulk density, flowability, and tensile strength) as discussed later (Sections 5.2.4 and 5.2.6). The difference in morphologies between various mixtures was clearly observed in the SEM micrographs (Figure 9). However, the VMDs (recorded by laser diffraction, Table 3) of the particles prepared by high energy (DHS, WHS, and HSH) conditions were larger than shown in the SEM micrographs (Figure 9), indicating the occurrence of particle aggregation for the preceding mixtures.

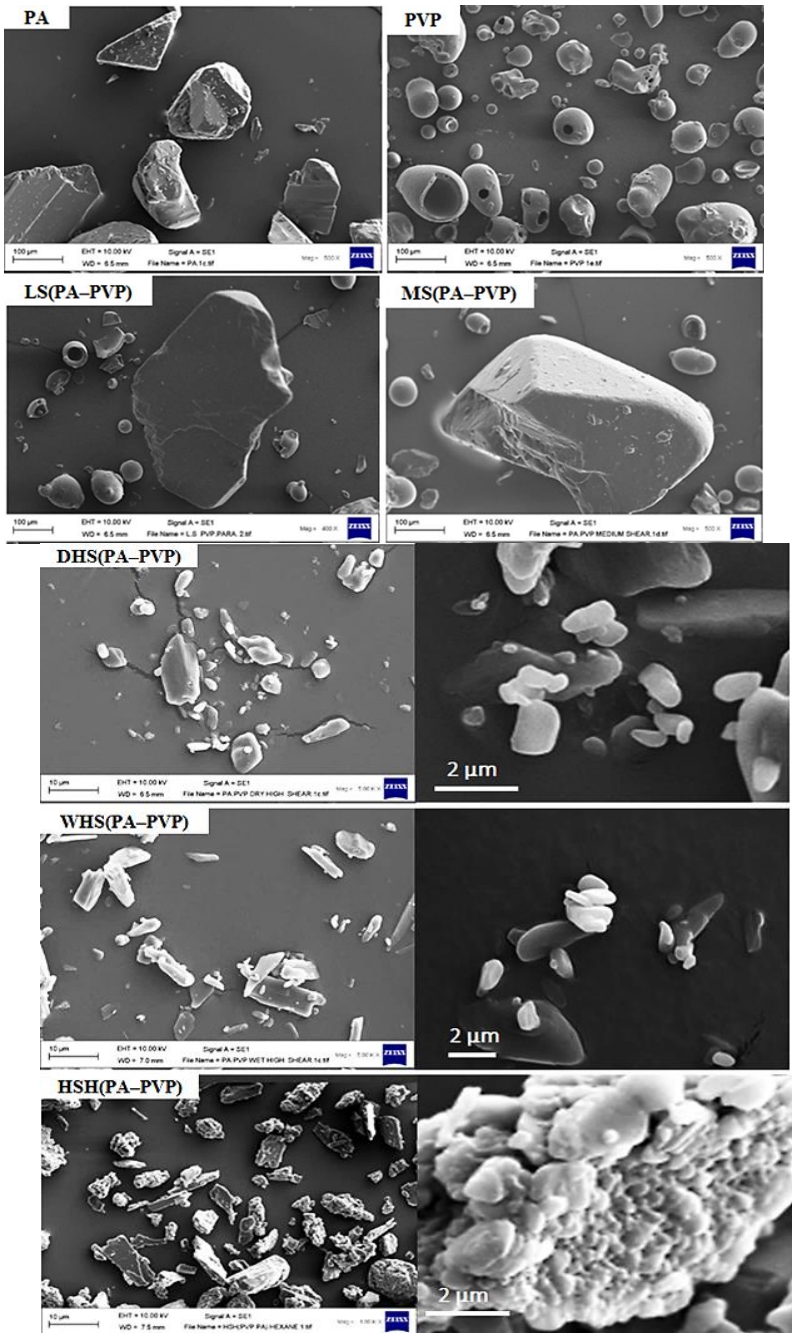

Figure 9. Scanning electron microscopy micrographs of commercial paracetamol (PA), commercial polyvinylpyrrolidone (PVP), and PA–PVP mixtures (5% PVP, w/w) prepared using low shear (LS), medium shear (MS), dry high shear(DHS), wet high shear (WHS) and high-speed homogenization (HSH) mixing conditions. Size bars denote magnification.

Table 3. Particle size distribution for commercial paracetamol (PA), commercial polyvinylpyrrolidone (PVP), and PA–PVP mixtures (5% PVP, *w/w*) prepared using, low shear (LS), medium shear (MS), dry high shear (DHS), wet high shear (WHS) and high-speed homogenization (HSH) mixing conditions. Data given for particle size at 10% ($d_{10\%}$), 50% ($d_{50\%}$, median diameter), and 90% ($d_{90\%}$) of the volume distribution, the volume mean diameter (VMD), and the span of the volume distribution (see Eq.(1)). Data expressed as mean ± SD, n = 3.

Product	$d_{10\%}$ (µm)	$d_{50\%}$ (µm)	$d_{90\%}$ (µm)	VMD (µm)	Span
PA	254 ± 22	506 ± 30	911 ± 39.3	548 ± 30.2	1.3 ± 0
PVP	42.1 ± 0.5	100.4 ± 1.1	209 ± 2	119.3 ± 4	1.7 ± 0
DHS(PA)	4 ± 0.1	25.2 ± 1	152 ± 8.3	53.3 ± 2.2	6 ± 0.3
LS(PA–PVP)	181± 13	487 ± 24.5	899 ± 42	521 ± 24	1.5 ± 0
MS(PA–PVP)	176 ± 6	468 ± 14	880 ± 21.4	504 ± 13	1.5 ± 0
DHS(PA–PVP)	4.5 ± 0.1	36 ± 0.3	211 ± 8	80 ± 4	6 ± 0.2
WHS(PA–PVP)	4 ± 0.1	25 ± 0.5	134.3 ± 7	52.3 ± 4	5.3 ± 0.3
HSH(PA–PVP)	9.6 ± 3	34.1 ± 5.3	128.4 ± 26	57 ± 13.5	3.5 ± 0.2

3.3.3. Powder density and cohesivity

All PA–PVP mixtures showed lower bulk and tap densities, higher cohesivities (1/*b*), and higher *CI* values than commercial PA (Table 4). The reductions in bulk and tap densities as well as the increases in cohesivity of PA–PVP mixtures when compared with PA showed increasing

trends with increasing mixing energy during dry mixing (LS < MS < DHS), although the bulk density, tap density, and cohesivity of the mixtures prepared using LS and MS conditions were not statistically different (p > 0.05) (Table 4). The mixtures prepared using wet mixing conditions (WHS and HSH) showed further reductions in bulk density (63.0% and 58.6% for WHS and HSH, respectively) as well as increases in cohesivity (197.1% and 487.1% for WHS and HSH, respectively) when compared with the original commercial PA powder (Table 4). The reduction in bulk density was previously shown to result in an increase in the tensile strength of tablets (Nokhodchi, Maghsoodi, Hassan-Zadeh, & Barzegar-Jalali, 2007; Zuurman, Riepma, Bolhuis, Vromans, & Lerk, 1994). The reductions in the bulk and tap densities for the mixtures prepared using low energy mixing conditions compared with commercial PA were caused by the presence of 5% (*w/w*) PVP powder, whose bulk and tap density values are less than those of commercial PA. The reductions in bulk and tap densities for the powders prepared using high energy conditions compared with mixtures prepared using low energy conditions were caused by their considerably smaller particle sizes (Table 3). This led to substantial increases in the strength of the interparticle forces as reflected by higher cohesivity values (Table 4).

Commercial PA powder showed free-flowing noncohesive behaviour (*CI*: 3.2% ± 0.3%) (Table 4). Such powders are not very compressible during the consolidation process because they will consolidate before

tapping because of weak interparticle forces. Consistent with the patterns in the bulk and tap density changes, all PA–PVP mixtures showed higher CI values than commercial PA (Table 4), indicating their poor flow properties. The mixtures prepared using high energy conditions demonstrated notably poor flowabilities than those prepared using low energy conditions as indicated by their considerably higher *CI* values (42.3% ± 2.1% to 46.3% ± 1% versus 8.3% ± 1% to 9% ± 0%) (Table 4). This provides further evidence for their stronger interparticle forces, which are attributable to their lower VMDs (Table 3) (Kaialy, Alhalaweh, Velaga, & Nokhodchi, 2012). These powders were highly compressible because of strong interparticle cohesive forces that produced inefficient packing and high voidage. The structures of such cohesive powders collapse considerably during consolidation, which is revealed as a large reduction in the volume of the powder bed.

Product	D_b (g/cm^3)	D_t (g/cm^3)	1/*b*	*CI* (%)	Flow character
PA	0.8 ± 0	0.8 ± 0	4 ± 0	3.2 ± 0.3	Excellent (*CI* <10%)
PVP	0.4 ± 0	0.5 ± 0	8 ± 3.3	22 ± 2.5	Fair 16<*CI*<*23%*
DHS(PA)	0.3 ± 0	0.6 ± 0	27 ± 2.3	45 ± 0.1	Extremely poor (*CI* >38%)
LS(PA–PVP)	0.7 ± 0	0.8 ± 0	9 ± 2.5	9 ± 0	Excellent (*CI* <10%)
MS(PA–PVP)	0.7 ± 0	0.8 ± 0	11 ± 1.2	8.3 ± 1	Excellent (*CI* <10%)
DHS(PA–PVP)	0.3 ± 0	0.5 ± 0	28 ± 8.3	42.3 ± 2.1	Extremely poor (*CI* >38%)
WHS(PA–PVP)	0.3 ± 0	0.5 ± 0	12 ± 0	43 ± 0	Extremely poor (*CI* >38%)
HSH(PA–PVP)	0.3 ± 0	0.6 ± 0	24 ± 13	46.3 ± 1	Extremely poor (*CI* >38%)

Table 4. Bulk density (D_b), tap density *(D_t)*, cohesivity (1/*b*), and Carr index (CI) for commercial paracetamol (PA), commercial polyvinylpyrrolidone (PVP), and PA–PVP mixtures (5% PVP, *w/w*) prepared using, low shear (LS), medium shear (MS), dry high shear (DHS), wet high shear (WHS) and high-speed homogenization (HSH) mixing conditions and PA processed using high shear mixing in the absence of PVP (DHS(PA)).Data expressed as mean ± SD, *n* = 3.

3.3.4. Solid-state properties

Commercial PA and all PA–PVP mixtures exhibited comparable, sharp, characteristic diffraction angles of 12.10°, 13.83°, 15.5°, 16.7°, 18.29°, 20.4°, and 24.40° 2θ corresponding to the monoclinic form of PA (Figure 10) (Khanmohammadi, Garmarudi, Moazzen, & Ghasemi, 2010; Di Martino et al., 1996). The absence of high reflections at 10.35°, 21.85°, and 24.03° 2θ (Khanmohammadi *et al*., 2010; Di Martino *et al*., 1996) from the PXRD patterns of all PA–PVP mixtures ruled out the transformation of the monoclinic form to the orthorhombic form, which is less stable than the monoclinic form and thus unsuitable for scaling up (Beyer *et al*., 2001). This indicated that the initial crystalline state of commercial PA is retained for all PA–PVP mixtures regardless of the mixing method. This is advantageous because it warrants the long-term physical stability of all mixtures during storage and allows direct comparative evaluation of the PA products. The high crystallinity of PA could be attributed to its relatively low glass transition temperature (23–25 °C) (Sibik, Sargent, Franklin, & Zeitler, 2014).

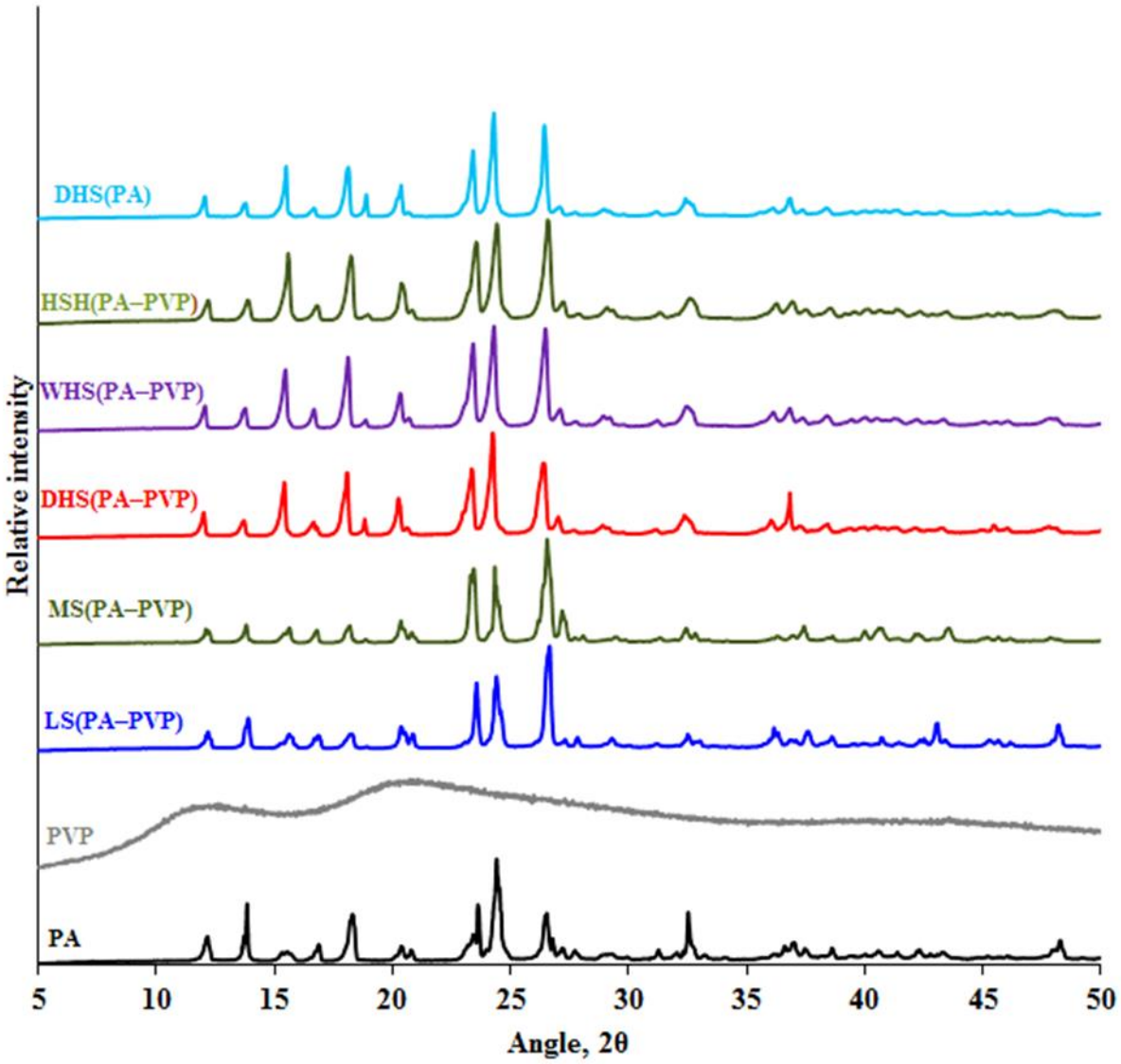

Figure 10. Powder X–ray diffraction (PXRD) patterns of commercial paracetamol (PA), commercial polyvinylpyrrolidone (PVP), and PA–PVP mixtures (5% PVP, *w/w*) prepared using, low shear (LS), medium shear (MS), dry high shear (DHS), wet high shear (WHS) and high-speed homogenization (HSH) mixing and PA processed using high shear mixing in the absence of PVP (DHS(PA)).

The FT–IR characteristic bands of the monoclinic form of PA (Table 5) were present in the spectra of commercial PA and all PA–PVP mixtures

(Figure 11). The diagnostic bands of the PA orthorhombic form (C–C aromatic stretching peaks at 1614, 1507, 1626, 1513, and 1453 cm^{-1}) (Al-Zoubi, Koundourellis, & Malamataris, 2002) were absent from the spectra of commercial PA and all PA–PVP mixtures, confirming the purity of the PA monoclinic form for all products under investigation. Analysis of the molecular structures of PA and PVP (Figure 1; Table 5) suggests that H-bonding may exist between the N–H or O–H moieties (H donors) of PA and the carbonyl group (C=O, H acceptor) of PVP. Such intermolecular interactions should be reflected by shifts in the N–H, O–H, and C=O stretches. The mixtures prepared using low energy conditions showed insignificant changes in absorption intensities in comparison to neat commercial PA (Figure 11), indicating a low level of interparticle interaction. The mixtures prepared using dry high shear (DHS) conditions showed minor reductions in absorption intensities (i.e., increased band broadening) between 3300 and 3350 cm^{-1} as well as between 3100 and 3200 cm^{-1} compared with the peaks observed for commercial PA (Figure 11). The band broadening became more pronounced for the mixtures prepared using wet high energy conditions (WHS and HSH) (Figure 11). This indicated a higher level of intermolecular hydrogen bonding between PA and PVP in the mixtures prepared using high energy conditions than those prepared using low energy conditions. In addition, the mixtures prepared using wet high energy (WHS and HSH) conditions showed decreases in the absorption intensities between 1640 and 1660 cm^{-1} (amide I, carbonyl stretch), between 1600 and 1620 cm^{-1} (skeletal aryl

C–C stretch) between 1560 and 1570 cm^{-1} (amide II, N–H in plane deformation), and between 1500 and 1520 cm^{-1} (aryl C=H, C=H symmetric bending). Such reductions in the absorption intensities indicate the presence of weak hydrophobic interactions between PA and PVP. Therefore, the FT–IR spectra indicated that hydrogen bonding and other types of weak hydrophobic interactions are more likely to occur in PA–PVP mixtures prepared using wet high energy mixing conditions (WHS and HSH), followed by minimal interactions observed in the mixture prepared using dry high energy (DHS) condition, and no interactions in the mixtures prepared using low energy conditions. Therefore, it is likely that the level of interparticle interactions between PA and PVP in a mixture depends on the energy (i.e., magnitude of shear/inertial forces) introduced during mixing. Higher shear forces introduced during mixing results in higher levels of PA–PVP interaction. This is probably because the increase in shear forces during mixing presses the PVP particles into the host PA particle surfaces.

Table 5. Chemical structure and characteristic FT-IR absorption bands of monoclinic paracetamol (PA) and polyvinylpyrrolidone (PVP).

Compound		Characteristic FT-IR absorbance bands (cm^{-1})	Reference
PA		3326 (associated N–H stretch), 3162 (H-bonded O–H stretch), 1654 (amide I, carbonyl stretch), 1610 (skeletal aryl C–C stretch), 1565 (amide II, N–H in plane deformation), 1507 (aryl C=H, C=H symmetric bending).	Moynihan and O'Hare (2002)
PVP	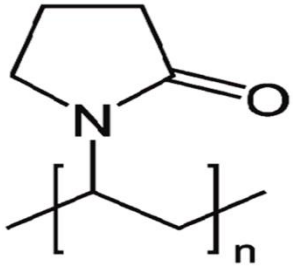	3469 (O–H stretching), 1698 (pyrrolidone group C=O stretching), 2987 (C–H asymmetric stretching-CH_2), 1427 (C–H bending), 1260 (C–N stretching), 931 (C–C stretching)	Sivaiah *et al*. (2011)

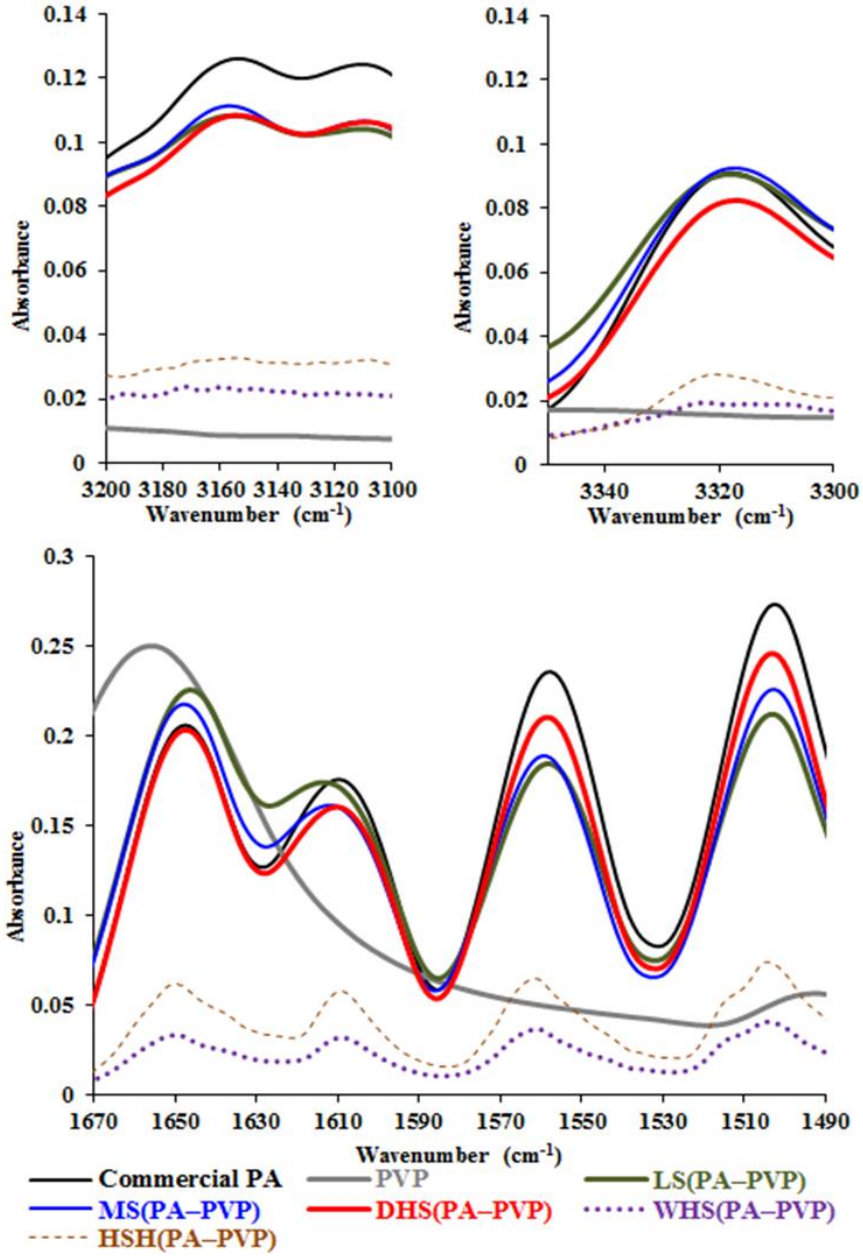

Figure 11. Fourier transform infrared (FT−IR) absorption spectra of commercial paracetamol (PA), commercial polyvinylpyrrolidone (PVP), and PA–PVP mixtures (5% PVP, *w/w*) prepared using, low shear (LS), medium shear (MS), dry high shear (DHS), wet high shear (WHS) and high-speed homogenization (HSH) mixing conditions.

The TGA curves of commercial PA and PA–PVP mixtures showed weight loss in the temperature range between 170 and 255 °C, corresponding to melting of the stable monoclinic form (de Oliveira *et al*., 2017) then there was a significant rapid weight loss due to degradation (Hughey, Keen, Brough, Saeger, & McGinity, 2011) (Figure 12). PVP showed weight loss that started at about 340 °C, implying that weight loss was caused by thermal degradation (i.e., thermal decomposition of PVP molecular chains). No weight loss occurred below 100 °C (Figure 12), indicating the absence of a significant amount of free (surface) water in all mixtures. A slight shift towards lower melting onsets was observed for the mixtures prepared using high energy conditions when compared with the mixtures prepared using low energy conditions (Figure 12). This difference may be attributable to their starkly different physical properties such as their considerably lower VMDs (Table 5) and/or because of the interaction between PA and PVP. Smaller particles could have slightly lower melting points than larger particles of the same material because of lower resistance to heat transfer (Kaialy *et al*., 2012).

The moisture content was measured in all mixtures under investigation. This is because the moisture content of a powder affects powder flowability through interparticle forces including capillary forces and liquid bridging (Leuenberger & Imanidis, 1986). The presence of water could also affect the particle surface microstructure by a dissolution–precipitation process (Finot, Lesniewska, Mutin, Hosain, &

Goudonnet, 1996), potentially affecting the mechanical properties of the particles exposed to high relative humidity. The results of the present study showed that commercial PA and all PA–PVP mixtures gained negligible amounts of moisture (< 0.7%, *w/w*) when stored at 75% RH (22°C) for six months, confirming their low hygroscopicity and potential for excellent stability.

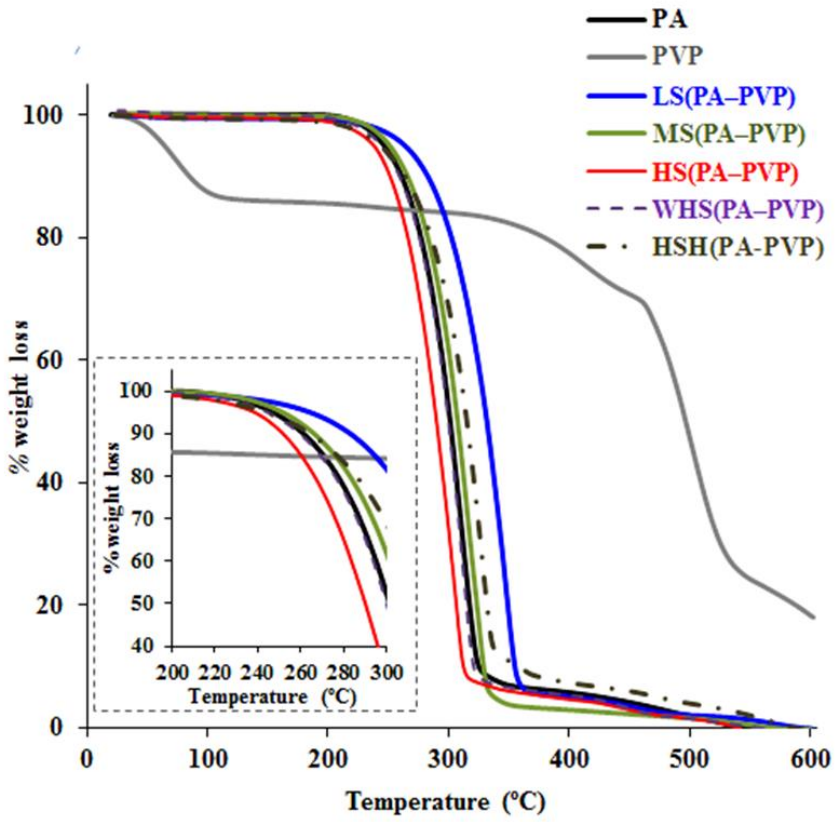

Figure 12. Thermogravimetric analysis curves of commercial paracetamol (PA), commercial polyvinylpyrrolidone (PVP), and PA–PVP mixtures (5% PVP, w/w) prepared using, low shear (LS), medium shear (MS), dry high shear (DHS), wet high shear (WHS) and high-speed homogenization (HSH) mixing conditions.

3.3.5. Tableting properties

Commercial PA showed poor mechanical properties, with the highest TS of only 0.18 ± 0.02 MPa at a compression pressure of 148 MPa. However, the mechanical properties of the commercial PA (TCI Chemicals, UK) investigated in this study were better than those for a previously reported commercial PA (Sigma–Aldrich, Gillingham, UK) (Kaialy *et al.*, 2014), which achieved no TS at all compression pressures. Such improved character could be attributed to morphological differences between these two commercial grades. While Sigma–Aldrich PA particles showed an elongated (needle) habit (Kaialy *et al.*, 2014), the TCI Chemicals product had particles with subangular, polyhedral shapes with relatively flat surfaces (Figure 9). These could have increased interparticle contact points and thus increased the degree of densification during compression. The presence of 5% (*w/w*) PVP as an additive improved the mechanical properties of paracetamol in all PA–PVP mixtures (Figure 13). For example, the TS of PA–PVP mixture compressed at 222 MPa was 0.5 ± 0.0 MPa, 1.4 ± 0.1 MPa, 1.9 ± 0.2 MPa, and 3.2 ± 0.2 MPa for the mixtures prepared using LS/MS, DHS, WHS, and HSH conditions (Figure 13). PA–PVP mixtures prepared using low energy conditions exhibited statistically similar ($p > 0.05$) tabletability profiles, whereas the mixture prepared using DHS conditions exhibited a remarkable improvement in tabletability compared with the mixtures prepared using LS and MS conditions. For example, with the compression pressure increasing from 37 to 222 MPa, the TS of tablets increased from 0.1 to 0.4 MPa and from

0.2 to 1.4 MPa for the mixtures prepared using LS/MS and DHS conditions, respectively (Figure 13). This indicated that the DHS conditions resulted in an increase in the TS of tablets from 1.8 to 3.5 times compare with the LS/MS conditions over the compression pressure range of 37 to 222 MPa. The mixtures prepared using wet high energy conditions (WHS and HSH) clearly exhibited further improvements of tabletability in comparison to the mixtures prepared using dry high shear (DHS) conditions. For example, when the compression pressure increased from 37 to 222 MPa, the TS of tablets prepared using WHS increased from 0.4 ± 0.1 MPa to 1.8 ± 0.3 MPa, while that prepared using HSH increased from 1.3 ± 0.1 MPa to 3.0 ± 0.2 MPa (Figure 13). It is therefore clear that the PA–PVP mixture prepared using HSH conditions showed the best compression properties among the mixtures under investigation, scoring a TS of 2.9 ± 0.1 MPa at a compression pressure of 148 MPa. Compared with the mixtures prepared using low energy conditions, the mixtures prepared using HSH gave tablets that were ~8–14 times stronger under the compression pressure range of 37 to 222 MPa. The improved tabletability for PA–PVP mixtures compared with commercial PA was caused by the combination of a brittle (PA) and plastic (PVP) material (Larhrib & Wells, 1998). The increased tensile strengths of the tablets containing mixtures prepared using high energy conditions compared with those mixed using low energy conditions are indicative of stronger interparticle bonding for the former products. Such superior tabletability is attributed to the higher level of PA–PVP interaction via hydrogen bonding

in the case of the mixtures prepared using high energy conditions (Figure 11). In addition, in contrast to the mixtures prepared using low energy mixing conditions, in which the morphologies of both commercial PA (subangular/polyhedral) and commercial PVP (hollow spherical) particles could be observed (Figure 9), no distinct individual commercial PVP particles were visualized in mixtures prepared using high energy conditions (Figure 9). This indicated that the low energy mixing conditions were unable to provide sufficient energy to extensively delaminate and spread PVP onto PA surfaces. In contrast, high energy mixing conditions caused attrition, corrosion, and compressive coating of PVP onto PA surfaces, or a combination of the foregoing effects. It is assumed that one contributor to the superior tableting performance of monoclinic PAs mixed with PVP using high energy conditions (compared with use of low energy conditions) must be the increased surface coating of plastic PVP wrapping the fragmenting PA. Vanhoorne, Peeters, Van Snick, Remon, and Vervaet (2014) indicated that the presence of amorphous lactose is crucial for the production of co–processed powders with improved mechanical properties. Although the PA–PVP mixture prepared in this study using HSH contained no amorphous lactose (Figure 13), its tabletability behavior outperformed that of the spray-dried formulation (75% paracetamol, 5% PVP, and 20% amorphous lactose) reported by Vanhoorne *et al*. (2014) (maximum TS of 1.9 MPa at a compression pressure of 288 MPa). The absence of amorphous products in the mixtures prepared in this study make them potentially more stable in the

long term than the formulations prepared by Vanhoorne *et al*. (2014). The tableting behaviour of PA processed using high shear mixing in the absence of PVP was as poor as commercial PA. Such results confirm that improvement in the PA mechanical properties was because of a higher level of PA–PVP interaction induced by high energy mixing, and not caused by a particle size reduction effect.

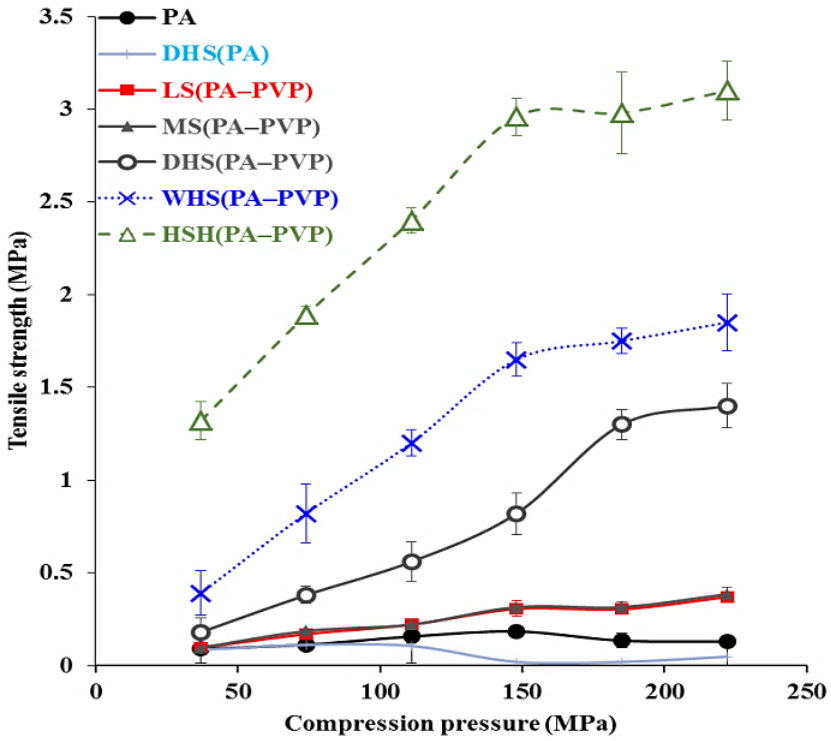

Figure 13. Tensile strength (mean ± SD, *n* = 5) versus compression pressure of commercial paracetamol (PA), commercial polyvinylpyrrolidone (PVP), and PA–PVP mixtures (5% PVP, *w/w*) prepared using, low shear (LS), medium shear (MS), dry high shear (DHS), wet high shear (WHS) and high-speed homogenization (HSH) mixing conditions and PA processed using high shear mixing in the absence of PVP (DHS(PA)).

3.4. Conclusions

The effects of mixing conditions on the micrometric and mechanical properties of PA–PVP mixture should not be ignored. In contrast to low energy mixing conditions, high energy mixing conditions promoted hydrogen bonding between PA and PVP with following improvements in the mechanical properties of the resultant mixtures. High energy mixing conditions were therefore successfully applied to produce PA with improved tensile strength in the presence of 5% (*w/w*) PVP additive. This method should have general applicability to many poorly compactible drug entities.

Cooperative research and development between mixing equipment providers and pharmaceutical manufacturers is required in the future to optimize the quality of interactive mixtures for tableting. Future studies should also concentrate on the application of various mixing methods to improve the functional properties of a wide range of drugs including chemical drugs and Chinese drugs and herbal extracts that are prepared using direct compression.

4 CHAPTER 4: EFFECT OF VARIOUS PREPARATION METHODS ON PARACETAMOL–POLYVINYLPYRROLIDONE MIXTURES

4.0. Introduction

Crystallisation has been referred to as an art rather than a science. The primary objective of crystallisation systems engineering is to develop an advanced understanding of its phenomena, enabling the efficient bulk processing of high–quality crystalline products. Crystallization in many industries is the most common way of production of high–value chemicals, with high purity and desired size and shape (Nowee *et al*., 2007), and it has been used over the past years as a particle engineering method to enhance the physicochemical properties of poorly compactible drugs (Garekani *et al*., 2000 a & b; Abioye *et al*., 2016). Crystallization process can be carried out using many methods including; cooling crystallisation (Joiris *et al*., 1998), antisolvent crystallisation (Kaialy *et al*. 2014), spray drying (Vanhoorne *et al*., 2014; Sagechi *et al*., 2004), co–spray drying (Vanhoorne *et al*. 2016; Gonnissen *et al*. 2008), modified polymorphic forms (Martino *et al*., 1996) and particle shape modification (Rasenack & Müller 2002; Kaialy *et al*. 2014) which were discussed in (Section 1.3.0). However, none of the authors has compared the tabletability properties of PA to PA–PVP mixtures using all at once the engineering techniques which includes: Physical mixing, cooling crystallisation, solvent evaporation, Freeze drying and milling.

Since many APIs possess poor tableting properties, co–processing methods will be very prevalent and invaluable in the presence of 5%(*w/w*) binder/polymer polyvinylpyrrolidone (PVP) incorporated in the formulation to improve the manufactured tablets' properties.

In this investigation, the tabletability properties of commercial PA will be compared to the mixtures of PA–PVP engineered using different preparation methods.

4.1. Engineering of PA–PVP formulations

4.1.1. Physical mixing

PA and PVP (95:5 *w/w*) powders were mixed using low shear mixing method as described in (Section 2.2.1.1).

4.1.2. Batch cooling crystallisation

25% *w/v* solution was prepared by dissolving 25 g of PA–PVP mixture in a hydro–alcoholic solution of (125 mL of ethanol and 375 mL) of deionised water) for a final volume of 500 mL under stirring (200 rpm) at 70 ºC. The resultant clear solution was left uncovered in laboratory conditions for seven days using batch cooling crystallisation method as described in (Section 2.2.1.4). The crystals obtained were sieved using the technique described in (Section 2.3).

4.1.3. Solvent evaporation (SE)

25% *w/v* solution was prepared by dissolving 25 g of PA–PVP mixture in a hydro–alcoholic solution of (125 mL of ethanol and 375 mL of deionised water) for a final volume of 500 mL under stirring (200 rpm) at 70 ºC. The solvents present were evaporated using Stuart heat–stirrer for 1h at a constant temperature of 70 ºC. The precipitated crystals obtained were left to dry using solvent evaporation method as described in (Section

2.2.1.5). The engineered powders were sieved as described in (Section 2.3).

4.1.4. Freeze drying

25% *w/v* solution was prepared by dissolving 25 g of PA–PVP mixture in a hydro–alcoholic solution of (125 mL of ethanol and 375 mL of deionised water) for a final volume of 500 mL under stirring (200 rpm) at 70 ºC. The resultant clear solution containing PA–PVP mixtures obtained was allowed to cool down and was frozen at –20 ºC, for two days then was freeze dried using the technique described in (Section 2.2.1.6). The FD (PA–PVP) formulations were sieved using the technique described in (Section 2.3).

4.1.5. Milling (PA–PVP)

PA–PVP powders (25 g *w/w*) were milled for five mins using the milling method as described in (Section 2.2.1.7).

4.1.6. Tablet preparation

Each tablet weighs 526.3 mg ± 0.5 mg for the various formulations and 500 mg ± 0.5 mg for PA compressed using the method described in (Section 2.14).

4.2. Results and discussions

4.2. 1. Content uniformity

The percentage drug content uniformity obtained from all PA–PVP mixtures was acceptable (LS, 100.6% ± 5.9%; BCC 94.8.% ± 3.8%; SE, 106.5% ± 5.9%; FD, 95.6% ± 5.1% and ML, 105.2% ± 5.8%). The %CV of PA content varied with (LS, 5.8%; BCC, 4.1%; SE, 5.3%; FD, 5.8% and ML, 5.3%) which falls in the adequate range which implies satisfactorily uniform PA content in all the mixtures using various preparation techniques.

4.2.2. Particle size distributions

Commercial PVP showed considerably smaller PSDs than commercial PA. PA–PVP mixture prepared using physical mixing showed statistically similar (P>0.05) VMD to commercial PA, whereas PA–PVP mixtures prepared using batch cooling, solvent evaporation, freeze-drying and milling showed considerably smaller PSDs compare to commercial PA (Table 6), as affirmed by SEM micrographs (Figure 14). The PSDs of PA–PVP mixtures showed the following descending rank order according to the preparing techniques: physical mixing > batch cooling > solvent evaporation > freeze–drying > milling (Table 6).

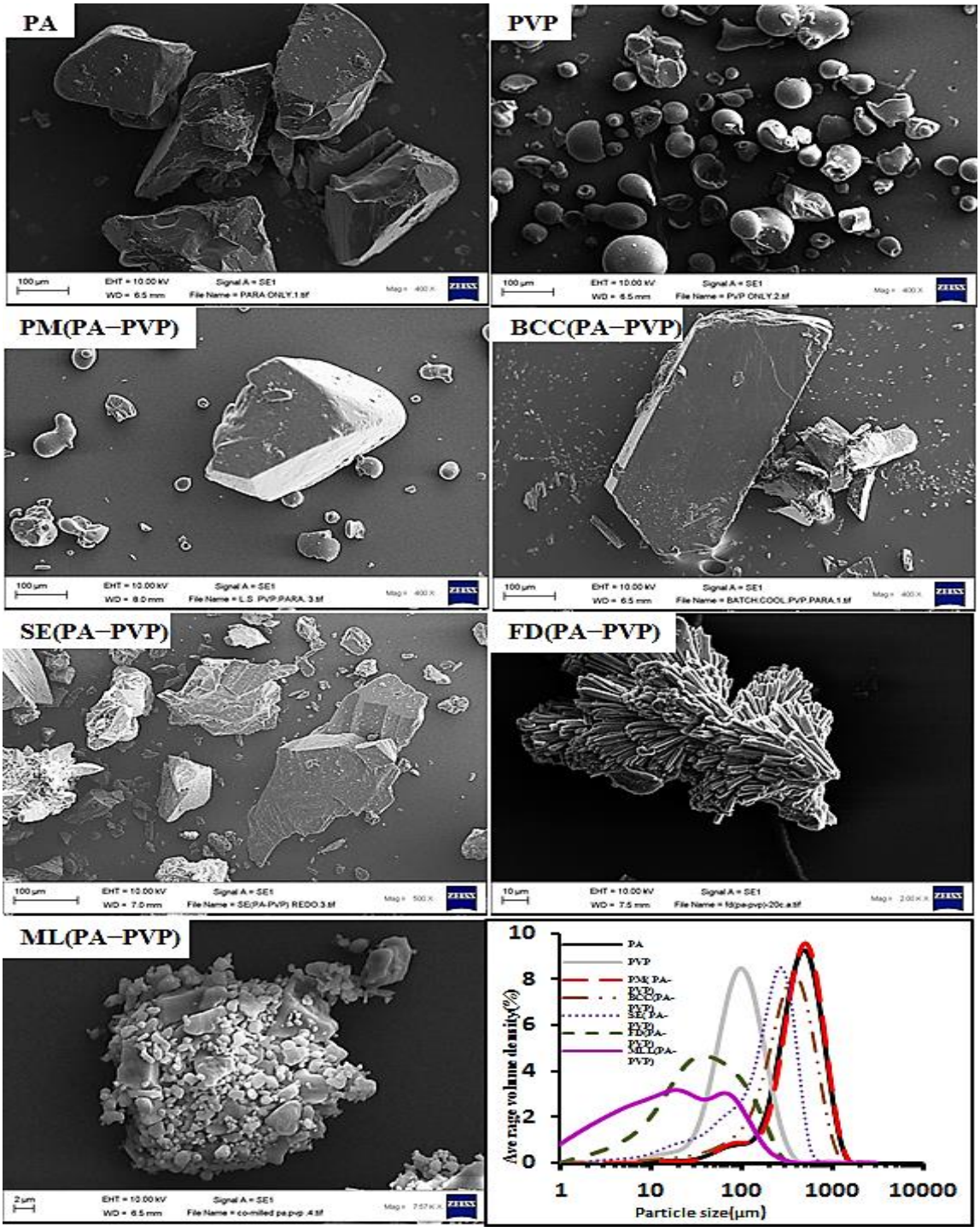

Figure 14. Scanning electron microscopy (SEM) and particles size distributions micrographs of commercial paracetamol (PA), commercial polyvinylpyrrolidone (PVP), and PA–PVP mixtures (95:5, *w*:*w*) co-processed by physical mixing (PM), batch cooling crystallisation (BCC), solvent evaporation (SE), freeze drying (FD), and milling (ML).

Across the mixtures investigated, the mixtures prepared using freeze−drying, and milling techniques showed a considerable reduction in their VMDs along with a significant increase in their span values indicating they are smaller and more heterogeneous in size distributions (Table 6). The significant reduction in PSDs in the case of freeze−dried PA−PVP mixture could be due to, the *in−situ* generation of intrinsic fine particles during the freezing drying process, whereas, in the case of milled PA−PVP mixture which is due to interparticle and particle−surface collisions and fracturing/attrition during milling, as evident by the reduction in $d_{10\%}$ values (Table 6). The generation of such fine particulates will have a significant influence on powder bulk properties (i.e. compactibilty, cohesivity, bulk density, flowability and tensile strength) as discussed later.

Product	$d_{10\%}$ (µm)	$d_{50\%}$ (µm)	$d_{90\%}$ (µm)	VMD (µm)	Span
PA	254 ± 22	506 ± 30	911 ± 39.3	548 ± 30.2	1.3 ± 0
PVP	42.1 ± 0.5	100.4 ± 1.1	209 ± 2	119.3 ± 4	1.7 ± 0
PM(PA−PVP)	181 ± 13	487 ± 14	899 ± 42	521 ± 24	1.5 ± 0
BCC(PA−PVP)	103 ± 0	348 ± 3	710 ± 12	383.3 ± 4	1.7 ± 0
SE(PA−PVP)	94.3 ± 6	212 ± 10.1	411 ± 36	219 ± 12	1.8 ± 0.2
FD(PA−PVP)	8.1 ± 0	38 ± 0.3	56 ± 1.3	81.3 ± 28.4	3.2 ± 0.1
ML(PA−PVP)	2.3 ± 0.1	17.3 ± 0.2	91 ± 2	35.3 ± 1.3	5.1 ± 0.1

Table 6. Particle size distribution (i.e. particle size at 10% ($d_{10\%}$), 50% ($d_{50\%}$, median diameter and 90% ($d_{90\%}$) volume distribution and span) (mean ± SD, n = 3) for commercial paracetamol (PA), commercial polyvinylpyrrolidone (PVP), and PA−PVP mixtures (95:5, w:w) co−processed by physical mixing (PM), batch cooling crystallisation (BCC), solvent evaporation (SE), freeze drying (FD), and milling (ML).

4.2. 3. Powder density and cohesivity

All PA−PVP mixtures displayed significantly lower bulk and tap densities, higher cohesivities and higher CI values than commercial PA (Table 7). The slight reductions in the bulk and tap densities for the mixture prepared using physical mixing technique compared to commercial PA are due to the presence of 5% (*w/w*) PVP powder whose bulk and tap density values are smaller than those of commercial PA (Table 7). The reductions in bulk and tap density, as well as the increase in cohesivity of PA−PVP mixtures compared to commercial PA (Table 7), are due to their smaller PSDs (Table 6). Interestingly, a direct relationship was established when plotting the bulk density of PA−PVP mixtures against their VMDs (Table 6), indicating that the bulk density (i.e. the porosity) of PA−PVP mixture powders decreased with decreasing their particle size. Commercial PA powder showed free–flowing no cohesive behaviour (CI: 3.2% ± 0.3%), (Table 7). Such powders are not very compressible during compaction because they will compact before tapping due to weak inter-particle forces. All PA− PVP mixtures showed higher CI values than commercial PA, which is consistent with the patterns observed for bulk and tap density changes (Table 7), indicating their relatively poorer flow properties. The mixtures prepared using freeze drying, and milling samples displayed exceptionally poor flowability as evident by their considerably high CI values (47.3% ± 1.1% and 40.0% ± 0.6% respectively (Table 7).

Table 7. Bulk density (D_b), tap density (D_t), cohesivity (1/*b*) and Carr's index (CI) (mean ± SD, n = 3) for commercial paracetamol (PA), commercial polyvinylpyrrolidone (PVP), and PA−PVP mixtures (95:5, *w*:*w*) processed by physical mixing (PM), batch cooling crystallisation (BCC), solvent evaporation (SE), freeze drying (FD), and milling (ML).

Product	D_b **(g/cm^3)**	D_t **(g/cm^3)**	**1/*b***	**CI (%)**	**Flow character**
PA	0.8 ± 0	0.8 ± 0	4 ± 0	3.2 ± 0.3	Excellent *CI* <10%
PVP	0.4 ± 0	0.5 ± 0	8 ± 3.3	22 ± 2.5	Fair 16 < *CI* <23
PM (PA−PVP)	0.7 ± 0	0.8 ± 0	9 ± 2.5	9 ± 0	Excellent *CI* <10%
BCC(PA−PVP)	0.7 ± 0	0.8 ± 0	15 ± 2.5	15 ± 0.6	Good *CI* <16%
SE(PA−PVP)	0.5 ± 0	0.6 ± 0	11.3 ± 2	22 ± 1.1	Fair 16 < *CI* <23%
FD(PA−PVP)	0.1 ± 0	0.3 ± 0	14 ± 1.5	47.3 ± 1.1	Extremely poor CI > 38%
ML(PA−PVP)	0.3 ± 0	0.5 ± 0	20.4 ± 3.5	40 ± 0.6	Extremely poor

4.2.4. Solid state properties

Commercial PA and all of the PA–PVP mixtures displayed PXRD characteristic angles at 2θ values of 12.10°, 13.83°, 15.5°, 16.7°, 18.29°, 20.4° and 24.40°, and FT–IR diagnostic bands at 3325 cm^{-1} (N–H stretching vibration), 3161 cm^{-1} (hydrogen–bonded, O–H stretching vibration), 1653 cm^{-1} (C=O stretching vibration), 1564 cm^{-1} (N–H in-plane bending), 1610 cm^{-1}, 1506 cm^{-1} and 1440 cm^{-1} (aromatic ring mode), and 1327 cm^{-1} (O–H, bending vibration), corresponding to the monoclinic form of paracetamol (form *I*) (Figure 15) (Nichols and Frampton, 1998; Di Martino *et al*.,1996; Wang *et al*., 2002). The absence of PXRD characteristic angles at 10.35º, 21.85º and 24.03º 2θ and FT–IR bands at 1658 cm^{-1}, 1558 cm^{-1}, 1440 cm^{-1}, 1240 cm^{-1}, and 837cm^{-1} from the PXRD patterns and FT–IR spectra in mixtures prepared using physical mixing, solvent evaporation, freeze–drying and milling ruled out the presence of the orthorhombic form (form *II*) (Di Martino *et al*., 1996; Moynihan and O'Hare, 2002) in the foregoing mixtures. However, the PA–PVP product prepared using batch cooling crystallisation showed mixtures of the monoclinic and the orthorhombic form, also, the orthorhombic form known to be relatively less stable than the monoclinic form. This indicated that the initial crystalline state of commercial PA is retained in all PA–PVP mixtures regardless of the processing method employed (Figure 16). Although, there was some difference in the relative intensity of the peaks which could be due to either the differences of the

size of the crystals or the alteration of the crystal habit because the relative abundance of the planes exposed to X–ray source is transformed (Garekani *et al*., 2001). PVP showed no detection of any prominent peak of the polymer, a characteristic of the amorphous state (Figure 16). The analysis of the molecular structures of PA and PVP shows that major H−bonding interactions may exist between the O–H stretch or the N–H stretch (strong H donors) of PA and the carbonyl group (C=O, strong H acceptor) of PVP. Such intermolecular interaction would be fed back by the change of shifts in the N–H stretch, O–H stretch and C=O stretch.

PA−PVP mixtures prepared using batch cooling crystallisation did not display remarkable changes in absorption intensities compared to the commercial PA (Figure 15), indicating insufficient miscibility to allow interaction. The PA−PVP mixture prepared using physical mixing showed minor reductions in absorption intensities (i.e. increased band broadening) between 3300 cm^{-1} and 3350 cm^{-1} as well as between 3100 cm^{-1} and 3200 cm^{-1} compared to the peaks observed with the commercial PA (Figure 15). The band broadening became more pronounced for the mixtures prepared using SE, FD and ML, indicating a higher level of intermolecular hydrogen bond interaction between PA and PVP in the preceding mixtures compared to the mixtures prepared using physical mixing and batch cooling crystallisation.

Additionally, PA–PVP co-processed using milling showed significant reductions in the absorption intensities between 1640 cm^{-1} and 1660 cm^{-1}

(due to amide I, i.e. carbonyl stretch), between 1600 cm^{-1} and 1620 cm^{-1} (skeletal aryl C–C stretch) between 1560 cm^{-1} and 1570 cm^{-1} (amide II, N–H in–plane deformation), and between 1500 cm^{-1} and 1520 cm^{-1} (due to aryl C=H, C=H symmetric bends). Such reductions in the absorption intensities indicate the presence of weak hydrophobic interactions between PA and PVP.

Therefore, the FT–IR spectra indicated that hydrogen bonding and other types of weak hydrophobic interactions are more likely to occur according to the following rank order based on the technique by which PA and PVP were co–processed: Batch cooling crystallisation < Physical mixing < Solvent evaporation < Freeze–drying <Milling. This could be because milling affords a higher level of interparticle interactions between PA and PVP than the other techniques under investigation due to higher magnitude of shear/inertial forces introduced during mixing caused by particle–particle and particle–surface collisions which can press PVP particles into the host PA particle surfaces, as evident by SEM micrographs.

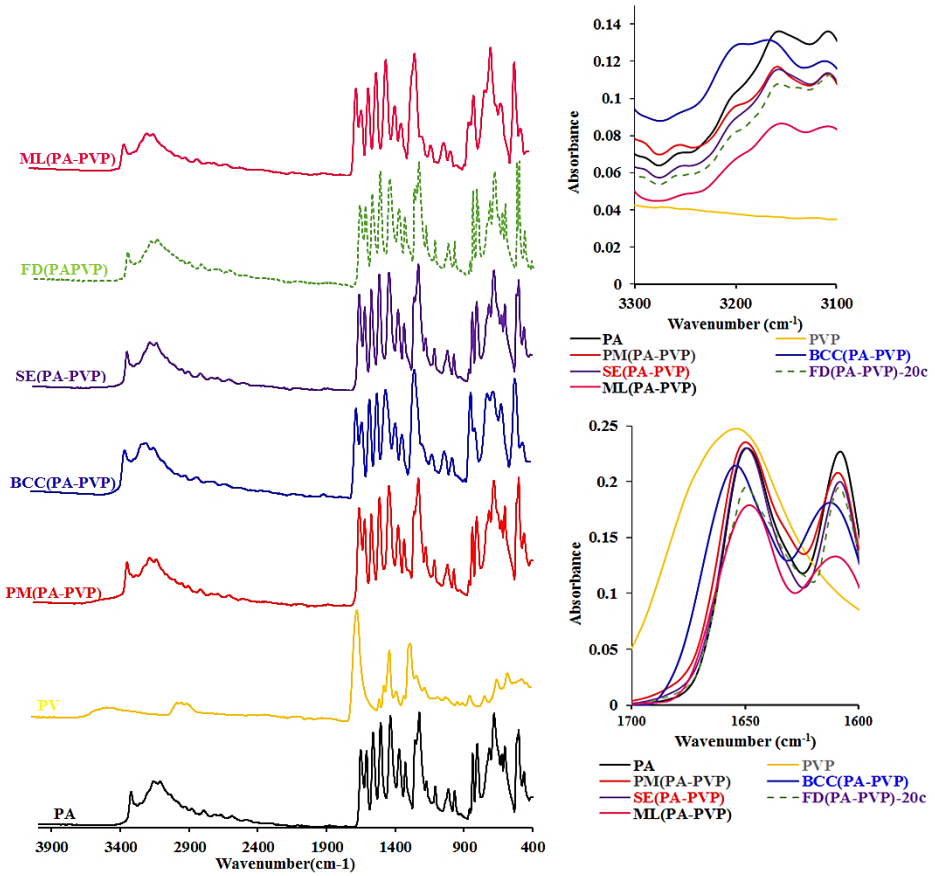

Figure 15. Fourier transform infrared spectroscopy (FT–IR) spectra of commercial paracetamol (PA), commercial polyvinylpyrrolidone (PVP), and PA–PVP mixtures (95:5, *w*: *w*) co–processed by physical mixing (PM), batch cooling crystallisation (BCC), solvent evaporation (SE), freeze drying (FD), and milling (ML) (%A: % Absorbance).

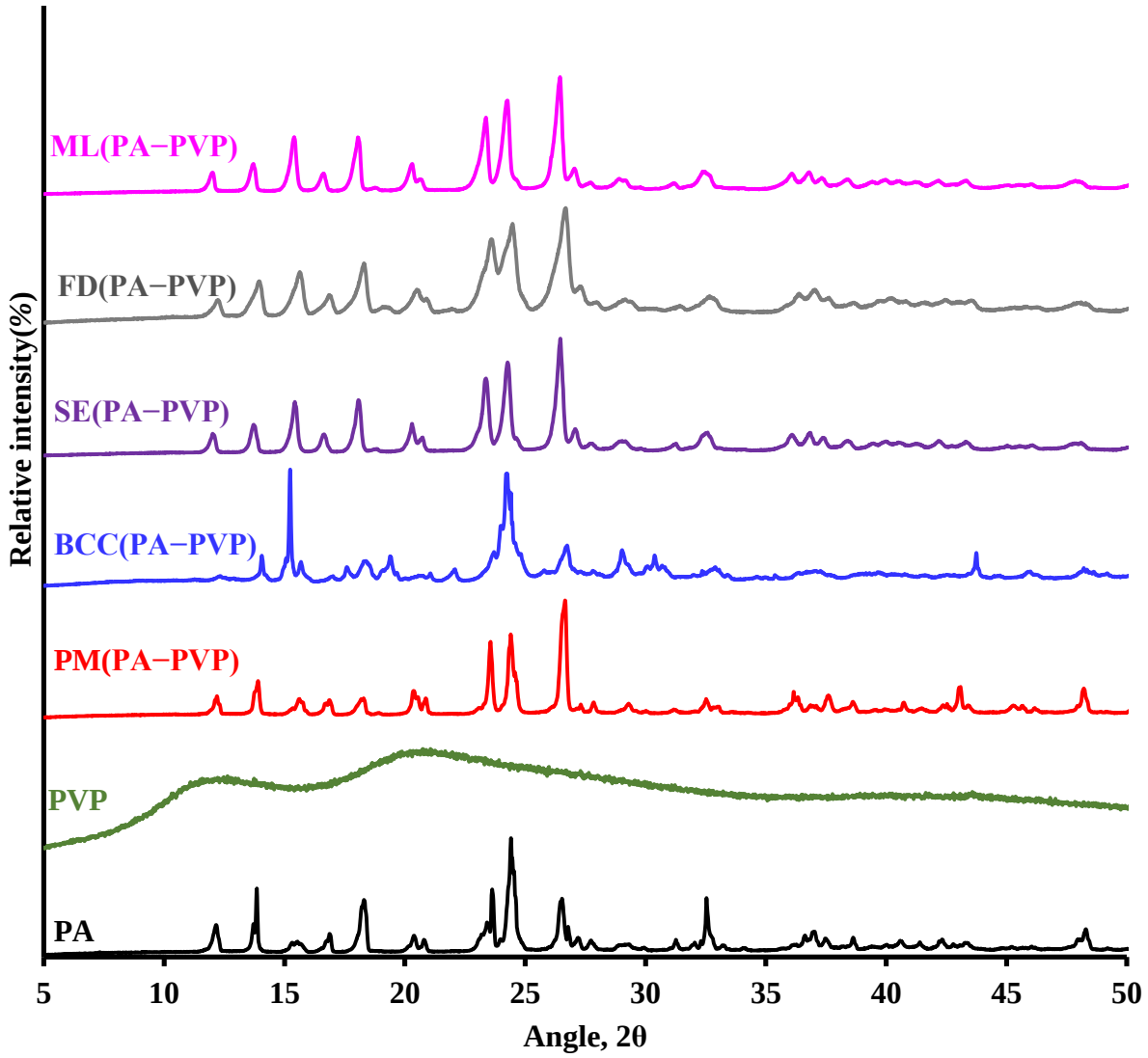

Figure 16. Powder X–ray diffraction (PXRD) patterns of commercial paracetamol (PA), commercial polyvinylpyrrolidone (PVP), and PA–PVP mixtures (95:5, *w: w*) co-processed by physical mixing (PM), batch cooling crystallisation (BCC), solvent evaporation (SE), freeze drying (FD), and milling (ML).

TGA analysis showed commercial PA and PA–PVP mixtures processed via physical mixing, batch cooling crystallisation, solvent evaporation, freeze drying, and milling were thermally stable until 254 ºC ± 2 ºC, which agrees with degradation temperatures results reported previously for PA (Tomassetti *et al*., 2005).

A slight shift towards lower melting onsets was observed for the PA–PVP mixture processed via freeze–drying, which could be attributed to the highly porous nature and the smaller PSDs of the freeze–dried PA–PVP formulation that can potentially lead to relatively lower resistance to heat transfer in comparison to PA–PVP mixture formulations prepared by other methods. Commercial PVP began to decompose at temperatures above 126 °C.

No significant weight loss was observed at temperatures below 100 °C for all samples (Figure 17) ruling out the presence of surface (free) water in all products under investigation as confirmed by their Karl fisher results which showed the water content in all the mixtures to be lower than 1% (Table 8).

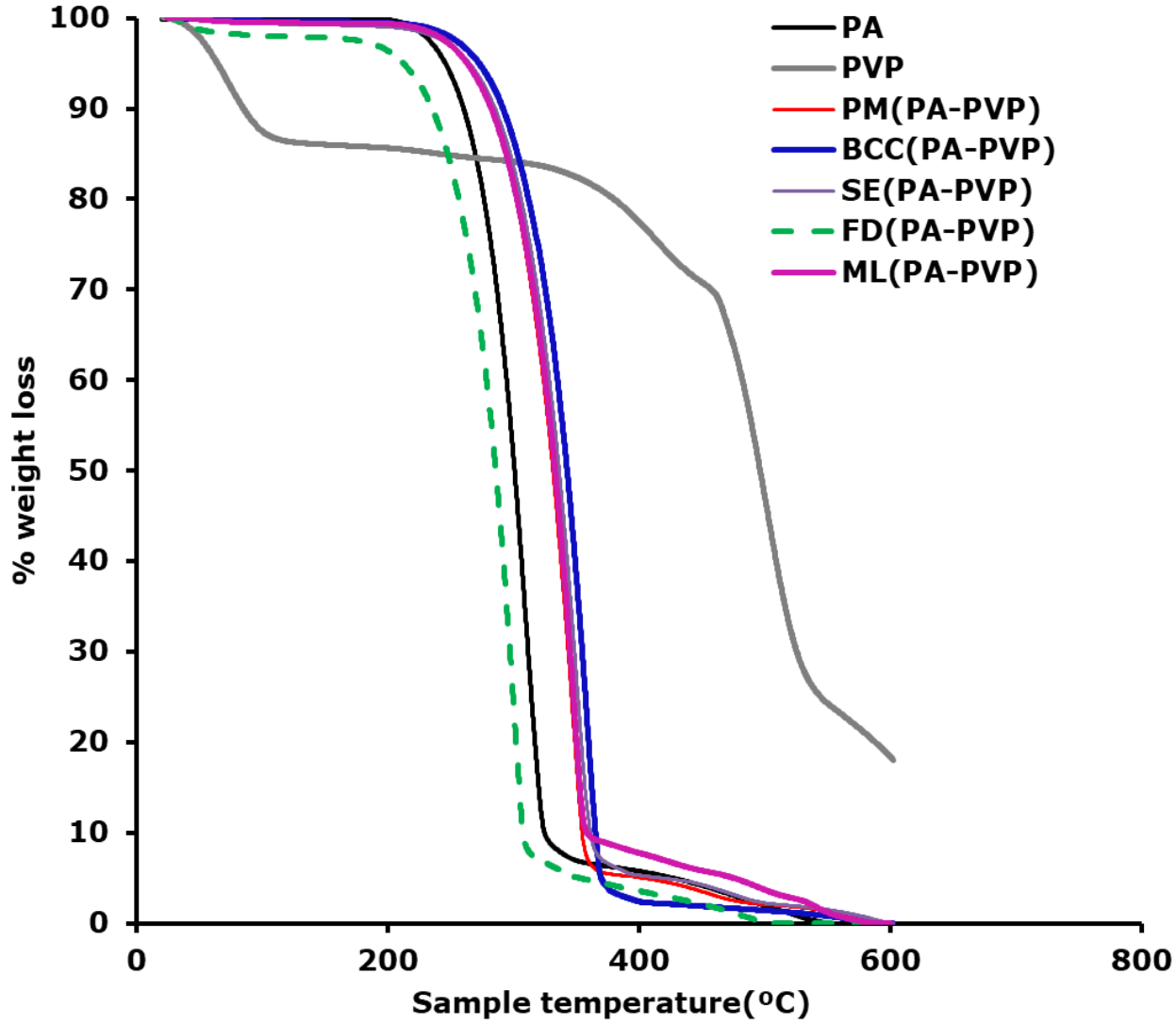

Figure 17. Thermogravimetric analysis (TGA) profiles of commercial paracetamol (PA), commercial polyvinylpyrrolidone (PVP), and PA–PVP mixtures (95:5, *w*:*w*) co–processed by physical mixing (PM), batch cooling crystallisation (BCC), solvent evaporation (SE), freeze drying (FD), and milling (ML).

Table 8. Water content of commercial paracetamol (PA), commercial polyvinylpyrrolidone (PVP), and PA–PVP mixtures (95:5, *w: w*) co-processed by physical mixing (PM), batch cooling crystallisation (BCC), solvent evaporation (SE), freeze drying (FD), and milling (ML).

Product	Moisture content (%)
PA	0.17 ± 0.0
PVP	6.62 ± 0.0
PM(PA–PVP)	0.73 ± 0.3
BCC(PA–PVP)	0.17 ± 0.1
SE(PA–PVP)	0.50 ± 0.0
FD(PA–PVP)	0.57 ± 0.0
ML(PA–PVP)	0.7 ± 0.1

4.2.5. Tableting properties

Commercial PA displayed poor mechanical properties, with the highest TS of only 0.18 ± 0.02 MPa at a compression pressure of 148 Mpa (Figure 18) like that obtained by (Agbor Rose and Kaialy, 2019). In comparison to commercial PA, the addition of PVP regardless of the method utilised showed an increase in tabletabilty of the PA–PVP mixtures (Figure 18). The TS of the mix of PA–PVP processed using different techniques compressed at 222 MPa was 0.4 ± 0.0 MPa, 0.4 ± 0.0 MPa, 1.2 ± 0.1 MPa, 3.4 ± 0.0 MPa and 4.1 ± 0.1 MPa for mixtures prepared using PM,

BCC, SE, FD and ML method (Figure 18). PA–PVP mixtures using PM and BCC method were not statically different (P>0.05) tabletability profiles, whereas, the mixture prepared using SE methods exhibited a notable improvement in tabletability compare to the mixtures prepared using PM and BCC (Figure 18).

For example, as the compression pressure increased from 37 MPa to 222 MPa, the TS tablets increased from 0.1 to 0.4 MPa, 0.2 to 0.4 MPa and from 0.3 to 1.2 MPa for the mixtures prepared using PM, BCC and SE methods correspondingly (Figure 18), indicating that the SE method resulted in an increase in the tensile strength of tablets in comparison to PM and BCC over the compression range of 37 MPa to 222 MPa .The mixtures prepared using FD and ML exhibited a further increase of tabletability compared to the mixtures prepared using the SE technique. When the compression pressure increased from 37 MPa to 222 MPa, the TS of tablets prepared using FD increased from 0.9 ± 0.0 MPa to 3.4 ± 0.0 MPa. Meanwhile, the PA–PVP mixture obtained using milling method increased from 0.4 ± 0.1 MPa to 4.1 ± 0.1 MPa (Figure 18). PA–PVP mixtures prepared using ML displayed the best compression properties among the combinations in this study, with a TS of 4.1 ± 0.1 MPa at a compression pressure of 222 MPa. In contrast to the other techniques applied, the mixtures prepared using ML achieved stronger tablets under compression pressure range of 37 MPa to 222 MPa.

The increased tensile strengths of the tablet mixtures prepared using FD and ML techniques compared to those prepared using (PM, BCC and SE) could be due to their differences in crystal habits (Figure 14), because crystal shape, through its effects on the relative alignment of crystallites throughout compression can impact compaction profiles (Higuchi *et al*., 1963; Celik, 2011). Moreover, Sun and Hou, (2008); Chow *et al*., 2014 showed that the formation of flat hydrogen–bonded layers or stacking hydrogen–bonded columns in the crystal structure could improve the tableting performance of poorly compressible powders.

The high content of fine particulates of the mixtures prepared using ML compared to (BCC and SE) could also contribute to the increased cohesive inter−particulate forces between PA and PVP (Table 6 & 7) (Kaialy *et al*.,2016) leading to the increased degree of particle deformation, densification and magnitude and extent of bond formation during compaction (Kaialy, 2016). The tabletability profile (Figure 18) of the co−processed PA−PVP mixture prepared using ML technique demonstrated a far better tensile strength (TS) than that of Vanhoorne *et al.* (2016) who applied spray drying method with a formulation which comprises of (75% paracetamol, 5% PVP and 20% δ-mannitol) with a tensile strength of 2.1 MPa at a compression pressure of 300Mpa.

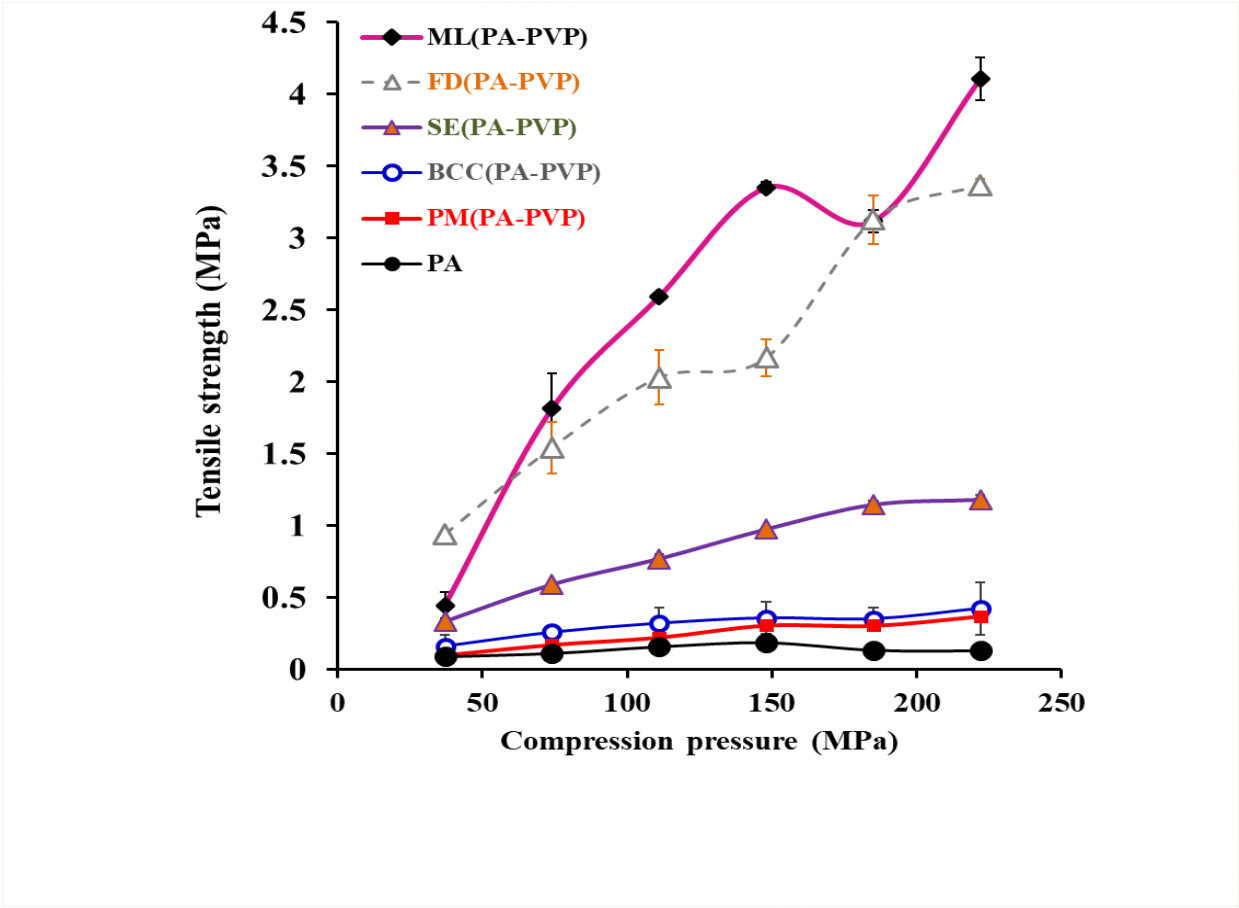

Figure 18. Tabletability profiles (mean ± SD, n = 5), of commercial paracetamol (PA), commercial polyvinylpyrrolidone (PVP), and PA−PVP mixtures (95:5, *w*:*w*) co-processed by physical mixing (PM), batch cooling crystallisation (BCC), solvent evaporation (SE), freeze drying (FD), and milling (ML).

4.3. Conclusions

It is remarkable how the methods of preparation have an immense impact on the micrometric and mechanical characteristics of paracetamol–Polyvinylpyrrolidone mixtures (PA: PVP; *95:5*; *w:w*) which is of great importance. Regardless of the engineered method employed, there was an improvement in tabletability for the mixtures of PA–PVP obtained using physical mixing, batch cooling crystallisation, solvent evaporation, freeze drying and milling techniques in comparison to the commercial paracetamol. Freeze drying and milling methods demonstrated excellent tabletability characteristics in comparison to the other techniques, which could be due to the increased hydrogen bonding interaction between paracetamol and polyvinylpyrrolidone leading to, subsequent reductions in bulk density and enhancement in mechanical properties. Freeze and milling methods should be considered in the future to improve the tabletability of poorly compactable drugs. Even though the flowability was not good, the content of uniformity of PA in all the different mixtures fell within the acceptable range.

5 CHAPTER 5: EFFECT OF FREEZING TEMPERATURES ON PA–PVP MIXTURES

5.0. Introduction

Freeze drying is a technical process which includes the desiccation of a substance, followed by sublimation of water from the solid state at reduced pressure (Craig *et al*., 1999). This process provides products with desired physicochemical properties, such as, improved mechanical properties and enhanced dissolution rates (Kaialy *et al*., 2016) and allows the stabilisation and preservation of thermal sensitive APIs and biologicals that have reduced shelf life in solution (Liu, 2006). Additionally, freeze drying made it possible to achieve a 1:1 paracetamol/2–hydroxypropyl–β–cyclodextrin host–guest complex, with solubility nearly six times higher than that of commercial paracetamol in comparison to kneading and physical mixing in water–ethanol mixture (Talegaonkar *et al.,* 2007).

Freeze drying technique was employed by Ogienko *et al.* (2011) to increase the tabletability of paracetamol, as discussed in (Section 1.7). However, the tablets obtained from the study were compressed using extremely high pressure. In this study for the first time, different freezing temperatures will be employed to obtain drug-polymer system to increase the tabletability of PA–PVP mixtures.

5.1. Engineering of PA and PA–PVP formulations

5.1.1 Freeze drying

25% w/*v* solutions were prepared by dissolving 25 g of PA and 25 g of PVP independently in hydro–alcoholic solutions of (125 mL of ethanol and 375 mL of deionised water) for a final volume of 500 mL under stirring

(200 rpm) at 70 ºC. The resultant clear solutions containing PA only and PVP only obtained were allowed to cool down and frozen using liquid nitrogen, while the vessel was stirred to allow maximum surface area for ten minutes and freeze dried using the method as discussed in (Section 2.2.1.6). The FD Pas powders were sieved using the technique described in (Section 2.3).

25% w/v solution was prepared by dissolving 25 g of PA–PVP mixture in a hydro–alcoholic solution of (125 mL of ethanol and 375 mL of deionised water) for a final volume of 500 mL under stirring (200 rpm) at 70 ºC. The resultant clear solution containing PA–PVP mixture obtained was allowed to cool down and was frozen at –20 ºC, –80 ºC and –196 ºC and was freeze dried using the technique described in (Section 2.2.1.6). The FD (PA–PVP) formulations were sieved using the technique described in (Section 2.3).

5.1.2. Physical mixing (PM)

Freeze–dried paracetamol (FD PA) and freeze–dried polyvinylpyrrolidone (FD PVP) (19:1 *w:w*) powders were mixed using low shear mixing technique as described in (Section 2.2.1.1).

5.1.3. Preparation of tablets

Each tablet has a weight of 526.3 ± 0.5 mg for the various formulations and 500 ± 0.5 mg for PA and FDPA, all compressed using the method described in (Section 2.14).

5.2. Results and discussions

5.2.1. Laser diffraction

As shown in (Table 9), the extent of agglomeration which is being expressed by the increase in mean median diameter (d_{50}%). It is quite evident that the degree of agglomeration increases as the temperatures decrease from –20 ºC to –196 ºC for example, the d_{50}% values range from 38 ± 0.3 µm to 64 ± 2.5 µm. Since PVP acted as a binder favouring agglomeration during the FD process which is affirmed by the SEM micrographs (Figure 19) which further demonstrate agglomerate comprises of, spherical and larger coalesced particles in which single particles are tough to differentiate (Figure 19). The mean diameter (VMD) of the FD samples increased with the decreased in temperatures (–20 ºC > –80 ºC > –196 ºC). For example, the VMD of the freeze–dried samples increased from 81.3 ± 28.4µm to 121 ± 11.2 µm when the temperature of freezing decreased from –20 ºC to –196 ºC as shown in (Table 9). The increased mean diameter of the freeze–dried samples is probably due to the increase in the size of the crystal ice formed during the freezing process at various temperatures. Also, it could be due to the presence of PVP which increases agglomeration and adhesion of particles–particles interaction (Vanhoorne *et al*., 2016). FD (PA–PVP) mixture frozen in liquid nitrogen exhibited narrow and broader PSDs (Table 9) in comparison to FPA, FD (PA–PVP) –20 ºC and FD (PA–PVP) –80 ºC.

Table 9. Particle size distribution (i.e. particle size at 10%($d_{10\%)}$,50%($d_{50\%}$, median diameter and 90%($d_{90\%)}$ volume distribution and span) (mean ± SD, n=3) for commercial paracetamol (PA) and freeze–dried paracetamol(FDPA), freeze–dried polyvinylpyrrolidone(FDPVP), and PA−PVP mixtures (95:5, w:w) co-processed by physical mixing (PM) and freeze drying(FD) with different freezing temperatures (–20 ºC, –80 ºC and –196 ºC).

Product	d_{10}**% (µm)**	d_{50}**% (µm)**	d_{90}**% (µm)**	**VMD (µm)**	**Span**
PA	254 ± 22	506 ± 30	911 ± 39.3	548 ± 30.2	1.3 ± 0
FDPA	4.2 ± 0	16 ± 0.1	86 ± 1.3	32 ± 1	5 ± 1
FDPVP	61 ± 3.2	279 ± 15.	550 ± 38.1	231 ± 29.1	2 ± 0.2
PM(FDPA−FDPVP)	4 ± 0	12.4 ± 0.1	56 ± 3.5	23 ± 1	4.1 ± 0.3
FD(PA−PVP)–20 ºC	8.1 ± 0	38 ± 0.3	56 ± 1.3	81.3 ± 28.4	3.2 ± 0.1
FD(PA−PVP)–80 ºC	10.4 ± 0.1	42.4 ± 1	56 ± 3.5	80.4 ±15	3.4 ± 0.3
FD(PAP−PVP)–196 ºC	14 ± 0.2	64 ± 2.5	255.3 ± 17.2	121 ± 11.2	4 ± 0.2

Table 10. Bulk density (D_b), tap density (D_t), cohesivity (1/*b*) and Carr's index (CI) (mean ± SD, n=3) for commercial paracetamol (PA) and freeze–dried paracetamol(FDPA), freeze–dried polyvinylpyrrolidone(FDPVP), and PA–PVP mixtures (95:5, *w*:*w*) co-processed by physical mixing (PM) and freeze drying(FD) with different freezing temperatures (–20 ºC, –80 ºC and –196 ºC).

Product	$D_{b(g/cm^3)}$	$D_{t(g/cm^3)}$	**1/*b***	***CI* (%)**
PA	0.8 ± 0	0.8 ± 0	4 ± 0	3.2 ± 0.3
FDPA	0.1 ± 0	0.3 ± 0	15.3 ± 0.2	52.3 ± 1
FDPVP	0.2 ± 0	0.2 ± 0	17.2 ± 1	23 ± 0
PM(FDPA–FDPVP)	0.1 ± 0	0.2 ± 0	13 ± 5	58 ± 4.3
FD(PA–PVP)–20 ºC	0.1 ± 0	0.3 ± 0	12.1 ± 1.5	47.3 ± 1.1
FD(PA–PVP)–80 ºC	0.1 ± 0	0.2 ± 0	9.3 ± 1.1	44 ± 2
FD(PAP–PVP) –196 ºC	0.1 ± 0	0.2 ± 0	9.5 ± 2.4	43 ± 0

The SEM micrographs as displayed in (Figure 19) shows that commercial PA portrays a polyhedral shape (Kaialy *et al*., 2014) whereas, in the case of FD PA, there was an alteration in shape from polyhedral to the plate–like habit with holes at the edges (Figure 19). The freeze–dried (PA–PVP) samples frozen from –20 ºC and –80 ºC also produced a flat surface with finger–like shaped edges which could increase the interlocking of the particles. The freeze–dried PA–PVP sample frozen from –196 ºC demonstrated an agglomerated shape with fissures. Sagechi *et al.* (2004)

reported a change in crystal habit of PA using the same amount of PVP (5% *w/w*) in a hydroalcoholic solution by applying spray freeze drying technique.

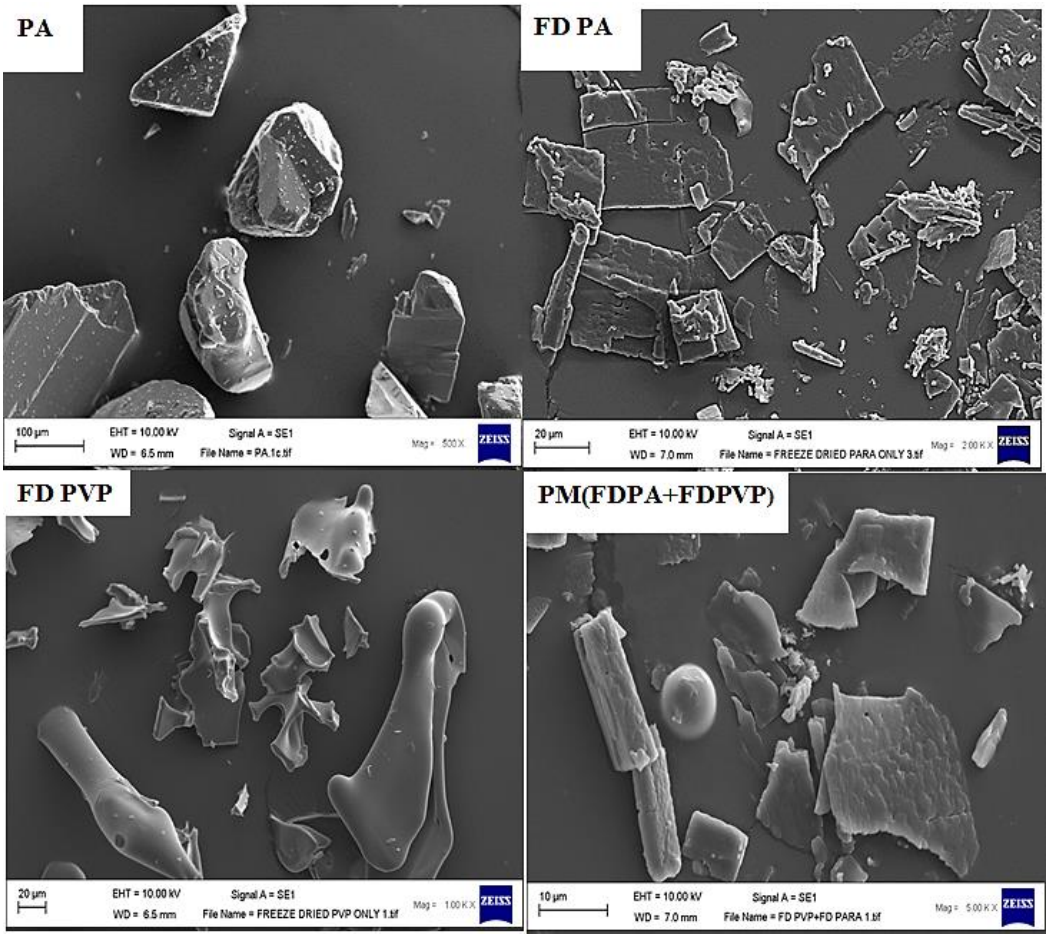

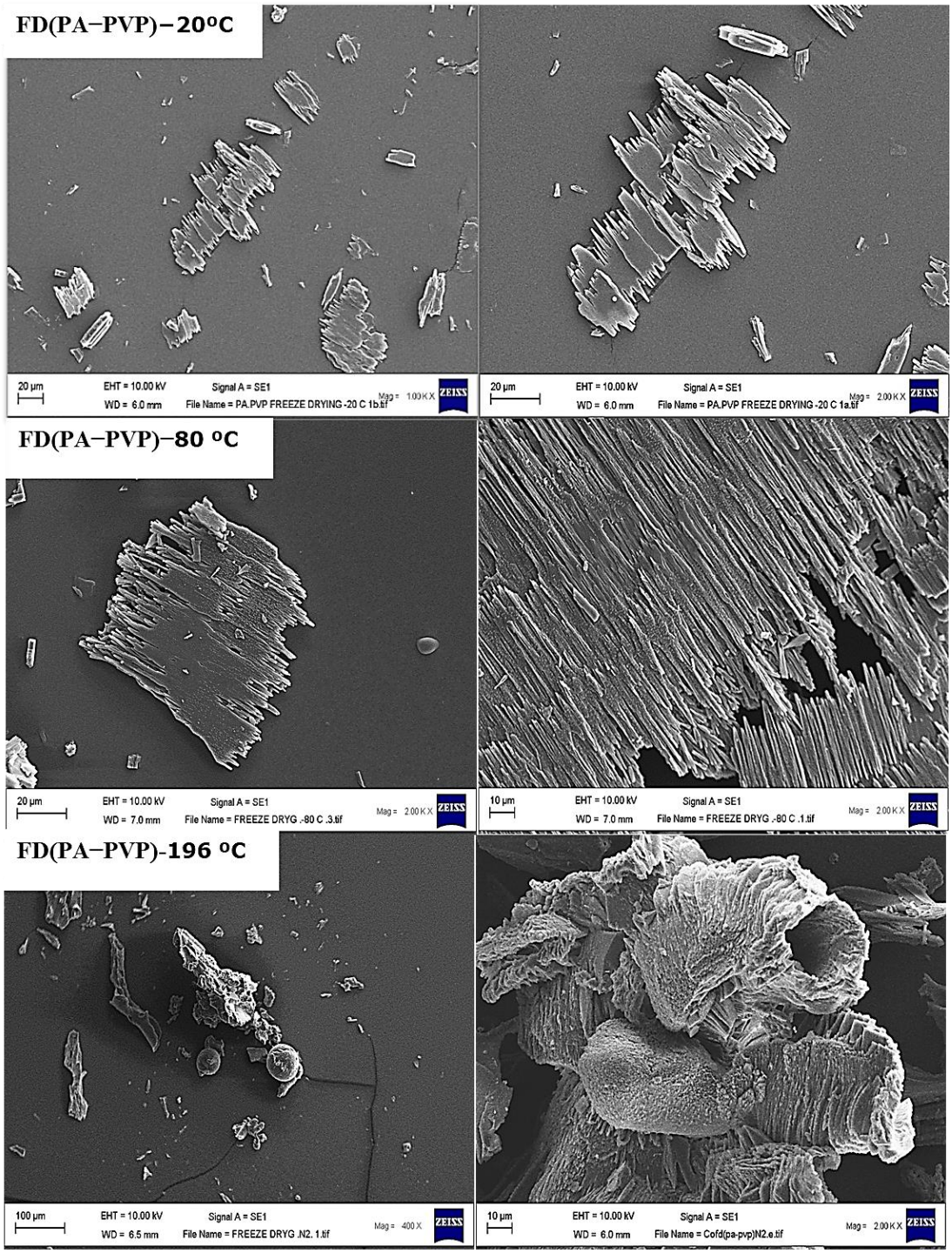

Figure 19. Scanning electron microscopy for commercial paracetamol (PA) and freeze–dried paracetamol (FDPA), freeze–dried polyvinylpyrrolidone(FDPVP), and PA–PVP mixtures (95:5, *w*:*w*) co-processed by physical mixing (PM) and freeze drying(FD) with different freezing temperatures (–20 ºC, –80 ºC and –196 ºC).

5.2.2. Solid state

Percentage of relative crystallinity of samples was calculated by the following equation (De Villiers *et al*., 1998)

% Relative crystallinity = (I_S / I_R) X 100 (Equation 9)

Here, I_S is the area under a distinct peak exactly at 24.41° 2θ in the freeze–dried samples and I_R is the area under a peak at the same position in commercial crystalline paracetamol. The peak at 24.41° 2θ is the largest and most distinguished peak in X–ray diffraction spectra of paracetamol (Figure 20).

Table 11. The relative peak intensity for paracetamol samples obtained based on the percentage of crystallinity at a specific peak in PXRD diffractogram.

Product	**The peak at 24.41 °2θ** **% Crystallinity**
PA	100
FDPA	94
FD(PA–PVP) –20 °C	82
FD(PA–PVP) –80 °C	43
FD(PA–PVP) –196 °C	39

The PXRD spectra of commercial PA and freeze–dried samples are displayed in (Figure 20). The PXRD spectra portrayed similar diffraction patterns at 2θ values for all the samples suggesting that all the FD particles did not undergo any structural changes (Figure 20). A significant reduction in relative to, the degree of crystallinity of the freeze–dried samples using various freezing temperatures (−20 ºC, −80 ºC, –196 ºC) were encountered as shown in (Table 11). For example, the freeze–dried PA sample obtained in the absence of PVP exhibited about 6% reduction in crystallinity, whereas as the temperatures decreased from −20 ºC to –196 ºC for the processed PA–PVP mixtures, there was a significant decrease in the percentage of crystallinity. The freeze–dried PA-PVP samples obtained from freezing using liquid nitrogen in the presence of 5% PVP displayed only 39% crystallinity compared to FD (PA−PVP) −20 ºC and FD (PA−PVP) −80 ºC that recorded 82% and 43% relative degree of crystallinity. According to (Sethia and Sequiilante, 2005; de Villiers, 1998; Frank, 1990), the production of partially amorphous paracetamol particles could be due to the rapid evaporation rate of the hydroalcoholic solvent and the use of reduced temperature which facilitates rapid solidification of the crystals leading to the production of the amorphous phase. Also, Kaialy *et al*., (2016) stated that freeze drying process could induce the formation of amorphous products. The PXRD and DSC techniques were used to demonstrate how lyophilised mannitol displayed lower degrees of crystallinities (RDCs) in comparison to commercial mannitol.

In this study, all the formulations showed a water content below (<1%) (Table 12), which is essential, especially when it comes to the stability of the freeze–dried samples. Also, all the freeze–dried samples were stable when exposed to higher temperatures as discussed in (Section 5.2.4).

Table 12. The water content (n=3) for commercial paracetamol (PA) and freeze–dried paracetamol (FDPA), freeze–dried polyvinylpyrrolidone (FDPVP), and PA–PVP mixtures (95:5, *w*:*w*) co-processed by physical mixing (PM) and freeze drying(FD) with different freezing temperatures (–20 ºC, –80 ºC and –196 ºC).

Product	Water content (%)
PA	0.2 ± 0
PVP	6.6 ± 0
FDPA	0.5 ± 0
FD PVP	8.4 ± 0
PM (FDPA– FD PVP)	0.9 ± 0
FD(PA–PVP)–20 ºC	0.6 ± 0
FD(PA–PVP)–80 ºC	0.5 ± 0
FD (PA–PVP) –196 ºC	0.7 ± 0

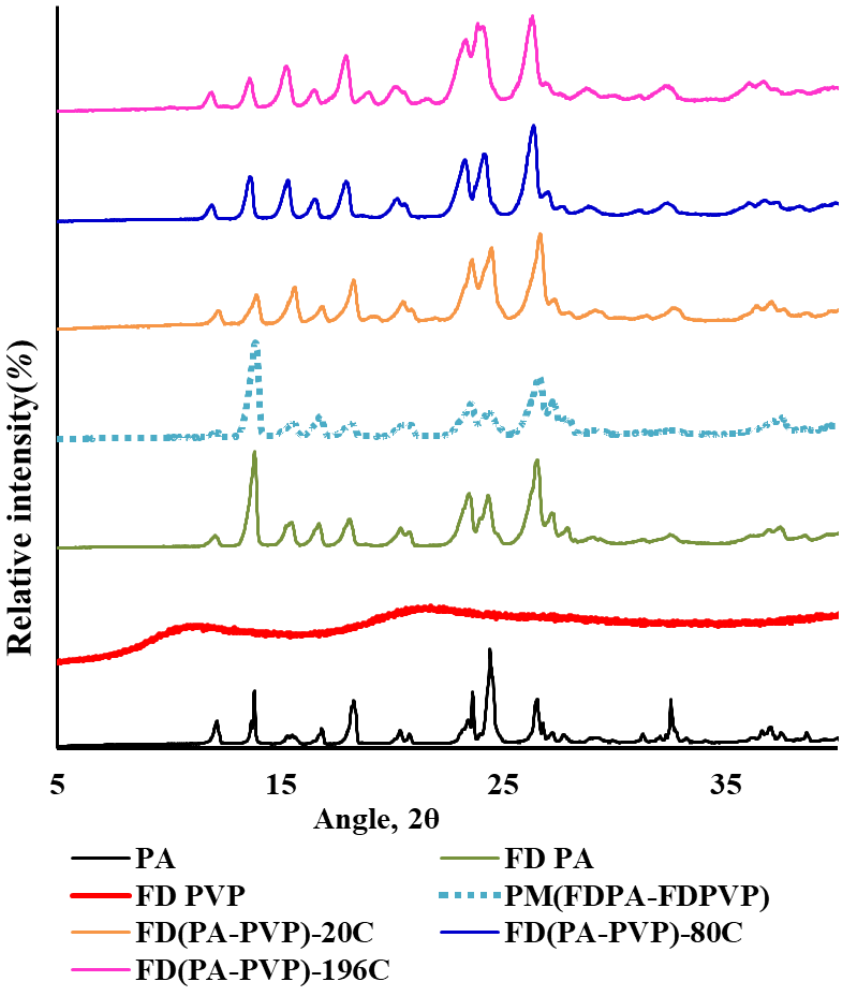

Figure 20. Powder X–ray diffraction (PXRD) patterns for commercial paracetamol (PA) and freeze–dried paracetamol (FDPA), freeze–dried polyvinylpyrrolidone (FDPVP), and PA–PVP mixtures (95:5, *w*:*w*) co-processed by physical mixing (PM) and freeze drying(FD) with different freezing temperatures (–20 ºC, –80 ºC and –196 ºC).

5.2.3. Fourier transform infrared

FT–IR studies were conducted to further investigate the nature and extent of interactions between the drug and polymeric carrier in the solid state. In polymer blends, mixing of two components at the molecular level will cause changes in the oscillating dipole of the molecules; this will manifest itself as changes in the frequency and bandwidth of interacting groups in the spectrum. Therefore, if interaction existed between the drug and polymer, the functional groups in the FT–IR spectra will show band shifts and broaden as compared to the spectra of the pure drug and polymer (Kovanda *et al*., 2011).

(Figure 21) Shows that PA infrared spectra were the monoclinic form *I* as reported in the literature (Al–zoubi *et al*., 2002). The FT–IR spectrum of PA was well discussed in (Section 3.3.4). As for FDPVP, the intense bandwidth at 1640.28 cm^{-1} corresponded to the non–hydrogen bonded amide C=O (Figure 21). The FD samples such as FD PA, FD (PA–PVP)–20 ºC, PM (FDPA–FDPVP) demonstrated slight reduction in absorbance intensity followed by FD (PA–PVP) –80 ºC and FD (PA–PVP) –196 ºC which demonstrated further reduction in absorbance intensity at 1644.37cm^{-1} which established as the freezing temperature decreases. The peak at 3300–3100 cm^{-1} is assigned to the non–hydrogen bonded N–H stretch of an amide of a PA molecule which is hydrogen bonded (3158.16 cm^{-1}) through the carbonyl group to a PVP molecule. The N–H band shifts to lower wavenumbers from 1558.68 cm^{-1} to 1556.64 cm^{-1} with broadening

indicating the formation of hydrogen bonding between the N–H groups of the drug and the carbonyl groups of the polymer. PA and PVP molecules are associated with intermolecular hydrogen bonding between the amide (PA) and carbonyl (PVP) functional and increased its bond strength. Therefore, in this investigation the presence of PVP in the amorphous phase of co–freeze dried PA–PVP mixtures could be stabilised by the intermolecular hydrogen bond between PA and PVP and improve its physical stability against recrystallisation. FT−IR spectra co–freeze dried PA–PVP mixtures demonstrated the presence of intermolecular interactions between PA and PVP molecules.

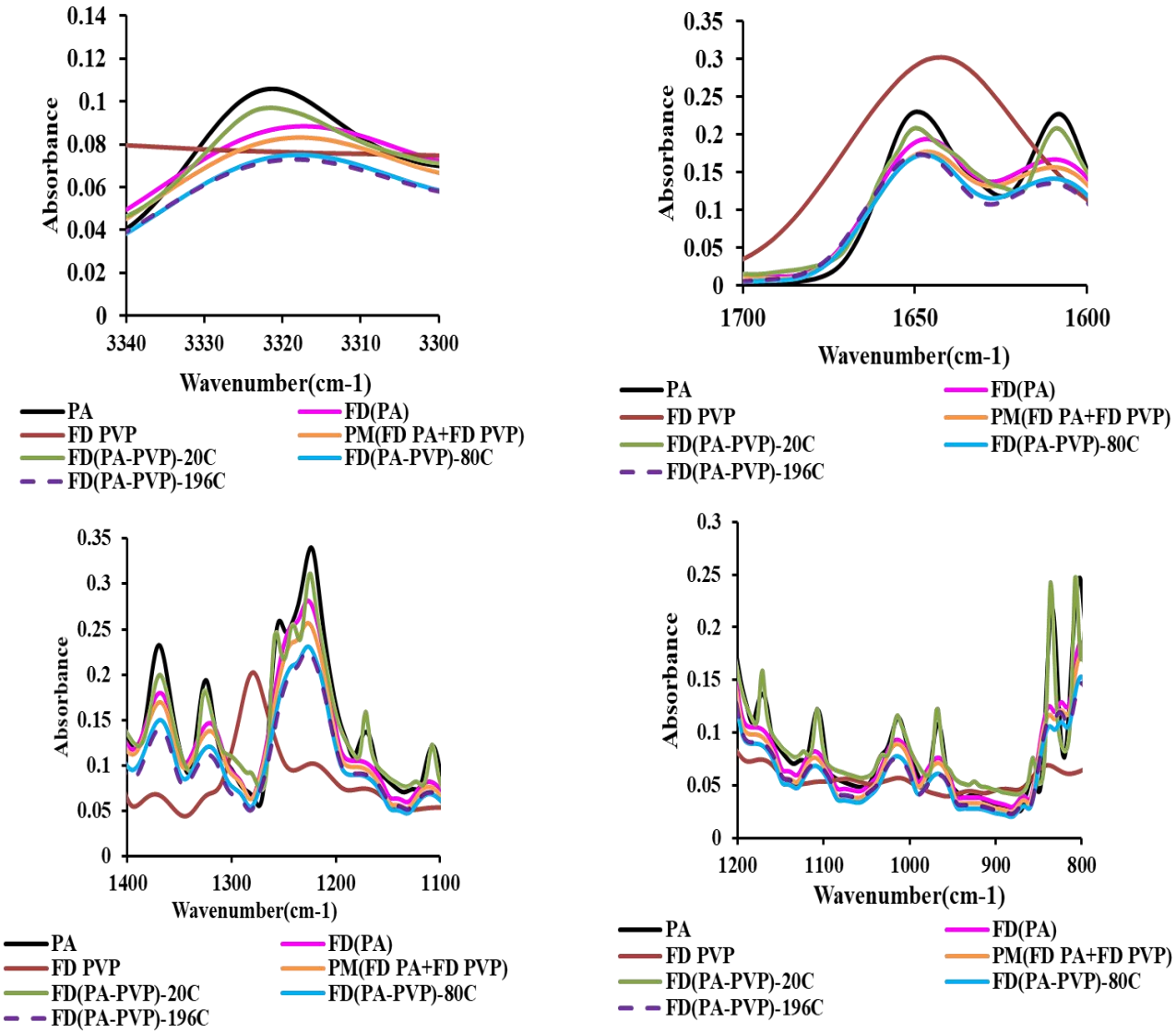

Figure 21. Fourier transform infrared (FT–IR) absorption spectra for commercial paracetamol (PA) and freeze–dried paracetamol (FDPA), freeze–dried polyvinylpyrrolidone(FDPVP), and PA–PVP mixtures (95:5, *w*:*w*) co-processed by physical mixing (PM) and freeze drying(FD) with different freezing temperatures (–20 ºC, –80 ºC and –196 ºC).

5.2.4. Thermogravimetric analysis

Figure 22 shows the thermograms of PA, PVP, FD PVP and their respective mixtures of PM(FDPA–FDPVP) and FD(PA–PVP) powders using various temperatures. All the formulations demonstrated a similar pattern and a reduction in water weight loss towards reduced temperature in comparison to PA, which could be due to the presence of PVP and the freeze drying technique applied. However, no water weight loss before 100°C implying the absence of surface water in all the formulations. The thermogram also shows the FD samples began to decompose at approximately 218°C. FDPVP started to lose weight below 100°C due to its hygroscopic nature and decomposed finally at approximately 434°C.

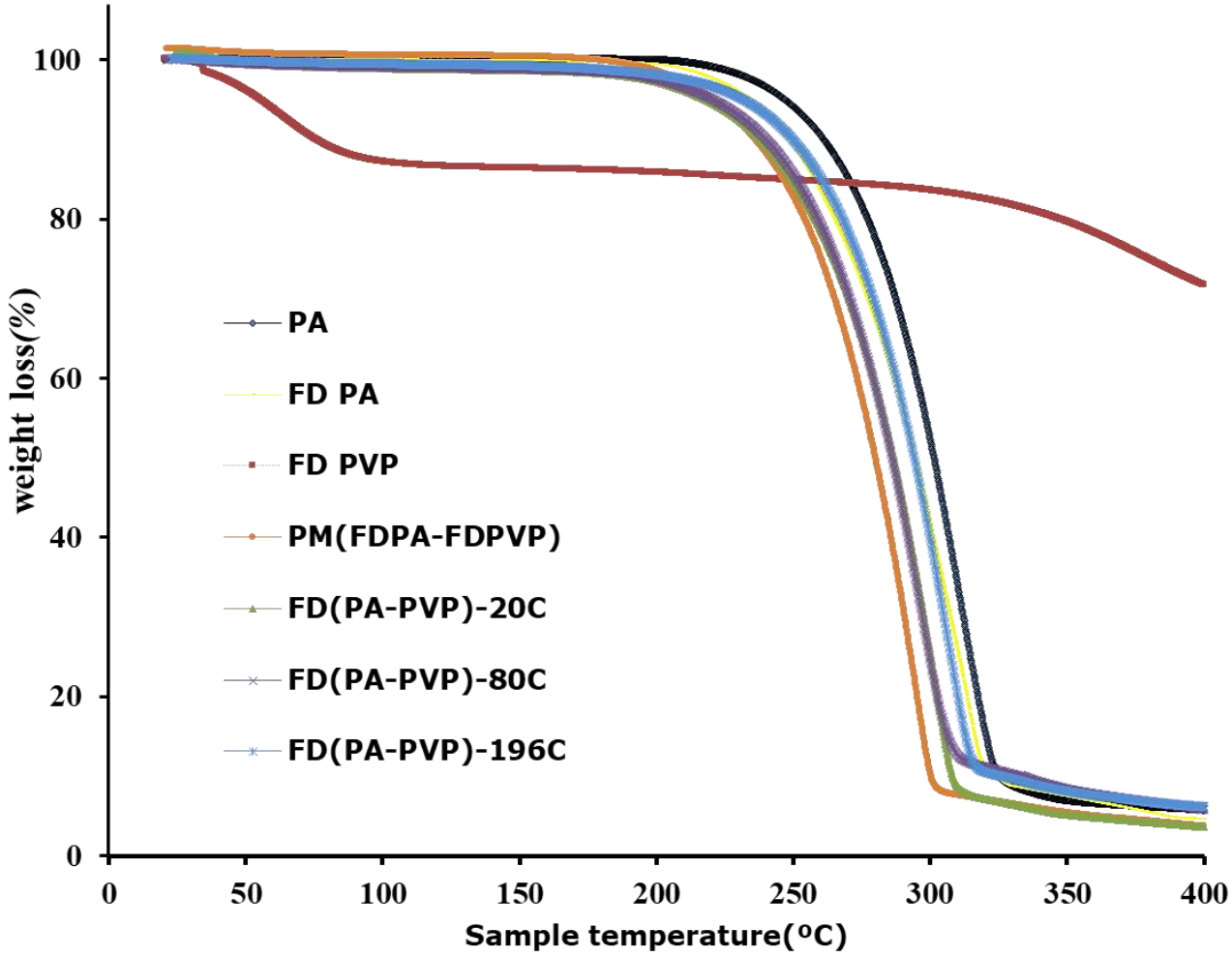

Figure 22. Thermogravimetric analysis (TGA) profiles for commercial paracetamol (PA) and freeze–dried paracetamol (FDPA), freeze–dried polyvinylpyrrolidone(FDPVP), and PA–PVP mixtures (95:5, *w*:*w*) co-processed by physical mixing (PM) and freeze drying(FD) with different freezing temperatures (–20 ºC, –80 ºC and –196 ºC).

5.2.5. Tableting properties

The influence of compression force on crushing strengths of tablets prepared from freeze drying PA in the absence or presence of PVP are shown in (Figure 23). Effect of compression force on the crushing strengths of tablets prepared from the physical mixing of PA with PVP using various freezing temperatures are displayed in (Figure 23). The tabletability profile shows that PA at all compression forces produced weak tablets with a measurable crushing strength and likewise with FDPA in the absence of PVP which produced weaker tablets at various compression pressure with high capping tendency in comparison to FD (PA–PVP) mixtures (Figure 23). The FD (PA–PVP) particles demonstrated an immense increase in their compaction properties compared to PA, and formed tablets with excellent crushing strength and the absence of tendency to cap for example, FD (PA–PVP)–20 ºC, FD (PA–PVP)–80 ºC and FD (PA–PVP)–196 ºC recorded TS values of, 3.4 ± 0.0 MPa, 3.8 ± 0.2 MPa and 4.2 ± 0.1MPa at 222 MPa. It was quite evident that the reduction in freezing temperatures employed on the various freeze–dried samples resulted in a profound increase in the crushing strength of the tablets and according to, Olusanmi *et al*. (2010) processing temperatures are known to impact mechanical properties especially, the hardness of the materials. In this investigation, the strong interparticulate bonding between PA and PVP particles which is indicated by, the higher crushing strength of the tablets could be due to the formation of the partially amorphous state that occurred during the co–freezing process at various freezing

temperatures, and the presence of the amorphous binder PVP is known to form strong hydrogen bonding with PA (Garekani *et al.,*2000b).

The tensile strength of the physical mixture of FDPA–FDPVP compressed at different compression pressure (Figure 23), clearly demonstrated that the tablets strength even at 5% *w/w* PVP content was 2.8 ± 0.1MPa, but that of FD(PA–PVP) –196 ºC in the presence of 5% PVP produced tablets with crushing strengths of 4.2 ± 0.1MPa (Figure 23). This was because the PA–PVP mixture freeze–dried with liquid nitrogen produced larger particles in comparison to the other samples under dissimilar freezing temperatures (–20 ºC and –80 ºC) and the physical mix, which was clearly shown by their differences in VMDs values (Table 10) and according to Osborne *et al*. (2011) bigger granules can be expected to possess more binder–rich domains which further produced tablets with considerable tensile strength and reduced friability. Also, these results show that the enhancement in tabletability of FD (PA–PVP) –196 ºC was not only due to the binding nature of PVP but also the solid properties and the semi–crystalline state of the crystals. The presence of the amorphous state in pharmaceutical powder plays a vital role in their compactibility (Vanhoorne *et al*., 2014; Takeuchi *et al*., 1998; Bauer-Brandl, 1996; York, 1992). The results obtained from this study showed superior compactibility properties using freeze drying technique compared to spray drying in the presence of plastically deforming particles like Lactose or δ-mannitol applied by (Vanhoorne *et al*., 2014; 2016).

Tablet with a minimum tensile strength of 2.0 MPa is required to safeguard the integrity of the pharmaceutical tablet, which indicates adequate strength for handling and transportation. Based on the observations in this study, all the values were >2.0 MPa suggesting an excellent tablet tensile strength from all the formulations regardless of the freezing temperatures.

The friability is a measure of the mechanical strength of the tablets. The friability data of the PM (FDPA–FD PVP); FD (PA–PVP) –20 ºC, FD (PA–PVP)-80 ºC tablets (mass loss of 21.31%; 1.25% and 1.30%) was higher compared to the FD(PA–PVP) –196 ºC tablets (mass loss of 0.91%). The differences in particle sizes, as shown by their VMD values (Table 11) can explain the differences in friability between the various freezing temperatures applied to the PA–PVP mixtures. Moreover, it appears from that FD (PA–PVP) –196 ºC had more intragranular pores and amorphous sites (Table 11; Figure 19) compared to their counterparts. Intragranular pores increased tablet strength, while the amorphous domains discourage tablets fragmentation/breakage under stress (oscillations in friability test) leading to reduced tablet friability.

The friability of the tablets consisting of the engineered powders of FD (PA–PVP) –196 ºC was acceptable as it ranged between 0.0% and 1%.

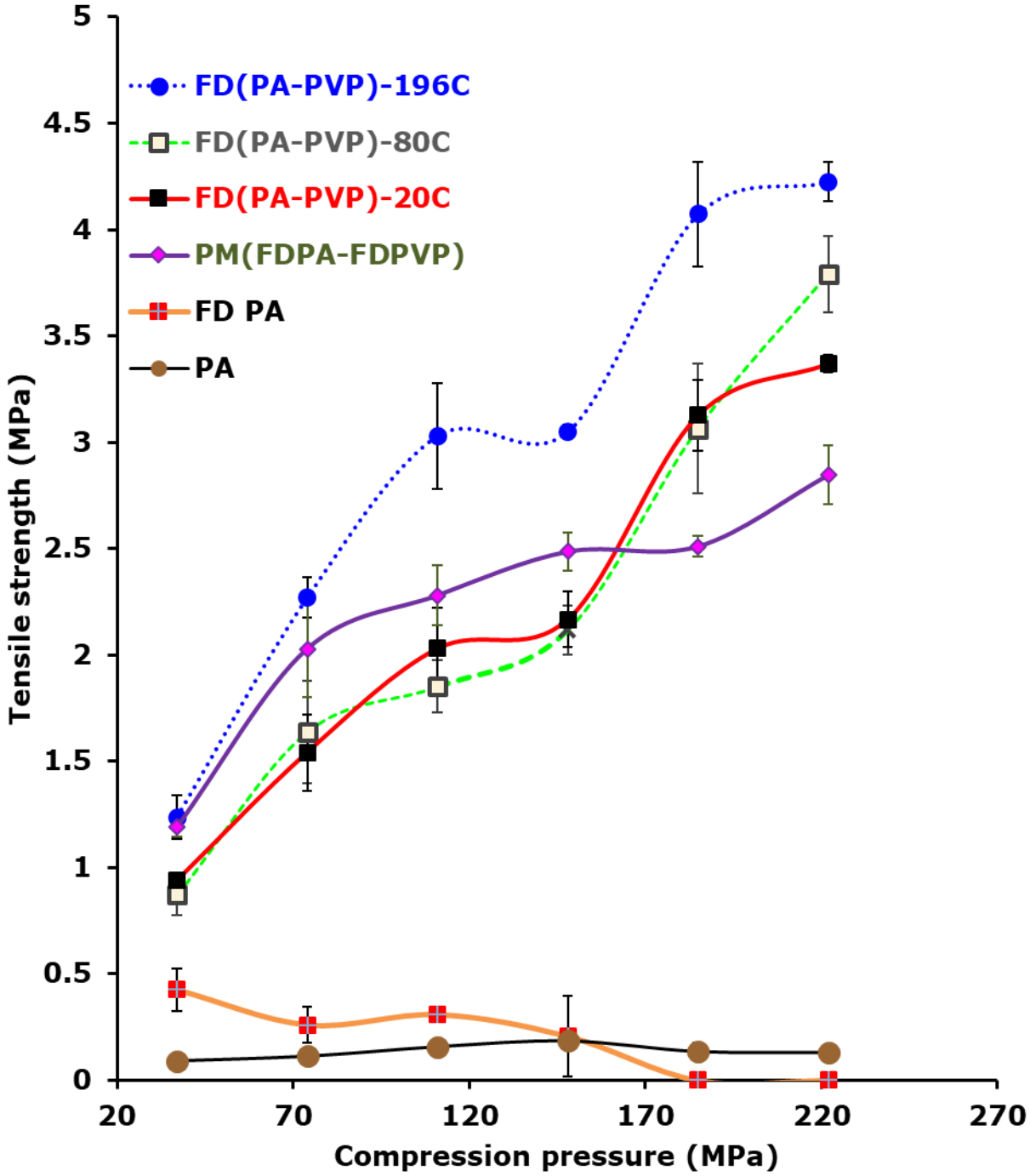

Figure 23. Tabletability profiles (mean ± SD, n = 5), for commercial paracetamol (PA) and freeze–dried paracetamol (FDPA), freeze–dried polyvinylpyrrolidone(FDPVP), and PA–PVP mixtures (95:5, *w*:*w*) co-processed by physical mixing (PM) and freeze drying(FD) with different freezing temperatures (–20 ºC, –80 ºC and –196 ºC).

5.3. Conclusions

This investigation clearly showed how the effect of freezing temperatures impacted the particle size, crystallinity and mechanical characteristics of paracetamol–Polyvinylpyrrolidone mixtures freeze–dried in the presence of 5% PVP *w/w* from a hydroalcoholic solution. It was quite evident that irrespective of the temperature of freezing employed, there was an enhancement in tabletability for the freeze–dried mixtures of PA–PVP in comparison to the commercial paracetamol. The best tabletability results were obtained with the PA–PVP mixture was frozen at –196 ºC compared to the other mixtures frozen at –20 ºC and –80 ºC. The PA–PVP mixtures frozen using liquid nitrogen had the best tabletability result which could be due to, the drastic reduction in the percentage of relative crystallinity which fosters hydrogen bonding interaction leading to an increased tabletability.

6 CHAPTER 6: EFFECT OF VARIOUS PREPARATION METHODS ON PARACETAMOL–IBUPROFEN MIXTURES

6.0. Introduction

Ibuprofen [$C_{13}H_{18}O_2$ – (RS)–2– (4– (2–methyl propyl) phenyl) propanoic acid] (IBU) is a non–steroidal anti–inflammatory drug used mainly as antipyretic and analgesic (Soares and Carneiro, 2014) also, the third most used anti–inflammatory agent in the world (Andini *et al*., 2012). At lower doses (0.6–1.2 g per day), IBU is well suited for the treatment of fever, pain, migraine, and dysmenorrhoea (De Brabander *et al*., 2004) and in the therapy of rheumatoid arthritis and osteoarthritis, it is used in high doses; 1800–3200 mg daily or 200–800 mg every 4–6 h as a single dose (Kachrimanis and Malamataris, 1998).

IBU is a colourless needle–like crystalline powder with a molecular weight of 206 g/mol with melting temperature ranges from 75–77 ºC and boiling points of 157 ºC (Paradkar *et al*.,2003; Krupta *et al*., 2007). IBU has two possible enantiomers, (R)–ibuprofen and (S)–ibuprofen (Qiao *et al*., 2011). However, it has poor water solubility at room temperature (Drug bank, Ibuprofen, 2012). The frequently used needle– shaped crystals of IBU demonstrates poor flowability due to high cohesivity and adhesivity, and it exhibits poor compaction behaviour; thus, must be granulated in most cases before tableting. Another problem in manufacturing is the high tendency of sticking to the punches (Rasenack and Müller, 2002; Mallick *et al*., 2013; Manish *et al*., 2005). Nonetheless, combining analgesics into a single product may ease compliance by reducing the total number of medications in which the patient is obliged to take to

manage pain, therefore, the use of a mixture of oral analgesics vs an individual agent offers numerous potential benefits (Raffa,2001; Tanner *et al*., 2010).

A combination of paracetamol–ibuprofen therapy is currently available in the market (NuromolTM) as a tablet. In this work is aimed to prepare direct compression grades of PA in the presence of IBU particles which are less brittle under compaction.

IBU contains one carboxylic acid group that can act as a hydrogen−bond donor, so it has the potential to interact via hydrogen bonding with drugs continuing amine groups like PA. The ratio of (5:2, *w/w*) of PA to IBU was used in this study. The effect of the different processing methods on the physicochemical and mechanical properties of PA–IBU mixtures was investigated.

6.1.0. Engineering of PA–IBU formulations

6.1.1 Physical mixing

PA and IBU (5:2 *w:w*) powders were mixed using low shear mixing technique as described in (Section 2.2.1.1).

6.1.2. Batch cooling crystallisation

PA and IBU powders (5:2, *w:w* ratio) were dissolved in a mixture of ethanol/distilled water (50/50, *v:v*). After being wholly dissolved, the resultant solution was left uncovered under laboratory conditions for seven days using batch cooling crystallisation method as described in

(Section 2.2.1.4). The crystals obtained were sieved using the technique described in (Section 2.3).

6.1.3. Freeze drying

PA and IBU powders (5:2, *w: w* ratio) were dissolved in the mixture of ethanol/distilled water (50/50). The resultant clear solution containing paracetamol−ibuprofen mixture obtained was allowed to cool down and was frozen using liquid nitrogen, while the vessel was stirred to allow maximum surface area for ten min then was freeze dried using the technique described in (Section 2.2.1.6). The FD (PA–IBU) powders were sieved using the technique described in (Section 2.3).

6.1.4. Compact milling (CPM) (PA−IBU)

PA and IBU powders (14 g in total at 5:2, *w: w* ratio) were compacted into a tablet using 3000 kp and were further milled for one min by applying the milling technique as described in (Section 2.2.1.7).

6.1.5 Milling (PA−IBU)

PA and IBU powders (14 g in total at 5:2, *w: w* ratio) were milled for five min by using the milling method as described in (Section 2.2.1.7).

6.1.6. Tablet preparation

Each tablet weighs 700 mg ± 0.5 mg for the various formulations of which 200 mg is of IBU and 500 mg of PA. Both the formulations and the commercial paracetamol and commercial Ibuprofen (500 mg ± 0.5 mg) were all compressed using the method described in (Section 2.14).

6.2. Results and Discussions

6.2.1. Particle size distributions

PA–IBU mixture prepared using PM mixing method displayed an increase in both VMD and span values compared to the marketed PA (Table 13) this could be due to the ratio of IBU to that of PA particles whose VMD values are lesser (Table 13) as affirmed by SEM micrographs (Figure 24). However, the mixtures obtained using both CPM and BCC processing methods demonstrated a drastic reduction in VMDs and an increased in span values compare to the commercial PA (Table 13), and their PSDs showed statistically different results. This is affirmed by the SEM observations, which showed a difference in the structure of mixtures prepared using (CPM and BCC) (Figure 24). On the other hand, the mixtures prepared using DHS, FD and ML processing techniques revealed smaller and varied PSDs (VMD of 30.3 ± 0.5 µm, 47 ± 4.3 µm and 43 ± 5.2 µm) in comparison to the mixtures using PM, CPM and BCC methods which displayed broader PSDs (VMDs ranging from span values ranging from 125 ± 4.5 µm to 821 ± 37.4 µm (Table 13). The change towards lower PSDs for the freeze–dried sample could be due to the *in–situ* generation of intrinsic fine particles during the FD preparation (as shown by its d_{10}% values) (Table 13). On the other hand, the fines particles during ML are due to the collisions of the metallic balls and the PA–IBU particles. The difference in morphologies between the various mixtures is envisaged from their SEM micrographs (Figure 24) as the engineered samples showed irregular–shaped structures compared to their

commercial components. This could lead to differences in tabletabilty properties.

Table 13. Particle size distribution (i.e. particle size at 10%($d_{10\%)}$,50%($d_{50\%,}$ median diameter and 90% ($d_{90\%)}$ volume distribution and span) (mean ± SD, n=3) of commercial paracetamol(PA), commercial ibuprofen(IBU) and the mixtures (PA:IBU, 5:2 *w/w*) prepared using physical mixing (PM), compact milling(CPM), batch cooling crystallisation(BCC), dry high shear (DHS), freeze drying (FD) and milling(ML)

Samples	$d_{10\%}$ **(µm)**	$d_{50\%}$ **(µm)**	$d_{90\%}$**(µm)**	**VMD (µm)**	**Span**
PA	254 ± 22	506 ± 30	911 ± 39.3	548. ± 30.2	1.3 ± 0
IBU	26.1 ± 0.5	88 ± 3.3	389.3 ± 8.5	144 ± 14	4 ± 0.5
PM(PA−IBU)	80 ± 5.2	634.3 ± 17	1780.3 ± 9	821 ± 37.4	3 ± 0.1
CPM(PA−IBU)	11 ± 0.4	76 ± 3.5	313 ± 11.5	125 ± 4.5	4 ± 0.1
BCC(PA−IBU)	16.4 ± 0.1	97.3 ± 1	595 ± 13	277 ± 29.3	6 ± 0.5
DHS(PA−IBU)	3.3 ± 0.1	15.3 ± 0.4	82.1 ± 1.1	30.3 ± 0.5	5.1 ± 0.1
FD(PA−IBU)	5 ± 0	19.4 ± 0.2	112 ± 9.4	47 ± 4.3	5.5 ± 0.4
ML(PA−IBU)	4 ± 0.1	23.3 ± 0.5	109.3 ± 10.1	43 ± 5.2	4.5 ± 0.4

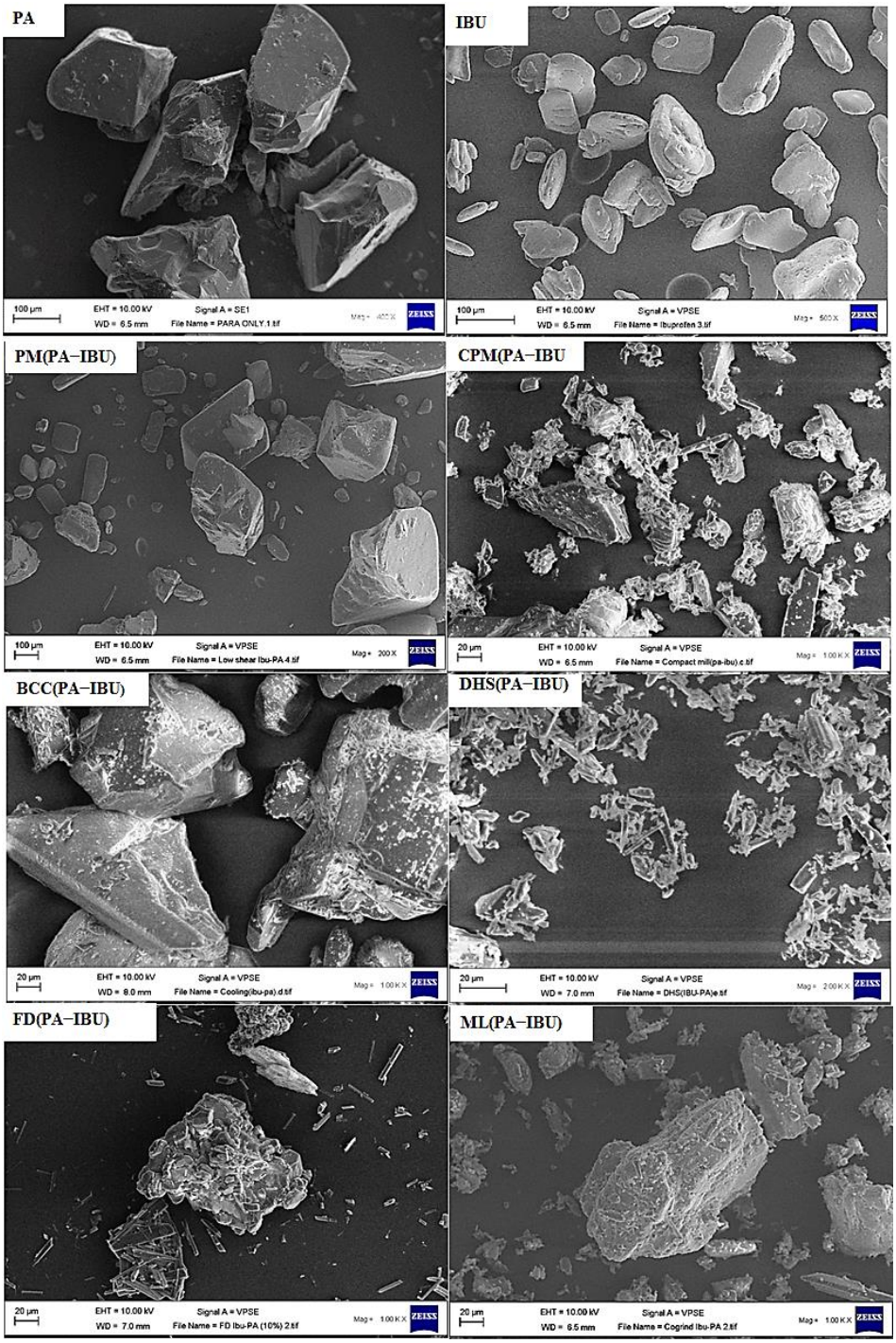

Figure 24. Scanning electron microscopy micrographs of commercial paracetamol(PA), commercial ibuprofen(IBU) and the mixtures (PA:IBU, 5:2 *w/w*) prepared using physical mixing (PM), compact milling(CPM), batch cooling crystallisation(BCC), dry high shear (DHS), freeze drying (FD) and milling (ML).

6.2.2. Powder density and Cohesivity

The various mixtures of PA–IBU exhibited lower bulk, high cohesivity and high CI values than the marketed PA (Table 14). The mixtures prepared using DHS, FD and milling methods showed a further reduction in bulk densities, increased in cohesivities compared to commercial PA, PM, CPM and BCC powders (Table 14). Additionally, as displayed in (Figure 24), the DHS (PA–IBU), FD (PA–IBU) and ML (PA–IBU) demonstrated irregular crystal shapes in comparison to PA PM (PA–IBU), CPM (PA–IBU) and BCC (PA–IBU) powders which influences the packing density (ter Horst *et al*., 1999).

The reduction in bulk and tap densities were shown to increase the tensile strength of tablets (Chen *et al*., 2018; Di Martino *et al*., 2002). Most powdered pharmaceuticals, compaction of smaller particles leads to the formation of stronger tablets as, the smaller particles offer a larger total area for bonding than larger particles (Grant and Sun, 2001). The slight reductions in the bulk for the mixture prepared using PM method compared to PA is due to the presence of (14%, *w/w*) IBU powders whose bulk and tap density values are slightly smaller than those of PA (Table 14).

The marketed paracetamol demonstrated the least CI value as shown in (Table 14) indicating a better flow property compared to the other powders under investigation. Such powders, present uniformed–sized shapes so it must be difficult to orient in different direction and fracture

during compaction resulting in poor compaction. All PA– IBU mixtures showed higher CI values which is consistent with the patterns in bulk and tap density changes compared to commercial PA (Table 14) indicating their relatively poorer flow properties. The mixtures prepared using FD and ML samples displayed poorer flowability than (PM, CPM and BCC) as shown by their considerably higher CI values (42% ± 0% and 51% ± 2% versus 12% ± 0 %, 40% ± 1% and 32 % ± 1% (Table 14). Which further, attribute to the lower PSDs to stronger interparticle forces (Li *et al*., 2004; Kaialy *et al*., 2012) likewise, the difference in bulk densities is also linked to their dissimilar crystal habits, leading to different contact points and cohesive and frictional forces between crystals. Those factors impact sliding of the particles against each other, which leads to different packing geometry and bulk densities (Garekani *et al*., 2001).

Table 14. Bulk density (D_b), tap density (D_t), cohesivity (1/*b*) and carr's index (CI) (mean ± SD, n=3) for commercial paracetamol(PA), commercial ibuprofen(IBU) and the mixtures (PA:IBU, 5:2 *w/w*) prepared using physical mixing (PM), compact milling(CPM), batch cooling crystallisation(BCC), dry high shear (DHS), freeze drying (FD) and milling (ML).

samples	$D_{b(g/cm^3)}$	$D_{t(g/cm^3)}$	1/*b*	*CI* (%)
PA	0.8 ± 0	0.8 ± 0	4 ± 0	3.2 ± 0.3
IBU	0.6 ± 0	0.71 ± 0	14 ± 0	22 ± 1
PM(PA–IBU)	0.74 ± 0	0.84 ± 0	7.5 ± 1	12 ± 0
CPM(PA–IBU)	0.5 ± 0	0.8 ± 0	7.2 ± 4.0	40 ± 1
BCC (PA–IBU)	0.43 ± 0	0.63 ± 0	41 ± 0	32 ± 1
DHS(PA–IBU)	0.24 ± 0	0.43 ± 0	29 ± 2	44 ± 1
FD(PA–IBU)	0.13 ± 0	0.3 ± 0	24.4 ± 2	51 ± 2
ML(PA–IBU)	0.31 ± 0	0.53 ± 0	52 ± 0	42 ± 0

6.3. Solid state properties

6.3.1. Powder X–ray diffraction

The PXRD analysis was carried out for Commercial PA, commercial IBU and all PA–IBU mixtures prepared using PM, BCC CPM, FD and ML techniques as shown in (Figure 25).

IBU displayed characteristic peaks at 2θ values of ~6^{O}, 12^{O}, 13.5^{O}, 16^{O}, 17^{O}, 18^{O}, 19^{O}, 20^{O}, 20.5^{O}, 22^{O}, and 22.5^{O} (Ali *et al*., 2010) and PA PXRD pattern as displayed in (Figure 25) and possessed characteristic peaks as discussed in (Section 3.3.3). Both commercial samples' PXRD patterns revealed their crystalline nature due to the numerous sharp and intense peaks present. All PXRPD values for PA–IBU mixtures showed that all diagnostic peaks for PA and IBU were present in PM (PA–IBU), CPM (PA–IBU), DHS (PA–IBU), FD (PA–IBU) and ML (PA–IBU) mixtures (Figure 25). The absence of high reflections at 10.35 ^{o}, 21.85^{o} and 24.03^{o} 2θ (Di Martino *et al*., 1996) in PM (PA–IBU), CPM (PA–IBU), DHS (PA–IBU), FD (PA–IBU) and ML (PA–IBU) mixtures ruled out the transformation of the monoclinic form to the orthorhombic form, which is less stable than the monoclinic form. However, the BCC method employed showed a different pattern (peak position) at 2θ values of 12.16°, 13.83°, 15.5° and 24.03° (Martino *et al*., 1996) an indication of the mixture of monoclinic PA and orthorhombic forms of PA. Also, IBU was less prevalent than PA in BCC (PA–IBU) mixture could be due to its lost during filtration using the batch cooling crystallisation process described in (Section 2.2.1.4) which will reduce the appearance of IBU in BCC (PA–IBU) mixture in the comparison the mixtures prepared using PM, CPM, DHS, FD and ML techniques. In some cases, the intensity of the peaks was higher than those of neat IBU and PA, which could be due to their high crystalline nature.

The residual moisture measured for the PA–IBU was insignificant (<0.16% *w/w*), which is ideal for storage stability (Barresi *et al*., 2009) (Table 15).

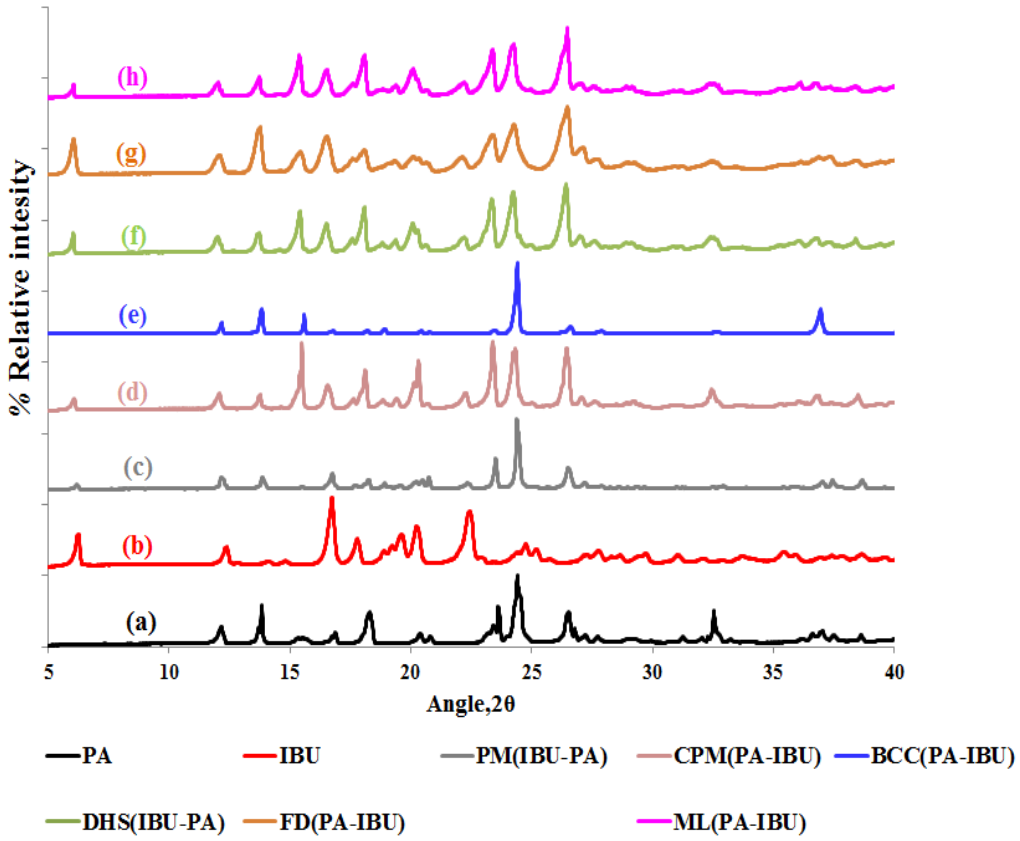

Figure 25. Powder X–ray diffraction (PXRD) patterns of (a) commercial paracetamol(PA), (b) commercial ibuprofen(IBU) and the mixtures (PA: IBU, 5: 2 *w/w*) prepared using (c) physical mixing (PM), (d) compact milling(CPM), (e) batch cooling crystallisation (BCC), (f) dry high shear (DHS), (g) freeze drying (FD)and (h) milling (ML).

6.3.2. Infrared spectroscopy

The FT–IR analysis of PA, IBU and PA–IBU mixtures (Figure 26) displays the spectra of PA and IBU confirming that the presence of both drugs in the various mixtures irrespective of the method applied which is vital

regarding any chemical changes/interactions at the molecular level during the engineering process.

The diagnostic bands for PA orthorhombic form (Section 3.3.4) were absent from the spectra of commercial PA and all PA–IBU mixtures, confirming the purity of PA monoclinic form phase for all products under investigation. From the molecular structures of PA and IBU (Table 5 & 15) indicate that H–bonding effect may exist between the N–H stretch or the O–H stretch (H donors) of PA and the carbonyl group (C=O, H acceptor) of IBU which could probably induce hydrogen bonding interactions in all the PA–IBU mixtures prepared using the various techniques. The marketed IBU spectra showed characteristic broad absorption peaks at 3078.60 cm^{-1} and 3066.36 cm^{-1} corresponding to OH group usually from carboxylic acid which has strong tendency to form hydrogen–bonded dimers, O–H group from carboxylic acid which is attributed by the presence of the broad absorption bands at 3500–2500 cm^{-1} (Coates, 2000).

IBU shows characteristic peaks at 2960 cm^{-1} for the aryl C–H stretching and three aliphatic alkyl groups. The carbonyl group can be found at approximately, 1700 cm^{-1} on IBU spectrum (Ma *et al*.,2013), 1513 cm^{-1}, 1463 cm^{-1}, 1378 cm^{-1} which are used by C=C vibration of the phenyl ring and the C– H bond vibration (Zhao *et al*., 2014; Ambrogi *et al*., 2001; Qiu *et al*., 2005; DeLeon *et al*.,2012). C–0 stretching at 1228.20 cm^{-1}, the C=O stretching of the carboxylic acid of IBU at 1703.05 cm^{-1} which

demonstrated high intensity which could be due to the immerse dipole moment of the carbonyl bond.

The FT–IR spectrum of (*5:2*; PA: IBU) of PM(PA–IBU), CPM(PA–IBU), BCC(PA–IBU), DHS(PA–IBU) and FD(PA–IBU) mixtures displayed in (Figure 26) showed specific bands corresponding to the bands in the individual components of the mixture remained the same indicating an insufficient intermolecular interaction between both drugs. However, the band corresponding to the stretching vibration of the carbonyl group of IBU shifted from 1709.75 cm^{-1} to 1731.83 cm^{-1} indicating a slightly stronger hydrogen bonding interaction in solid state between PA and IBU for the mixture prepared using milling (ML (PA–IBU) technique as shown in (Figure 26).

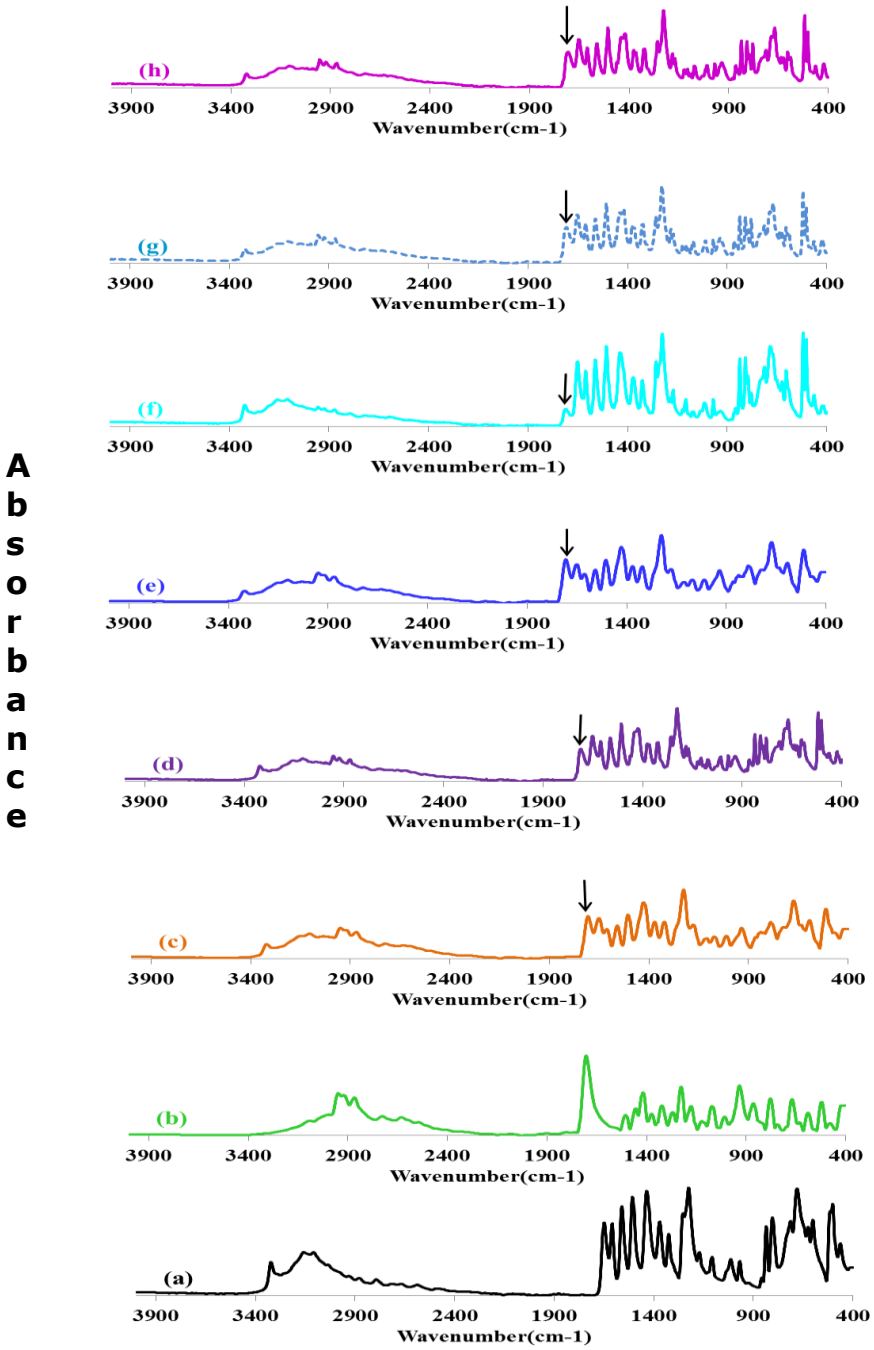

Figure 26. Fourier transform infrared spectroscopy (FT–IR) spectra of (a) commercial paracetamol(PA), (b) commercial ibuprofen(IBU) and the mixtures (PA:IBU, 5:2 *w/w*) prepared using (c)physical mixing (PM), (d)compact milling(CPM), (e) batch cooling crystallisation(BCC), (f) dry high shear (DHS), (g) freeze drying (FD) and (h) milling (ML).

Table 15. Chemical structure and characteristic FT–IR absorption bands of Ibuprofen (IBU) (Namur, 2009).

Chemical structure	Functional groups	Absorbance bands
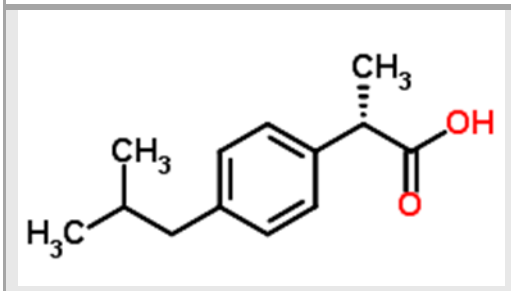	C=O stretching (COOH) C–C ring vibrations C–H asymmetric bending (CH_3) and C–H scissoring (CH_2) C–O stretching (COOH) O–H bending	1708 cm^{-1} 1512 cm^{-1} 1412 cm^{-1} 1268 cm^{-1} 1230 cm^{-1} 1184 cm^{-1}

6.3.3. Thermogravimetric analysis

The TGA profiles of commercial PA, commercial IBU and PA–IBU mixtures are displayed in (Figure 27). Single step mass loss and decomposition

were observed in both PA and IBU, and the various (PA–IBU) mixtures in the TGA derivative curves. The melting point of IBU has been reported to be at 71.7± 0.1 ºC (Passerini *et al*., 2002). A weight loss in PA particles as the temperature increases as discussed in (Section 3.3.4) whereas, IBU showed 100% mass loss at 292 ºC, due to the complete melting of the sample which is closer to the result obtained by (Krupa *et al*., 2010). No apparent water loss is found near the temperature of 100 ºC for PA, IBU and PA–IBU mixtures. The TGA curves of the IBU and PA binary mixtures (Figure 27) showed slightly significant weight loss in the temperature from 200 ºC to a final decomposition at 500 ºC. BCC and DHS samples displayed a shift from 200 ºC towards lower melting points, which could be attributed to the decomposition of the organic fraction of IBU at a higher temperature. Meanwhile, in FD sample, the weight loss at 148 ºC may be due to the highly porous nature of the sample (Table 14).

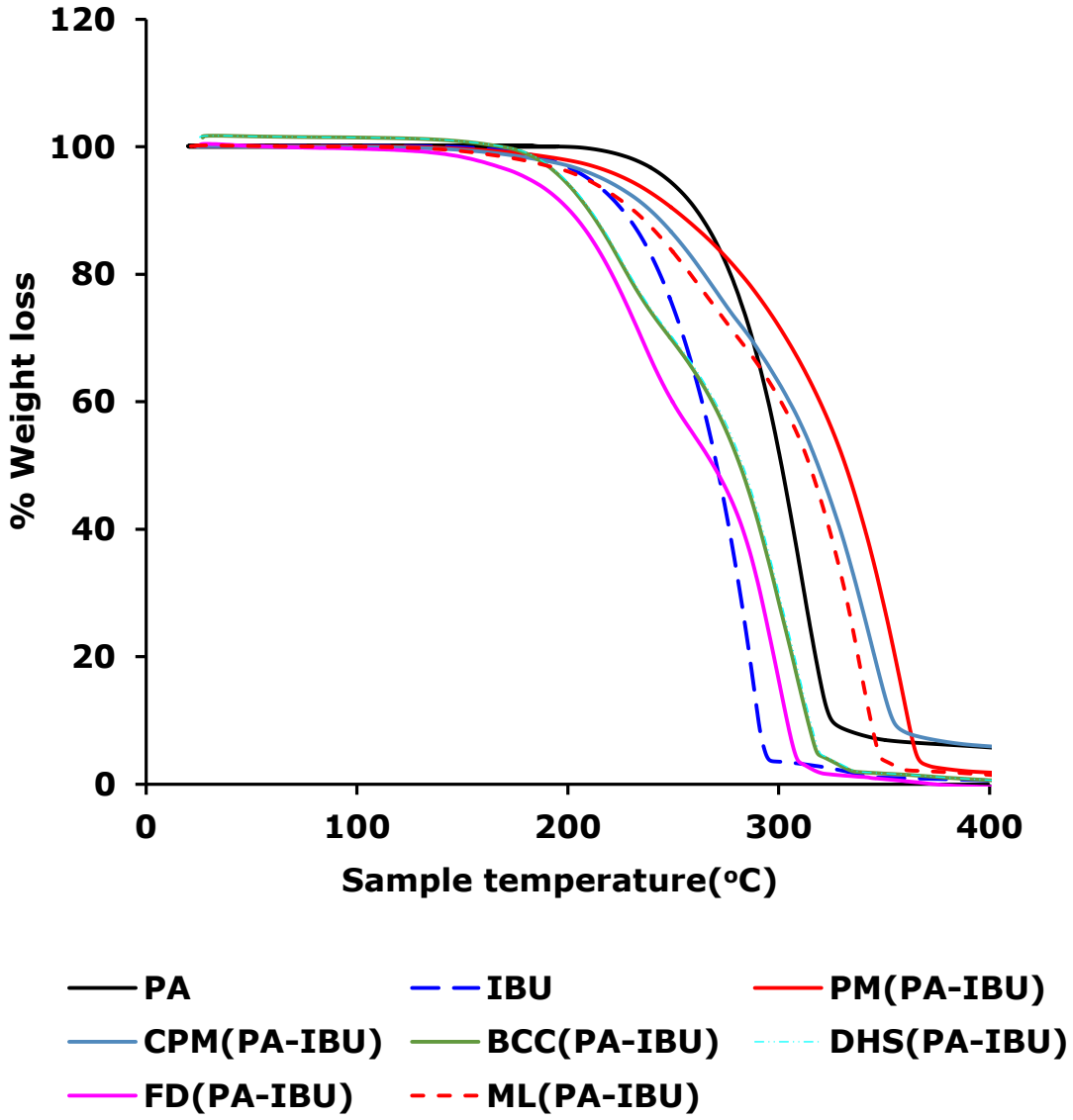

Figure 27. TGA thermal profiles of commercial paracetamol(PA), commercial ibuprofen(IBU) and the mixtures (PA:IBU, 5:2 *w/w*) prepared using physical mixing (PM), compact milling(CPM), batch cooling crystallisation(BCC), dry high shear (DHS), freeze drying (FD) and milling (ML).

6.4.4. Stability studies

The results of the current investigation, showed that the PA and all PA–IBU mixtures gained negligible amounts of moisture (<0.08%, *w/w*) when stored at 75% RH conditions (22 ºC) for three months, confirming their low hygroscopicity and thereby, potentially excellent stability (SM 1).

6.5. Tableting properties

PA showed poor mechanical properties, as discussed in (Section 3.3.5) (Figure 28). Similarly, the compression of IBU crystals at all compaction pressures produced weak compacts with low tensile strength, with its highest tensile strength recorded at 148 MPa was (0.98 ± 0.07 MPa). The engineered samples of PA–IBU (5:2, *w/w* PA: IBU) showed an improved tabletability (Figure 28). For example, the TS of PA–IBU mixture compressed at 222 MPa was 0.3 ± 0.0 MPa, 0.8 ± 0.2 MPa, 1.2 ± 0.0 MPa, 1.4 ± 0.0 MPa, 1.7 ± 0.2 MPa and 1.9 ± 0.1 MPa for the mixtures prepared using PM, CPM, BCC, DHS, FD, and ML methods (Figure 28). The mixture prepared using DHS method exhibited a remarkable improvement in tabletability compared to the mixtures prepared using PM, CPM and BCC methods. For example, the compression pressure increasing from 37 MPa to 222 MPa, the TS of tablets increased, from 0.2 MPa to 0.3 MPa and from 0.4 MPa to 1.4 MPa, for the mixture prepared using PM and DHS methods respectively (Figure 28) which implies that the DHS method resulted in an increase in the TS of tablets compared to PM method as fines from this product must have filled cavities between comparatively

larger particles and DHS showed smaller particles sizes compared to PM crystals (Table 14) (Aher *et al*., 2003; Di Martino *et al*., 2001). The mixtures prepared using, FD and ML techniques demonstrated additional enhancement of tabletability compared to DHS method. As the compression pressure increased from 37 MPa to 222 MPa, the TS of tablets prepared using FD increased from 0.8 ± 0.1 MPa to 1.7 ± 0.2 MPa. Meanwhile, the ML mixture increased from 0.7 ± 0.1 MPa to 1.9 ± 0.1 MPa (Figure 28). It is evident, that the PA–IBU mixture prepared using ML method showed the best compression properties among the mixtures under investigation, recording a TS of 1.9 ± 0.1 MPa at a compression pressure of 222 MPa. In comparison to the mixtures prepared using PM, CPM and BCC. Such superior tabletability is attributed to the decrease in particle size which is known to enhance tensile strength by an increase in the overall bonding area (Liu *et al*., 2013; Alderborn, 2002). Additionally, the ductile fracture caused by shear stresses in the mill could be assumed as, one of the contributing factors to the superior tableting performance of monoclinic PA mixed with IBU in comparison to PA and IBU mixed using the other methods as, IBU plastically deform during milling (Larsson and Kristensen, 2000; More *et al*., 2013) by covering the brittle PA. Furthermore, during compression crystal habit can also influence compaction profiles through its effect on the relative orientation of crystallites (Lin *et al*., 2017; Celik, 2011; Nokhodchi *et al*.,2008; Bandyopadhyay, 1998; Sun and Grant,1999; Wong and Pilpel, 1990; Garekani et al., 2000a and Garekani et al., 2000b). The ML

samples (Figure 24) depicts an irregular shape in comparison the other methods applied, and the better compaction is being observed in case of particles of more irregular size and shape (Aher *et al.*, 2013).

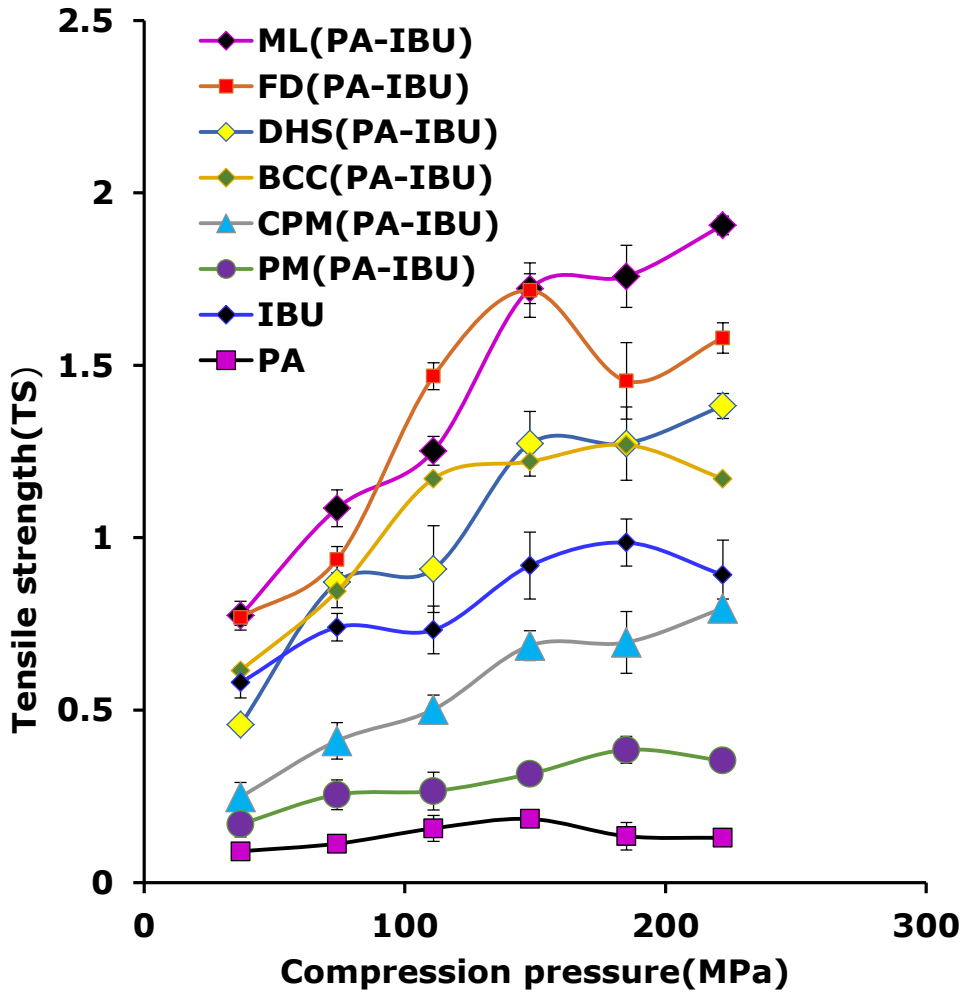

Figure 28. Tabletability profiles (mean ± SD, n = 5) for commercial paracetamol(PA), commercial ibuprofen(IBU) and the mixtures (PA:IBU, 5:2 *w/w*) prepared using physical mixing (PM), compact milling(CPM), batch cooling crystallisation(BCC), dry high shear (DHS), freeze drying (FD) and milling (ML).

6.6. Conclusions

In this study, the engineered crystals of PA–IBU mixtures displayed improved tableting properties in comparison to the commercial grades of PA, IBU, and their conventional physical mixture in the presence of (2% IBU *w/w*). The tablets obtained using the milling technique demonstrated far better tabletability results in comparison to the compact milling, batch cooling, dry high shear and freeze drying methods, which was due to their enhanced micrometric properties and strong hydrogen bonding interactions leading to improved mechanical properties between the PA and IBU particles. Thus, paracetamol and ibuprofen can be simultaneously milled to obtain engineered PA–IBU mixtures with improved mechanical properties.

7 CHAPTER 7: EFFECT OF VARIOUS PROCESSING METHODS ON PARACETAMOL–ASPIRIN–CAFFEINE MIXTURES

7.0. Introduction

Particle size reduction of pharmaceutical materials is frequently performed by applying micronisation methods which have been well discussed in (Section 1.8.1.2). Grinding (milling) technique has been employed over the years to improve the physicochemical properties of drugs (Al–Hamidi *et al*., 2013; 2010). Dichi *et al*. (2018) applied dry grinding technique to reinvestigate paracetamol–caffeine, aspirin–caffeine, and paracetamol–aspirin phase equilibria diagrams. On the other hand, Jain *et al*. (2014) formulated a eutectic mixture of aspirin−paracetamol with enhanced physico–mechanical properties in comparison to paracetamol and aspirin physical mixture which was well discussed in (Section.1.3.4).

Aspirin (acetylsalicylic acid, $C_6H_5C_3O_4H_4$) (ASP) is a drug widely used as antipyretic (pain reliever), anti–inflammatory (reduces swelling) and analgesic (fever reducer) mainly because of its high effectiveness, low cost and low toxicity (Brayfield, 2014; Linares *et al*., 2004) and it is administered extensively via the oral route (BNF, 2016). On the other hand, Caffeine ($C_8H_{10}N_40_2$; 1, 3, 7−trimethylpurine-2, 6−dione,) (CAF) is inexpensive, readily available and broadly used psychoactive drug in the world (Sahoo *et al*., 2015) and is widely used cold remedies for its stimulant action and consumed in coffee, tea and a variety of soft drinks (Dichi *et al*., 2014). Many pharmaceutical molecules including, CAF shows polymorphism which is a common phenomenon in pharmaceutical fields and possesses two known polymorphic structures the form *I* which is

stable at ambient pressure from the transition temperature (145 °C) to its melting point of 236°C and the Form *II* is stable polymorph at room temperature until 145 °C (Pinto *et al*., 2006; Dichi *et al*., 2014). However, it has poor flowability due to its needle–like shaped crystals leading to aggregates (Garekani *et al*., 2015; Jbilou et al., 2015). UK Medicines and Healthcare Regulatory Authority (MHRA) in 1991 first permitted the combination of PA and CAF for medical use (MHRA, 1991). Besides, the increase in the content of CAF in the mixture immensely enhances the solubility of paracetamol (Tkachenko *et al*., 2003).

The combination of PA, ASP and CAF is being used in the United Kingdom as Anadin extra, which contributes to the efficacy of oral analgesics with better performance than their individually active pharmaceutical ingredients. Therefore, in this study, two plastically deforming drugs (ASP and CAF) will be combined to enhance the tabletability performance of PA with no binder added and, it is more likely for hydrogen bonding interaction, to occur between these three drugs.

There is no published work which has attempted to increase the tableting performance of paracetamol with caffeine and aspirin by employing various processing methods. In order to avoid pseudo–polymorphs formation (Hydrates or solvates) of ASP and CAF, no water or organic solvent was introduced in the preparation of the samples.

Table 16. Some Chemical properties of aspirin and caffeine.

Product	**Physical properties**	**References**
Aspirin (ASP)	Melting point: 135 ºC Solubility (37 ºC) (10 mg/ml)	Chomcharn, and Xanthos, (2013)
	Enthalpy of fusion: $\Delta_{fus}h$ = 93.19 J g^{-1}	(Jain *et al.*, 2014)
	Solubility pH $_{(1.2)}$ (25 ºC): 0.061 mg/ml PKa (25 ºC): 3.5	(Rasool *et al.*, 2010)
Caffeine (CAF)	Melting point: 235.6 ºC Enthalpy of fusion: $\Delta_{fus}h$ = 104.9 J g^{-1}	(Klimova and Leitner, 2012)
	the solubility of (37.47± 1.01 mg/ml) in water at 37 ºC	(Sriamornsak and Kennedy,2007)
	pKa: 3.6	(Johnson and Rumon,1965)

7.1. Engineering of PA–ASP–CAF formulations

7.1.1. Physical mixing

PA, ASP and CAF (25:25:13 *w: w*) powders were mixed using low shear mixing technique as described in (Section 2.2.1.1).

7.1.2. Dry high shear mixing

PA, ASP and CAF (25:25:13 *w: w*) powders were blended for 1 min and 2 min by applying high shear mixing technique as described in (Section 2.2.1.2).

7.1.3. Milling

PA, ASP and CAF (25:25:13 *w: w*) powders were milled for 5 min (ML5) and 10 min (ML10) using milling method as described in (Section 2.2.1.7).

7.1.4. Tablet preparation

Each tablet has a weight of 565 ± 0.5 mg for the various formulations and 500 ± 0.5 mg for PA, ASP and CAF were compressed using the method described in (Section 2.14).

7.2. Results and discussions

7.2.1. Particle size distribution

All spans calculated from the ML and DHS data were higher than 2, indicating that the breadth of the distributions was relatively broad (Fan *et al.* (2005). Both commercial ASP and commercial CAF demonstrated smaller PSDs compared to PA. The physical mixing of PA–ASP–CAF

displayed reduced VMDs compared to PA. Meanwhile, the dry high shear (1 min & 2 min) and milling (5 min & 10 min) displayed significantly reduced PSDs compare to PA (Table 17). The PSDs (d_{10}% values) of PA–ASP–CAF mixture demonstrated subsequent order PM> DHS1=DHS2 > ML5 = ML10 (Table 17). It is remarkable that mixtures prepared using DHS and ML processes displayed a remarkable decrease in their VMDs as their span values increases which deduced their smaller PSDs. The reduced size in PSDs in the DHS (PA–ASP–CAF) (1 min & 2 min) could be due to higher energy applied to the mixtures. Meanwhile for the mixtures using milling (5 min & 10 min), the increase in the particle size due to the collisions between the metallic balls and the particles, as evident the increased in d_{10}% values (Table 17). The latter results will have an impact on powder properties such as compactibility and tensile strength.

Table 17. Particle size distribution (i.e. particle size at 10%($d_{10\%)}$,50%($d_{50\%,}$ median diameter and 90%($d_{90\%)}$ volume distribution and span) (mean ± SD, n=3) of commercial paracetamol (PA), commercial aspirin (ASP), commercial Caffeine (CAF) and PA–ASP–CAF mixtures co–processed using physical mixing (PM), dry high shear for 1min (DHS1), dry high shear for 2 min (DHS2), milling for 5 min (ML5) and milling for 10 min (ML10).

Product	$d_{10\%}$ **(µm)**	$d_{50\%}$ **(µm)**	$d_{90\%}$**(µm)**	**VMD (µm)**	**Span**
PA	254 ± 22	506 ± 30	911 ± 39.3	548 ± 30.2	1.3 ± 0
ASP	250.3 ± 7.2	423.3 ± 13	676 ± 22.5	444 ±11.5	1 ± 0
CAF	8.5 ± 0.1	52.3 ± 0.5	163.3 ± 1.1	72.3 ± 1	3 ± 0
PM(PA–ASP–CAF)	71 ± 1.2	388 ± 10.1	709 ± 34	401.3 ± 15	2 ± 0
DHS1(PA–ASP–CAF)	4.1 ± 0.2	26 ± 2.4	155 ± 3.5	55.3 ± 1	6 ± 0
DHS2(PA–ASP–CAF)	4.2 ± 0.1	28.3 ± 1	193.3 ± 6.4	62 ± 12	7 ± 0.2
ML5(PA–ASP–CAF)	3 ± 0	24.1 ± 1	110 ± 5	43.4 ± 2	4.4 ± 0.2
ML10(PA–ASP–CAF)	3 ± 0	29 ± 1.2	133.3 ± 28.3	49.3 ± 7	4.5 ±1

7.2.1. Scanning electron microscopy

Many pharmaceutical parameters such as flow properties and compaction characteristic of drug powder can be impacted by the morphology of the API, which makes it a vital parameter in the pharmaceutical process (Dhumal *et al*., 2010). (Figure 29) displays the SEM micrographs of PA, ASP, CAF and PA–ASP–CAF mixtures. PA morphology was explained in (Section 3.3.5), and ASP displayed an oblong shape meanwhile, CAF crystals exhibited a columnar shape (Figure 29), the physical mixture (PM) displayed a mix of crystal habits of the marketed products. Whereas, the SEM of all the engineered mixtures (DHS1, DHS2, ML5, ML10) showed an irregular crystal habit compared to their commercial components (Figure 29).

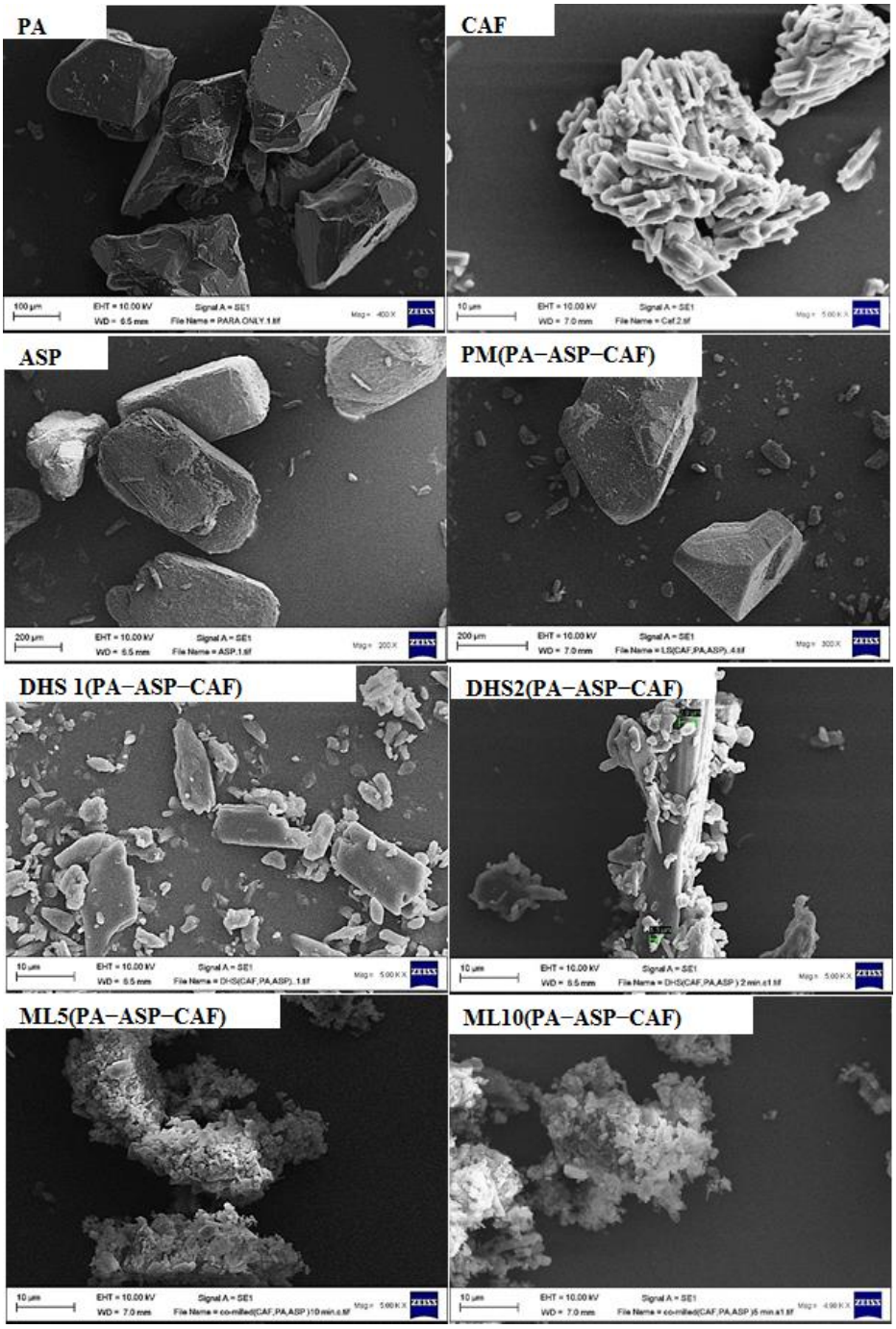

Figure 29. Scanning electron microscopy (SEM) and particles size distributions micrographs of commercial paracetamol (PA), commercial aspirin (ASP), commercial Caffeine (CAF) and PA–ASP–CAF mixtures co–processed using physical mixing (PM), dry high shear for 1min (DHS1), dry high shear for 2 min (DHS2), milling for 5 min (ML5) and milling for 10 min (ML10).

7.2.2. Solid state properties

7.2.2.1. Powder X–ray diffraction

The PXRD patterns of the various samples are shown in (Figure 30). The PXRD patterns of the commercial PA displayed various characteristic angles at 2θ values, as seen in (Section 3.3.4). Whereas the diffraction pattern of commercial ASP displayed different characteristic peaks specifically at 15.6°, 23.1° and 27.0° that were noticeable and the main peak at 15.6° was particularly distinctive (Lin, *et al.*, 2012). On the other hand, CAF (form *II*) showed prominent diffraction peaks at 12.06°, 24.1°, 26.4°, and 27.1° (Park and Yeo, 2008; Illangakoon *et al.*, 2014). The diffractogram of physical mixing PM (PA–ASP–CAF) displayed an overlap of the various characteristic peaks of Form *I* PA, ASP (form *I*) and (form *II* CAF) samples. Also, the PXRD patterns of the products obtained using dry high shear mixing (DHS1 (PA–ASP–CAF) and DHS2 (PA–ASP–CAF) and milling (ML5 (PA–ASP–CAF) and ML10 (PA–ASP–CAF) methods showed the same pattern that matches the sum of the marketed samples as observed in the physical mixing but with reduced peak intensities due to the differences in particle sizes. Regardless of the method employed, the engineered ternary mixtures showed the absence of any unstable forms from the marketed products (orthorhombic forms of PA, CAF form *I*), which is very important to the stability of the final product.

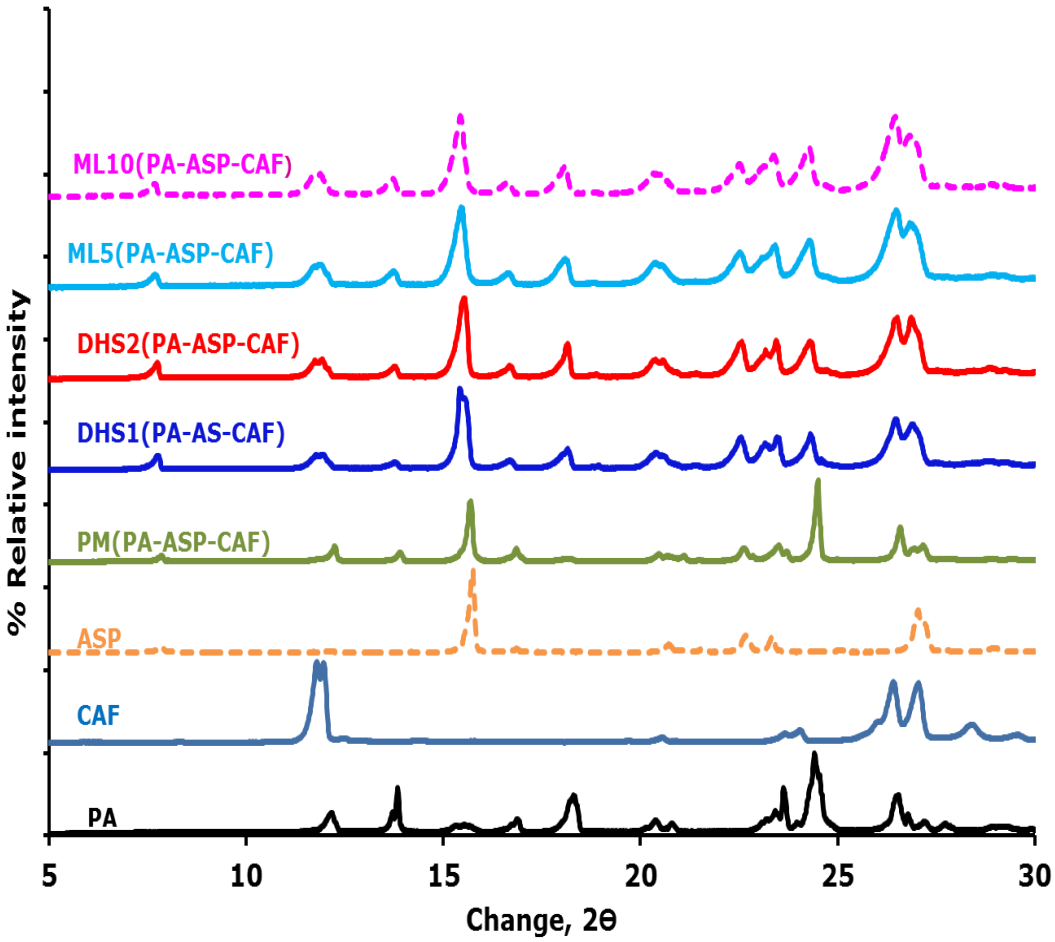

Figure 30. Powder X–ray diffraction of commercial paracetamol (PA), commercial aspirin (ASP), commercial Caffeine (CAF) and PA–ASP–CAF mixtures co–processed using physical mixing (PM), dry high shear for 1min (DHS1), dry high shear for 2 min (DHS2), milling for 5 min (ML5) and milling for 10 min (ML10).

7.2.2.2. Fourier transform infrared spectroscopy

FT–IR studies were conducted to explore the nature and extent of interactions between drugs in the solid state. The mixing or blending of

two or more drugs causes changes in the oscillating dipole of the molecules; this will manifest itself as changes in the frequency and bandwidth of interacting groups in the FT–IR spectra (Figure 31). If interaction existed between the various drugs, the functional groups in the FT–IR spectra will show band shifts and widening as compared to the spectra of the pure drugs before mixing (Figure 31). The FT–IR characteristic bands of the monoclinic form of PA (Table 5) were present in the spectra of commercial PA and all PA–ASP–CAF mixtures (Figure 31). The diagnostic bands of the PA orthorhombic form as discussed in (Section 3.3.4) were not present in the spectra of commercial PA and all PA–ASP–CAF mixtures indicating the presence of the PA monoclinic form in all the mixtures under study.

Analysis of the molecular structures of, PA as displayed in (Figure 1; Table 5), ASP and CAF as shown in (Table 18). Because of the presence of –NH and –OH in paracetamol's structure it suggests that H–bonding may exist between the N–H or O–H moieties (H donors) of PA with the carbonyl group (C=O, H acceptor) of ASP and two carbonyl groups (C=O, H acceptor) and one basic imidazole nitrogen group (proton acceptors) of CAF. Such intermolecular interactions should be revealed by shifts in the N–H, O–H, and C=O stretches. Additionally, the formation of hydrogen bonds or dipolar occurs between PA with other compounds having identical group(s) and the carbonyl groups have been reported (Grant *et al.*, 1980). The FT–IR spectra of PA, ASP, CAF and PA–ASP–CAF mixtures

are shown in (Figure 31). The physical mixture prepared using physical mixing showed insignificant changes in absorption intensities in comparison to the marketed paracetamol, suggesting a reduced interparticulate interaction between PA, ASP and CAF (Figure 31).

The mixtures prepared using dry high shear mixing (DHS1 and DHS2) showed minor reductions in absorption intensities (i.e., increased band broadening) between 3100 cm^{-1} and 3200 cm^{-1} compared with the peaks observed from marketed PA (Figure 31). The band broadening became more pronounced for the mixtures prepared using milling technique for five minutes and ten minutes at (ML5 and ML10) (Figure 31). This indicated a strong intermolecular hydrogen bonding between the PA, ASP and CAF mixtures compared to the mixture obtained using physical mixing. The mixtures prepared using milling technique (ML5 and ML10) showed decreases in the absorption intensities between 1605 and 1660 cm^{-1} (amide I, carbonyl stretch), between 1600 and 1620 cm^{-1} (skeletal aryl C–C stretch) and between 1500 and 1200 cm^{-1} (aryl C=H, C=H symmetric bending, C–0 stretch). The presence of weak hydrophobic interactions is observed in these mixtures due to the reductions in the absorption intensities between PA, ASP and CAF. However, with the physical mixing, there were no hydrophobic interactions between the drugs (Figure 31). A drastic reduction in absorption intensity was noticeable for PA–ASP–CAF mixtures prepared using milling technique in the region between 1605 cm^{-1} to 1656 cm^{-1} (C=0, keto–amide groups) of CAF. This indicated the intermolecular hydrogen bond interaction between

amide group of PA and carbonyl of CAF molecule via either one of the two keto–amide groups of CAF (N−H···O). Additionally, there was no shift or any reduction in intensities at 1755 cm^{-1} and 1692 cm^{-1}, which indicated that the two keto–amide groups of CAF overshadowed the one carbonyl group of ASP, implying insignificant interaction between the carbonyl of ASP and PA. This highlighted that the carbonyl groups of CAF were more prominent and formed strong hydrogen bonds with PA (Figure 31).

In conclusion, paracetamol and caffeine formed strong hydrogen bonding compared to PA and ASP. This implies that, the effect of introducing a competing two strong carbonyl groups (H bond acceptors) (CAF) in the presence of PA, the basic nitrogen preferentially forms O−H· · ·N hydrogen bonds; the N–H donor adhering to the rule that all good donors and acceptors are typically used in hydrogen bonding pairs.

Table 18. Chemical structure and FT–IR characteristic absorption bands of, aspirin (ASP) (Ajun *et al*., 2009), caffeine (CAF) (Illangakoon *et al*., 2014) and paracetamol (PA)(Section 3.3.5; Table 5).

Compound	Chemical structure	Characteristic FT–IR absorbance bands (cm^{-1})
CAF	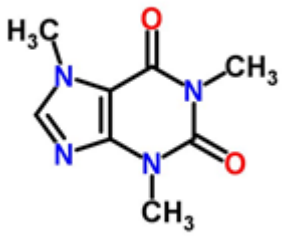	1650 cm^{-1}(C=O stretch) of the amide group; 1435 cm^{-1} and 1504 cm^{-1} (C=C stretch)
ASP	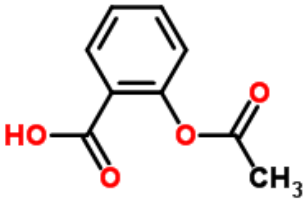	C=C (carbons of the Benzene ring) 1605 cm^{-1} ; 1755 cm^{-1} (=C–0 an ester), 1692 cm^{-1} (–C=0), 2500–3200 cm^{-1} (O–H)

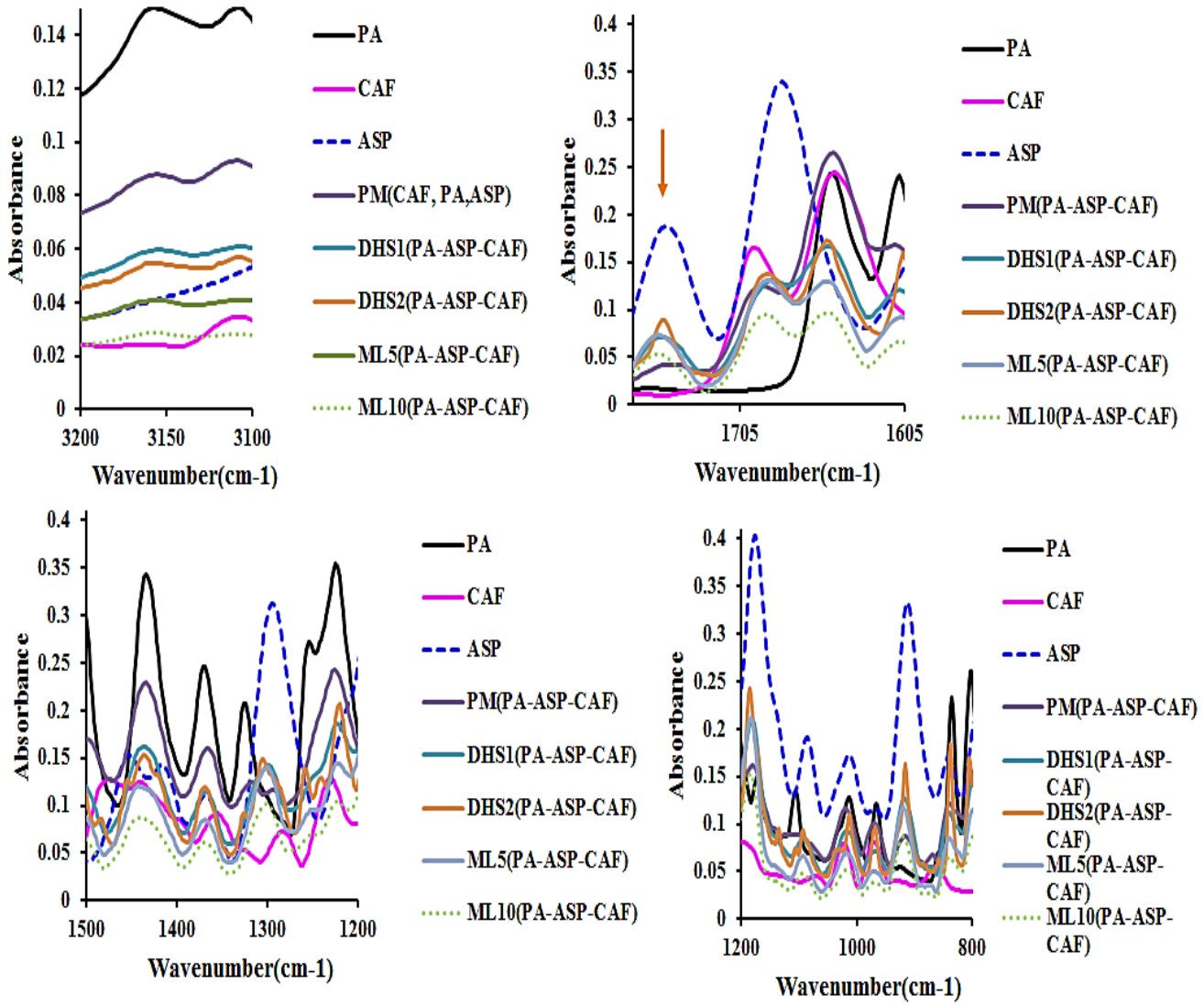

Figure 31. Fourier transform infrared spectroscopy (FT–IR) of commercial paracetamol (PA), commercial aspirin (ASP), commercial Caffeine (CAF) and PA–ASP–CAF mixtures co–processed using physical mixing (PM), dry high shear for 1min (DHS1), dry high shear for 2 min (DHS2), milling for 5 min (ML5) and milling for 10 min (ML10).

7.2.2.3. Thermogravimetric analysis

Figure 32 shows the TGA curves of the tested commercial drugs and their various co−processed mixtures. In the TGA curves, the decomposition of drugs depicted well–defined thermal events. The samples showed no weight loss below their melting points, which implies no surface water formation. The TGA curves showed that PA, ASP and CAF remained stable until 222.1 ºC, 183 ºC and 213.4 ºC. CAF and PA drugs weight loss is due to degradation at a higher temperature. Also, a mass loss event recorded a maximum of 363 ºC for CAF. ASP depicted two events at 187 ºC and 390.6 ºC. Above 150 ºC, two weight loss steps are shown as follows: (*1*) release of salicylic acid and acetic acid with the formation of an intermediary compound (ASP dimmers) and (*2*) thermal degradation of the intermediary compound (Edna *et al*., 2004). The data recorded by TGA confirm those shown in (Figure 32). It is noticeable that PM (PA–ASP–CAF) demonstrated no considerable weight loss below 387.3 ºC and begins to degrade due to its exposure to higher temperatures. ML10(PA–ASP–CAF) showed a further weight loss towards lower temperature, which could either be due to, the exposure of ASP sample to the harsh environment and the reduction in particles size (Figure 32, Table 17).

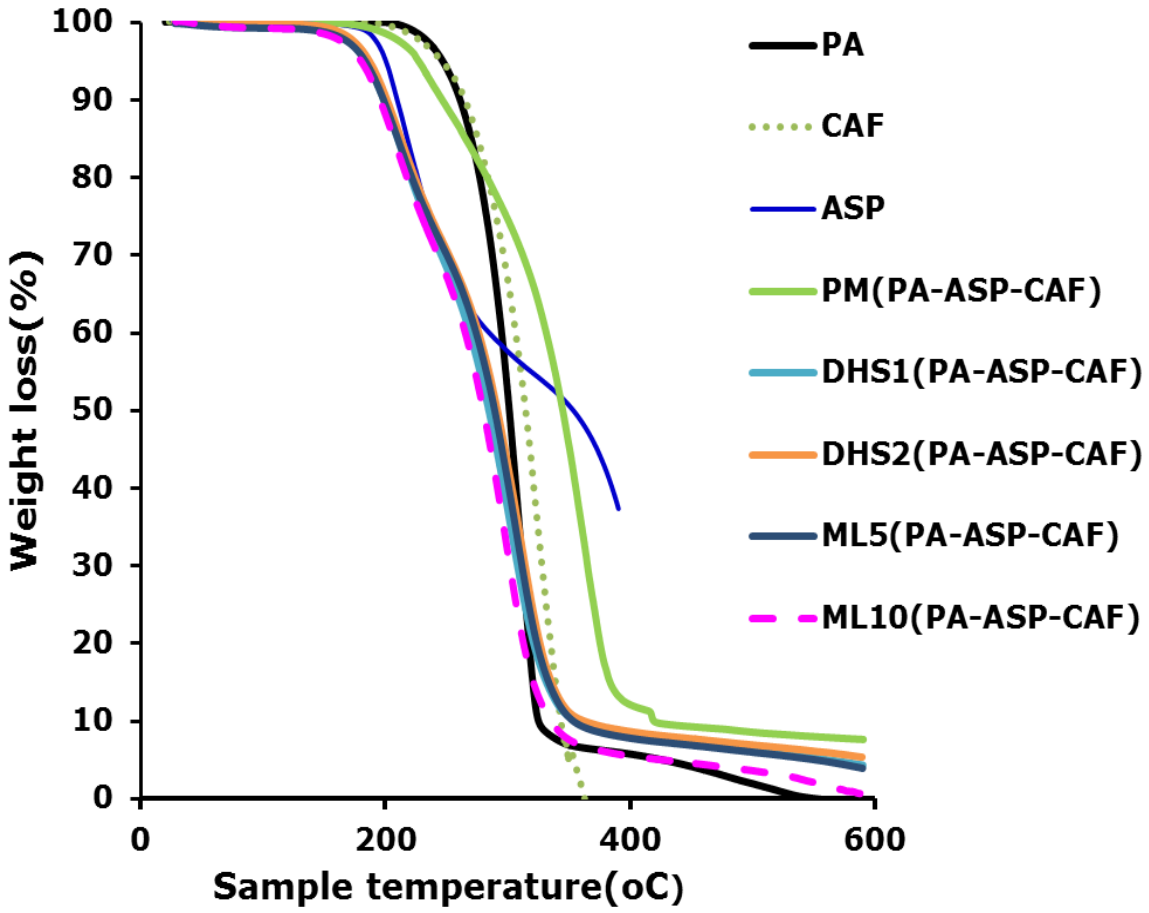

Figure 32. Thermogravimetric analysis (TGA) profiles of commercial paracetamol (PA), commercial aspirin (ASP), commercial Caffeine (CAF) and PA–ASP–CAF mixtures co–processed using physical mixing (PM), dry high shear for 1min (DHS1), dry high shear for 2 min (DHS2), milling for 5 min (ML5) and milling for 10 min (ML10).

7.3. Tableting properties

ASP is plastically deforming (Pedersen and Kristensen, 1994), CAF form *II* (plastically deforming and soft upon grinding (Ghosh *et al*., 2013).

PA is brittle and known to undergo brittle fracture as it exhibits poor tableting characteristics because the particles of this drug are very stiff and therefore, inter–particulate bonding is very weak (Joiris *et al*., 1998).

PA in this study displayed poor compactibility, as discussed in (Section 3.3.5). The presence of ASP and CAF increased the tensile strength of PA–ASP–CAF mixtures, regardless of the method of application (Figure 33). The TS of the PA–ASP–CAF mixtures compressed at 222 MPa was 0.76 ± 0.0 MPa, 1.9 ± 0.0 MPa, 2.4 ± 0.1 MPa, 2.4 ± 0.2 MPa and 3.4 ± 0.3 MPa for mixtures prepared using PM, DHS1, DHS2, ML5 and ML10 techniques (Figure 33). PA–ASP–CAF prepared using, PM displayed statically different tabletability results ($P<0.05$) compare to PA. Whereas, the mixture prepared using DHS1 and DHS2 methods exhibited a remarkable increased in tabletability compare to the mixtures prepared using PM (Figure 33) for example, as the compression pressure increases from 37 MPa to 222 MPa, the TS tablets increased from 0.3 MPa to 0.8 MPa, 0.7 MPa to 1.9 MPa and from 0.4 MPa to 2.4 MPa for the mixtures prepared using PM, DHS1 and DHS2 methods respectively (Figure 33) indicating that the DHS2 technique resulted in an increase in the tensile of tablets in comparison to PM and DHS1 over the compression range of 37 MPa to 222 MPa. The mixtures prepared using ML exhibited a further increase of

tabletability compare to the mixtures prepared using DHS technique when the compression pressure increased from 37 MPa to 222 MPa, the TS of tablets prepared using ML5 increased from 1.2 ± 0.1 MPa to 2.4 ± 0.1 MPa meanwhile, the mixture prepared by doubling the ML time improved from 1.3 ± 0.2 MPa to 3.4 ± 0.3 MPa (Figure 33) and gave the best tabletability result at compression pressure of 222 MPa in contrast to the other techniques applied. So, the increased tensile strength of the tablets using ML method compared to the other methods could be due to the higher content of fine particles as seen in (Table 18) which could also contribute to the increased surface area and increase inter−particulate forces which further increased the degree of particle deformation and increase in hardness (Cantor *et al*.,2009).

The mixture obtained using PM technique, all the drugs (PA, ASP and CAF) retained their initial shapes. Meanwhile, DHS1, DHS2 ML5 and ML10 demonstrated irregular shapes with ultrafine particles at their surfaces (Figure 29). Additionally, the pronounced hydrogen bonding interactions observed between PA, ASP and CAF especially, using the milling technique. The PA–ASP–CAF mixture prepared using ML (ML10) technique demonstrated a far better tensile strength (TS) (Figure 33).

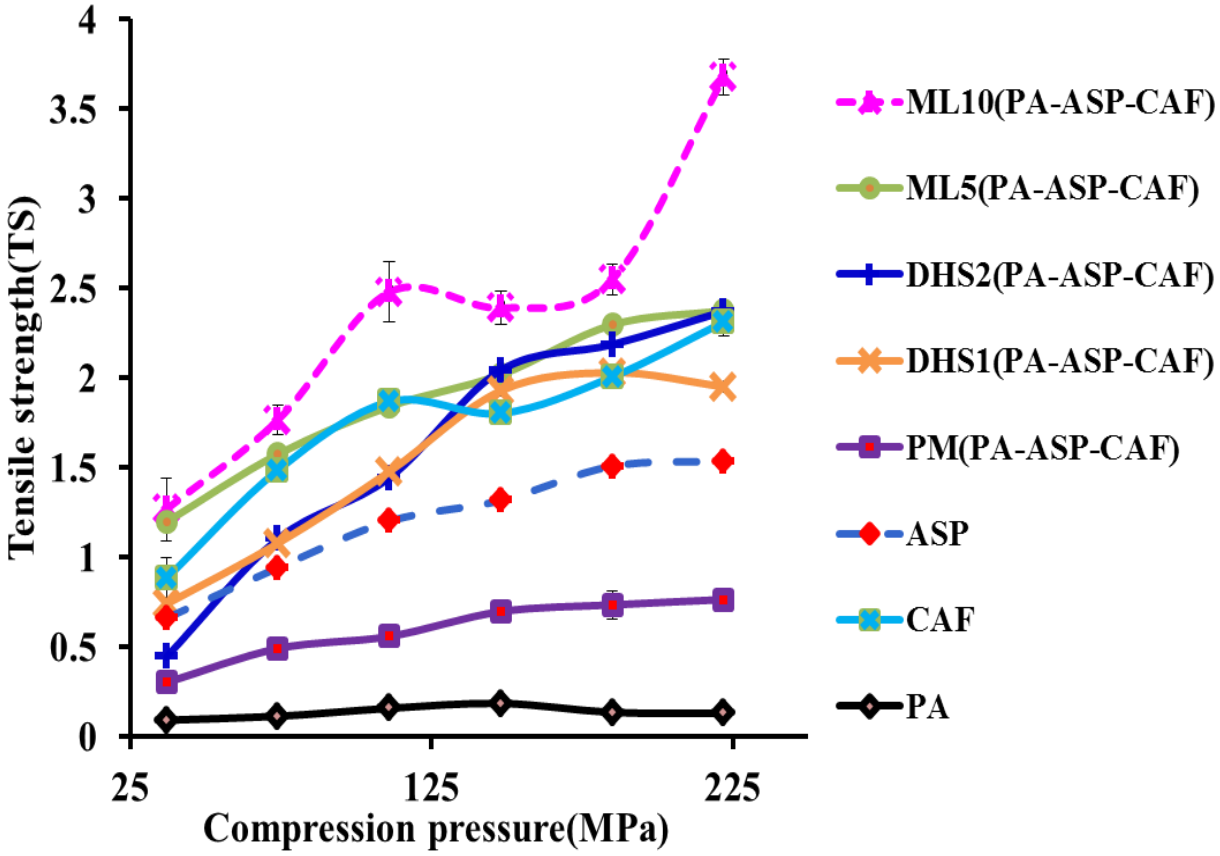

Figure 33. Tabletability profiles(mean ± SD, n = 5), of commercial paracetamol (PA), commercial aspirin (ASP), commercial Caffeine (CAF) and PA–ASP–CAF mixtures co–processed using physical mixing (PM), dry high shear for 1min (DHS1), dry high shear for 2 min (DHS2), milling for 5 min (ML5) and milling for 10 min (ML10).

7.4. Conclusions

Engineered mixtures of PA–ASP–CAF gave better tablets with enhanced tensile strength in comparison to the individual marketed form of PA and ASP and their usual physical mixture, which could be due to their enhanced micrometric properties, morphological features and the drastic reduction in absorbance intensity leading to the increased mechanical properties of the PA–ASP–CAF powders. Milling technique used for 10 min of the PA–ASP–CAF mixture gave the best tablets. Thus, PA, ASP and CAF can be simultaneously milled to acquire engineered PA–ASP–CAF mixtures with improved mechanical properties.

8 CHAPTER 8: PREPARATION OF PARACETAMOL–5– NITROISOPHTHALIC ACID COCRYSTALS USING VARIOUS ENGINEERING METHODS

8.0. Introduction

A cocrystal is a multiple component crystal in which all components are solid under ambient conditions when in their pure form. These components co–exist as a stoichiometric ratio of a target molecule or ion and a neutral molecular cocrystal former(s)(Shan and Zaworotko, 2008).

It has been shown that, paracetamol can form cocrystals with pyridines, carboxylic acid (Sander *et al.*,2010) and, bipyridines as shown by, Oswald *et al.*,2002 who demonstrated various multi–components crystal forms of PA with 1,4–dioxane, 4,4–bipyridine, *N*–methylmorpholine, *N*,*N*–dimethylpiperazine, morpholine and piperazine. Additionally, a new ternary cocrystal containing paracetamol, piperazine and ethanol was obtained at elevated pressure via formation of the intermolecular interaction of ArO–H of paracetamol and amine (N–H) piperazine (Oswald and Pulham, 2008).

From some systematic studies on cocrystals, it was recognised that, in general, all good hydrogen bond donors and acceptors would be used in hydrogen bonding formation; which is of great importance to the design of the cocrystals. As it was noted that, the best hydrogen bond acceptor in a given crystal structure, is inclined to interact with the best hydrogen bond donor (Trask *et al.*, 2006). PA and its cocrystal forms have shown that hydrogen–bonded PA… PA chains are robust motifs that commonly occur either through phenol (O–H …O=C) interactions or through the

coformer moieties which accept hydrogen bonds from the phenolic H, through N−H…0=C interactions (Oswald *et al*., 2002).

5− Nitroisophthalic acid (5NIP) (Figure 34) possesses functional groups which can generate hydrogen–bond motifs (supramolecular synthons) with PA. The coformer (5NIP) contains two carboxylic acid groups that can act as hydrogen–bond donors and acceptor, respectively. It is expected that PA and 5NIP can interact via formation of heterosynthons between amide···carboxylic acid functional groups.

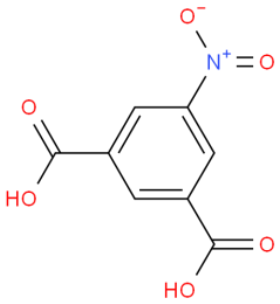

Figure 34. Chemical structure of 5–Nitroisophthalic acid (5NIP).

Additionally, 5NIP has been employed as a coformer in the cocrystallisation with active ingredients including; paracetamol, levetiracetam, etiracetam, carbamazepine and dapsone (Hiendrawan *et al*.,2016; George *et al*., 2014; Fleischman *et al*., 2003; Smith and Wermuth, 2013).

Over the past years, several authors have studied the enhancement of the physicomechanical properties of different APIs. However, no marketed drug products utilise cocrystals despite, the positive application of

cocrystallisation to influence the physical properties of a drug, which could be due to the thermodynamic stability of cocrystals (Schartman, 2009).

In this investigation, the formation of pure cocrystals of PA and the coformer (5NIP) were attempted through different techniques including; slow cooling crystallisation, water evaporation, dry milling, high shear, freeze−drying and wet−milling. The wet−milling process performed at different milling times (1s, 1min, 10 min, 15 min, 20 min and 30 min) and using various solvents (hexane, acetone, methanol, water, butanol and ethanol). The processing techniques including, milling time and solvents were used to produce pure cocrystals were achieved only with slow cooling with methanol, slow cooling with water and wet−milling (methanol, butanol and ethanol) for 30 min.

No published work is available in the presence of different techniques to improve the physicomechanical properties of PA via PA−5NIP cocrystal formation.

8.1. Engineering of PA−5NIP formulations

8.1.1. Effect of various preparation methods.

(*i*) Low shear mixing

An equimolar mixture of paracetamol and 5−Nitroisophthalic acid (PA−5NIP) powders was prepared using low shear mixing technique as described in (Section 2.2.1.1).

(*ii*) Milling

An equimolar mixture of paracetamol and 5−Nitroisophthalic acid (PA−5NIP) powders) were milled for 30 min after adding 5 mL of different solvents including; ethanol, butanol and methanol and applying the milling method as described in (Section 2.2.1.7). All the mixtures were kept in the fume cupboard for 24h for complete evaporation of the solvents and were stored in a sealed glass vial for at least seven days at the laboratory conditions (22 ºC, RH = 50%). The engineered powders were sieved as described in (Section 2.3).

(iii) Cooling crystallisation

(6% *w/v*) solutions of an equimolar mixture of paracetamol and 5–Nitroisophthalic acid (PA−5NIP) were prepared by dissolving PA–5NIP in 200 mL of deionised water under stirring (200 rpm) at 70 ºC and methanol (without heat). The resultant clear solution was left uncovered in laboratory conditions for five days using batch cooling crystallisation method as described in (Section 2.2.1.4). The cocrystals obtained were sieved using the technique described in (Section 2.3).

8.2. Results and Discussions

8.2.1. Scanning electron microscopy and particle size distribution

(Figure 35) displays micrographs of PA, 5NIP, PM (PA–5NIP) and PA–5NIP cocrystals powders. The PM (PA–5NIP) and 5NIP crystals exhibited angular habits. The SEM micrographs under high magnification revealed

that the cocrystals prepared using various techniques including, SCW (PA–5NIP) showed irregular shape whereas, and SCM (PA–5NIP) displayed agglomerates consisting of needle–shaped individual cocrystals entangled. MLM (PA–5NIP), MLB (PA–5NIP) and MLE (PA–5NIP) powders displayed an irregular shaped structure.

The mixture of PA and 5NIP prepared using low shear mixing method PM (PA–5NIP) displayed a decrease in mean diameter (VMD) compared to the marketed PA (Table 19) this could be due to the molar ratio differences between PA and 5NIP; as 5NIP particles whose VMD values are higher compared to PA (Table 19) as affirmed by SEM micrographs (Figure 35). On the other hand, the cocrystals of PA–5NIP obtained using both cooling crystallisation, and milling techniques demonstrated a drastic reduction in VMDs values compare to the commercial PA and PM (PA–5NIP) (Table 19), and their PSDs showed statistically different results ($P<0.05$). This is affirmed by the SEM observations, which showed a difference in the structure of mixtures prepared using milling and slow cooling crystallisation methods (Figure 35). As it should be noted that the largest mean size diameter of the cocrystals recorded was around 232 ± 18.2 µm in comparison to the PA and 5NIP starting materials which were around 548 ± 30.2 µm and 826.3 ± 3.3 µm.

The slight reduction in the bulk for the mixture prepared using PM method compared to PA is due to the presence of 5NIP powders whose bulk and tap density values are smaller than those of PA (Table 19). Whereas, all

the cocrystals prepared using both slow cooling crystallisation and milling techniques showed higher CI values which is consistent with the patterns in bulk and tap density changes compared to PA (Table 19) and, as confirmed by the SEM micrographs displayed in (Figure 35).

Table 19. Particle size distribution (i.e. particle size at 10%(d_{10}%), 50%(d_{50}%, median diameter and 90%(d_{90}%) mean diameter (VMD) (mean ± SD, n=3), bulk density (D_b), tap density (D_t), cohesivity (1/b) and Carr's index (CI) (mean ± SD, n=3) of PA, 5NIP, physical mixing(PM) and PA−5NIP cocrystals prepared using slow cooling crystallisation and wet−milling.

Product	$d_{10\%}$ **(µm)**	$d_{50\%}$ **(µm)**	$d_{90\%}$ **(µm)**	**VMD (µm)**	$D_{b(g/cm^3)}$	$D_{t(g/cm^3)}$	**1/*b***	***CI* (%)**
PA	254 ± 22	506 ± 30	911 ± 39.3	548 ± 30.2	0.8 ± 0	0.8 ± 0	4 ± 0	3.2 ± 0.3
5NIP	14 ± 0.2	280 ± 18.3	2217 ± 6	826.3 ± 3.2	0.5 ± 0	0.73 ± 0	6 ± 0	32.7 ± 1.5
PM(PA-5NIP)	62.3 ± 10	439 ± 23	866 ± 40.3	461.3 ± 26	0.62 ± 0	0.84 ± 0	3 ± 0	26.7 ± 0.6
SCW(PA-5NIP)	5.2 ± 0	42.1 ± 0	226 ± 2	84.1 ± 0.3	0.4 ± 0	0.4 ± 0	7 ±1.1	37.0 ± 0.0
SCM(PA-5NIP)	5.2 ± 0	155 ± 9	396 ± 7	1756 ± 3.5	0.5 ± 0	0.7 ± 0	4 ± 0	32.0 ± 0.0
MLM(PA−5NIP)	20.2 ± 1.1	192 ± 16.1	441 ± 21	213 ± 13	0.6 ± 0	0.8 ± 0	8 ± 0	28.0 ±0.0
MLB(PA-5NIP)	6.4 ± 0	86 ± 6	386.3 ± 34.1	147.3 ± 12	0.5 ± 0	0.8 ± 0	27 ± 0	37.0 ± 0.0
MLE(PA-5NIP)	17 ± 0.4	210.3 ± 8.1	489.3 ± 52.3	232 ± 18.2	0.6 ± 0	0.82 ± 0	9 ± 3.3	29.3 ± 0.6

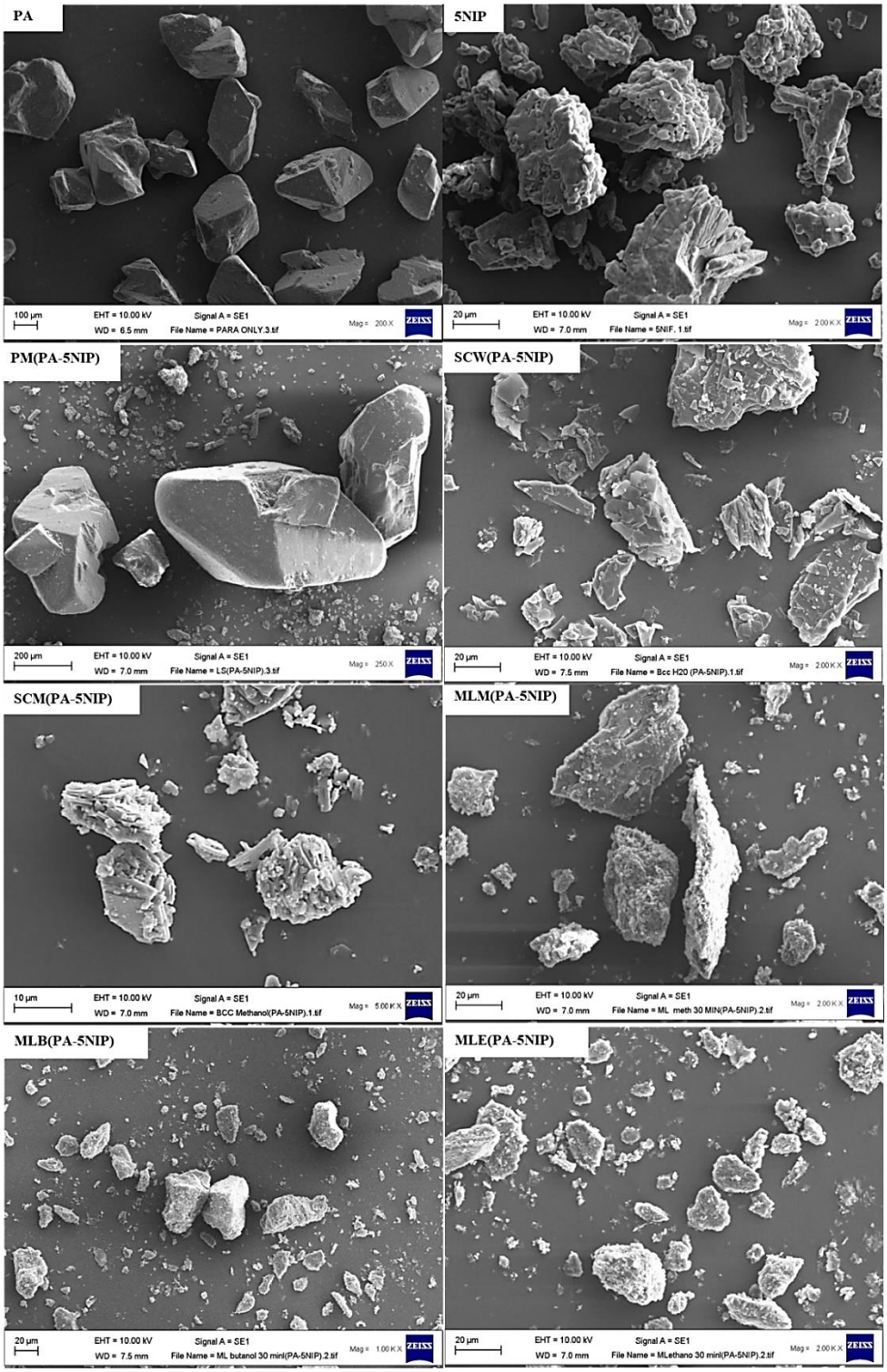

Figure 35. Scanning electron microscopy micrographs of PA, 5NIP, physical mixing (PM) and PA−5NIP cocrystals prepared using slow cooling crystallisation and wet−milling.

8.3. Solid state properties

8.3.1 Powder X–ray diffraction

In the solid state, the formation of a new crystalline phase can be categorised by applying PXRD and DSC to monitor the phase purity of the cocrystals formed using various preparation methods. The binary mixture of the components under consideration with the molar ratio (1:1) was coprocessed using PM, SCW, SCM, MLM, MLB and MLE.

The PXRD analysis was carried out for Commercial PA, commercial 5NIP, PM (PA–5NIP) and all the cocrystals of PA–5NIP coprocessed using SCW, SCM, MLM, MLB and MLE techniques as shown in (Figure 36). The commercial PA's PXRD pattern, as displayed in (Figure 26) possessed characteristic peaks which are well discussed in (Section 3.3.3). Whereas, the commercial 5NIP displayed characteristic peaks at 2θ values of, 18.01°, 20.37°, 21.32°, 23.83° and 28.60°. The diffractogram of the physical mixture presented an overlap of the characteristic peaks of each component; whereas, the cocrystals prepared showed a singular pattern that matches neither, each species nor the sum as observed in the physical mixing (Figure 36). The diffractogram of SCW (PA–5NIP) and SCM (PA–5NIP) cocrystals showed identical characteristic peaks at 2θ values of 5.38°, 11.20°, 18.79°, 21.31°, 25.68° and 27.45°). Whereas, the cocrystals of PA–5NIP obtained using wet–milling technique in the presence of methanol (MLM(PA–5NIP)); butanol(MLB(PA–5NIP)) and ethanol(MLE(PA–5NIP)) displayed characteristic peaks at 2θ values at

(5.40°, 11.31°, 18.92°, 21.42°, 25.79°, 27.44°); (5.47°, 10.91°, 18.94°, 21.48°, 25.63°, 27.44°) and (5.52°, 11.36°, 18.82°, 21.49°, 25.92°) and 27.57°). All the cocrystals obtained using the various techniques in this research are corroborating with the formation of a new crystallographic structure, suggesting that these samples are pure cocrystals. The diffraction patterns obtained from all the cocrystals were closer to the result obtained from the pure cocrystal of PA–5NIP diffraction pattern obtained using rapid solvent evaporation technique (Hiendrawan *et al*., 2016).

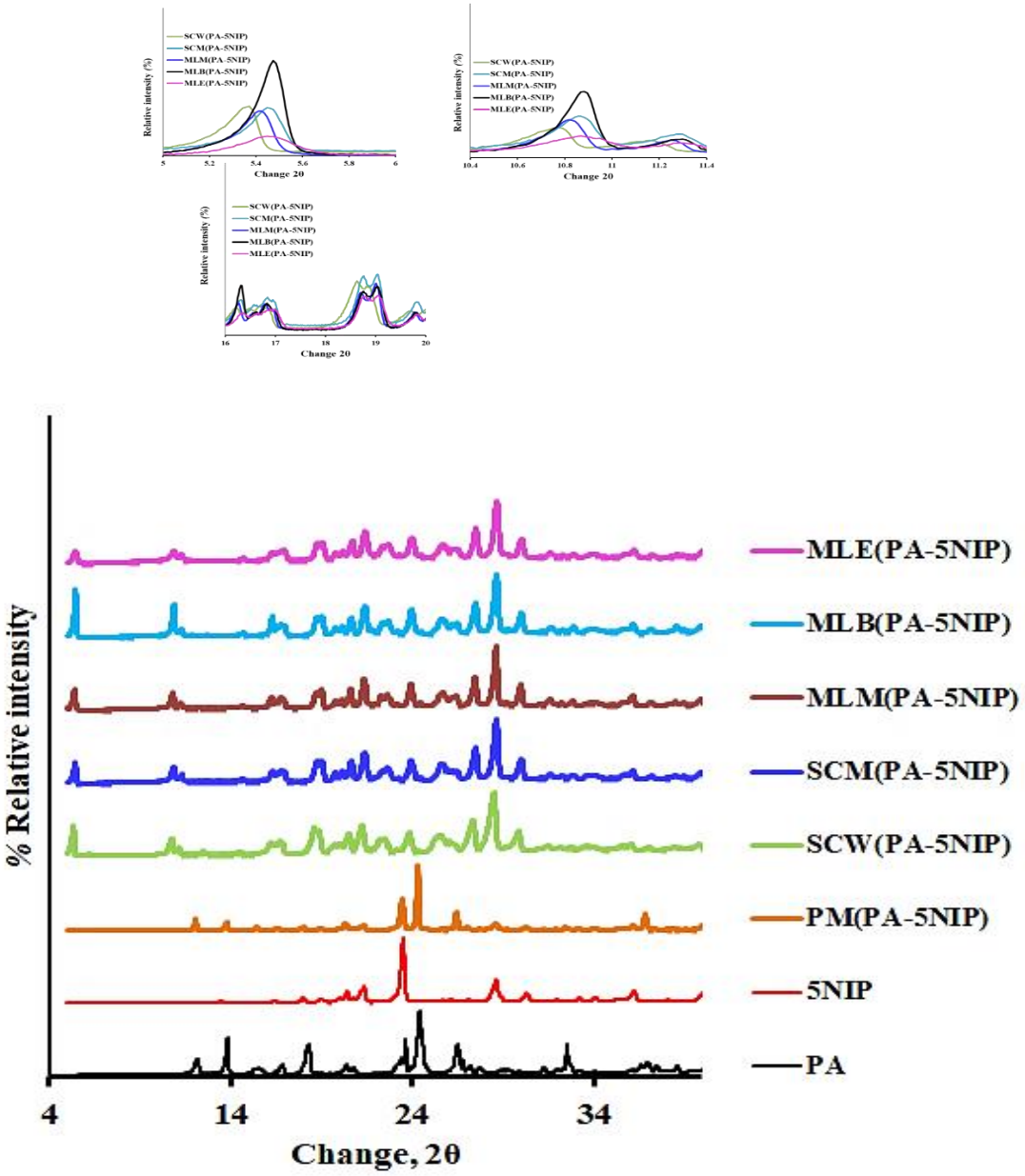

Figure 36. Powder X–ray diffraction of PA, 5NIP, physical mixing (PM) and PA–5NIP cocrystals prepared using slow cooling crystallisation and wet–milling and reduction in % of relative crystallinity in comparison to their specific peaks.

8.3.1.2. Fourier transform infrared spectroscopy

Formation of cocrystal or a eutectic is dependent on the dominance of heteromeric and homomeric molecular interactions in a given combination of materials. Various factors like nature of intermolecular interactions and supramolecular synthons, functional group disposition and complementarity, interaction strength, and packing efficiency play a vital role in the formation of eutectic or cocrystal (Cherukuvada, 2016).

Furthermore, the presence of functional groups including, amides and carboxylic acids provide an ability to engage in a supramolecular event with cocrystal formers, which possesses complementary hydrogen bond donor and acceptor sites, thus forming pharmaceutical cocrystals (Padrela *et al*., 2009). The FT−IR spectra of PA, 5NIP and PA−5NIP cocrystals are shown in (Figure 37). From the chemical structures of PA and 5NIP, the coformer (5NIP) possesses two carboxylic groups in its structure, which are functional groups particularly amenable to the formation of supramolecular hetero–synthons with complimenting a functional group including, the amide group found in the structure of PA, providing evidence of the new hydrogen bond (NH……O and HO…C=O). Also, bonds between the acid and each paracetamol represent the fulfilment of the 'best-donor–best–acceptor' rule, whereby the acid and the basic nitrogen play these respective roles (Trask *et al*.,2006).

PA shows characteristic absorption peaks at 1630 cm^{-1} and 3304 $cm^{-1,}$ which are assigned to C=O and N–H stretching of the secondary amide (Figure 37). Whereas, the spectrum of 5NIP has peaks corresponding to

carboxylic C=O and O–H stretching at 1697 cm^{-1} and 2939 cm^{-1}, respectively (Figure 37) suggesting the structural units of the hydrogen–bonded carboxylic acid dimers form in the 5NIP crystalline lattice. The spectrum of the PA–5NIP cocrystal has three new distinctive peaks at 1611.77 cm^{-1}, 1695.42 cm^{-1} and 1697.46 cm^{-1} that did not exist before and which are assigned to C=O stretching of the amide group in PA and the two carboxylic acid groups in 5NIP, respectively (Figure 37). The shift in the C=O stretching frequency from 1646.41cm^{-1} and 1626 cm^{-1} in the component phases to 1611.77 cm^{-1} and 1696.42 cm^{-1} in the cocrystal implies that the C=O groups participate in weaker hydrogen bonds accompanying cocrystal formation. A hypsochromic shift in the O–H and N–H stretching frequency verifies the formation of weaker hydrogen bonds is accompanying cocrystallisation in absorption bands at 3348.00 cm^{-1} and 3464.29 cm^{-1}. We also pointed out the carbonyl stretch C=O of PA−5NIP cocrystal showed stretching band at 1697.46 cm^{-1}, indicated that the carboxylic acid group is in the neutral state thus, confirms that proton transfer did not occur between PA and 5NIP and the resulting product was a cocrystal (Trask *et al.*, 2006).

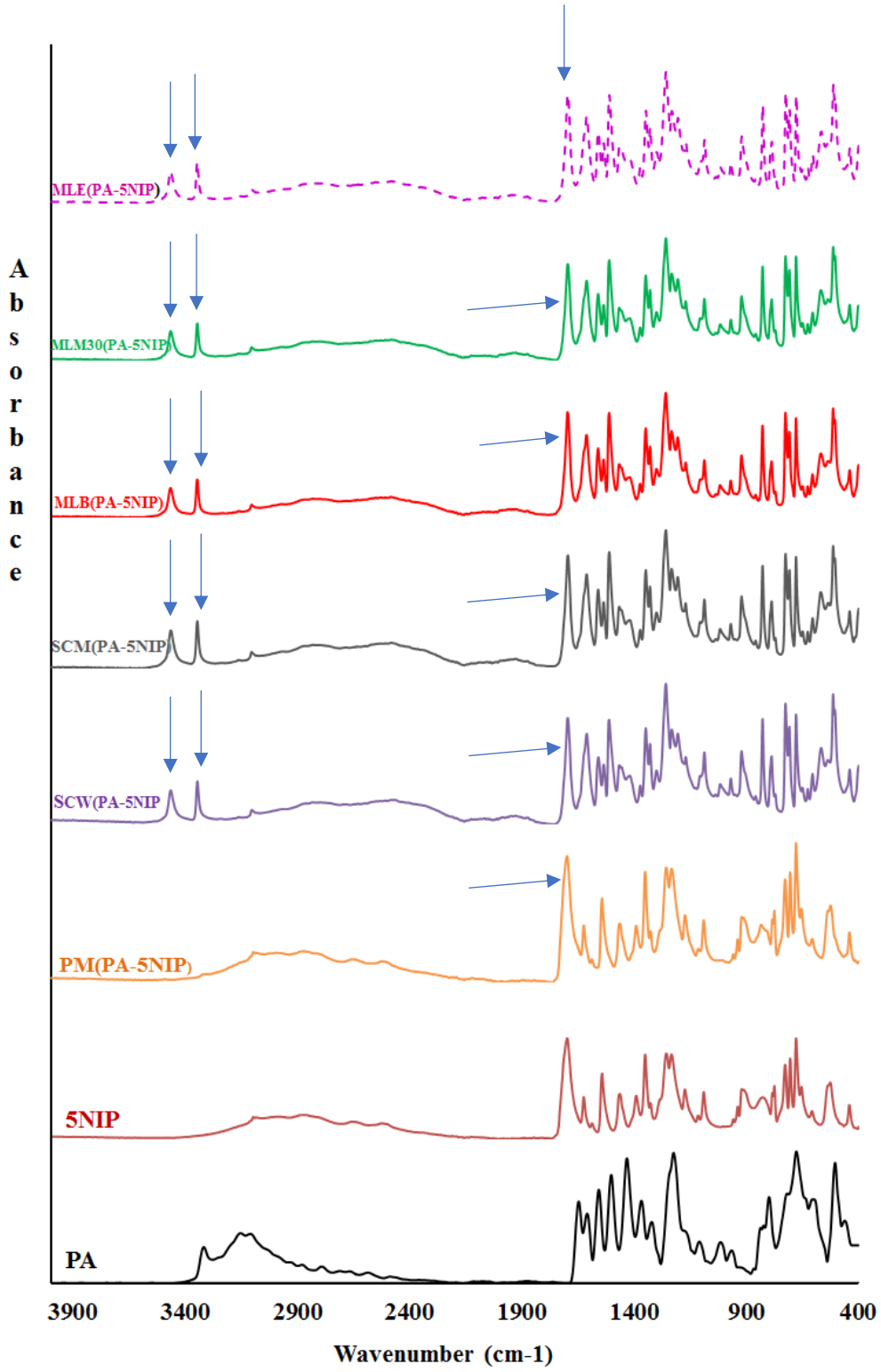

Figure 37. Fourier transform infrared of PA, 5NIP, physical mixing (PM) and PA−5NIP cocrystals prepared using slow cooling crystallisation and wet−milling.

8.3.1.3. Thermal analysis

DSC experiments were carried out to investigate the thermal behaviour of PA, 5NIP, and 5NIP physical mixture (1:1 molar ratio) and PA–5NIP cocrystals (Figure 38). It shows that PA and 5NIP exhibited an endothermic melting peaks at (169.3 ± 0.3) °C and (261.5± 0.7) °C as shown in (Table 20; Figure 38) indicating their melting points and the PA–5NIP cocrystals exhibited single endothermic melting point (Figure 38). The melting temperatures of all the cocrystals were between corresponding pure starting solids (Figure 38). Whereas, that DSC analysis of the physical mixture of PA and 5NIP (1:1 molar ratio); PM (PA–5NIP) showed three endothermic peaks (Figure 38); First endothermic peak at (171.1 ± 0.7) °C is ascribed as cocrystal eutectic melting with an excess of high–melting component. The second peak at (211.9 ± 0.3) °C could be the melting point of the cocrystal, followed by the endothermic peak (264.7± 0.1) °C corresponding to the decomposition of cocrystal as confirmed by thermal gravimetric analysis (TGA) results whereby PA, 5NIP and PA–5NIP cocrystals were thermally stable until 254 ºC, which agrees for degradation temperatures reported previously for PA (Section 3.3.4) (Figure 38). In conclusion, the phase purity of cocrystals was established based on the absence of characteristic peaks of 5NIP and PA in the PXRD pattern and clean baseline and unique melting temperatures in DSC thermograms of the pure cocrystals obtained.

Table 20. Thermal properties of PA, 5NIP and the five cocrystals of (PA–5NIP (n=3).

Product	Onset temperature (°C)	Peak temperature(°C)	Enthalpy(j/g)
PA	169.3 ± 0.3	170.8 ± 0.3	164.5 ± 0.6
5NIP	261.5 ± 0.7	263.1 ± 0.7	160.0 ± 0.2
SCW(PA–5NIP)	206.1± 0.1	208.5 ± 0.1	153.9 ± 0.1
SCM(PA–5NIP)	206.5± 0.8	209.1 ± 0.8	150.7 ± 0.6
MLM(PA–5NIP)	204.9± 0.7	207.0 ± 0.7	149.7 ± 0.4
MLB(PA–5NIP)	204.7± 0.4	206.7 ± 0.4	152.9 ± 0.6
MLE(PA–5NIP)	204.6± 1.2	206.8 ± 1.2	154.8 ± 1.3

TGA was conducted to analyse the changes in cocrystals weight in comparison to the change of temperature (Figure 39). TGA curve showed no weight loss on PA–5NIP cocrystals until their various melting points which indicates the absence of solvate or hydrate rather than PA–5NIP cocrystals. TGA of PA–5NIP cocrystal also showed a mass loss after its melting point, which could be attributed to the degradation of the cocrystal (Figure 39).

The amount of water present in all the mixtures was less than 1% (Table 21).

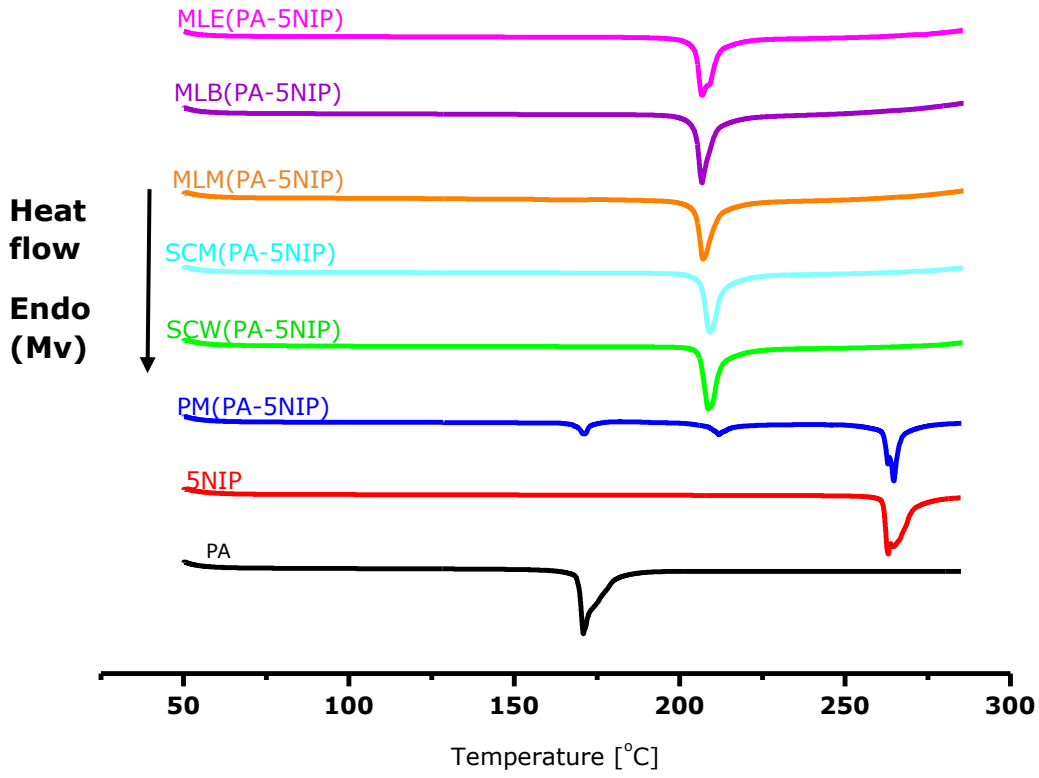

Figure 38. Differential Scanning calorimetry of PA, 5NIP, physical mixing (PM) and PA−5NIP cocrystals prepared using slow cooling crystallisation and wet−milling.

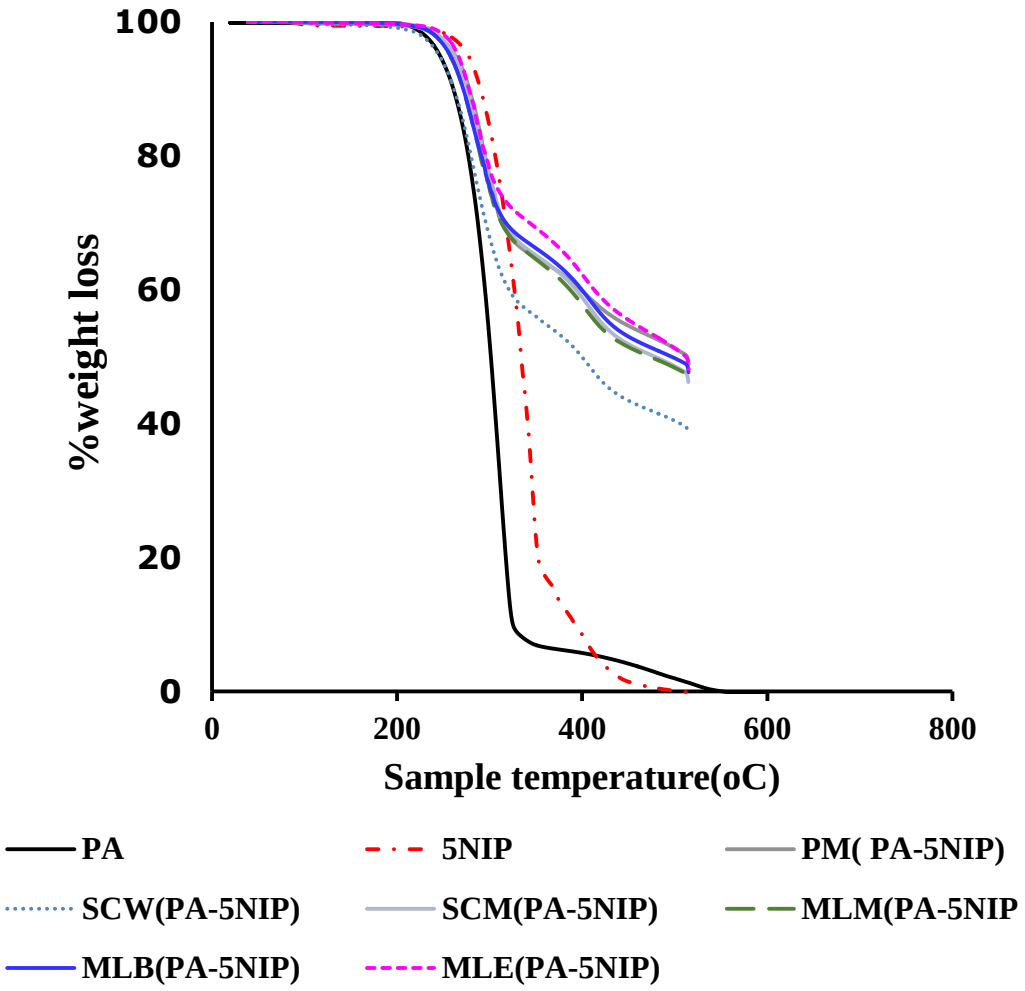

Figure 39. Thermogravimetric analysis of PA, 5NIP, physical mixing (PM) and PA−5NIP cocrystals prepared using slow cooling crystallisation and wet−milling.

Table 21. Percentage of crystallinity and Water content (n=3) recorded of PA, 5NIP, physical mixing (PM) and PA−5NIP cocrystals prepared using slow cooling crystallisation and wet−milling.

Product	Percentage of Crystallinity (%)	% Moisture content
PA	100%	0.2 ± 0
5NIP	99%	0.5 ± 0
PM (PA–5NIP)	96%	0.4 ± 0
SCW (PA–5NIP)	36.2%	0.4 ± 0
SCM (PA–5NIP)	34.9%	0.2 ± 0
MLM (PA–5NIP)	32.6%	0.6 ± 0
MLB (PA–5NIP)	30.2%	1 ± 0
MLE (PA–5NIP)	28.7%	0.7 ± 0

8.3.1.4. Relative humidity (*Rh*) and stability comparison

Due to the practical effects of hydrate formation upon processing, formulation, packaging and storage, the stability of solid drug material relative to atmospheric moisture is vital to the pharmaceutical industry. Thus, the stability profiles of 5NIP and all the cocrystals (PA–5NIP) were performed to assess whether these cocrystals offered enhanced physical stability profiles after being stored at 75% RH for six months and, further compared to the PXRD patterns of the samples before exposure. The results of PXRD analysis displayed that PXRD patterns of 5NIP and all the

PA–5NIP cocrystals stay the same (SM 3). All the PA–5NIP cocrystals investigated under the accelerated humidity condition were all physically stable, which indicates the non–hygroscopicity of the synthesised molecular cocrystals.

8.3.1.5. Tableting properties

The cocrystal powders were compressed into tablets to examine their mechanical behaviour in dependence of the solid–state form of the PA. Compactability was investigated by plotting the tensile strength of the tablets as a function of compaction pressure (Figure 40). This observation can be explained by either 5NIP or the cocrystal formation, changing the tableting behaviour of the PA. In other to eliminate the influence of 5NIP, a physical mixture of PA and 5NIP was tableted at different compaction pressures. The compactability of this physical mixture was lower compared to that of the cocrystal powders across the compaction range of 37 to 222 Mpa. Even though the crushing strength of 5NIP compacts was increased from 37 Mpa to 111 Mpa but suddenly decreased with further compression pressure. Also, severe lamination was observed at 148 Mpa, an indication of poor compactibility.

The results displayed in (Figure 40) showed an increased tabletability of paracetamol which resulted due to the formation of 1:1 cocrystal of PA and 5NIP. Hiendrawan *et al.* (2016) reported the formation of PA cocrystal using 5NIP as a coformer by applying rapid solvent evaporation technique which displayed an enhancement in the tabletability property.

During the tabletability test using 29.4 KN compaction pressure, tablets of PA–5NIP showed tensile strength value of 2.78 MPa. This study revealed that tabletability properties of the reported PA–5NIP cocrystal were superior to the past study using wet milling. MLE(PA–5NIP) demonstrated the highest tensile strength, compared to the others (SCW, SCM, MLM and MLB) could be due to the drastic reduction in crystallinity which is known to impact the tabletablity performance of powders by increasing their tensile strength (Kaialy *et al.*, 2016)(Table 21) or it was also suggested that MLE (PA–5NIP) might have different molecular packing compared to the other cocrystals due to its slightly reduced melting point (Walsh *et al.*, 2002)(Figure 38) or maybe MLE (PA–5NIP) has higher slip planes in its crystal structure compared to other cocrystals as, slip planes in the crystal lattice allow easier slip, enable greater plasticity (greater bonding area) therefore, form stronger tablets (Karki *et al.*, 2009). Overall, this may indicate that PA–5NIP cocrystallised from ethanol underwent more plastic and less elastic deformation during compression than the other samples.

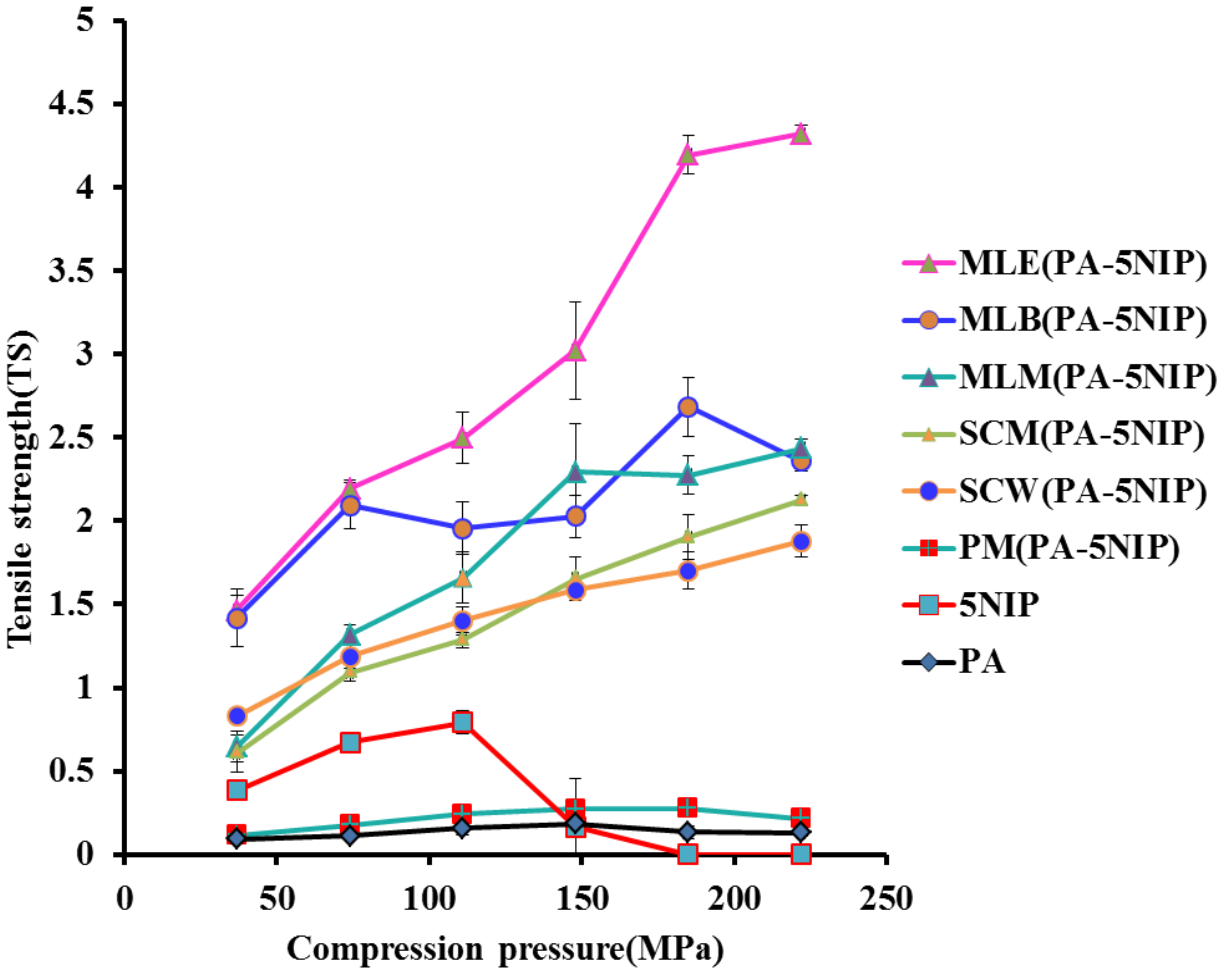

Figure 40. Tableting profile of PA, 5NIP, physical mixing (PM) and PA–5NIP cocrystals prepared using slow cooling crystallisation and wet–milling.

8.4. Conclusions

PA–5NIP cocrystal was successfully prepared using various methods and different solvents, namely, slow solvent cooling, slow water cooling, and wet milling with (methanol, butanol and ethanol).

The resultant cocrystals were characterised by PXRD, DSC, TGA and FT–IR. In comparison to the starting materials, the preparation methods

and the solvents had a significant effect on the physicochemical and mechanical properties of the cocrystals obtained. The cocrystal prepared using wet−milling in the presence of ethanol showed the best tableting properties due to the reduced relative degree of crystallinity. Also, PA–5NIP cocrystals were stable at 40 ºC /75% RH throughout six months confirmed by stability studies. The results of this investigation demonstrate that cocrystallisation with 5NIP shows an invaluable way to enhance the mechanical properties of PA.

9 CHAPTER 9: FREEZE DRYING OF PARACETAMOL–CHONDROITIN MIXTURES

9.0. Introduction

Many studies have demonstrated the pharmacological benefits Of CHONS which includes, Anti–inflammatory effect (Vergés *et al*., 2005; Abe *et al*., 2016; Linares *et al*., 2015), Anti–oxidant (Xiong *et al*., 2007), Malaria (Fried *et al*., 2000), Allergic response (Sakai *et al*., 2002) and chondroprotective effects (Das and Hammad, 2000; Orth *et al*., 2002). Chondroitin sulfates (CHONSs) (Figure 41) are abundantly and broadly distributed in nasal septa (Nakano *et al*., 2000) and they are also found in humans' cartilage, bone, cornea, skin and the arterial wall. The molecular weight of CHONS comprises of ~15 to 150 basic units of D–galactosamine and D–glucuronic acid, which ranges from 5000 to 50 000 d (Avachat and Kotwal, 2007). CHONSs are heteropolysaccharides with different sulfated residues of N–acetyl–D–galactosamine that are connected by β (1–>3) bonds, and these CHONSs are purified from several tissues made–up of other sequences of uronic acids (D–glucuronic or L–iduronic) (Mucci *et al*., 2000; Imanari *et al.,* 1996; Cassaro and Dietrich, 1977). The disaccharides inside the polysaccharide chains have different number and position of sulfate groups. For example, Chondroitin sulfate (chondroitin–6 sulfate) is principally constituted of a disaccharide unit [(1–>4) –O– (D–glucopyranosyluronic acid) – (1–>3) –O– (2–N-acetamido–2–deoxy–D–galactopyranosyl–6–sulfate and the regular disaccharide sequence of chondroitin sulfate A is chondroitin–4–sulfate which is composed of [(1–>4) –O– (D–glucopyranosyluronic acid) – (1–>3) –O– (2–N–acetamido–2–deoxy–D–galactopyranosyl–4–sulfate)].

CHONS is administered at a dosage of 1200 mg divided into three doses per day and has now become a part of the therapeutic armoury of the French rheumatologist. At the range of dosages commonly consumed, the evidence shows that chondroitin sulfate produces no identifiable pattern of adverse effect; thus, it is not lethal (Hathcock and Shao, 2007).

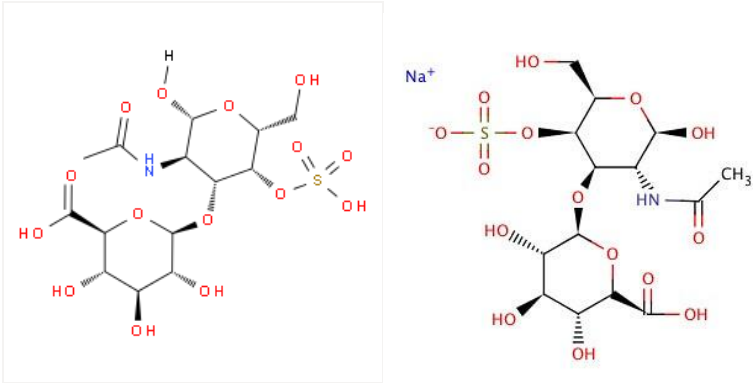

Figure 41. Chemical structure of chondroitin sulfate C and its salt form

It has been suggested that if PA is inadequately effective, the physician should contemplate halting and swapping treatment or adding on other therapies (Bruyère *et al.*, 2016). Therefore, since no published work has ever been conducted using paracetamol and chondroitin sulfates. For the very first time, the combination of PA and CHONS will be investigated in order to enhance the mechanical properties of paracetamol.

9.1. Engineering of PA–CHONS formulations

9.1.1. Low shear mixing

Commercial PA and commercial CHONS (10:4 *w/w*) powders and freeze–dried PA and freeze–dried CHON (10:4 *w/w*) were mixed separately using low shear mixing method as described in (Section 2.2.1.1).

9.1.2. Freeze drying

10% *w/v* solution was prepared by dissolving 10 g (*w/w*) of CHON in deionised water for a final volume of 100 mL. The flasks containing CHON solution were frozen using liquid nitrogen, while the flasks were stirred to allow maximum surface area for ten minutes and were freeze dried using the technique described in (Section 2.2.1.6). The FD CHONS powders were sieved using the technique described in (Section 2.3).

3.5% *w/v* solution was prepared by dissolving 14 g of PA–CHON in deionised water for a final volume of 400 mL. The flasks containing PA–CHON solution was frozen using liquid nitrogen, while the flasks were stirred to allow maximum surface area for ten minutes and were freeze dried using the technique described in (Section 2.2.1.6). The FD (PA–CHONS) powders were sieved using the technique described in (Section 2.3).

9.1.3. Tablet preparation

Each tablet weighs 700 mg ± 0.5 mg for the various formulations, and 500 mg ± 0.5 mg for PA and CHONS were all compressed using the method described in (Section 2.14).

9.2. Results and Discussions

9.2.1. Morphology and particle size distribution

Commercial PA, freeze–dried paracetamol (FDPA), commercial chondroitin (CHONS), freeze–dried chondroitin sulfate sodium salt (FDCHONS),

Physical mixing of PA and CHONS (PM (PA–CHONS)), physical mixing of FDPA and FD CHONS (PM (FDPA–FDCHONS)) and freeze–dried PA–CHONS FD (PA–CHONS) showed different sizes and morphologies as characterized by SEM (Figure 42). The morphology of the PA was well described in (Section 3.3.5) whereas, the commercial CHONS is visualised as smooth–surfaced spherical particles. The PM (PA–CHONS) displays a mixture of two different habits, an angular and smooth–surfaced spherical shaped, which affirms the presence of both PA and CHONS particles (Figure 42). The FDPA obtained in the absence of the polysaccharide demonstrates that the PA crystals changed from angular shape to elongated/flattened shape (Figure 42), and the crystal size of commercial PA decreases from a mean diameter (VMD) of 548 ± 30.2 µm to a VMD of 21 ± 2.1 µm for FDPA (Table 22). The physical mixture of both commercial products PA: CHONS displays a mean diameter of 194 ± 5.1 µm and FDPA: FDCHONS physical mixture showed an irregular shape (Figure 42) with a VMD of 756 ± 15 µm (Table 22)

SEM micrographs of FD (PA–CHONS) displayed continuous and porous structures, with the pores being the result of ice crystal formation during the freeze drying process (Tan *et al*., 2009). Additionally, those pores in the formation are also due to the presence of CHONS (Figure 42).

The bulk density of FD PA crystals was > to that of PA (0.03 ± 0 g/cm^3 versus 0.8 ± 0 g/cm^3) (Table 23). FDPA in the absence of CHONS showed a considerably lower tap density than PA (0.07 ± 0 g/cm^3 versus 0.8 ± 0 g/cm^3) (Table 23), this could be attributed to the pronounced internal

friction (i.e., additional void space) between FD crystals due to their irregular shape (Figure 42).

(Table 23) Show that all FDPA powders showed increased (*1/b* values), compared to the PA, indicating their slightly increased cohesivity. It is generally known that particles of the same material with smaller size tend to have higher cohesivity compared to larger particle size, consequently more cohesive (Agbor Rose and Kaialy, 2019; Kaialy *et al*., 2012a). This validates the latter statement for the case of FDPA crystals which showed a slight increase in cohesivity compared to commercial PA. Also, both PM (FDPA–FDCHONS) and FD (PA–CHONS) demonstrated dissimilar particle sizes (Span values, $P<0.05$) compared to that of PM(PA–CHONS) (Figure 42, Table 22) which could also be linked to their irregular and flaky crystal shapes, thus increased in their cohesivity compared to PM(PA–CHONS) powder.

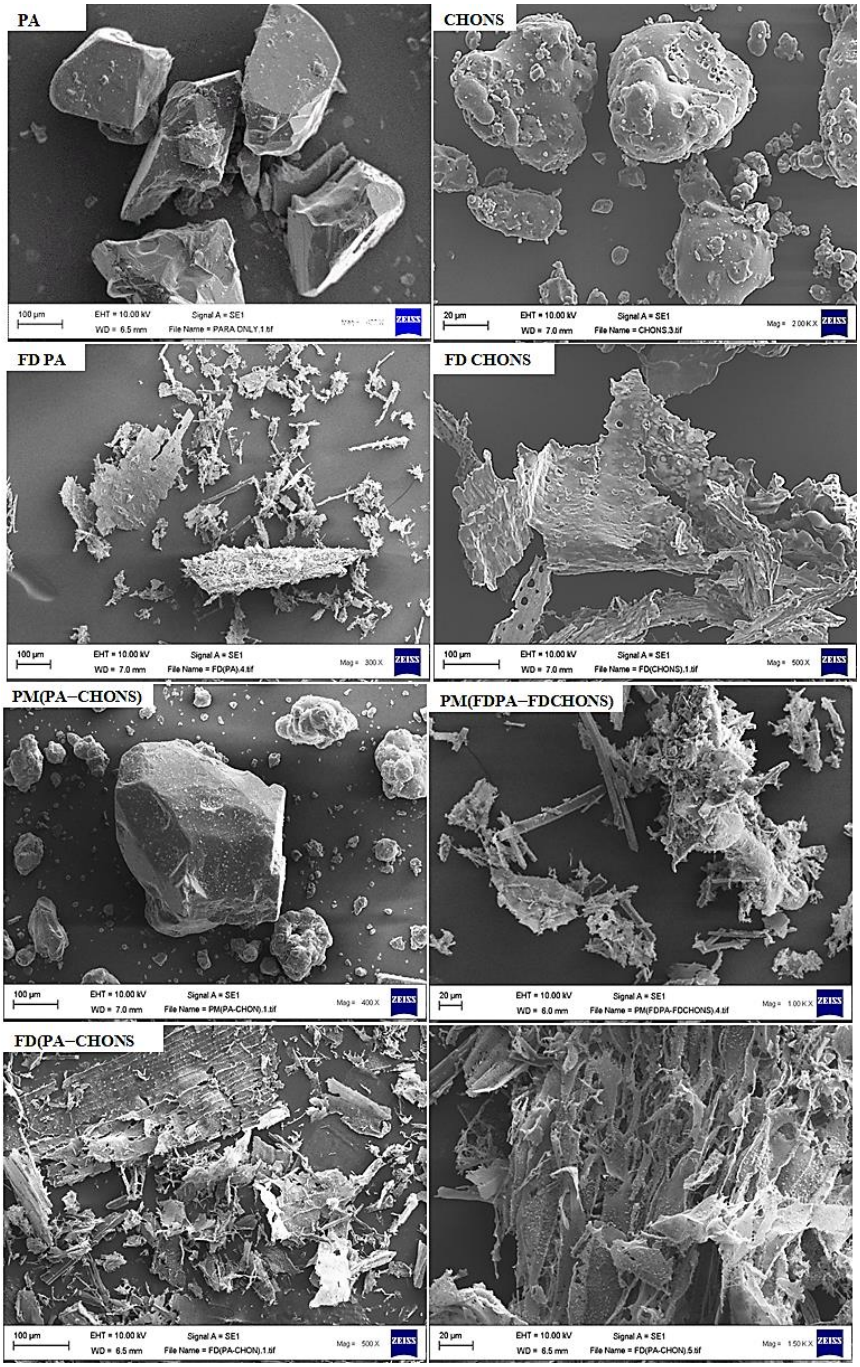

Figure 42. Scanning electron microscopy micrographs of commercial paracetamol (PA), commercial chondroitin sulfate sodium salt (CHONS), freeze dried paracetamol (FDPA), freeze dried chondroitin sulfate sodium salt (FDCHONS), and PA–CHONS mixtures (5:2, *w:w*) co–processed by physical mixing (PM) and freeze drying (FD).

Table 22. Particle size distribution (i.e. particle size at 10% ($d_{10\%}$), 50% ($d_{50\%}$, median diameter and 90% ($d_{90\%}$) volume distribution and span) (mean ± SD, n = 3) for commercial paracetamol (PA), commercial chondroitin sulfate sodium salt (CHONS), freeze dried paracetamol (FDPA), freeze dried chondroitin sulfate sodium salt (FDCHONS), and PA−CHONS mixtures (5:2, *w:w*) coprocessed by physical mixing (PM) and freeze drying (FD).

Product	$d_{10\%}$ **(μm)**	$d_{50\%}$ **(μm)**	$d_{90\%}$ **(μm)**	**VMD (μm)**	**Span**
PA	254 ± 22	506 ± 30	911 ± 39.3	548 ± 30.2	1.3 ± 0
CHONS	32 ± 0.2	80.4 ± 0.5	137 ± 1	82.3 ± 1	1.4 ± 0
FDPA	2.3 ± 0.1	16 ± 8.4	43 ± 2	21 ± 2.1	3 ± 1.1
FDCHONS	89.3 ± 4.3	222 ± 9	394.3 ± 14	233 ± 7	1.4 ± 0
PM(PA–CHONS)	80 ± 9	170 ± 6.2	348 ± 4.3	194 ± 5.1	2 ± 0
PM(FDPA–FDCHONS)	8.3 ± 1	597 ± 15	1777 ± 15.3	756 ± 15	3 ± 0
FD(PA–CHONS)	11.4 ± 0.1	31 ± 2.0	120 ± 8.1	56 ± 4	3.5 ± 0.2

Table 23. Bulk density *(D_b)*, tap density *(D_t)* and cohesivity *(1/b)* (mean ± SD, n = 3) for commercial paracetamol (PA), commercial chondroitin sulfate sodium salt (CHONS), freeze–dried paracetamol (FDPA) and PA–CHONS mixtures (5:2, *w:w*) co–processed by physical mixing (PM) and freeze drying (FD).

Product	**D_b (g/cm^3)**	**D_t (g/cm^3)**	**1/*b***
PA	0.8 ± 0	0.8 ± 0	4 ± 0
CHONS	0.7 ± 0	0.9 ± 0	4 ± 1
FDPA	0.03 ± 0	0.1 ± 0	4.5 ± 0
PM(PA–CHONS)	0.6 ± 0.5	0.6 ± 0.5	3 ± 1.1
PM(FDPA–FDCHONS)	0.2 ± 0	0.3 ± 0	4.4 ± 0
FD(PA–CHONS)	0.01 ± 0	0.02 ± 0	6 ± 1

9.2.2. Powder X–ray diffraction

The CHONS used in this work due to the inhomogeneity of its composition and the fact that they are studied in their salt forms makes them relatively amorphous in the solid state which falls in accordance with (Denuziere *et al.*, 1996). (Figure 43) depicts a hollow shape which indicates the amorphous nature of CHONS whereas, PA, which is crystalline displays various characteristic peaks at 2θ values which were well discussed in (Section 3.3.4). As shown in (Figure 43), the X–ray pattern of FD (PA–CHONS) shows a reduced peak height from 11–30°

that implies reduced crystallinity of the drug**.** The intensity in FD (PA–CHONS) has been found to reduce to a greater extent in comparison to the other mixtures, which may be attributed to the presence of CHONS in its lyophilised form. Additionally, the decrease in crystallinity (Figure 43) occurs, perhaps due to strong chemical bond formation between PA and CHONS.

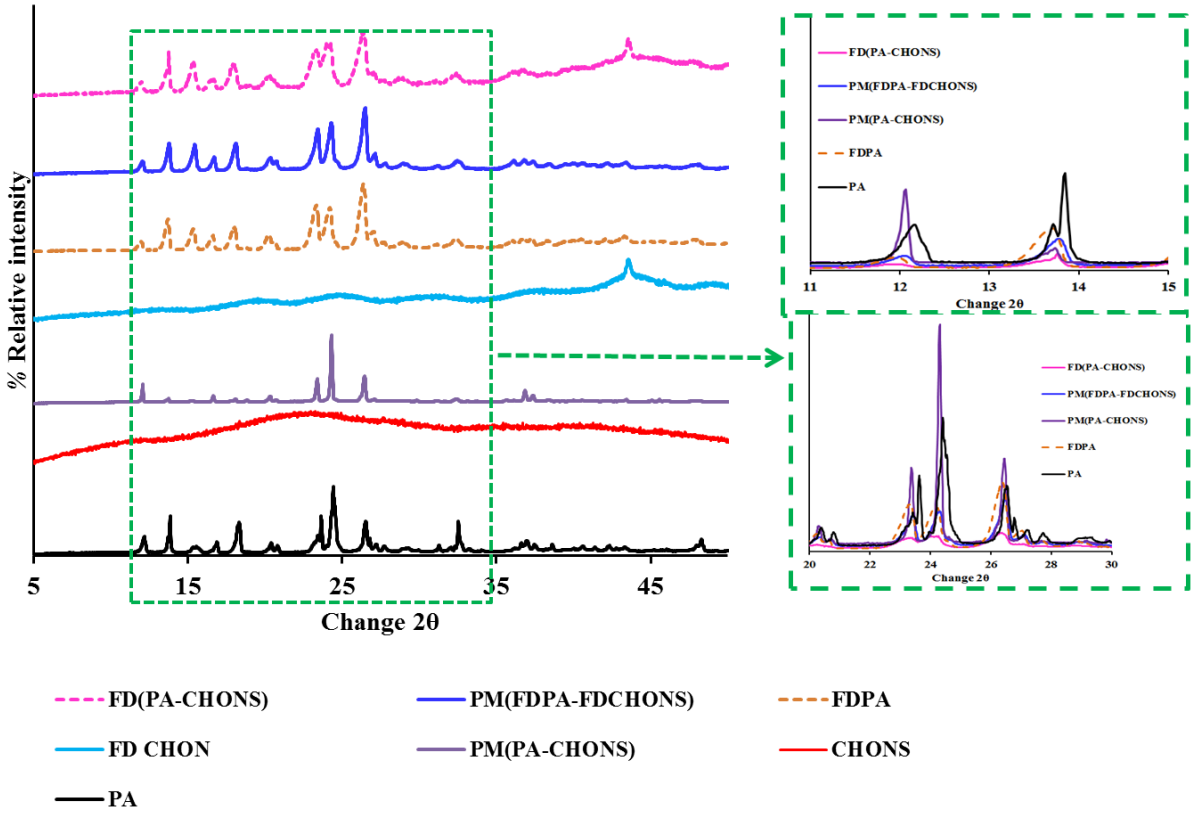

Figure 43. Powder X–ray diffraction (PXRD) patterns of commercial paracetamol (PA), commercial chondroitin sulfate sodium salt (CHONS), freeze dried paracetamol (FDPA), freeze dried chondroitin sulfate sodium salt (FDCHONS), and PA–CHONS mixtures (5:2, *w: w*) co–processed by physical mixing (PM) and freeze drying (FD).

9.2.3. Fourier transform infrared

The FT−IR spectrum of commercial PA depicts characteristic peaks which were well discussed in (Section 3.3.4). The FT−IR spectrum of commercial CHONS (Figure 44) shows a broad band between 3100–3600 cm^{-1} assigned to –OH and to N–H vibrational stretching in which, the –OH stretching overlaps the N–H. The presence of the amide groups (*I* and *II*) are depicted by characteristic peaks at 1606 cm^{-1}, COO− anti−symmetry stretching (1558 cm^{-1}), COO− symmetry stretching (1413 cm^{-1}). Bands at 1410 cm^{-1} and 1375 cm^{-1} are indicating towards overlapping of C–O stretching and –OH variable−angle vibrations and confirms the presence of carboxyl group. Amide III region (~ from 1200–1300 cm^{-1}) is related to the C–N and C–C stretching, N–H bonds, and CH_2 wagging from the glycine backbone and proline side chain (Corradetti *et al*., 2016). The peaks at 1222 cm^{-1} and 1046 cm^{-1} signified S—O and —C—O—S stretching vibrations, respectively for both commercial and freeze dried CHONS. These results were closer to that obtained by (Crispim *et al*., 2012; Khan *et al*., 2013). The peak at approximately 850 cm^{-1} was used to identify chondroitin-4-sulfate, and a peak at 820 cm^{-1} was used to indicate chondroitin-6-sulfate (Wang *et al*.,2019). The spectra of the commercial CHONS and freeze dried CHONS from bovine exhibited peaks at 820.17 cm^{-1}, suggesting that the marketed product and the freeze dried CHONS obtained mainly consisted of chondroitin-6-sulfate (Garnjanagoonchorn *et al*., 2007).

No significant change in band intensity was observed in the FDPA spectrum. However, the insertion of CHONS caused a significant change within the various formulations (Figure 44). The reduction in absorbance intensity of the band assigned to –OH, could be due to an increase of spread of CHONS in the freeze dried formulation. Also, slight shifts in absorbance intensities were observed for the freeze dried formulation (FD(PA–CHONS) at the carbonyl region (C=O) from 1650 cm^{-1} to 1654 cm^{-1} which indicated the intermolecular or intramolecular H–bonding among N–H groups in PA which were disrupted by S=0– groups in CHONS. Furthermore, the co–freeze dried mixture demonstrate a shift in band at 1226 cm^{-1} due to stretching vibrations of S=O– bond from sulfate groups of CHONS (1222 cm^{-1}) and N–H group of PA (1224 cm^{-1}), followed by another shift from 1434 to 1440 cm^{-1} could be due to the presence of protonated NH_3^+, this strongly affirms the new H–bonding was formed between N–H group in PA as hydrogen donor, and the by S=0 group in CHONS, as hydrogen acceptors via (N–H…..O–S) interaction. (Denuziere, *et al*.1996; Tan *et al.* 2018) successfully prepared a complex of chitosan and GAGs (Chondroitin sulfate) in their salt form and suggested that the complex corresponded to the interaction between NH_3^+ and $–OSO_3–$ and/or –COO–.

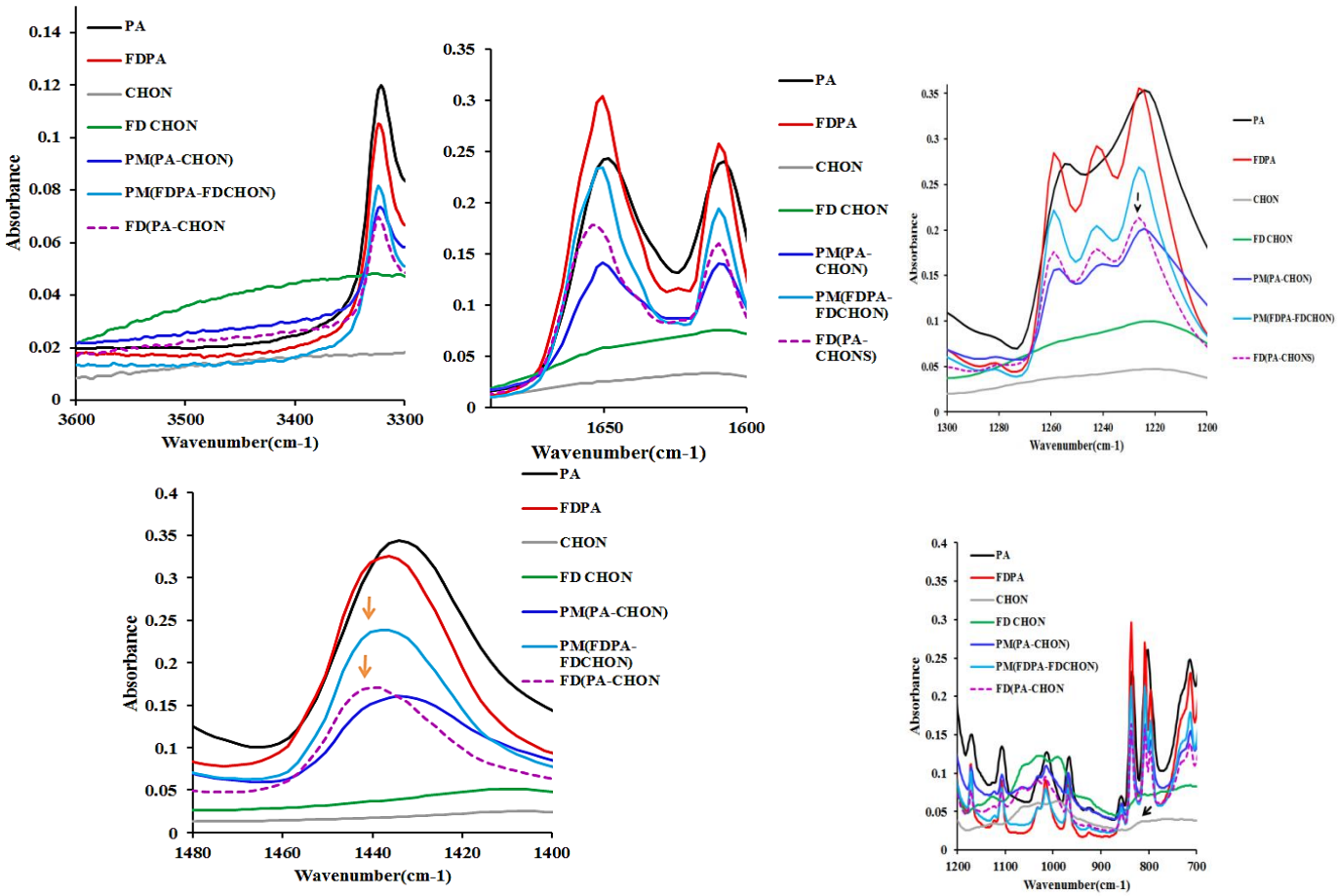

Figure 44. Fourier transform infrared (FT-IR) absorption spectra of commercial paracetamol (PA), commercial chondroitin sulfate sodium salt (CHONS), freeze–dried paracetamol (FDPA), freeze–dried chondroitin sulfate sodium salt (FDCHONS), and PA–CHONS mixtures (5:2, *w: w*) co–processed by physical mixing (PM) and freeze drying (FD).

9.2.4. Thermogravimetric analysis

TGA thermogram of PA was shown and discussed in (Section 3.3.4). The thermogram of FDPA was thermally stable till 168 ºC but, a slight shift was observed to a lower temperature in comparison to PA due to the

presence of fine particles (reduced d_{10}% values) as demonstrated by SEM (Figure 42, Table 23). CHONS demonstrated a weight loss stage one of 2wt % loss at 76 ºC due to the evaporation of surface water (dehydration) caused by the presence of functional groups (COO– and –$OS0_30$–) in CHONS which are known to be highly hydrophilic and could tightly interact with water molecules via dipole−dipole or ion−dipole and CHONS incorporated impact the water content in various samples (Bonkovoski *et al*., 2014). As heating ramps to 233 ºC, approximately 10 wt % mass loss of the original product at this stage were encountered. All the fraction and bound water were desorbed from the molecules. A drastic pattern of mass loss was shown when CHONS was further heated from 242 ºC to 410 ºC range, which may be due to the random breakage of polymeric backbone by decomposition of carboxylate and sulfonic acid groups (SO_2 and SO_3) (Qiao *et al*.,2005). To tell whether the thermal stability was enhanced after the CHONS was introduced in the different formulations of PM (PA–CHONS), PM (FDPA–FDCHONS) and FD (PA−CHONS). The PM (PA–CHONS) sample was comparatively thermally stable but less stable than PA, which could be linked to the presence of CHONS molecules, as seen by the slight shift (Figure 45).

The weight loss of the FD(PA−CHONS) mixture showed two degradation stages; (***i***) ~ 4 *wt%* (FD(PA-CHONS)) and 5 *wt %* PM (FDPA −FDCHONS) loss 76 ºC (dehydration), ~ wt 8% (at 200 ºC) and (*ii*) the events related to the degradation happened at 242 ºC to 410 ºC range. The first degradation temperature of FD (PA−CHONS) was lower than the

commercial CHONS because during the FD process, a small amount of water molecules could be present at the surface and the presence of CHONS could contribute to the slight increase in the amount of water. However, the weight loss amounts were not too significant in the FD (PA–CHONS) mixture (Figure 45). It was obvious that, PM(FDPA–FDCHONS) was slightly thermally stable than the FD(PA–CHONS) which could be linked to the higher structural organisation (crystallinity) (da Silva *et al*., 2017) which is confirmed by the PXRD results (Figure 44) and its very porous nature (Figure 42). Conclusively, the effect of PA on CHONS on the thermal stability was significant.

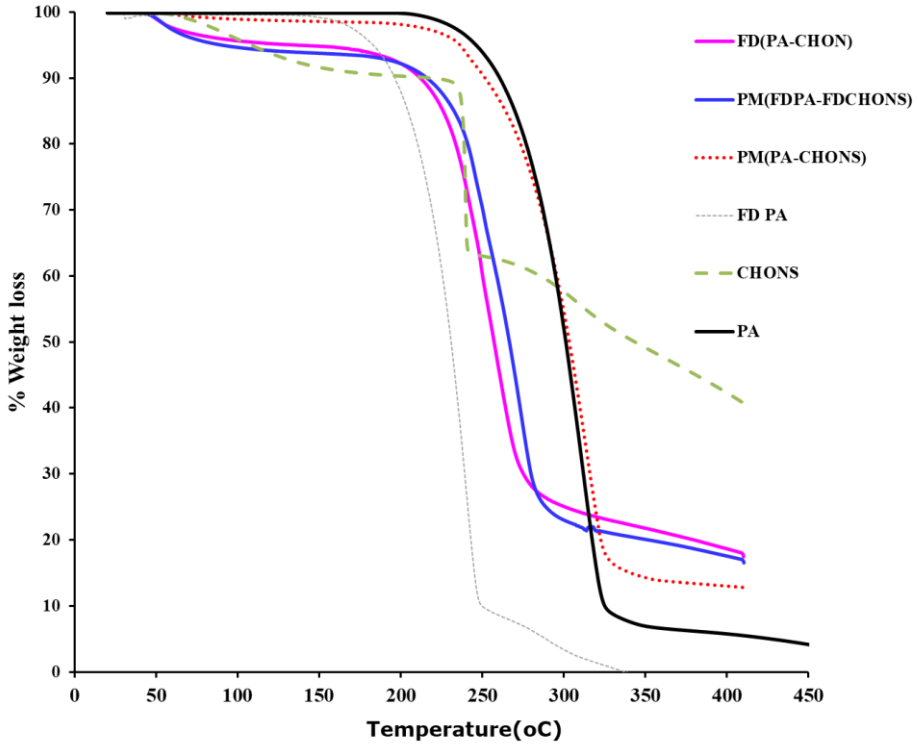

Figure 45. Thermogravimetric analysis curves of commercial paracetamol (PA), commercial chondroitin sulfate sodium salt (CHONS), freeze–dried paracetamol (FDPA), freeze–dried chondroitin sulfate sodium salt (FDCHONS), and PA–CHONS mixtures (5:2, *w: w*) co–processed by physical mixing (PM) and freeze drying (FD).

9.2.5. Tableting properties

Both commercial PA and commercial CHONS showed poor mechanical properties, with the highest TS of only 0.18 ± 0.02 MPa and 0.16 ± 0.03 MPa at a compression pressure of 148 MPa (Figure 16 & 46). The lyophilised PA in the absence of CHONS demonstrated a slight improvement of mechanical properties, with the highest TS of 0.56 ± 0.02 MPa at a compression pressure of 74 MPa. The presence of CHONS used

as biopolymer did not improve the mechanical properties of PA in physical mixing as no TS at all compression pressures were achieved (Figure 46). On the other hand, the tabletability profiles of the physical mix of FDPA and FDCHONS (PM(FDPA–FDCHONS)) demonstrated an enhancement in tabletability compared to the physical mixing of both marketed forms, i.e., with the compression pressure increasing from 37 to 222 MPa, the TS for PM(PA–CHONS) was zero whereas, that of (PM(FDPA–FDCHONS)) increased from 1.28 to 3.8 MPa, for the mixture obtained using the same method (Figure 46) which implies that, the physical mixing of both lyophilised PA and lyophilised CHONS increased the TS of tablets compared to the physical mixing of the two commercial products over the compression pressure range of 37 to 222 MPa. The mixture prepared using co–freeze dried of both PA and CHONS (FD (PA–CHONS)) showed an outstanding enhancement in tabletability in comparison to PM (FDPA–FDCHONS)). For example, when the compression pressure increased from 37 to 222 MPa, the TS of tablets prepared using PM (FDPA–FDCHONS) increased from 1.3 ± 0.1 MPa to 3.8 ± 0.0 MPa, whilst that prepared using FD (PA–CHONS) increased from 2.7 ± 0.2 MPa to 3.9 ± 0.0 MPa (Figure 46). It is quite evident that the co–freeze dried (PA–CHONS) mixture showed the best compression properties among the mixtures under this study recording TS of 3.9 ± 0.0 MPa at a compression pressure of 222 MPa. The increased tensile strength of the tablets of the mixture obtained using freeze drying method in comparison to the PM of the two commercial products (PA and CHONS) was due to the presence of the

strong intermolecular bond formation through hydrogen bonding especially in the FD(PA−CHONS) mixture (Figure 46). Also, in disparity to the mixture prepared using physical mixing (PM (PA−CHONS) in which the shapes of both PA and CHONS retained their morphology whereas, no distinct individual PA or CHONS particles were envisaged in FD (PA−CHONS) (Figure 46), this implies the inhomogeneity in PM (PA−CHONS) for CHONS to bind tightly to onto PA surfaces. The lyophilised method in the presence of CHONS drastically reduces the crystallinity of the mixture (Figure 42). Consequently, it can be confirmed that reduced crystallinity is one of the contributors to the superior tableting performance of monoclinic paracetamols freeze dried with CHONS in comparison to PM (PA–CHONS).

The tableting behaviour of PA processed using FD method in the absence of CHONS was comparatively poor as PA (Figure 46). The enhancement of the mechanical properties as shown in the results proved the strong intermolecular hydrogen bonding interaction induced via freeze drying method in the presence of CHONS thus, the effect of the size of particles was ruled out (Table 24).

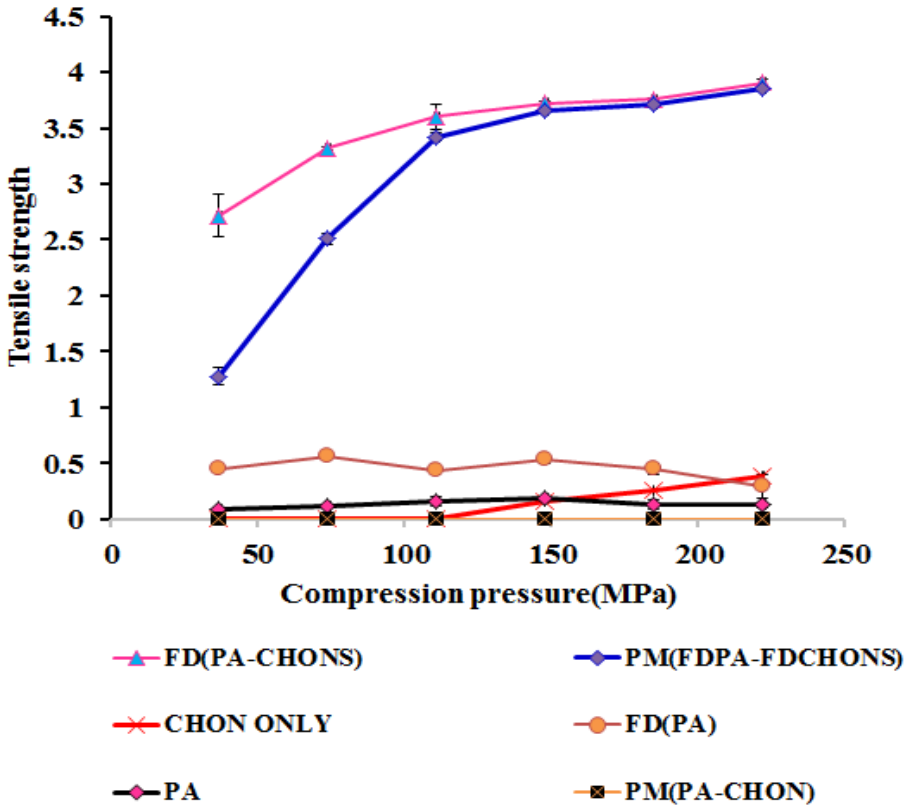

Figure 46. Tensile strength (mean ± SD, n=5) versus compression pressure for commercial paracetamol (PA), commercial chondroitin sulfate sodium salt (CHONS), freeze–dried paracetamol (FDPA), freeze–dried chondroitin sulfate sodium salt (FDCHONS), and PA–CHONS mixtures (5:2, *w: w*) co–processed by physical mixing (PM) and freeze drying (FD).

Weak tablets are often prone to breakage during production, transportation and end use which can result in waste that no longer meets required product specifications. Furthermore, surface damage by chipping is aesthetically undesirable and can affect content uniformity (Hare *et al.*, 2018). The percent friability of the subsequent tablets

obtained from commercial PA, FDPA, and commercial CHONS was above 1%. Whereas, PM (FDPA–FDPA) and FD (PA–CHONS) mixtures recorded (0.73% and 0.17%) and were shown by using a compression pressure of 148 MPa and all tablets obtained from the latter mixtures showed friability values less than 1%. For an existing uncoated and compressed tablet product in general, ≤1% weight loss is acceptable. Although, it is suggested for new formulations not yet having adequate packaging data, a more conservative weight loss of ≤0.8% is preferable (USP, 2014; Pharm Eur, 2013; JP, 2011).

9.3. *In–vitro* studies

The comparison of dissolution profile using *f*2 has also been adopted by food and drug administration (FDA) in the assessment of similarity between two dissolution profiles (Boateng *et al*., 2009; Yuksel et al., 2000; Hiendrawan *et al*., 2014). It was observed that dissolution profile of FDPA, PM (FDPA–FDCHONS)) and FD (PA–CHONS) and were all similar to PA as indicated by *f*1 and *f*2 value (6.30 & 67.17(FDPA); (8.37 & 63.32)(PM(FDPA–FDCHONS)) and (13.38 & 54.67)FD(PA–CHONS) which subsequently supports the claim as the dissolution parameters for the water soluble (DE%; MDR(min) and MDR(min) for PA(68.4 ± 8; 0.8 ± 0.1; 54.2 ± 11) values in comparison to FDPA(72.5 ± 3; 0.8 ± 0.0 and 46.1 ± 6), PM(FDPA–FDCHONS)(63.2 ± 4; 0.6 ± 0 and 59.1 ± 6.2) and FD(PA–CHONS)(61 ± 4; 0.6 ± 0 and 59.1 ± 6.2) were all similar (P >0.05)(Figure 47).

Solubility may be defined as the amount of a substance that dissolves in each volume of solvent at a specified temperature (Bergström *et al.*, 2004). The solubility of PA, FDPA and PA–CHONS samples were measured in deionised water by slurring excessed solids in water at 37 ºC for 24 h. The solubility value of, PA–CHONS samples were 15.54 mg/mL for (PM (FDPA–FDCHONS)) and 15.54 mg/mL for FD (PA–CHONS which were very slightly lower than the solubility of, PA (17.54 mg/mL) and FDPA (16.94 mg/mL). Nonetheless, all the samples were classified as sparingly soluble. The very slight reduced solubility values of PA–CHONS samples did not cause any problem in the dissolution of PA.

In general, the value of the commercial PA is in good agreement with (Sumathi and Ray, 2002). The aqueous solubility measured deviate in average 10% concerning the data presented by (Mota *et al.*, 2009) and 5.8% with (Etman and Naggar, 1990). These deviations of this magnitude are typically found when comparing solubility data from different authors. The effective arrangement of crystal packing in the samples through the strong intermolecular interactions such a hydrogen bonding holding the compacts together or the relatively higher cohesive forces with the processed powders could potentially reduce the effective surface area for solubility. Alternatively, the presence of hydrophilic additive could decrease the resistance to the effective diffusion of the solubilised PA in the case of the FD (PA–CHONS) mixture. The present study showed that the presence of the additive did not retard the dissolution rate of PA, however slightly reduced the solubility.

Nonetheless, it immensely improved the mechanical properties of PA tablets, especially, with FD (PA–CHONS) powders. Some other techniques were conducted; however failed to enhance the physicomechanical properties of PA (e.g., (dry and wet) high shear mixing, batch cooling, water evaporation and milling).

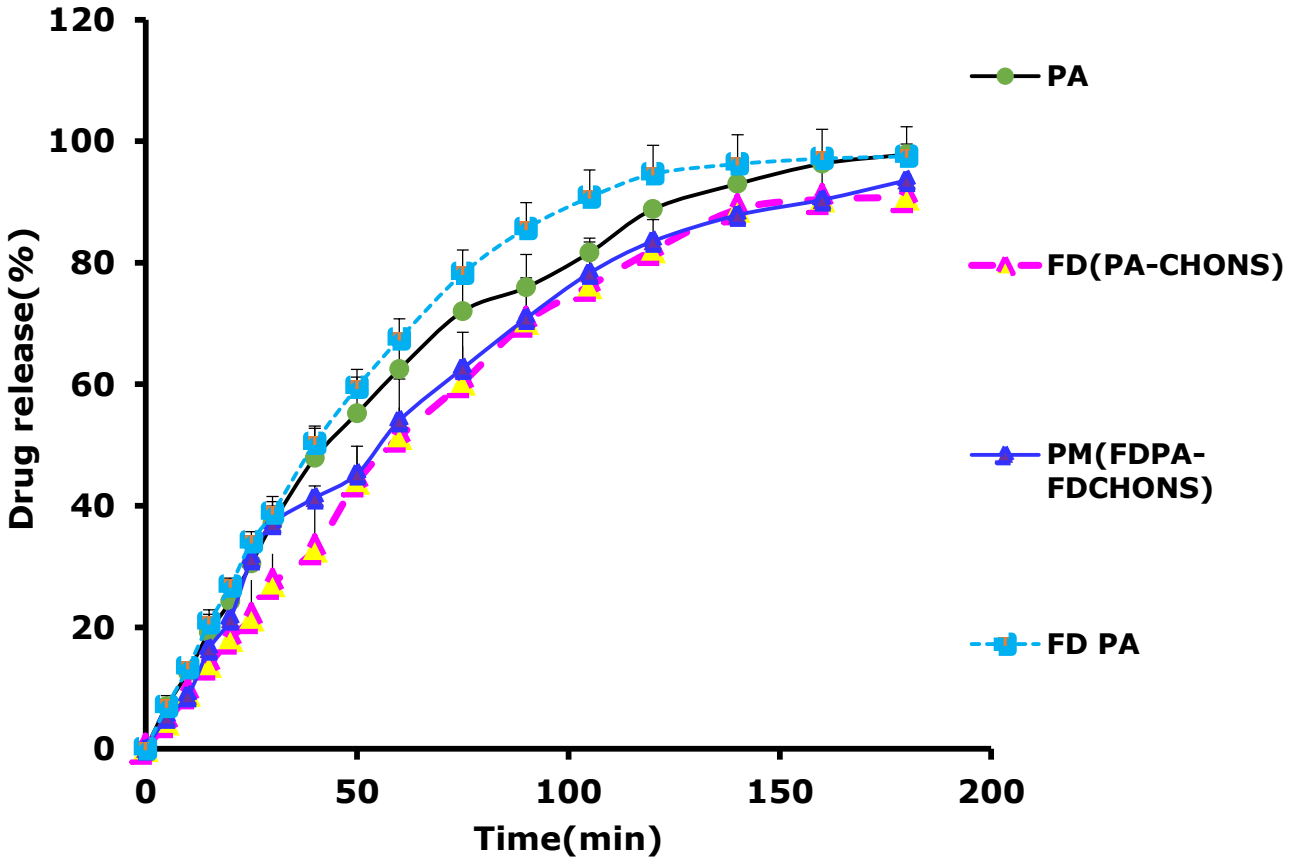

Figure 47. Release profiles for commercial paracetamol (PA), freeze dried paracetamol (FDPA) and PA–CHONS mixtures (5:2, *w: w*) co–processed by physical mixing (PM) and freeze drying (FD).

9.5. Conclusions

A novel mixture of PA–CHONS was obtained and possessed improved micromeritic and mechanical properties via freeze drying technique in the presence of the highly hydrophilic polysaccharide (biopolymer). No polymorphic transformation was induced by the freeze drying process. However, reduced crystallinity which was influenced by the presence of the biopolymer used during freeze drying was observed. The change in crystal habit and reduction in crystallinity, in turn, influenced the compaction behaviour of paracetamol crystals. The co–freeze dried PA–CHONS produced stronger tablets than the commercial paracetamol.

Physicomechanical properties of PA can be immensely improved via the selection of a suitable additive during FD. The physical mixtures of FDPA and FDCHONS or co–freeze dried PA and CHONS samples were more valuable and showed the best tabletability when compared to other paracetamols at compression pressures from 37 to 222 MPa. However, there was no difference in dissolution performance between the commercial paracetamol and the binary mixtures.

10 CHAPTER 10: MILLING OF PARACETAMOL–CURCUMIN MIXTURES

10.1. Introduction

Commercial curcumin (CUR) is a hydrophobic compound having the chemical name of (1,7–bis(4–hydroxy–3–methoxyphenyl)–1,6–heptadiene–3,5–dione)(Figure 48) with a molecular weight of 368g/mol and a melting point of 183 ºC. CUR is composed of three main components together denoted to as curcuminoid which are bisdemethoxycurcumin (3%), demethoxycurcumin (17%) and curcumin (77%) (Anand *et al.*, 2007). CUR is a golden–yellow solid, natural compound primarily used for food colouring and, often used as a dye owing to its vibrant colour. Furthermore, it is derived from the rhizome of *curcuma longa* with a wide variety of medicinal benefits (Salem *et al.*, 2014) including, anti–inflammatory (Sharma *et al.*, 2005), antioxidant (Joe and Lokesh, 1994), anti–cancer (Ireson *et al.*, 2001), wound healing and rheumatoid arthritis (Dcodhar *et al.*, 2013).

CUR is safe even at high doses of 12 g/day in humans (Lao *et al.*, 2006). However, it is hindered by its enormously reduced aqueous solubility of aqueous buffer pH=5.0 (Tønnesen *et al.*, 2002), also, relatively insoluble in water (Sharma *et al.*, 2005). CUR has poor absorption from the gastrointestinal tract, thermal treatment, light, metallic ions, enzymes, oxygen and ascorbic acid (Paramera *et al.*, 2011; Gowthamarajan *et al.*, 2012). Also, when taken orally, only traces appear in the blood. Meanwhile most of the dose is excreted through the faeces (38–75%). Chemically CUR decomposes rapidly in neutral and alkaline medium,

above 90% of CUR, decomposition occurs within 30 min in pH 7.4 buffer medium (Wang *et al*., 1997).

CUR has a potential as a pharmaceutical excipient (Tønnesen *et al*., 2002; Salem *et al*., 2014), and an interesting model compound as it possesses three polymorphic forms, form *I* (monoclinic) and orthorhombic form *II* and *III,* commercially available CUR crystals are the monoclinic forms and the space group is P2/n and exists primarily in its enolic form in solution. CUR molecule also exists as tautomers of β–diketonic form (di–keto) and enolic form (enol) (Sanphui *et al*., 2014; Thorat *et al*., 2015) (Figure 48).

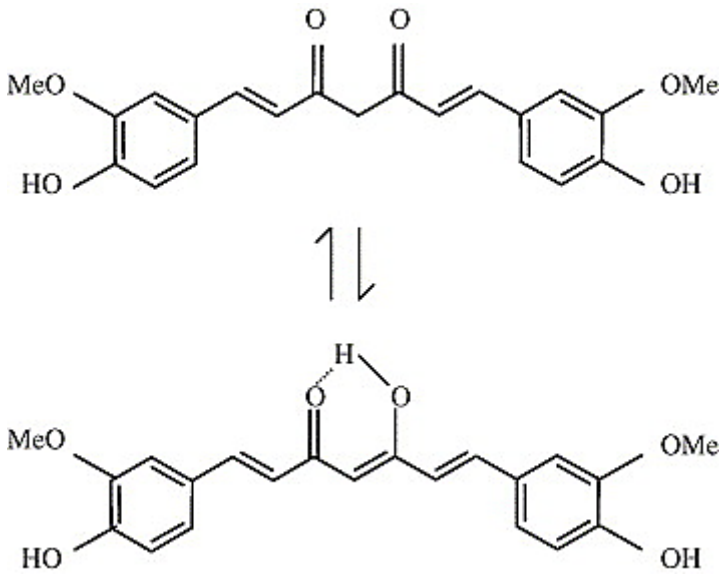

Figure 48. Chemical structure of curcumin (Keto and enol form).

CUR has been selected for blending and milling with PA. The main focus of the present study is to develop paracetamol–curcumin (PA–CUR) tablets with improved tableting properties. Until now, no study is available

on PA–CUR tableting properties. For the first time, the tableting properties of PA will be improved in the presence of CUR via milling technique.

10.2. Engineering of PA–CUR formulations

10.2.1. Low shear mixing

PA and CUR (10:4 *w: w*) powders were mixed using low shear mixing technique as described in (Section 2.2.1.1).

10.2.2. Dry Milling

PA and CUR (10:4 *w: w*) powders were milled for 5min (ML5), 6min (ML6), 7min (ML7) and 10min (ML10) using the milling technique described in (Section 2.2.1.7).

10.2.3. Tablet preparation

Each tablet weighs 700 mg ± 0.5 mg for the various formulations, and 500 mg ± 0.5 mg for PA and 500 mg ± 0.5 mg CUR were all compressed using the method described (Section 2.14).

10.3. Results and Discussions

10.3.1. Morphology and particle size distribution

Scanning electron microscopy was used to envisage the morphology of commercial PA, commercial CUR and the various mixtures of PA–CUR using techniques such as, physical mixing PM (PA–CUR) and milling ML (PA–CUR) using various time intervals; 5 min, 6 min, 7 min and 10 min (ML5, ML6, ML7 and ML10) (Figure 49). The morphology of PA was well discussed in (Section 3.3.4) whereas; CUR revealed a clear crystalline

nature and showed the presence of large prismatic–cube/tabular crystalline particles with rough surface edges (Figure 49). In the case of the PM (PA–CUR) mixture which demonstrated two distinct shapes consisting of both PA and CUR habits. Meanwhile, PA–CUR mixture milled at various time intervals (ML5, ML6, ML7 and ML10) morphologies were neither a flake−like structure nor polyhedral crystals but exhibited a combination of large and small aggregates/clumps of PA–CUR assemblies (Figure 49). The apparent morphological change from tabular structures to smaller aggregates must be due to well–mixed PA and CUR in PA–CUR mixtures (ML5, ML6, ML7 and ML10). Also, most of the large aggregates disappeared with an increase in milling time of PA and CUR, i.e., ML5 (PA–CUR) to ML10 (PA–CUR). The ML10 (PA–CUR) mixture demonstrated tiny clusters/aggregates compared to other blends (ML5, ML6 and ML7) (Figure 49). This alteration of crystal structure further suggests the formation of well spread CUR on PA particles.

PA–CUR mixture prepared using physical mixing technique showed increased span values compared with marketed PA (Table 25). This was caused by the span value of the CUR particles, which was higher than that of commercial PA (Table 25), as confirmed by SEM micrographs. A trend of higher span values could be observed with the increased in milling time (i.e., ML5 < ML6 <ML7< ML10) (Table 25). For example, the span values of PA–CUR mixtures using various timing (ML5, ML6, ML7 and ML10) were 3 ± 0.1 µm, 4.2 ± 0.1 µm, 9.5 ± 0.4 µm, and 11 ± 0 µm, respectively (Table 25). Additionally, the mixtures above showed smaller mean

diameters (VMDs ranging from 858 ± 25.3 µm to 86 ± 6 µm) compared with the mixture prepared using physical mixing (PM) technique with a VMD of 1237 ± 51 µm (Table 25). The lower VMDs for the mixtures prepared using milling compared to PM was due to the reduced *d*10% values (ML10<ML7<ML6<ML5<PM) as shown in (Table 25).

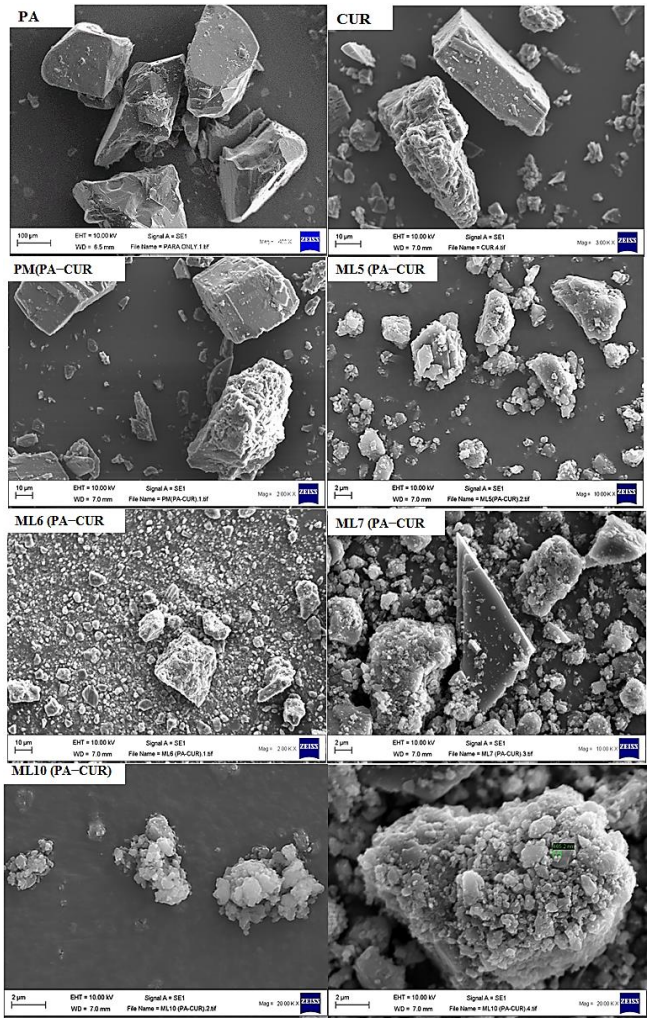

Figure 49. Scanning electron microscopy micrographs of commercial paracetamol (PA), commercial curcumin (CUR), and PA–CUR mixtures (5:2, *w/w*) prepared using physical mixing (PM (PA–CUR)), and milling at various timing (ML5, ML6, ML7 and ML10).

10.3.2. Powder density and cohesivity

All PA–CUR mixtures showed lower bulk and tap densities, higher cohesivity (1/*b*), and higher *CI* values than PA (Table 24). However, the bulk density, tap density and cohesivity of the mixtures prepared using milling method were not statistically different ($p > 0.05$) (Table 24). The mixtures prepared using milling for 10 min (ML10) showed further reductions in bulk density as well as increases in cohesivity compared to the PA powder (Table 24). The reductions in the bulk and tap densities for the mixtures prepared using physical mixing method compared with commercial PA were due to the presence of smaller particle sizes of CUR powder, whose bulk and tap density values are less than those of commercial PA (Table 24). The reductions in bulk and tap densities for the powders prepared using milling technique compared with a mixture prepared using physical mixing method were caused by their considerably smaller particle sizes (VMD, *d*10%) as shown in (Table 25). As revealed by the higher cohesivity values which are associated with considerable increases in the strength of the interparticle forces (Table 25). The mixtures prepared using milling technique exhibited reduced flowabilities compared to the physical mixing method as indicated by their considerably higher *CI* values from 28 ± 0% to 34 ± 0% as shown in (Table 24) this is linked to their increased span values and higher fines particles (d_{10}%). This provides further evidence for their stronger interparticle forces (Table 25).

Product	$D_{b(g/cm^3)}$	$D_{t(g/cm^3)}$	1/*b*	*CI* (%)
PA	0.8 ± 0	0.8 ± 0	4 ± 0	3.2 ± 0.3
CUR	0.4 ± 0	0.6 ± 0	28.3 ± 0	34 ± 0
PM(PA–CUR)	0.63 ± 0	0.9 ± 0	11 ± 0	28 ± 0
ML5(PA–CUR)	0.42 ± 2.3	0.63 ± 0	59 ± 2.3	34 ± 0
ML6(PA–CUR)	0.34 ± 0	0.54 ± 0	59 ± 2.3	34 ± 0
ML7(PA–CUR)	0.4 ± 0	0.6 ± 0	60 ± 0	34 ± 0
ML10(PA–CUR)	0.42 ± 0	0.64 ± 0	60 ± 0	34 ± 0

Table 24. Bulk density (D_b), tap density (D_t), cohesivity (1/*b*), and Carr index (*CI*) for commercial paracetamol (PA), commercial curcumin (CUR), and PA–CUR mixtures (5:2, *w/w*) prepared using physical mixing (PM), and milling at various timing (ML5, ML6, ML7 and ML10).

Product	$d_{10\%}$ (µm)	$d_{50\%}$ (µm)	$d_{90\%}$ (µm)	VMD (µm)	Span
PA	254 ± 22	506 ± 30	911 ± 39.3	548 ± 30.2	1.3 ± 0
CUR	4 ± 0	18 ± 1	85.2 ± 5	44 ± 4	5 ± 0
PM(PA–CUR)	53.3 ± 24	1200 ± 46	2350 ± 20	1237 ± 51.3	2 ± 0
ML5(PA–CUR)	5 ± 1	789 ± 40.2	2133.3 ± 32.1	858 ± 25.3	3 ± 0
ML6(PA–CUR)	3.4 ± 0.2	490 ± 17	2073.3 ± 32.1	796 ± 17.3	4.2 ± 0
ML7(PA–CUR)	3 ± 0.3	25.3 ± 5	243 ± 37.2	76.3 ± 13	10 ± 0
ML10(PA–CUR)	3 ± 0.0	25.3 ± 1	276 ± 18	86 ± 6	10 ± 0.0

Table 25. Particle size distribution for commercial paracetamol (PA), commercial curcumin (CUR), and PA–CUR mixtures (5:2, *w/w*) prepared using physical mixing (PM), and milling at various timing (ML5, ML6, ML7 and ML10). Data given for particle size at 10% ($d_{10\%}$), 50% ($d_{50\%}$, median diameter), and 90% ($d_{90\%}$) of the volume distribution, the volume mean diameter (VMD), and the span of the volume distribution (see Eq. (1)). Data expressed as mean ± SD,n=3.

10.4. Solid–state properties

10.4.1. Powder X–ray diffraction

After numerous attempts to prepare cocrystals of PA–CUR using grinding and solution–based techniques, a pure cocrystal was not obtained. Instead, the physical mixing of PA: CUR (10:4, *w/w* in total 14g) was milled. The X–ray diffraction patterns of PA, CUR, PM (PA–CUR) and ML5 (PA–CUR), ML6 (PA–CUR), ML7 (PA–CUR) and ML10 (PA–CUR) are shown in (Figure 50). The commercial PA exhibited diffraction angles as well discussed in (Section 3.3.4). On the other hand, the marketed available CUR used for this investigation was the known Form *I* (monoclinic form) (Sanphui *et al.*, 2011). Its sharp characteristic peak indicates the crystalline structure of CUR as shown by distinct peak at 2θ values of, 8.85°, 17.46°, 23.32°, 24.49°, 25.56° and a series of small peaks at 12.19°, 14.48°, 18.13°, 19.41°, 21.13°, 23.32°, 24.49°, 26.07°, 26.73°, 27.34° and 28.91° similar to the results obtained by (Pushpalatha *et al.*, 2018). The diffractogram of physical mixture PM (PA–CUR) and all the milled mixtures (ML5, ML6, ML7, ML10 (PA–CUR)) presented only an overlap of the characteristic peaks of each component that matches the sum of both species (Figure 50). The PXRD patterns of all the PA–CUR mixtures ruled out the transformation of the monoclinic form to the orthorhombic form, in both PA and CUR which indicated that the initial crystalline state of commercial PA and CUR are maintained for all PA–CUR mixtures regardless of the mixing technique. The height of the peaks of curcumin reduces as the milling time increases, which could be due to the

entrapment of CUR particles on PA particles, thereby reducing their occurrence (Figure 50).

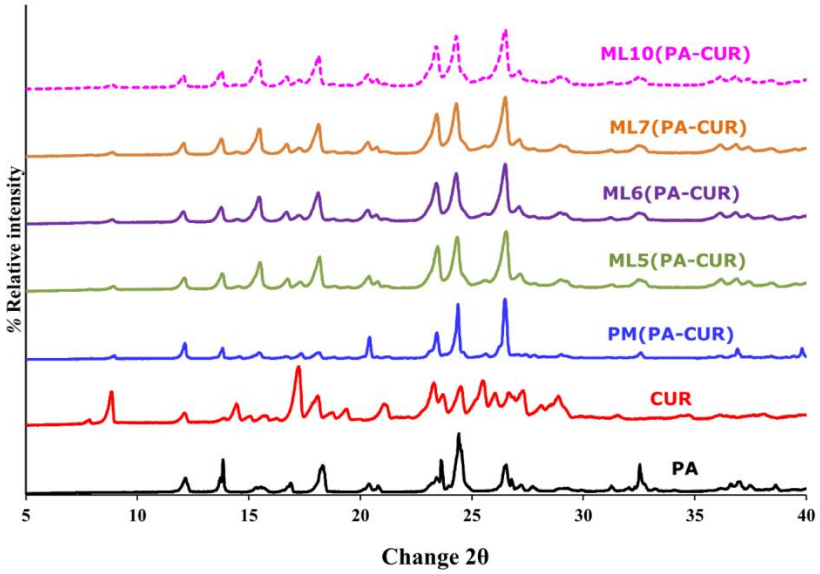

Figure 50. Powder X–ray diffraction of commercial paracetamol (PA), commercial curcumin (CUR), and PA–CUR mixtures (5:2, w/w) prepared using physical mixing (PM (PA–CUR)), and milling method at various timing (ML5, ML6, ML7 and ML10)

10.4.2. Fourier transform infrared spectrum

FT–IR spectroscopy was used to ascertain the hydrogen bonding interactions between PA and CUR molecules, which was also relevant to supplement microstructural change of PA and PA–CUR mixtures. FT–IR spectra of PA, CUR, PM (PA–CUR), ML5 (PA–CUR), ML6 (PA–CUR), ML7 (PA–CUR) and ML10 (PA–CUR) are displayed in (Figure 51). A broad absorption band at the range of 3400 and 3450 cm^{-1} was due to overlapping of a hydroxyl group and amino group stretching vibrations

(Liu *et al*., 2016) was observed in all five spectra. The peaks at 2963, 1430 and 1376 cm^{-1} can be assigned to the C–H stretching modes and deformation of methyl groups. Likewise, the broad absorbance band at 1601.59 cm^{-1} assigned to C=C stretching of aromatic rings. The C–O stretching absorption bands appear at, 1428.17 cm^{-1}, (enol C–O) and 1273.11 cm^{-1} (phenol C–O) (Liu *et al*., 2016). Also, in the FT−IR spectrum, a sharp absorption peak at 967.07 cm^{-1} can be observed which corresponds to the in–plane bending mode of the C–H aromatic and the peak at 820 cm^{-1} relates to the stretching vibrations of C–O groups present in commercial CUR (Mai *et al*., 2012). Peaks at 1626.07 and 1601.59 cm^{-1} represents the C–O (amide *I* band) stretching of CUR (Govindaraj *et al*., 2014) and N–H (amide *II* band) of PA carbon chains as discussed in (Section 3.3.4) respectively. The FT−IR characteristic bands of the monoclinic form of PA as discussed in (Section 3.3.4) retained the diagnostic bands indicative of form *I* in all the mixtures of PA−CUR.

The carbonyl group (C=0, H) of CUR being a stronger electron acceptor than the hydroxyl group of the CUR might be favoured in H–bonding with PA (N−H, H) a strong hydrogen bond donor. Small changes in the drug N−H stretching and the O−H regions can be used to provide information about PA−CUR intermolecular hydrogen−bonding interactions. The shift and reduction in absorbance intensity have been found across the spectra of PA mixed with CUR compared to PA. The mixtures prepared using physical mixing showed a slight decrease in absorption intensities in comparison to PA (Figure 51), which implies a reduced inter−particle

interaction between PA and CUR. On the other hand, the band broadening became more noticeable for the mixtures prepared using milling at different timing (i.e. ML5, ML6 and ML7)(Figure 51) hence; it implies a higher level of intermolecular hydrogen bonding between PA and CUR in the mixtures prepared using milling. Also, the mixture milled for 10 min (ML10) exhibited decreased furthermore probably because of the strong hydrogen bonding interaction formed between two ketone groups of CUR and amide of PA molecule i.e the hydrogen bond interaction brings about the reduction of absorption intensity of N−H and the slight shift to higher wavenumber from 3321.37 cm^{-1} to 3327.64 cm^{-1}. The peak at 1281.27 cm^{-1} was assigned to the C−O stretching vibration of the benzene ring (Feng, Liu, Zhao, & Hu, 2012), which was regarded as a characteristic peak found in CUR and PA–CUR mixtures. The changes of the C−O bond and N−H bond are observed by FT−IR spectrum as seen in (Figure 51).

The mixture of PA−CUR milled for 10 min showed a drastic reduction in absorbance intensity at various typical peaks in PA and CUR, which demonstrated that PA and CUR had been homogeneously blended. A more substantial shift indicates stronger/more extensive hydrogen bonding) (Wegiel *et al*., 2014). Therefore, the FT–IR spectra showed that hydrogen bonding interactions are more likely to occur in the mixtures using milling compared to the physical mixing where the interaction is minimal. Higher milling time during grinding results in higher levels of PA–CUR interaction; this is probably because the increase in shear forces during milling causes

entrapment of CUR particles into the host PA particle surfaces. So, it can be concluded that milling did not change the chemical composition of PA.

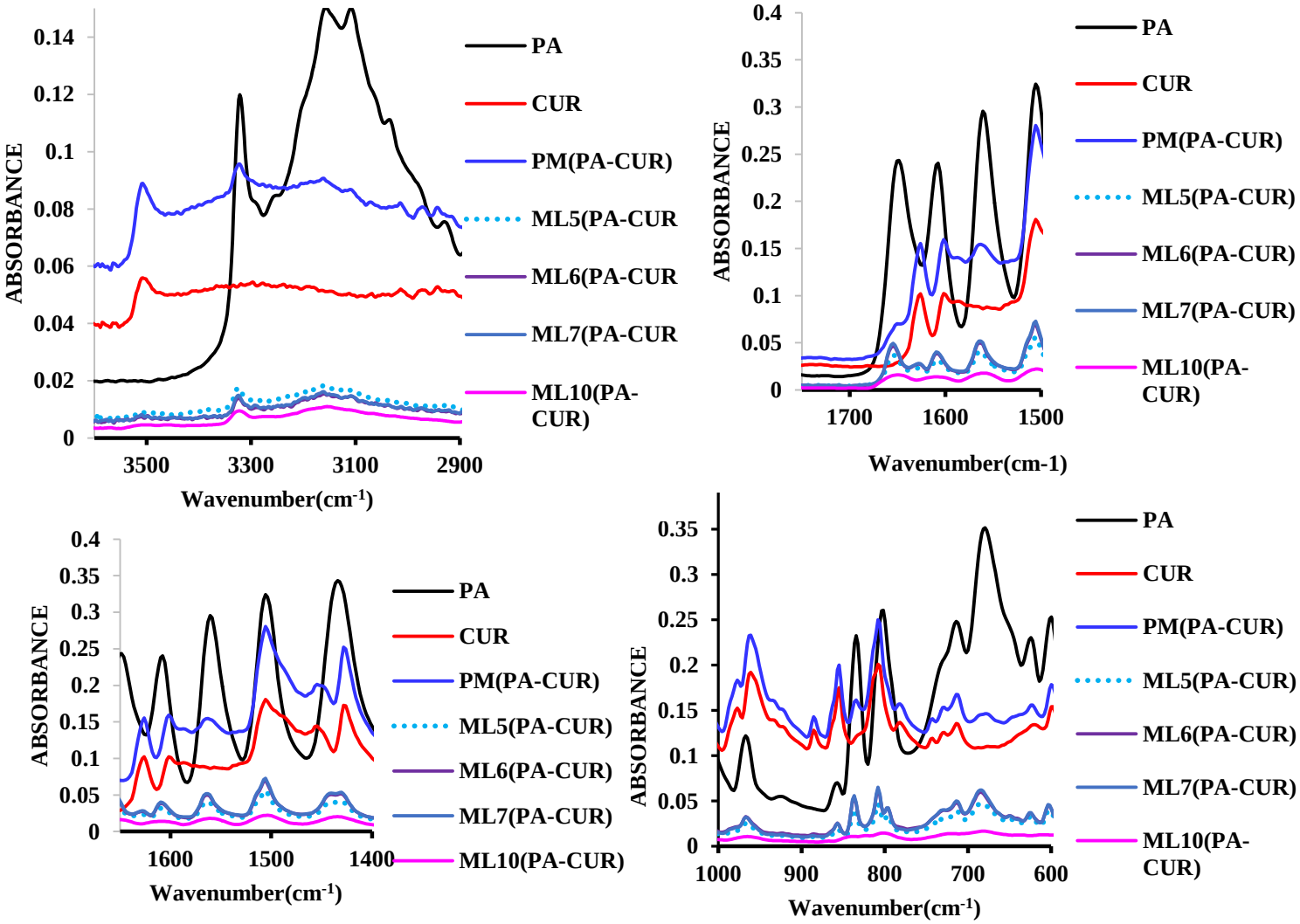

Figure 51. Fourier transform infrared spectroscopy (FT–IR) spectra of commercial paracetamol (PA), commercial curcumin (CUR), and PA–CUR mixtures (5:2, *w/w*) prepared using physical mixing (PM (PA–CUR)), and milling method at various timing (ML5, ML6, ML7 and ML10).

10.4.3. Thermogravimetric analysis

Thermogravimetric Curve for commercial materials and PA–CUR mixtures were carried out to assess their thermal behaviour as shown in (Figure 52), where the mass versus temperature curve was portrayed showing the degradation of PA, CUR and PA–CUR mixtures with increasing temperature. The TGA curves of PA and PA–CUR mixtures showed weight loss in the temperature range close to the range as discussed in (Section 3.3.4) which denotes the melting point of monoclinic PA, then subsequent weight loss due to degradation. CUR molecule remained thermally stable up to 150.2ºC and then began to lose weight continuously reaching the first maximum rate of weight loss at 168.7 ºC, as depicted in the TGA curve (Figure 52). The loss of volatile impurities during the melting of CUR is linked to the step above followed with the loss of two water molecules due to dehydroxylation of O–H groups (Zebib *et al*., 2010; Souguir *et al*., 2013). No weight loss occurred below 100 ºC (Figure 52), indicating the absence of a significant amount of free water in all mixtures. A slight shift towards lower melting onsets was observed for the mixtures prepared using milling technique when compared with the mixture prepared using physical mixing method (Figure 52). This difference may be attributable to their starkly different physical properties such as their considerably lower VMDs (Table 27; Figure 52).

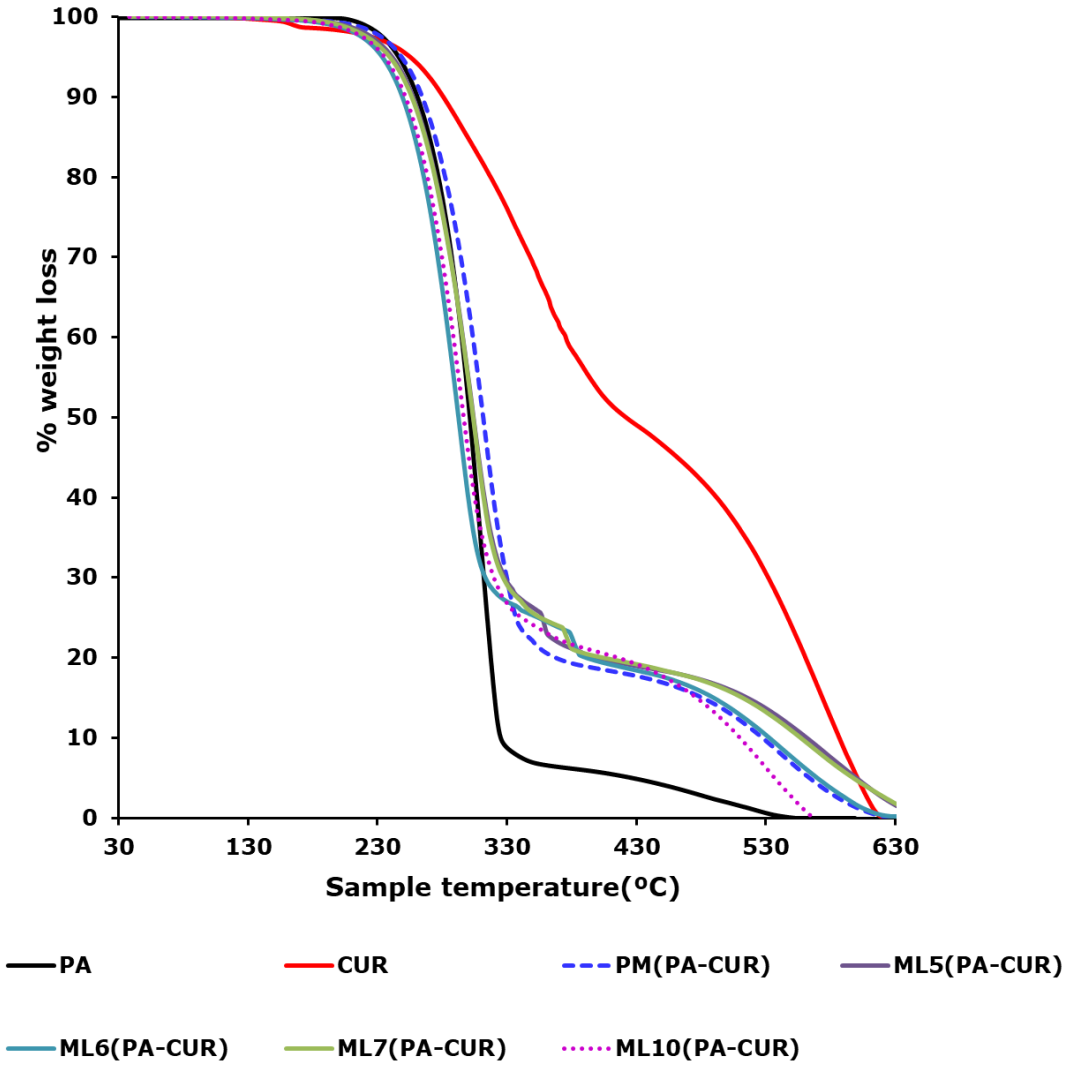

Figure 52. Thermogravimetric analysis curves of commercial paracetamol (PA), commercial curcumin (CUR), and PA–CUR mixtures (5:2, *w/w*) prepared using physical mixing (PM (PA–CUR)), and milling method at various timing (ML5, ML6, ML7 and ML10).

10.4.4. Tableting properties

The tabletability of PA was poor at various compression pressures, as discussed in (Section 3.3.5). In contrast, CUR exhibited far much better tabletability as the TS of CUR tablets increased with increasing pressure and reached ~ 2.2 ± 0.1 MPa at the compaction pressure of 222 MPa with

low variability in the tablet tensile strength. The presence of the drug to CUR (5:2 ratio *w/w*) improved the mechanical properties of PA in all PA–CUR mixtures (Figure 53).

The TS of PA–CUR mixture compressed at 222 MPa was 0.9 ± 0.1 MPa, 3.0 ± 0.0 MPa, 2.9 ± 0.1 MPa and 3.2 ± 0.0 MPa for the mixtures prepared using PM, ML5, ML6/ML7, and ML10 methods (Figure 53).

The tableting performance of PA was slightly improved by physically mixing with CUR and was intermediate between those of PA and CUR (Figure 53) for example, with the compression pressure increasing from 37 to 222 MPa, the TS of tablets increased from 0.2 to 0.9 MPa.

Compressed tablets with TS of at least 2 MPa was obtained at 185 MPa from the milling mixtures of PA–CUR (ML5, ML6 and ML7) (Figure 53), for example, the TS of 0.6 to 3.0 MPa was obtained at a compression pressure of 37 to 222 MPa (Figure 53). On the other hand, tabletability of PA was substantially improved after milling with CUR for 10 min. For example, when the compression pressure increased from 37 to 222 MPa, the TS of tablets increased from 0.6 ± 0.0 MPa to 3.2 ± 0.0 MPa (Figure 53). It is apparent that the PA–CUR mixture prepared using ML10 showed the best compression properties among the mixtures obtained during this study showed, TS of 3.3 ± 0.0 MPa at a compression pressure of 185 MPa. Compared with the mixtures prepared using PM technique, the mixtures acquired with ML10 produced the best tablets under the compression pressure range of 37 to 222 MPa.

The increased tensile strengths of the tablets containing mixtures prepared with ML10 technique shows of stronger interparticle bonding for between PA and CUR. Such superior tabletability is attributed to the higher level of PA–CUR interaction via hydrogen bonding, especially with the milling sample (Figure 52). Also, in disparity to the mixtures prepared using PM technique in which the morphologies of both PA (subangular/polyhedral) and CUR (tabular) particles could be observed (Figure 49), no distinct individual CUR particles were seen in mixtures prepared using milling method (Figure 49).

The mechanistic understanding of the superior tableting performance of ML10 (PA−CUR) would require elucidation of its crystal structure if it is possible that the component molecules in ML10 (PA−CUR) mixture form either a flat hydrogen column since the molecular arrangement is known to improve crystal plasticity and tabletabilty (Karki *et al.,* 2009). According to (Sun, 2011) when plasticity is enhanced, crystals can form a larger bonding area under pressure and therefore a strong tablet.

Overall, irrespective of the milling timing, the enhanced tableting performance in this investigation demonstrated the applicability of milling technique for enhancing the tableting performance of PA.

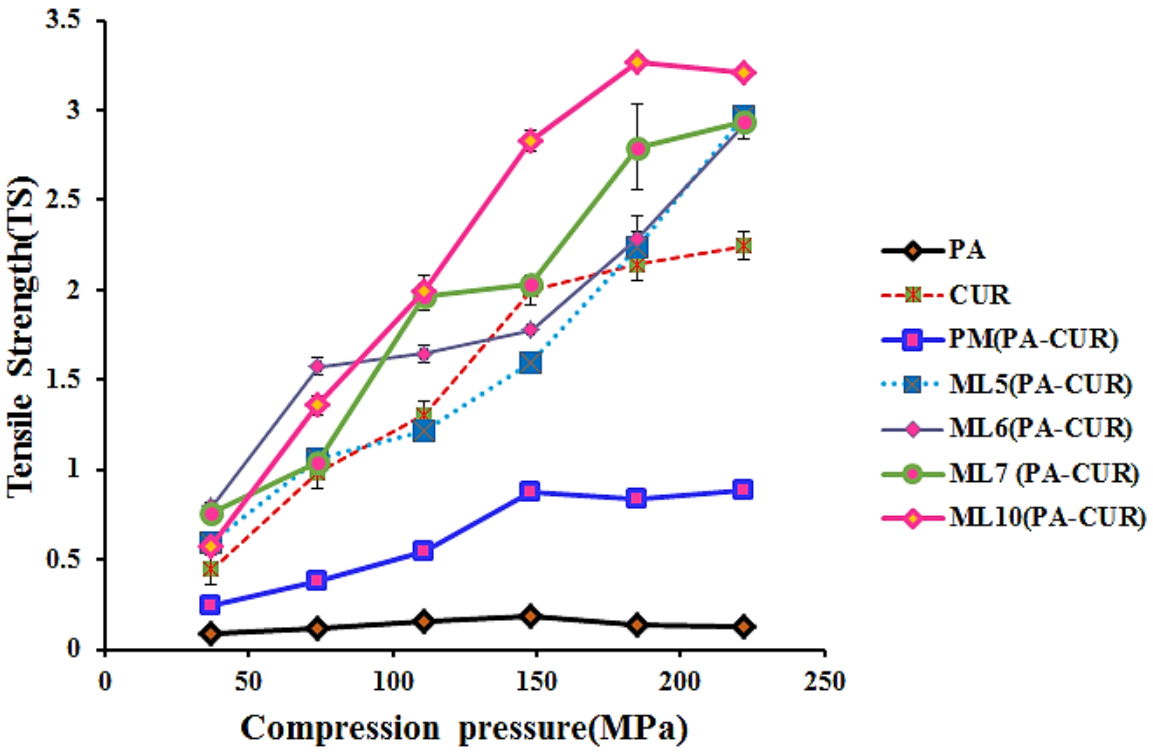

Figure 53. Tensile strength (mean ± SD, n = 5) versus compression pressure for commercial paracetamol (PA), commercial curcumin (CUR), and PA–CUR mixtures (5:2, *w/w*) prepared using physical mixing (PM) and milling at various timing (ML5, ML6, ML7 and ML10).

10.5. Dissolution Studies

The dissolution profile of commercial PA and the mixtures of PA–CUR products are shown in (Figure 54). After 3 min, the milled PA–CUR had the highest percentage of PA released (Figure 54) and a complete drug dissolution was achieved within the first 21 min, which was further reflected by the highest dissolution efficiency ($DE_{180\ min}$ of 90.8 ± 1.3%) and the shortest mean dissolution time (MDT of 2.9 ± 0.5 min) in the presence of 5% sodium starch glycolate (Primojel) among the mixtures studied. On the other hand, commercial PA demonstrated the slowest

dissolution compared to the engineered PA and CUR products which was also reflected by the lowest dissolution efficiency ($DE_{180\ min}$ of 68.4 ± 7.5%) and the highest mean dissolution time (MDT of 54.2 ± 11.4 % min) among paracetamols mixtures studied (Figure 54).

Results of this investigation indicate that 5% *w/w* of primogel in the mixture as dissolution medium is suitable for routine *in vitro* dissolution testing of PA formulations. PA–CUR obtained using physical mixing also showed an enhancement of PA dissolution, as it released PA within 30 min, whereas the dissolution of the commercial PA took about 3h. Also, it was observed that the mean dissolution rate of PA from the physical mixture was ~2.2 times higher than that of commercial PA; this may be due to a better dispersion of PA particles in the form of the physical mixture with CUR. The release rate of PA was 80% with ML10 (PA–CUR) compared to PM (PA–CUR) within 15 min under the same test conditions. Also, these results indicate that milling is an effective approach for improving the dissolution rate of PA. The greater dissolution of PA from ML10 (PA–CUR) can be attributed to the change in crystallinity pattern (reduced peak heights), morphology (*i.e.*, crystal habit), shape and size of ML10 (PA–CUR) that led in enhancing in the dissolution medium (Panzade *et al.*, 2017); for example, the physical mixing method tends to produce larger primary particles with a broader size distribution and a lower specific surface area, consequently giving a reduced dissolution rate of PA.

On the other hand, the sharp increased and highest rate (90%) in the dissolution rate were due to the enlarged surface area of the micronised drug particles, as particle size reduction leads to an enlarged effective surface area in the diffusion layer, which would increase the drug dissolution rate (Noyes and Whitney, 1897).

Nevertheless, the dissolution of these mixtures ML10(PA–CUR) and PM(PA–CUR) due to the release of more than 80% PA in dissolution medium within 30 min, as required according to the requirement (USP, 2008).

The present investigation showed that the milling technique not only improved the mechanical properties of paracetamol tablets but also the processed PA in some cases had better dissolution performance than the commercial PA and physical mixing of both commercial PA and commercial CUR.

.

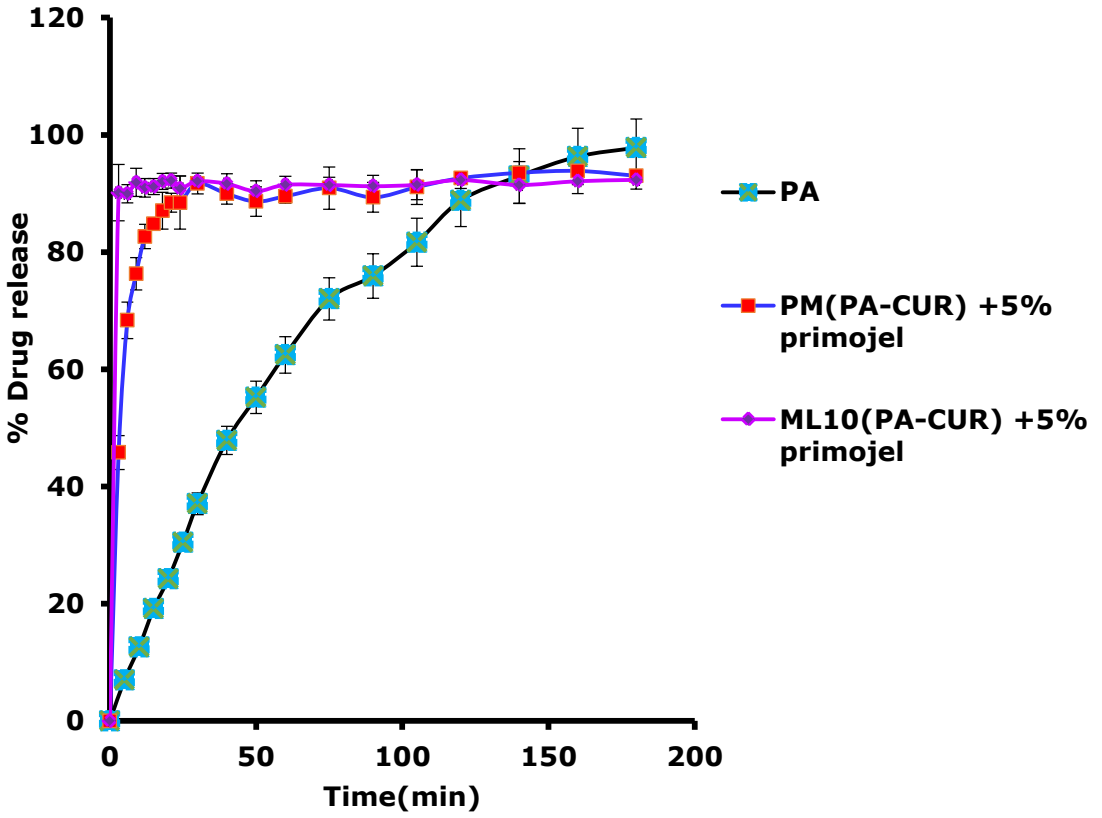

Figure 54. Release profiles for commercial paracetamol (PA), PA–CUR mixtures (5:2, w/w) prepared using physical mixing (PM) and milling for 10 min ML10

10.7. Conclusions

Processing of PA−CUR mixtures on the micrometric and mechanical properties should be well considered. In disparity to physical mixing and milling techniques promoted hydrogen bonding between PA and CUR with subsequent improvements in the mechanical properties of the resultant mixtures in the presence of 5:2 (*w/w*) CUR. Henceforth, such improved material properties with milling may be exploitable in the formulation development and manufacturing of high−quality PA products

CHAPTER 11: SUMMARY AND FUTURE WORKS

Solid oral drug administration entails steps such as, the formation of a stable drug compact which can withstand mechanical shock upon transportation, drug release and transport to the site of action.

Oral drug administration is the most versatile and popular route among other routes due to the ease of ingestion, patient compliance and pain avoidance. Also, the solid oral dosage forms such as tablets are cheap to manufacture and do not require a sterile environment.

Many new chemical entities developed possess a poor mechanical characteristic, which is one of the major hurdles that formulation scientists and pharmaceutical companies face every day.

In this research study, the tableting deficiency of paracetamol was overcome by applying various engineering methods via processing drug–excipient and drug/drug formulations. Consequently, employing suitable processing techniques in the presence of plastically deforming excipient or drugs particles is vital for enhancing solid dosage performance. Therefore, numerous methods including, blending, milling, solvent evaporation, batch cooling crystallisation, freeze drying and cocrystallisation were used in the presence of the known plastically deforming binder polyvinylpyrrolidone and other common drugs including; Ibuprofen, caffeine, aspirin, curcumin, chondroitin sulphate and the coformer 5–nitroisophthalic acid, in order to enhance the mechanical performance of paracetamol from the binary and ternary mixtures.

Important parameters affecting the outcomes of the particles' properties were identified. It was shown that the micrometric properties for

paracetamol: polyvinylpyrrolidone mixtures blended were dependent on the energy of mixing employed as, the energy of mixing increased so is the tensile strength of paracetamol: polyvinylpyrrolidone mixtures. Also, the milling time in the cases of paracetamol: Curcumin and paracetamol/aspirin/caffeine as the timing increase, so was the tabletability. The temperature of freezing on paracetamol–polyvinylpyrrolidone mixtures by applying freeze drying technique appeared to be a critical factor in the control of the mechanical behaviour, for example, enhanced mechanical performance was obtained for the formulations containing paracetamol−polyvinylpyrrolidone mixture frozen at considerable low temperature with liquid nitrogen (−196 ºC), as the tensile strength of the tablets increased with decreased in temperatures (−196 ºC > −80 ºC >−20 ºC). Among all the processing techniques investigate, freeze drying with liquid nitrogen was shown to be the ultimate method in preparing engineered particles with an immense increase in tabletability. The effect of other drugs properties, when combined with paracetamol on their performance, was evaluated. Processing of two or more drugs was proven to be a promising approach to enhance the mechanical properties of paracetamol, as paracetamol and ibuprofen tablets showed better tensile than their marketed component, the same applies to paracetamol/aspirin/caffeine. Cocrystals of paracetamol and the coformer 5–nitroisophthalic acid demonstrated far much better mechanical properties than their commercial components through processing in the presence of polar solvents specifically. The use

of co–engineering techniques on the poorly compactable drug offers great prospect at improving mechanical performance via the manipulation of their physicochemical properties. Also, mechanical properties enhancement can be linked to changes in key physicochemical properties of the excipient/other drugs, which can be heightened via the processing technique applied.

Future work

In the present study, in order to appraise the impact of the various engineered methods in the presence of the excipient/drugs on the physicochemical and mechanical performance, paracetamol was included in all processed formulations as the model drug. Nonetheless, substantial data are essential where the performance of various formulations is compared in the case of different hydrophobic and highly hydrophilic drugs. It was noteworthy that numerous factors impacted the performance of the co–processing formulations. Analyses such as surface properties could be performed to identify the most vital parameters holding the engineered particle in a stable compact in the acquired formulations. Some formulations demonstrated slightly reduced flow; thus, the employability of lubricants and anti adherents should be added into the formulations in other to obtain a great product.

Further investigations in the future such as the use of other engineering techniques including, antisolvent crystallisation, spray drying or hot melt extrusion should be applied in the mixtures of paracetamol–chondroitin to enhance the mechanical properties of PA will be much needed.

In vivo tests should be performed in order to evaluate their pharmacokinetic performance/ characteristics, especially on paracetamol–chondroitin and paracetamol−curcumin formulations on osteoarthritis and arthritis patients upon oral absorption in order to further reduce pain.

REFERENCES

Abe, S., Obata, Y., Oka, S., Koji, T., Nishino, T. and Izumikawa, K (2016). Chondroitin sulfate prevents peritoneal fibrosis in mice by suppressing NF-κB activation. *Medical molecular morphology*, **49**(3), pp.144-153.

Abioye, A. O., Chi, G. T., Simone, E. and Nagy, Z. (2016) 'Real-time monitoring of the mechanism of ibuprofen-cationic dextran crystanule formation using crystallization process informatics system (CryPRINS). *International journal of pharmaceutics*, **509**(1–2), pp. 264–78.

Abdelwahed, W., Degobert, G., Stainmesse, S. and Fessi, H(2006). Freeze-drying of nanoparticles: formulation, process and storage considerations. *Advanced drug delivery reviews*, **58**(15), pp.1688-1713.

Aher, S., Dhumal, R., Mahadik, K., Ketolainen, J. and Paradkar, A(2013). Effect of cocrystallization techniques on compressional properties of caffeine/oxalic acid 2: 1 cocrystal. *Pharmaceutical development and technology*, **18**(1), pp.55-60.

Ainouz, A., Authelin, J.R., Billot, P. and Lieberman, H(2009). Modeling and prediction of cocrystal phase diagrams. *International journal of pharmaceutics*, **374**(1-2), pp.82-89.

Alderborn,G(2002) Tablets and compaction, In: in: M.E. Aulton (Ed.), Pharmaceutics: The Science of Dosage Form Design, Churchill Livingstone.

Ali, W., Williams, A.C. and Rawlinson, C.F(2010). Stochiometrically governed molecular interactions in drug: poloxamer solid dispersions. *International journal of pharmaceutics*, **391**(1-2), pp.162-168.

Al-Hamidi, H., Edwards, A.A., Douroumis, D., Asare-Addo, K., Nayebi, A.M., Reyhani-Rad, S., Mahmoudi, J. and Nokhodchi, A(2013). Effect of glucosamine HCl on dissolution and solid state behaviours of piroxicam upon milling. *Colloids and Surfaces B: Biointerfaces*, **103**, pp.189-199.

Al-Hamidi, H., Edwards, A.A., Mohammad, M.A. and Nokhodchi, A(2010). Glucosamine HCl as a new carrier for improved dissolution behaviour: Effect of grinding. *Colloids and Surfaces B: Biointerfaces*, **81**(1), pp.96-109.

Amrutkar, J.R. and Gattani, S.G(2009). Chitosan–chondroitin sulfate based matrix tablets for colon specific delivery of indomethacin. *Aaps Pharmscitech*, **10**(2), pp.670-677.

Afshari, E. and Ghambari, M(2016). Characterization of pre-alloyed tin bronze powder prepared by recycling machining chips using jet milling. Materials & Design, **103**, pp.201-208.

Acevedo, D., Peña, R., Yang, Y., Barton, A., Firth, P. and Nagy, Z.K(2016). Evaluation of Mixed Suspension Mixed Product Removal Crystallization Processes Coupled with a Continuous Filtration System. Chemical Engineering and Processing: Process Intensification

Afrasiabi Garekani, H., Sadeghi, Fatemeh and Ghazi, A(2003). Increasing the aqueous solubility of acetaminophen in the presence of polyvinylpyrrolidone and investigation of the mechanisms involved. Drug development and industrial pharmacy, **29**(2), pp.173-179.

Ajun, W., Yan, S., Li, G., Huili, L(2009). Preparation of aspirin and probucol in combination loaded chitosan nanoparticles and in vitro release study. Carbohydr. Polym**. 75**, 566–57

Alderborn, G. and Ahlneck, C(1991). Moisture adsorption and tableting. III. Effect on tablet strenght-post compaction storage time profiles. International journal of pharmaceutics, **73**(3), pp.249-258.

Alderborn, G. and Nystrom, C(1996). Pharmaceutical powder compaction technology. Marcel Dekker, Inc ..

Al–Zoubi, N., Koundourellis, J.E., & Malamataris, S. (2002). FT-IR and Raman spectroscopic methods for identification and quantitation of orthorhombic and monoclinic paracetamol in powder mixes. *Journal of Pharmaceutical and Biomedical Analysis,* **29**, 459–467.

Ambrogi, V., Fardella, G., Grandolini, G. and Perioli, L., 2001. Intercalation compounds of hydrotalcite-like anionic clays with antiinflammatory agents—I. Intercalation and in vitro release of ibuprofen. International Journal of Pharmaceutics, **220**(1), pp.23-32.

Andini, S., Bolognese, A., Formisano, D., Manfra, M., Montagnaro, F. and Santoro, L., 2012. Mechanochemistry of ibuprofen pharmaceutical. *Chemosphere*, **88**(5), pp.548-553.

Anand, P., Kunnumakkara, A.B., Newman, R.A. and Aggarwal, B.B (2007). Bioavailability of curcumin: problems and promises. *Molecular pharmaceutics*, **4**(6), pp.807-818.

Armstrong, N. A. (2007). Tablet manufacture by direct compression. In J. Swarbrick (Ed.), *Encyclopedia of pharmaceutical technology* (pp. 3673–3683). New York: Informa Healthcare Inc.

Avachat, A. and Kotwal, V(2007). Design and evaluation of matrix-based controlled release tablets of diclofenac sodium and chondroitin sulphate. *Aaps pharmscitech*, **8**(4), pp.51-56.

Ayensu, I., Mitchell, J.C. and Boateng, J.S(2012). Development and physico-mechanical characterisation of lyophilised chitosan wafers as potential protein drug delivery systems via the buccal mucosa. Colloids and Surfaces B: Biointerfaces, **91**, pp.258-265.

Bannwarth, B. and Pehourcq, F(2003). Pharmacological rationale for the clinical use of paracetamol: pharmacokinetic and pharmacodynamic issues. *Drugs*, **63**, pp.5-13.

Barresi, A.A., Ghio, S., Fissore, D., Pisano, R(2009). Freeze drying of pharmaceutical excipients close to collapse temperature: influence of the process conditions on process time and product quality. Dry. Technol. **27**, 805–816.

Bauer-Brandl, A(1996). Polymorphic transitions of cimetidine during manufacture of solid dosage forms. International Journal of Pharmaceutics, **140**(2), pp.195-206.

Berggren, J., Frenning, G., & Alderborn, G. (2004). Compression behaviour and tablet-forming ability of spray-dried amorphous composite

particles. *European Journal of Pharmaceutical Sciences,* **22**, 191–200.

Bergström, C.A., Luthman, K. and Artursson, P(2004). Accuracy of calculated pH-dependent aqueous drug solubility. *European Journal of Pharmaceutical Sciences*, **22**(5), pp.387-398.

Bertolini, A., Ferrari, A., Ottani, A., Guerzoni, S., Tacchi, R. and Leone, S., 2006. Paracetamol: new vistas of an old drug. *CNS drug reviews*, **12**(3-4), pp.250-275.

Beyer, T., Day, G. M., & Price, S.L. (2001). The prediction, morphology, and mechanical properties of the polymorphs of paracetamol. *Journal of the American Chemical Society,* **123**, 5086–5094.

Blagden, N., Berry, D.J., Parkin, A., Javed, H., Ibrahim, A., Gavan, P.T., De Matos, L.L. and Seaton, C.C(2008). Current directions in co-crystal growth. *New Journal of Chemistry*, **32**(10), pp.1659-1672.

BNF 71: British National Formulary 71. (2016). British Medical Association & Royal Pharmaceutical Society of Great Britain.

Boateng, J.S., Matthews, K.H., Auffret, A.D., Humphrey, M.J., Stevens, H.N. and Eccleston, G.M(2009). In vitro drug release studies of polymeric freeze-dried wafers and solvent-cast films using paracetamol as a model soluble drug. *International journal of pharmaceutics*, **378**(1-2), pp.66-72.

Bonkovoski, L.C., Martins, A.F., Bellettini, I.C., Garcia, F.P., Nakamura, C.V., Rubira, A.F. and Muniz, E.C(2014). Polyelectrolyte complexes of poly [(2-dimethylamino) ethyl methacrylate]/chondroitin sulfate obtained at

different pHs: I. Preparation, characterization, cytotoxicity and controlled release of chondroitin sulfate. *International journal of pharmaceutics*, **477**(1-2), pp.197-207.

Booth, S.W. and Newton, J.M(1987). Experimental investigation of adhesion between powders and surfaces. Journal of pharmacy and pharmacology, **39**(9), pp.679-684.

Bonkovoski, L.C., Martins, A.F., Bellettini, I.C., Garcia, F.P., Nakamura, C.V., Rubira, A.F. and Muniz, E.C (2014). Polyelectrolyte complexes of poly [(2-dimethylamino) ethyl methacrylate]/chondroitin sulfate obtained at different pHs: I. Preparation, characterization, cytotoxicity and controlled release of chondroitin sulfate. *International journal of pharmaceutics*, **477**(1-2), pp.197-207.

Brayfield (Ed.), "Aspirin". Martindale: The Complete Drug Reference, Pharmaceutical Press, January 14 2014 (Retrieved 3 April 2014).

Breitenbach, J (2002). Melt extrusion: from process to drug delivery technology. *European journal of pharmaceutics and biopharmaceutics*, **54**(2), pp.107-117.

Brniak, W., Maślak, E. and Jachowicz, R(2015). Orodispersible films and tablets with prednisolone microparticles. *European Journal of Pharmaceutical Sciences*, **75**, pp.81-90.

Bruyère, O., Cooper, C., Pelletier, J.P., Maheu, E., Rannou, F., Branco, J., Brandi, M.L., Kanis, J.A., Altman, R.D., Hochberg, M.C. and Martel-Pelletier, J(2016), February. A consensus statement on the European

Society for Clinical and Economic Aspects of Osteoporosis and Osteoarthritis (ESCEO) algorithm for the management of knee osteoarthritis—from evidence-based medicine to the real-life setting. In *Seminars in arthritis and rheumatism* (Vol. **45**, No. 4, pp. S3-S11). Elsevier.

Bučar, D.K., Elliott, J.A., Eddleston, M.D., Cockcroft, J.K. and Jones, W(2015). Sonocrystallization yields monoclinic paracetamol with significantly improved compaction behavior. *Angewandte Chemie*, **127**(1), pp.251-255.

Burley, J.C., Duer, M.J., Stein, R.S. and Vrcelj, R.M (2007). Enforcing Ostwald's rule of stages: Isolation of paracetamol forms III and II. *European journal of pharmaceutical sciences*, **31**(5), pp.271-276.

Bustamante, P.,Romero, S., Escalera, B., Cirri, M. and Mura, P(2004). Characterization of the solid phases of paracetamol and fenamates at equilibrium in saturated solutions. Journal of thermal analysis and calorimetry, **77**(2), pp.541-554.

Cahn, A. and Hepp, P(1886). Antifebrin, a new antipyretic. *American Journal of Pharmacy (1835-1907)*, **58**(11), p.565.

Cai, A.H., Xiong, X., Liu, Y., Zhou, Y., An, W.K. and Luo, Y(2010). Regular Cu-based amorphous alloy powder. Journal of Alloys and Compounds, **497**(1), pp.234-238.

Cassaro, C.M. and Dietrich, C.P(1977). Distribution of sulfated mucopolysaccharides in invertebrates. *Journal of Biological Chemistry*, **252**(7), pp.2254-2261.

Celik, M(2011). Pharmaceutical Powder Compaction Technology. Informa Healthcare, London UK, pp. 236–241

Chattoraj, S., Shi, L. and Sun, C.C(2010). Understanding the relationship between crystal structure, plasticity and compaction behaviour of theophylline, methyl gallate, and their 1: 1 co-crystal. *CrystEngComm*, **12**(8), pp.2466-2472.

Cherukuvada, S(2016). On the issues of resolving a low melting combination as a definite eutectic or an elusive cocrystal: a critical evaluation. J. Chem. Sci. **128**, 1–13.

Chemat, F. and Khan, M.K (2011). Applications of ultrasound in food technology: processing, preservation and extraction. *Ultrasonics sonochemistry*, **18**(4), pp.813-835.

Chieng, N., Hubert, M., Saville, D., Rades, T. and Aaltonen, J(2009). Formation kinetics and stability of carbamazepine– nicotinamide cocrystals prepared by mechanical activation. *Crystal Growth and Design*, **9**(5), pp.2377-2386.

Childs, S.L., Chyall, L.J., Dunlap, J.T., Smolenskaya, V.N., Stahly, B.C. and Stahly, G.P(2004). Crystal engineering approach to forming cocrystals of amine hydrochlorides with organic acids. Molecular complexes of fluoxetine hydrochloride with benzoic, succinic, and fumaric

acids. *Journal of the American Chemical Society*, **126**(41), pp.13335-13342.

Chomcharn, N. and Xanthos, M., 2013. Properties of aspirin modified enteric polymer prepared by hot-melt mixing. *International journal of pharmaceutics*, *450*(1), pp.259-267

Chow, S.F., Shi, L., Ng, W.W., Leung, K.H.Y., Nagapudi, K., Sun, C.C. and Chow, A.H(2014). Kinetic entrapment of a hidden curcumin cocrystal with phloroglucinol. *Crystal Growth & Design*, **14**(10), pp.5079-5089.

Chowdary, K.P.R .,Kumar, S.,. and Suresh, P(2012). Preparation Characterization and Evaluation of PGS-PVP Co-Processed Excipient as Directly Compressible Vehicle in the Formulation Development of Antiretroviral Drugs. *IJRPC*, **2**(3), pp.860-865.

Coates, J(2000). Interpretation of infrared spectra, a practical approach. In: Meyers, R.A. (Ed.), Encyclopedia of Analytical Chemistry, pp. 10815–10837

Craig, D.Q., Royall, P.G., Kett, V.L. and Hopton, M.L(1999). The relevance of the amorphous state to pharmaceutical dosage forms: glassy drugs and freeze dried systems. *International Journal of Pharmaceutics*, **179**(2), pp.179-207.

Crowley, M.M., Zhang, F., Repka, M.A., Thumma, S., Upadhye, S.B., Kumar Battu, S., McGinity, J.W. and Martin, C (2007). Pharmaceutical applications of hot-melt extrusion: part I. *Drug development and industrial pharmacy*, **33**(9), pp.909-926.

Corradetti, B., Taraballi, F., Minardi, S., Van Eps, J., Cabrera, F., Francis, L.W., Gazze, S.A., Ferrari, M., Weiner, B.K. and Tasciotti, E(2016). Chondroitin sulfate immobilized on a biomimetic scaffold modulates inflammation while driving chondrogenesis. *Stem cells translational medicine*, **5**(5), pp.670-682.

Crispim, E.G., Piai, J.F., Fajardo, A.R., Ramos, E.R.F., Nakamura, T.U., Nakamura, C.V., Rubira, A.F. and Muniz, E.C(2012). Hydrogels based on chemically modified poly (vinyl alcohol)(PVA-GMA) and PVA-GMA/chondroitin sulfate: Preparation and characterization. *Express Polymer Letters*, **6**(5).

Das, A. and Hammad, T.A(2000). Efficacy of a combination of FCHG49™ glucosamine hydrochloride, TRH122™ low molecular weight sodium chondroitin sulfate and manganese ascorbate* in the management of knee osteoarthritis. *Osteoarthritis and Cartilage*, **8**(5), pp.343-350.

da Silva, G.T., Voss, G.T., Kaplum, V., Nakamura, C.V., Wilhelm, E.A., Luchese, C. and Fajardo, A.R(2017). Development, characterization and biocompatibility of chondroitin sulfate/poly (vinyl alcohol)/bovine bone powder porous biocomposite. *Materials Science and Engineering: C*, **72**, pp.526-535.

Dcodhar, S.D., Sethi, R. and Srimal, R.C(2013). Preliminary study on antirheumatic activity of curcumin (diferuloyl methane). *Indian journal of medical research*, **138**(1).

De Brabander, C., Vervaet, C., Van Bortel, L. and Remon, J.P(2004). Bioavailability of ibuprofen from hot-melt extruded mini-matrices. *International journal of pharmaceutics*, **271**(1-2), pp.77-84.

DeLeon, V.H., Nguyen, T.D., Nar, M., D'Souza, N.A. and Golden, T.D(2012). Polymer nanocomposites for improved drug delivery efficiency. *Materials Chemistry and Physics*, ***132*****(**2), pp.409-415.

Denuziere, A., Ferrier, D. and Domard, A(1996). Chitosan-chondroitin sulfate and chitosan-hyaluronate polyelectrolyte complexes. Physico-chemical aspects. *Carbohydrate polymers*, **29**(4), pp.317-323.

de Oliveira, G. G. G., Feitosa, A., Loureiro, K., Fernandes, A. R., Souto, E. B., & Severino, P. (2017). Compatibility study of paracetamol, chlorpheniramine maleate and phenylephrine hydrochloride in physical mixtures. *Saudi Pharmaceutical Journal,* **25**(1), 99-103.

Depré, M., Hecken, A., Verbesselt, R., Tjandra-Maga, T.B., Gerin, M. and Schepper, P.J(1992). Tolerance and pharmacokinetics of propacetamol, a paracetamol formulation for intravenous use. *Fundamental & clinical pharmacology*, **6**(6), pp.259-262.

de Villiers, M.M., Wurster, D.E., Van der Watt, J.G. and Ketkar, A(1998). X-Ray powder diffraction determination of the relative amount of crystalline acetaminophen in solid dispersions with polyvinylpyrrolidone. *International journal of pharmaceutics*, **163**(1), pp.219-224.

Dhumal, R.S., Kelly, A.L., York, P., Coates, P.D. and Paradkar, A.(2010). Cocrystalization and simultaneous agglomeration using hot melt extrusion. *Pharmaceutical research*, **27**(12), pp.2725-2733.

Dichi, E., Legendre, B. and Sghaier, M(2014). Physico-chemical characterisation of a new polymorph of caffeine. *Journal of Thermal Analysis and Calorimetry*, **115**(2), pp.1551-1561.

Dichi, E., Sghaier, M. and Guiblin, N(2018). Reinvestigation of the paracetamol–caffeine, aspirin–caffeine, and paracetamol–aspirin phase equilibria diagrams. *Journal of Thermal Analysis and Calorimetry*, **131**(3), pp.2141-2155.

Di Martino, P., Guyot-Hermann, A.-M., Conflant, P., Drache, M., & Guyot, J.-C. (1996). A new pure paracetamol for direct compression: The orthorhombic form. *International Journal of Pharmaceutics,* **128**, 1–8.

Di Martino, P., Conflant, P., Drache, M., Huvenne, J.P. and Guyot-Hermann, A.M (1997). Preparation and physical characterization of forms II and III of paracetamol. *Journal of Thermal Analysis and Calorimetry*, **48**(3), pp.447-458.

Di Martino, P., Scoppa, M., Joiris, E., Palmieri, G.F., Andres, C., Pourcelot, Y. and Martelli, S(2001). The spray drying of acetazolamide as method to modify crystal properties and to improve compression behaviour. *International journal of pharmaceutics*, **213**(1-2), pp.209-221.

Di Martino, P., Beccerica, M., Joiris, E., Palmieri, G.F., Gayot, A. and

Doelker, E. and Massuelle, D(2004). Benefits of die-wall instrumentation for research and development in tableting. European journal of pharmaceutics and biopharmaceutics, **58**(2), pp.427-444.

Drug Bank: Ibuprofen, APRD 00372. www.drgbank.ca (assessed 25.02.2018).

Edna, M.D.A., Dulce, M.D.A., de Moura, M.D.F. and de Farias, R.F (2004). An investigation about the solid state thermal degradation of acetylsalicylic acid: polymer formation. *Thermochimica acta*, **414**(1), pp.101-104.

Elbagerma, M.A., Edwards, H.G.M., Munshi, T. and Scowen, I.J(2011). Identification of a new cocrystal of citric acid and paracetamol of pharmaceutical relevance. *CrystEngComm*, **13**(6), pp.1877-1884.

Eraga, S.O., Arhewoh, M.I., Uhumwangho, M.U. and Iwuagwu, M.A(2015). Characterisation of a novel, multifunctional, co-processed excipient and its effect on release profile of paracetamol from tablets prepared by direct compression. Asian Pacific Journal of Tropical Biomedicine, **5**(9), pp.768-772.

Etman, M.A. and Naggar, V.F(1990). Thermodynamics of paracetamol solubility in sugar-water cosolvent systems. *International journal of pharmaceutics*, **58**(3), pp.177-184.

Fachaux, J.M., Guyot-Hermann, A.M., Guyot, J.C., Conflant, P., Drache, M., Veesler, S. and Boistelle, R(1995). Pure paracetamol for direct compression Part II. Study of the physicochemical and mechanical

properties of sintered-like crystals of paracetamol. Powder technology, **82**(2), pp.129-133.

Fan, S. Pallerla, G. C, Ladipo,D, Dukich, R.J, Capella, S. L(2005).Effect of particle size distribution and flow property of powder blend on tablet weight variation. Amer. Pharm. Rev. **8** pp. 73-78.

Fell, J.T., & Newton, J.M. (1970). Determination of tablet strength by the diametral-compression test. *Journal of Pharmaceutical Sciences,* **59**, 688–691.

Finot, E., Lesniewska, E., Mutin, J. C., Hosain, S. I., & Goudonnet, J. P. (1996). Contact force dependence on relative humidity: investigations using atomic force microscopy. *Scanning Microscopy,* **10**(3), 697-708.

Fleischman, S.G., Kuduva, S.S., McMahon, J.A., Moulton, B., Bailey Walsh, R.D., Rodríguez-Hornedo, N. and Zaworotko, M.J(2003). Crystal engineering of the composition of pharmaceutical phases: multiple-component crystalline solids involving carbamazepine. *Crystal Growth & Design*, **3**(6), pp.909-919.

Forgione, M., Birpoutsoukis, G., Bombois, X., Mesbah, A., Daudey, P.J. and Van den Hof, P.M(2015). Batch-to-batch model improvement for cooling crystallization. Control Engineering Practice, **41**, pp.72-82.

Frank, F(1990). Freeze-drying from empiricism to predictability ,Cryo-lett, **11** pp 93-110.

Fried, M., Lauder, R.M. and Duffy, P.E(2000). Plasmodium falciparum: adhesion of placental isolates modulated by the sulfation characteristic CHONS of the glycosaminoglycan receptor. *Experimental parasitology*, **95**(1), pp.75-78.

Friščić, T. and Jones, W(2010). Benefits of cocrystallisation in pharmaceutical materials science: an update. *Journal of Pharmacy and Pharmacology*, **62**(11), pp.1547-1559.

Gaisford, S., Buanz, A.B. and Jethwa, N(2010). Characterisation of paracetamol form III with rapid-heating DSC. Journal of pharmaceutical and biomedical analysis, **53**(3), pp.366-370.

Garekani, H.A., Ford, J.L., Rubinstein, M.H., & Rajabi-Siahboomi, A.R. (2000). Highly compressible paracetamol: I: Crystallization and characterization. *International Journal of Pharmaceutics,* **208**, 87–99.

Garr, J.S.M. and Rubinstein, M.H(1991). An investigation into the capping of paracetamol at increasing speeds of compression. International journal of pharmaceutics, **72**(2), pp.117-122.

Garekani, H.A., Ford, J.L., Rubinstein, M.H. and Rajabi-Siahboomi, A.R(1999). Formation and compression characteristics of prismatic polyhedral and thin plate-like crystals of paracetamol. *International journal of pharmaceutics*, **187**(1), pp.77-89.

Garekani, H.A., Sadeghi, F.A.T.E.M.E.H., Badiee, A., Mostafa, S.A., Rajabi-Siahboomi, A.R. and Rajabi-Siahboomi, A.R(2001). Crystal habit

modifications of ibuprofen and their physicomechanical characteristics. *Drug development and industrial pharmacy*, **27**(8), pp.803-809.

Gharaibeh, S.F. and Iba'a, N(2011). Mechanical energies associated with compaction of form I and form II paracetamol powder. *Powder technology*, **214**(1), pp.161-168.

Craig, D.Q., Royall, P.G., Kett, V.L. and Hopton, M.L(1999). The relevance of the amorphous state to pharmaceutical dosage forms: glassy drugs and freeze dried systems. *International Journal of Pharmaceutics*, **179**(2), pp.179-207

Feng, F., Liu, Y., Zhao, B. and Hu, K(2012). Characterization of half N-acetylated chitosan powders and films. *Procedia Engineering*, **27**, pp.718-732.

Garnjanagoonchorn, W., Wongekalak, L. and Engkagul, A(2007). Determination of chondroitin sulfate from different sources of cartilage. *Chemical Engineering and Processing: Process Intensification*, **46**(5), pp.465-471.

George, F., Tumanov, N., Norberg, B., Robeyns, K., Filinchuk, Y., Wouters, J. and Leyssens, T(2014). Does chirality influence the tendency toward cocrystal formation?. *Crystal Growth & Design*, **14**(6), pp.2880-2892.

Ghosh, S., Mondal, A., Kiran, M.S.R.N., Ramamurty, U. and Reddy, C.M(2013). The role of weak interactions in the phase transition and distinct mechanical behavior of two structurally similar caffeine co-crystal

polymorphs studied by nanoindentation. *Crystal Growth & Design*, **13**(10), pp.4435-4441.

Gohel, M.C., & Jogani, P.D. (2005). A review of co-processed directly compressible excipients. *Journal of Pharmacy and Pharmaceutical Sciences,* **8**, 76–93.

Gonnissen, Y., Remon, J.P. and Vervaet, C (2007). Development of directly compressible powders via co-spray drying. *European journal of pharmaceutics and biopharmaceutics*, **67**(1), pp.220-226.

Govindaraj, P., Kandasubramanian, B. and Kodam, K.M(2014). Molecular interactions and antimicrobial activity of curcumin (Curcuma longa) loaded polyacrylonitrile films. *Materials Chemistry and Physics*, **147**(3), pp.934-941.

Gowthamarajan, K., Kumar, G.K.P., Gaikwad, N.B. and Suresh, B(2011). Preliminary study of Anacardium occidentale gum as binder in formulation of paracetamol tablets. Carbohydrate Polymers, **83**(2), pp.506-511.

Gowthamarajan, K., Jawahar, N., Wake, P., Jain, K. and Sood, S (2012). Development of buccal tablets for curcumin using Anacardium occidentale gum. *Carbohydrate polymers*, **88**(4), pp.1177-1183.

Craig, D.Q., Royall, P.G., Kett, V.L. and Hopton, M.L(1999). The relevance of the amorphous state to pharmaceutical dosage forms: glassy drugs and freeze dried systems. *International journal of pharmaceutics*, **179**(2), pp.179-207.

Grant, D.J.W., Jacobson, H., Fairbrother, J.E. and Patel, C.G(1980). Phases in the paracetamol-phenazone system. *International Journal of Pharmaceutics*, **5**(2), pp.109-116.

Griffin, D.J., Kawajiri, Y., Rousseau, R.W. and Grover, M.A(2017). Using MC plots for control of paracetamol crystallization. *Chemical Engineering Science*, **164**, pp.344-360.

Grodowska, K. and Parczewski, A(2010). Organic solvents in the pharmaceutical industry. *Acta Pol Pharm*, **67**(1), pp.3-12.

Gupta, A., Peck, G.E., Miller, R.W. and Morris, K.R(2005). Influence of ambient moisture on the compaction behavior of microcrystalline cellulose powder undergoing uni-axial compression and roller-compaction: A comparative study using near-infrared spectroscopy. *Journal of pharmaceutical sciences*, **94**(10), pp.2301-2313.

Han, X. and Poliakoff, M (2012). Continuous reactions in supercritical carbon dioxide: problems, solutions and possible ways forward. *Chemical Society Reviews*, **41**(4), pp.1428-1436.

Hare, C., Bonakdar, T., Ghadiri, M. and Strong, J(2018). Impact breakage of pharmaceutical tablets. International journal of pharmaceutics, **536**(1), pp.370-376.

Hathcock, J.N. and Shao, A(2007). Risk assessment for glucosamine and chondroitin sulfate. *Regulatory Toxicology and Pharmacology*, **47**(1), pp.78-83.

Heng, J.Y.Y., Thielmann, F., Williams, D.R(2006). The effects of milling on the surface properties of form I paracetamol crystals. Pharm. Res. **23**, 1918–1927.

Hiendrawan, S., Veriansyah, B., Widjojokusumo, E., Soewandhi, S.N., Wikarsa, S. and Tjandrawinata, R.R(2016). Physicochemical and mechanical properties of paracetamol cocrystal with 5-nitroisophthalic acid. *International journal of pharmaceutics*, **497**(1-2), pp.106-113.

Hiendrawan, S.T.E.V.A.N.U.S., Veriansyah, B.A.M.B.A.N.G., Widjojokusumo, E.D.W.A.R.D., Soewandhi, S.N., Wikarsa, S. and Tjandrawinata, R.R(2016). Simultaneous cocrystallization and micronization of paracetamol-dipicolinic acid cocrystal by supercritical antisolvent (SAS). *Int J Pharm Pharm Sci*, **8**, pp.89-98.

Hughey, J.R., Keen, J.M., Brough, C., Saeger, S., & McGinity, J.W. (2011). Thermal processing of a poorly water-soluble drug substance exhibiting a high melting point: the utility of KinetiSol® Dispersing. *International Journal of Pharmaceutics,* **419**, 222–230.

Illangakoon, U.E., Gill, H., Shearman, G.C., Parhizkar, M., Mahalingam, S., Chatterton, N.P. and Williams, G.R(2014). Fast dissolving paracetamol/caffeine nanofibers prepared by electrospinning. *International journal of pharmaceutics*, **477**(1-2), pp.369-379.

Imanari, T(2002). Effect of chondroitin sulfate on murine splenocytes sensitized with ovalbumin. *Immunology letters*, **84**(3), pp.211-216.

Ireson, C., Orr, S., Jones, D.J., Verschoyle, R., Lim, C.K., Luo, J.L., Howells, L., Plummer, S., Jukes, R., Williams, M. and Steward, W.P(2001). Characterization of metabolites of the chemopreventive agent curcumin in human and rat hepatocytes and in the rat in vivo, and evaluation of their ability to inhibit phorbol ester-induced prostaglandin E2 production. *Cancer research*, **61**(3), pp.1058-1064.

Jain, H., Khomane, K.S. and Bansal, A.K(2014). Implication of microstructure on the mechanical behaviour of an aspirin–paracetamol eutectic mixture. *CrystEngComm*, **16**(36), pp.8471-8478.

Jbilou, M., Ettabia, A., Guyot-Hermann, A.-M., Guyot, J.-C(2015). Ibuprofen agglomerates preparation by phase separationDrug Dev. Ind. Pharm.

Jardim, K.V., Joanitti, G.A., Azevedo, R.B. and Parize, A.L(2015). Physico-chemical characterization and cytotoxicity evaluation of curcumin loaded in chitosan/chondroitin sulfate nanoparticles. *Materials Science and Engineering: C*, **56**, pp.294-304.

Jayasankar, A., Somwangthanaroj, A., Shao, Z.J., Rodriguez-Hornedo, N(2006). Cocrystal formation during cogrinding and storage is mediated by amorphous phase. Pharm. Res. **23**, 2381–2392

Pharm. Eur(2013). 2.9.7: Friability of Uncoated Tablets, eighth ed. European Directorate for the Quality of Medicine and Health (EDQM).

Jindal, S., Jindal, K., Gupta, G.D., Garg, R. and Awasthi, R(2016). Gastroretentive floating tablets: An investigation of excipients effect on tablet properties. Marmara Pharmaceutical Journal, **20**(2), pp.100-110.

Jivraj, M., Martini, L.G., & Thomson, C.M. (2000). An overview of the different excipients useful for the direct compression of tablets. *Pharmaceutical Science & Technology Today,* **3**, 58–63.

Joe, B. and Lokesh, B.R(1994). Role of capsaicin, curcumin and dietary n—3 fatty acids in lowering the generation of reactive oxygen species in rat peritoneal macrophages. *Biochimica et Biophysica Acta (BBA)-Molecular Cell Research*, **1224**(2), pp.255-263.

Johnson, S.L. and Rumon, K.A(1965). Infrared spectra of solid 1: 1 pyridine-benzoic acid complexes; the nature of the hydrogen bond as a function of the acid-base levels in the complex1. *The Journal of Physical Chemistry*, **69**(1), pp.74-86.

Joiris, E., Di Martino, P., Berneron, C., Guyot-Hermann, A.M. and Guyot, J.C(1998). Compression behavior of orthorhombic paracetamol. Pharmaceutical research, **15**(7), pp.1122-1130

Jovanovic, S.V., Steenken, S., Boone, C.W. and Simic, M.G(1999). H-atom transfer is a preferred antioxidant mechanism of curcumin. *Journal of the American Chemical Society*, **121**(41), pp.9677-9681.

JP(2011). G6: Tablet Friability Test, sixteenth ed. Minister of Health, Labour and Welfare, Japan.

Kachrimanis, K., Ktistis, G. and Malamataris, S(1998). Crystallisation conditions and physicomechanical properties of ibuprofen–Eudragit® S100 spherical crystal agglomerates prepared by the solvent-change technique. *International journal of pharmaceutics*, **173**(1-2), pp.61-74

Kaialy, W. (2016a). A review of factors affecting electrostatic charging of pharmaceuticals and adhesive mixtures for inhalation. *International Journal of Pharmaceutics,* **503**, 262–276.

Kaialy, W. (2016b). On the effects of blending, physicochemical properties, and their interactions on the performance of carrier-based dry powders for inhalation — A review. *Advances in Colloid & Interface Science,* **235**, 70–89.

Kaialy, W., Alhalaweh, A., Velaga, S.P., & Nokhodchi, A. (2012). Influence of lactose carrier particle size on the aerosol performance of budesonide from a dry powder inhaler. *Powder Technology,* **227**, 74–85.

Kaialy, W., Larhrib, H., Chikwanha, B., Shojaee, S., & Nokhodchi, A. (2014). An approach to engineer paracetamol crystals by antisolvent crystallization technique in presence of various additives for direct compression. *International Journal of Pharmaceutics,* **464**, 53–64.

Kalantzi, L., Reppas, C., Dressman, J.B., Amidon, G.L., Junginger, H.E., Midha, K.K., Shah, V.P., Stavchansky, S.A. and Barends, D.M(2006). Biowaiver monographs for immediate release solid oral dosage forms:

Acetaminophen (paracetamol). *Journal of Pharmaceutical Sciences*, **95**(1), pp.4-14.

Karki, S., Friščić, T., Fabian, L., Laity, P.R., Day, G.M. and Jones, W(2009). Improving mechanical properties of crystalline solids by cocrystal formation: new compressible forms of paracetamol. *Advanced materials*, **21**(38-39), pp.3905-3909.

Kaur, G., Rana, V., Jain, S. and Tiwary, A.K(2010). Colon delivery of budesonide: evaluation of chitosan–chondroitin sulfate interpolymer complex. *AAPS PharmSciTech*, **11**(1), pp.36-45.

Kawakita, K., & Lüdde, K.-H. (1971). Some considerations on powder compression equations. *Powder Technology,* **4**, 61–68.

Kendall, K (1994). Adhesion: molecules and mechanics. Science **263**, 1720–1725.

Khadka, P., Ro, J., Kim, H., Kim, I., Kim, J.T., Kim, H., Cho, J.M., Yun, G. and Lee, J(2014). Pharmaceutical particle technologies: An approach to improve drug solubility, dissolution and bioavailability. asian journal of pharmaceutical sciences, **9**(6), pp.304-316.

Khan, H.M., Ashraf, M., Hashmi, A.S., Ahmad, M.U.D. and Anjum, A.A(2013). Extraction and biochemical characterization of sulphated glycosaminoglycans from chicken keel cartilage. *Pak Vet J*, **33**, pp.471-475.

Khan, K.A(1975). The concept of dissolution efficiency. *Journal of pharmacy and pharmacology*, **27**(1), pp.48-49.

Khanmohammadi, M., Garmarudi, A.B., Moazzen, N., & Ghasemi, K. (2010). Qualitative discrimination between paracetamol tablets made by near infrared spectroscopy and chemometrics with regard to polymorphism. *Journal of Structural Chemistry,* **51**, 663–669.

King, J.C., Li, H., Grover, M.A., Kawajiri, Y. and Rousseau, R.W(2015). Optimization of two-stage cooling profile in unseeded batch crystallization∗. *IFAC-PapersOnLine*, **48**(8), pp.297-302.

Klimova, K. and Leitner, J(2012). DSC study and phase diagrams calculation of binary systems of paracetamol. *Thermochimica acta*, **550**, pp.59-64.

Kovanda, F., Maryšková, Z. and Kovář, P(2011). Intercalation of paracetamol into the hydrotalcite-like host. *Journal of Solid State Chemistry*, **184(**12), pp.3329-3335.

Krokida, M.K. and Philippopoulos, C(2006). Volatility of apples during air and freeze drying. Journal of Food Engineering, **73**(2), pp.135-141.

Krupa, A., Majda, D., Jachowicz, R. and Mozgawa, W(2010). Solid-state interaction of ibuprofen and Neusilin US2. *Thermochimica Acta*, **509**(1), pp.12-17

Kuminek, G., Cao, F., da Rocha, A.B.D.O., Cardoso, S.G. and Rodríguez-Hornedo, N(2016). Cocrystals to facilitate delivery of poorly soluble

compounds beyond-rule-of-5. *Advanced drug delivery reviews*, **101**, pp.143-166.

Lao, C.D., Ruffin, M.T., Normolle, D., Heath, D.D., Murray, S.I., Bailey, J.M., Boggs, M.E., Crowell, J., Rock, C.L. and Brenner, D.E(2006). Dose escalation of a curcuminoid formulation. *BMC complementary and alternative medicine*, **6**(1), p.10.

Larhrib, H., & Wells, J. (1998). Compression speed on polyethylene glycol and dicalcium phosphate tableted mixtures. *International Journal of Pharmaceutics,* **160**, 197–206.

Larsson, I. and Kristensen, H.G(2000). Comminution of a brittle/ductile material in a Micros Ring Mill. *Powder technology*, **107**(1-2), pp.175-178.

Larson, I., Mangal, S., Meiser, F., Tan, G., Gengenbach, T and Morton, D.A(2016). Applying surface energy derived cohesive–adhesive balance model in predicting the mixing, flow and compaction behaviour of interactive mixtures.European Journal of Pharmaceutics and Biopharmaceutics, **104**, pp.110-116.

Lerdkanchanaporn, S. and Dollimore, D(2000). The evaporation of Ibuprofen from Ibuprofen-starch mixtures using simultaneous TG-DTA. Thermochimica acta, **357**, pp.71-78.

Leuenberger, H., & Imanidis, G. (1986). Monitoring mass transfer processes to control moist agglomeration. *Pharmaceutical Technology,*

10, 56–73.

Leuner, C. and Dressman, J(2000). Improving drug solubility for oral delivery using solid dispersions. *European journal of Pharmaceutics and Biopharmaceutics*, **50**(1), pp.47-60.

Levina, M. and Rubinstein, M.H (2000). The effect of ultrasonic vibration on the compaction characteristics of paracetamol. *Journal of pharmaceutical sciences*, **89**(6), pp.705-723.

Li, Q., Rudolph, V., Weigl, B. and Earl, A(2004). Interparticle van der Waals force in powder flowability and compactibility. *International journal of pharmaceutics*, **280**(1-2), pp.77-93.

Lin, X., Gao, W., Li, C., Chen, J., Yang, C. and Wu, H(2012). Nano-sized flake carboxymethyl cassava starch as excipient for solid dispersions. *International journal of pharmaceutics*, **423**(2), pp.435-439

Linares, P.M., Chaparro, M., Algaba, A., Román, M., Arza, I.M., Santos, F.A., Ochoa, D., Guerra, I., Bermejo, F. and Gisbert, J.P(2015). Effect of chondroitin sulphate on pro-inflammatory mediators and disease activity in patients with Inflammatory Bowel Disease. *Digestion*, **92**(4), pp.203-210.

Liu, Y., Cai, Y., Jiang, X., Wu, J. and Le, X (2016). Molecular interactions, characterization and antimicrobial activity of curcumin–chitosan blend films. *Food Hydrocolloids*, **52**, pp.564-572.

Liu, L.X., Marziano, I., Bentham, A.C., Litster, J.D., White, E.T. and Howes, T(2013). Influence of particle size on the direct compression of ibuprofen and its binary mixtures. *Powder technology*, **240**, pp.66-73.

Liu, J (2006). Physical characterization of pharmaceutical formulations in frozen and freeze-dried solid states: techniques and applications in freeze-drying development. *Pharmaceutical development and technology*, *11*(1), pp.3-28.

Lladó, J., Lao-Luque, C., Ruiz, B., Fuente, E., Solé-Sardans, M. and Dorado, A.D(2015). Role of activated carbon properties in atrazine and paracetamol adsorption equilibrium and kinetics. *Process Safety and Environmental Protection*, **95**, pp.51-59.

Lu, J. and Rohani, S(2010). Synthesis and preliminary characterization of sulfamethazine-theophylline co-crystal. *Journal of pharmaceutical sciences*, **99**(9), pp.4042-4047.

Machatha, S.G. and Yalkowsky, S.H., 2004. Estimation of the ethanol/water solubility profile from the octanol/water partition coefficient. *International journal of pharmaceutics*, *286*(1-2), pp.111-115.

Marshall, K(1986). Compression and consolidation of powdered solids. The Theory and Practice of Industrial Pharmacy. Bombay: Varghese Publishing House, pp.66-99 .

Maeno, Y., Fukami, T., Kawahata, M., Yamaguchi, K., Tagami, T., Ozeki, T., Suzuki, T. and Tomono, K(2014). Novel pharmaceutical cocrystal

consisting of paracetamol and trimethylglycine, a new promising cocrystal former. *International journal of pharmaceutics*, **473**(1), pp.179-186.

Mai, T.T.T., Nguyen, T.T.T., Le, Q.D., Nguyen, T.N., Ba, T.C., Nguyen, H.B., Phan, T.B.H., Nguyen, X.P. and Park, J.S(2012). A novel nanofiber Cur-loaded polylactic acid constructed by electrospinning. *Advances in Natural Sciences: Nanoscience and Nanotechnology*, **3**(2), p.025014.

Mallick, S., Pradhan, S.K. and Mohapatra, R(2013). Effects of microcrystalline cellulose based comilled powder on the compression and dissolution of ibuprofen. *International journal of biological macromolecules***, 60,** pp.148-155.

Manin, A.N., Voronin, A.P., Drozd, K.V., Manin, N.G., Bauer-Brandl, A. and Perlovich, G.L(2014). Cocrystal screening of hydroxybenzamides with benzoic acid derivatives: a comparative study of thermal and solution-based methods. *European Journal of Pharmaceutical Sciences*, **65**, pp.56-64.

Manish, M., Harshal, J. and Anant, P(2005). Melt sonocrystallization of ibuprofen: Effect on crystal properties. *European journal of pharmaceutical sciences*, **25**(1), pp.41-48.

Martín, A. and Cocero, M.J (2008). Micronization processes with supercritical fluids: fundamentals and mechanisms. *Advanced Drug Delivery Reviews*, **60**(3), pp.339-350.

Martínez, L.M., Videa, M., López-Silva, G.A., Carlos, A., Cruz-Angeles, J. and González, N(2014). Stabilization of amorphous paracetamol based

systems using traditional and novel strategies. *International journal of pharmaceutics*, **477**(1-2), pp.294-305.

Masters, K(1991).Spray−drying Handbook.Longman Scientific and Technical, New York.

Martelli, S(2002). Influence of crystal habit on the compression and densification mechanism of ibuprofen. *Journal of crystal growth*, **243**(2), pp.345-355.

McNamara, D.P., Childs, S.L., Giordano, J., Iarriccio, A., Cassidy, J., Shet, M.S., Mannion, R., O'donnell, E. and Park, A(2006). Use of a glutaric acid cocrystal to improve oral bioavailability of a low solubility API. *Pharmaceutical research*, **23**(8), pp.1888-1897.

MHRA(1991). Panadol Soluble Tablets Marketing Authorisation. Medicines and Healthcare Products Regulatory Agency PL 71/00379.

Miroshnyk, I., Mirza, S. and Sandler, N(2009). Pharmaceutical co-crystals–an opportunity for drug product enhancement. *Expert opinion on drug delivery*, **6**(4), pp.333-341.

Mohammad, M.A., Alhalaweh, A. and Velaga, S.P(2011). Hansen solubility parameter as a tool to predict cocrystal formation. *International journal of pharmaceutics*, **407**(1-2), pp.63-71

More, P.K., Khomane, K.S. and Bansal, A.K(2013). Flow and compaction behaviour of ultrafine coated ibuprofen. International journal of pharmaceutics, **441**(1), pp.527-534.

Morissette, S.L., Almarsson, Ö., Peterson, M.L., Remenar, J.F., Read, M.J., Lemmo, A.V., Ellis, S., Cima, M.J. and Gardner, C.R(2004). High-throughput crystallization: polymorphs, salts, co-crystals and solvates of pharmaceutical solids. Advanced drug delivery reviews, **56**(3), pp.275-300.

Mota, F.L., Carneiro, A.P., Queimada, A.J., Pinho, S.P. and Macedo, E.A(2009). Temperature and solvent effects in the solubility of some pharmaceutical compounds: measurements and modeling. *European Journal of Pharmaceutical Sciences*, **37**(3-4), pp.499-507.

Moynihan, H.A., & O'Hare, I.P. (2002). Spectroscopic characterisation of the monoclinic and orthorhombic forms of paracetamol. *International Journal of Pharmaceutics,* **247**, 179–185.

Mucci, A., Schenetti, L. and Volpi, N(2000). 1H and 13C nuclear magnetic resonance identification and characterization of components of chondroitin sulfates of various origin. *Carbohydrate Polymers*, **41**(1), pp.37-45.

Nada, A.H. and Graf, E., 1998. Evaluation of Vitacel M80K as a new direct compressible vehicle. *European journal of pharmaceutics and biopharmaceutics*, *46*(3), pp.347-353.

Nakano, T., Ikawa, N. and Ozimek, L(2000). An economical method to extract chondroitin sulphate-peptide from bovine nasal cartilage. *Canadian agricultural engineering*, **42**(4), pp.205-208.

Namur, J., Wassef, M., Pelage, J.P., Lewis, A., Manfait, M. and Laurent, A(2009). Infrared microspectroscopy analysis of ibuprofen release from drug eluting beads in uterine tissue. *Journal of Controlled Release*, **135**(3), pp.198-202.

Nagy, Z.K., Fujiwara, M. and Braatz, R.D (2008). Modelling and control of combined cooling and antisolvent crystallization processes. *Journal of Process Control*, **18**(9), pp.856-864.

Ndindayino, F., Vervaet, C., Van den Mooter, G. and Remon, J.P(2002). Direct compression and moulding properties of co-extruded isomalt/drug mixtures. *International journal of pharmaceutics*, **235**(1-2), pp.159-168.

Nichols, G. and Frampton, C.S(1998). Physicochemical characterization of the orthorhombic polymorph of paracetamol crystallized from solution. *Journal of pharmaceutical sciences*, **87**(6), pp.684-693.

Nokhodchi, A., Maghsoodi, M., Hassan-Zadeh, D., & Barzegar-Jalali, M. (2007). Preparation of agglomerated crystals for improving flowability and compactibility of poorly flowable and compactible drugs and excipients. *Powder Technology,* **175**, 73–81.

Nowee, S.M., Abbas, A. and Romagnoli, J.A(2007). Optimization in seeded cooling crystallization: A parameter estimation and dynamic optimization study. *Chemical Engineering and Processing: Process Intensification*, **46**(11), pp.1096-1106.

Noyes, A.A. and Whitney, W.R(1897). The rate of solution of solid substances in their own solutions. *Journal of the American Chemical Society*, **19**(12), pp.930-934.

Okoye, E.I., Onyekweli, A.O., Olobayo, O.K. and Arhewoh, M.I(2010). Brittle fracture index (BFI) as a tool in the classification, grouping and ranking of some binders used in tablet formulation: Lactose tablets. Sci Res Ess, **5**(5), pp.500-506.

Ogienko, A.G., Boldyreva, E.V., Manakov, A.Y., Boldyrev, V.V., Yunoshev, A.S., Ogienko, A.A., Myz, S.A., Ancharov, A.I., Achkasov, A.F. and Drebushchak, T.N(2011). A new method of producing monoclinic paracetamol suitable for direct compression. Pharmaceutical research, **28**(12), pp.3116-3127

Oliveira, J.E., Bonan, R.F., Bonan, P.R., Batista, A.U., Sampaio, F.C., Albuquerque, A.J., Moraes, M.C., Mattoso, L.H., Glenn, G.M and Medeiros, E.S(2015). In vitro antimicrobial activity of solution blow spun poly (lactic acid)/polyvinylpyrrolidone nanofibers loaded with Copaiba (Copaifera sp.) oil.Materials Science and Engineering: C, **48**, pp.372-377.

Olusanmi, D., Wang, C., Ghadiri, M., Ding, Y. and Roberts, K.J(2010). Effect of temperature and humidity on the breakage behaviour of Aspirin and sucrose particles. *Powder Technology*, **201**(3), pp.248-252.

Orth, M.W., Peters, T.L. and Hawkins, J.N(2002). Inhibition of articular cartilage degradation by glucosamine-HCl and chondroitin sulphate. *Equine Veterinary Journal*, **34**(S34), pp.224-229.

Osborne, J.D., Sochon, R.P., Cartwright, J.J., Doughty, D.G., Hounslow, M.J. and Salman, A.D(2011). Binder addition methods and binder distribution in high shear and fluidised bed granulation. *Chemical Engineering Research and Design*, **89(**5), pp.553-559.

Oswald, I.D. and Pulham, C.R(2008). Co-crystallisation at high pressure—an additional tool for the preparation and study of co-crystals. *CrystEngComm*, **10**(9), pp.1114-1116.

Oswald, I.D., Allan, D.R., McGregor, P.A., Motherwell, W.S., Parsons, S. and Pulham, C.R(2002). The formation of paracetamol (acetaminophen) adducts with hydrogen-bond acceptors. *Acta Crystallographica Section B: Structural Science*, **58**(6), pp.1057-1066.

Otsuka, A(1998). Adhesive properties and related phenomena for powdered pharmaceuticals. Yakugaku zasshi: Journal of the Pharmaceutical Society of Japan, **118**(4), pp.127-142 .

Panzade, P., Shendarkar, G., Shaikh, S. and Rathi, P.B., 2017. Pharmaceutical Cocrystal of Piroxicam: Design, Formulation and Evaluation. *Advanced pharmaceutical bulletin*, *7*(3), p.399.

Patra, C.N., Swain, S., Mahanty, S. and Panigrahi, K.C(2015). Design and characterization of aceclofenac and paracetamol spherical crystals and their tableting properties. *Powder Technology*, **274**, pp.446-454.

Padrela, L., Rodrigues, M.A., Velaga, S.P., Matos, H.A. and de Azevedo, E.G(2009). Formation of indomethacin–saccharin cocrystals using supercritical fluid technology. *European Journal of Pharmaceutical Sciences*, **38**(1), pp.9-17.

Pal, S., Roopa, B.N., Abu, K., Manjunath, S.G. and Nambiar, S(2014). Thermal studies of furosemide–caffeine binary system that forms a cocrystal. *Journal of Thermal Analysis and Calorimetry*, **115**(3), pp.2261-2268.

Passerini, N., Albertini, B., González-Rodŕiguez, M.L., Cavallari, C. and Rodriguez, L(2002). Preparation and characterisation of ibuprofen–poloxamer 188 granules obtained by melt granulation. *European Journal of Pharmaceutical Sciences*, **15**(1), pp.71-78.

Patist, A. and Bates, D (2008). Ultrasonic innovations in the food industry: From the laboratory to commercial production. *Innovative food science & emerging technologies*, **9**(2), pp.147-154.

Paradkar, A.R., Maheshwari, M., Ketkar, A.R. and Chauhan, B(2003). Preparation and evaluation of ibuprofen beads by melt solidification technique. International journal of pharmaceutics, **255**(1), pp.33-42

Park, S.J. and Yeo, S.D(2008). Recrystallization of caffeine using gas antisolvent process. *The Journal of Supercritical Fluids*, **47**(1), pp.85-92.

Pedersen, S. and Kristensen, H.G(1994). Change in crystal density of acetylsalicylic acid during compaction. *STP pharma sciences*, **4**(3), pp.201-206.

Perumalla, S.R., Sun, C.C(2014). Enabling tablet product development of 5- fluorocytosine through integrated crystal and particle engineering. J. Pharm. Sci. **103**, 1126–1132

Perumalla, S.R., Shi, L. and Sun, C.C(2012). Ionized form of acetaminophen with improved compaction properties. *CrystEngComm*, **14**(7), pp.2389-2390.

Pikal, M.J., Shah, S., Roy, M.L. and Putman, R(1990). The secondary drying stage of freeze drying: drying kinetics as a function of temperature and chamber pressure. *International journal of pharmaceutics*, **60**(3), pp.203-207.

Pikal, J.M(2002) Freeze drying, in: J. Swarbrick (Ed.), Encyclopedia of Pharmaceutical Technology, vol. **2,** Marcel Dekker, New York, pp. 1299–1326.

Pinto, S.S. and Diogo, H.P(2006). Thermochemical study of two anhydrous polymorphs of caffeine. *The Journal of Chemical Thermodynamics*, **38**(12), pp.1515-1522.

Pushpalatha, R., Selvamuthukumar, S. and Kilimozhi, D (2018). Cross-linked, cyclodextrin-based nanosponges for curcumin delivery-Physicochemical characterization, drug release, stability and cytotoxicity. *Journal of Drug Delivery Science and Technology*, **45**, pp.45-53.

Qi, S., Avalle, P., Saklatvala, R. and Craig, D.Q(2008). An investigation into the effects of thermal history on the crystallisation behaviour of

amorphous paracetamol. *European Journal of Pharmaceutics and Biopharmaceutics*, **69**(1), pp.364-371.

Qiao, N., Li, M., Schlindwein, W., Malek, N., Davies, A. and Trappitt, G(2011). Pharmaceutical cocrystals: an overview. International journal of pharmaceutics, **419**(1), pp.1-11.

Qiao, J., Hamaya, T. and Okada, T(2005). New highly proton-conducting membrane poly (vinylpyrrolidone)(PVP) modified poly (vinyl alcohol)/2-acrylamido-2-methyl-1-propanesulfonic acid (PVA–PAMPS) for low temperature direct methanol fuel cells (DMFCs). *Polymer*, **46**(24), pp.10809-10816.

Qiu, L., Chen, W. and Qu, B., 2005. Structural characterisation and thermal properties of exfoliated polystyrene/ZnAl layered double hydroxide nanocomposites prepared via solution intercalation. *Polymer Degradation and Stability*, ***87*(**3), pp.433-440.

Raffa,RB.Pharmacologyoforalcombinationanalgesic:rationaltherapyforpain. J Clin PharmTher2001;**26**:257–64

Rasenack, N. and Müller, B.W(2002). Ibuprofen crystals with optimized properties. International journal of pharmaceutics, **245**(1), pp.9-24.

Rasool, B.K.A., Abu-Gharbieh, E.F., Al-Mahdy, J.J., Nessa, F. and Ramzi, H.R(2010). Preparation and Characterization of Aspirin-Chitosan Complex: An Attempt for Its Solubil-ity and Stability Improvement. *Journal of Pharmacy Research Vol*, **3**(6), pp.1349-1354.

Rattes, A.L.R. and Oliveira, W.P (2007). Spray drying conditions and encapsulating composition effects on formation and properties of sodium diclofenac microparticles. *Powder Technology*, **171**(1), pp.7-14.

Richardson, G.M., & Malthus, R.S. (1955). Salts for static control of humidity at relatively low levels. *Journal of Chemical Technology and Biotechnology,* **5**, 557–567.

Rose, A.A. and Kaialy, W (2019). Improved tableting behavior of paracetamol in the presence of polyvinylpyrrolidone additive: Effect of mixing conditions. *Particuology*, **43**, pp.9-18.

Rossi, A., Savioli, A., Bini, M., Capsoni, D., Massarotti, V., Bettini, R., Gazzaniga, A., Sangalli, M.E. and Giordano, F (2003). Solid-state characterization of paracetamol metastable polymorphs formed in binary mixtures with hydroxypropylmethylcellulose. *Thermochimica acta*, **406**(1-2), pp.55-67.

Sadeghi, F., Torab, M., Khattab, M., Homayouni, A. and Garekani, H.A(2013). Improvement of physico-mechanical properties of partially amorphous acetaminophen developed from hydroalcoholic solution using spray drying technique. *Iranian journal of basic medical sciences*, **16**(10), p.1100.

Sahajwalla, C.G. and Ayres, J.W(1991). Multiple-dose acetaminophen pharmacokinetics. Journal of pharmaceutical sciences, **80**(9), pp.855-860.

Sakata, Y., Tanabe, E., Sumikawa, T., Shiraishi, S., Tokudome, Y. and Otsuka, M(2007). Effects of solid-state reaction between paracetamol and cloperastine hydrochloride on the pharmaceutical properties of their preparations. International journal of pharmaceutics, **335**(1), pp.12-19.

Sallam, E., & Orr, N. (1985). Content uniformity of ethinyldestradiol tablets 10 μG: Effect of variations in processing on the homogeneity after dry mixing and after tableting. *Drug Development and Industrial Pharmacy,* **11**, 607–633.

Sahoo, P(2015). Molecular recognition of caffeine in solution and solid state. *Bioorganic chemistry*, **58**, pp.26-47.

Sakai, S., Onose, J.I., Nakamura, H., Toyoda, H., Toida, T., Imanari, T. and Linhardt, R.J(2002). Pretreatment procedure for the microdetermination of chondroitin sulfate in plasma and urine. *Analytical biochemistry*, **302**(2), pp.169-174.

Sakai, S., Akiyama, H., Harikai, N., Toyoda, H., Toida, T., Maitani, T. and Imanari, T(2002). Effect of chondroitin sulfate on murine splenocytes sensitized with ovalbumin. *Immunology letters*, **84**(3), pp.211-216.

Salem, M., Rohani, S. and Gillies, E.R(2014). Curcumin, a promising anti-cancer therapeutic: a review of its chemical properties, bioactivity and approaches to cancer cell delivery. *Rsc Advances*, **4**(21), pp.10815-10829.

Sander, J.R., Bučar, D.K., Henry, R.F., Baltrusaitis, J., Zhang, G.G. and MacGillivray, L.R(2010). A red zwitterionic co-crystal of acetaminophen

and 2, 4-pyridinedicarboxylic acid. *Journal of pharmaceutical sciences*, **99**(9), pp.3676-3683.

Sanphui, P., Goud, N.R., Khandavilli, U.R., Bhanoth, S. and Nangia, A(2011). New polymorphs of curcumin. *Chemical Communications*, **47**(17), pp.5013-5015.

Santos, H.M.M., Sousa, J.J.M.S (2008). Tablet compression. In: Gad, S.C. (Ed.), Pharmaceutical Manufacturing Handbook. John Wiley & Sons, Hoboken, New Jersey, pp. 1133–1164

Sauceau, M., Fages, J., Common, A., Nikitine, C. and Rodier, E (2011). New challenges in polymer foaming: A review of extrusion processes assisted by supercritical carbon dioxide. *Progress in Polymer Science*, **36**(6), pp.749-766.

Schartman, R.R(2009). On the thermodynamics of cocrystal formation. *International journal of pharmaceutics*, **365**(1-2), pp.77-80.

Seki, H. and Su, Y(2015). Robust optimal temperature swing operations for size control of seeded batch cooling crystallization. Chemical Engineering Science, **133**, pp.16-23.

Sebhatu, T., Angberg, M. and Ahlneck, C(1994). Assessment of the degree of disorder in crystalline solids by isothermal microcalorimetry. *International Journal of Pharmaceutics*, **104**(2), pp.135-144.

Sethia, S. and Squillante, E(2004). Solid dispersion of carbamazepine in PVP K30 by conventional solvent evaporation and supercritical methods. *International Journal of Pharmaceutics*, **272**(1-2), pp.1-10.

Shan, N., Toda, F. and Jones, W(2002). Mechanochemistry and co-crystal formation: effect of solvent on reaction kinetics. *Chemical Communications*, (**20**), pp.2372-2373.

Shan, N. and Zaworotko, M.J(2008). The role of cocrystals in pharmaceutical science. *Drug discovery today*, **13**(9-10), pp.440-446.

Shariare, M.H., Leusen, F.J., de Matas, M., York, P. and Anwar, J(2012). Prediction of the mechanical behaviour of crystalline solids. *Pharmaceutical research*, **29**(1), pp.319-331.

Sharma, R.A., Gescher, A.J. and Steward, W.P(2005). Curcumin: the story so far. *European journal of cancer*, **41**(13), pp.1955°8.

Shekunov, B.Y., Baldyga, J. and York, P (2001). Particle formation by mixing with supercritical antisolvent at high Reynolds numbers. *Chemical Engineering Science*, **56**(7), pp.2421-2433.

Shi, L. and Sun, C.C(2010). Transforming powder mechanical properties by core/shell structure: compressible sand. Journal of pharmaceutical sciences, **99**(11), pp.4458-4462.

Shi, L. and Sun, C.C(2011). Overcoming poor tabletability of pharmaceutical crystals by surface modification. *Pharmaceutical research*, **28**(12), pp.3248-3255.

Sibik, J., Sargent, M.J., Franklin, M., & Zeitler, J.A. (2014). Crystallization and phase changes in paracetamol from the amorphous solid to the liquid phase. *Molecular Pharmaceutics,* **11**, 1326–1334.

Siissalo, S., Laine, L., Tolonen, A., Kaukonen, A.M., Finel, M. and Hirvonen, J(2010). Caco-2 cell monolayers as a tool to study simultaneous phase II metabolism and metabolite efflux of indomethacin, paracetamol and 1-naphthol. *International journal of pharmaceutics*, **383**(1), pp.24-29.

Sivaiah, K., Kumar, K.N., Naresh, V., & Buddhudu, S. (2011). Structural and optical properties of Li^+: PVP & Ag^+: PVP polymer films. *Materials Sciences and Applications,* **2**, 1688–1696.

Shah, U.V., Karde, V., Ghoroi, C. and Heng, J.Y(2017). Influence of particle properties on powder bulk behaviour and processability. International journal of pharmaceutics, **518**(1-2), pp.138-154.

Smith, S.J., Bishop, M.M., Montgomery, J.M., Hamilton, T.P. and Vohra, Y.K(2014). Polymorphism in paracetamol: evidence of additional forms IV and V at high pressure. *The Journal of Physical Chemistry A*, **118**(31), pp.6068-6077.

Smith, G. and Wermuth, U.D(2013). Proton-transfer and non-transfer compounds of the multi-purpose drug dapsone [4-(4-Aminophenylsulfonyl) aniline] with 3, 5-dinitrosalicylic acid and 5-nitroisophthalic acid. *Journal of Chemical Crystallography*, **43**(12), pp.664-670.

Soares, F.L.F. and Carneiro, R.L., 2014. Evaluation of analytical tools and multivariate methods for quantification of co-former crystals in ibuprofen-

nicotinamide co-crystals. Journal of pharmaceutical and biomedical analysis, **89**, pp.166-175.

Souguir, H., Salaün, F., Douillet, P., Vroman, I. and Chatterjee, S., 2013. Nanoencapsulation of curcumin in polyurethane and polyurea shells by an emulsion diffusion method. *Chemical Engineering Journal*, *221*, pp.133-145.

Sriamornsak, P., Kennedy, R.A., 2007. Effect of drug solubility on release behavior of calcium polysaccharide gel coated pellets. Eur. J. Pharm. Sci. **32**, 231–239.

Srirambhatla, V.K., Kraft, A., Watt, S. and Powell, A.V(2012). Crystal design approaches for the synthesis of paracetamol co-crystals. *Crystal Growth & Design*, **12**(10), pp.4870-4879.

Sumathi, S. and Ray, A.R(2002). Release behaviour of drugs from tamarind seed polysaccharide tablets. *J Pharm Pharm Sci*, **5**(1), pp.12-18.

Sun, C.C(2009). Materials science tetrahedron—A useful tool for pharmaceutical research and development. Journal of pharmaceutical sciences, 98(5), pp.1671-1687.

Sun, C.C(2008). Mechanism of moisture induced variations in true density and compaction properties of microcrystalline cellulose. *International journal of pharmaceutics*, **346**(1-2), pp.93-101.

Sun, C.C(2011). Decoding powder tabletability: roles of particle adhesion and plasticity. *Journal of Adhesion Science and Technology*, **25**(4-5), pp.483-499.

Sun, C.C. and Himmelspach, M.W(2006). Reduced tabletability of roller compacted granules as a result of granule size enlargement. *Journal of pharmaceutical sciences*, **95**(1), pp.200-206.

Sun, C. and Grant, D.J(2001). Effects of initial particle size on the tableting properties of L-lysine monohydrochloride dihydrate powder. *International journal of pharmaceutics*, **215**(1-2), pp.221-228.

Sun, C.C. and Hou, H(2008). Improving mechanical properties of caffeine and methyl gallate crystals by cocrystallization. *Crystal Growth and Design*, **8**(5), pp.1575-1579.

Sunada, H. and Bi, Y(2002). Preparation, evaluation and optimization of rapidly disintegrating tablets. *Powder technology*, **122**(2-3), pp.188-198.

Thipparaboina, R., Thumuri, D., Chavan, R., Naidu, V.G.M. and Shastri, N.R(2017). Fast dissolving drug-drug eutectics with improved compressibility and synergistic effects. *European Journal of Pharmaceutical Sciences*, **104**, pp.82-89.

Takeuchi, H., Yasuji, T., Hino, T., Yamamoto, H. and Kawashima, Y(1998). Spray-dried composite particles of lactose and sodium alginate for direct tableting and controlled releasing. International journal of pharmaceutics, **174**(1), pp.91-100.

Talegaonkar, S., Yakoob Khan, A., Kishan Khar, R., Jalees Ahmad, F. and Khan, Z(2010). Development and Characterization of Paracetamol Complexes with Hydroxypropyl-?-Cyclodextrin. *Iranian Journal of Pharmaceutical Research*, pp.95-99.

Tan, H., Chu, C.R., Payne, K.A. and Marra, K.G(2009). Injectable *in situ* forming biodegradable chitosan–hyaluronic acid based hydrogels for cartilage tissue engineering. *Biomaterials*, **30**(13), pp.2499-2506.

Tan, C., Selig, M.J. and Abbaspourrad, A.(2018). Anthocyanin stabilization by chitosan-chondroitin sulfate polyelectrolyte complexation integrating catechin co-pigmentation. *Carbohydrate polymers*, **181**, pp.124-131.

Tanner, T., Aspley, S., Munn, A. and Thomas, T(2010). The pharmacokinetic profile of a novel fixed-dose combination tablet of ibuprofen and paracetamol. *BMC clinical pharmacology*, **10**(1), p.10.

Takiyama, H., Otsuhata, T. and Matsuoka, M (1998). Morphology of NaCl crystals in drowning-out precipitation operation. *Chemical Engineering Research and Design*, **76**(7), pp.809-814.

Ter Horst, J.H., Geertman, R.M., Van der Heijden, A.E. and Van Rosmalen, G.M(1999). The influence of a solvent on the crystal morphology of RDX. *Journal of crystal growth*, **198**, pp.773-779.

Thipparaboina, R., Kumar, D., Chavan, R.B. and Shastri, N.R(2016). Multidrug co-crystals: towards the development of effective therapeutic hybrids. *Drug Discovery Today*, **21**(3), pp.481-490.

Thomsen, M.S., Loft, S., Roberts, D.W. and Poulsen, H.E(1995). Cytochrome P4502E1 inhibition by propylene glycol prevents acetaminophen (paracetamol) hepatotoxicity in mice without cytochrome P4501A2 inhibition. *Basic & Clinical Pharmacology & Toxicology*, **76**(6), pp.395-399.

Thorat, A.A. and Dalvi, S.V (2015). Solid-state phase transformations and storage stability of curcumin polymorphs. *Crystal Growth & Design*, **15**(4), pp.1757-1770.

Titapiwatanakun, V., Tankul, J., Basit, A.W. and Gaisford, S(2016). Laser irradiation to produce amorphous pharmaceuticals. *International journal of pharmaceutics*, **514**(1), pp.282-289.

Tjandrawinata, R.R., Hiendrawan, S., Veriansyah, B., Widjojokusumo, E., Soewandhi, S.N and Wikarsa, S(2016). Physicochemical and mechanical properties of paracetamol cocrystal with 5-nitroisophthalic acid. International journal of pharmaceutics, **497(**1), pp.106-113.

Tkachenko, M.L., Zhnyakina, L.E. and Kosmynin, A.S(2003). Physicochemical investigation of paracetamol–caffeine solid mixtures. *Pharmaceutical Chemistry Journal*, **37**(8), pp.430-432

Tomassetti, M., Catalani, A., Rossi, V. and Vecchio, S(2005). Thermal analysis study of the interactions between acetaminophen and excipients in solid dosage forms and in some binary mixtures. *Journal of pharmaceutical and biomedical analysis*, **37**(5), pp.949-955.

Tønnesen, H.H., Másson, M. and Loftsson, T(2002). Studies of curcumin and curcuminoids. XXVII. Cyclodextrin complexation: solubility, chemical and photochemical stability. *International Journal of Pharmaceutics*, **244**(1-2), pp.127-135.

Trask, A.V., Motherwell, W.S. and Jones, W(2006). Physical stability enhancement of theophylline via cocrystallization. *International journal of pharmaceutics*, **320**(1), pp.114-123.

Tunçal, T., Çifçi, D.İ., Pala, A. and Uslu, O(2016). Determination of optimum extinction wavelength for paracetamol removal through energy efficient thin film reactor. Journal of Photochemistry and Photobiology A: Chemistry, **322**, pp.102-109.

, M. and Bolten, D(2016). Polymorphic properties of micronized mefenamic acid, nabumetone, paracetamol and tolbutamide produced by rapid expansion of supercritical solutions (RESS). *The Journal of Supercritical Fluids*, **116**, pp.239-250.

Twycross, R., Pace, V., Mihalyo, M. and Wilcock, A(2013). Acetaminophen (paracetamol). *Journal of pain and symptom management*, **46**(5), pp.747-755.

USP, 2014. USP37/NF32 (Online), General Chapters: Tablet Friability. United States Pharmacopoeial Convention, Rockville, MD.

The United States pharmacopeia (2008).The United States Pharmacopeia, 31st ed., 2008. United States Pharmacopeia Convention, Inc.

van Rongen, A., Välitalo, P.A., Peeters, M.Y., Boerma, D., Huisman, F.W., van Ramshorst, B., van Dongen, E.P., van den Anker, J.N. and Knibbe, C.A(2016). Morbidly obese patients exhibit increased CYP2E1-mediated oxidation of acetaminophen. *Clinical pharmacokinetics*, **55**(7), pp.833-847.

Vanhoorne, V., Peeters, E., Van Snick, B., Remon, J.P., & Vervaet, C. (2014). Crystal coating via spray drying to improve powder tabletability. *European Journal of Pharmaceutics and Biopharmaceutics,* **88**, 939–944.

Vanhoorne, V., Van Bockstal, P.J., Van Snick, B., Peeters, E., Monteyne, T., Gomes, P., De Beer, T., Remon, J.P. and Vervaet, C(2016). Continuous manufacturing of delta mannitol by cospray drying with PVP. *International journal of pharmaceutics*, **501**(1), pp.139-147.

Varshosaz, J., Eskandari, S. and Tabbakhian, M(2012). Freeze-drying of nanostructure lipid carriers by different carbohydrate polymers used as cryoprotectants. Carbohydrate polymers, **88**(4), pp.1157-1163.

Vergés, J., Montell, E., Herrero, M., Perna, C., Cuevas, J., Dalmau, J., Pérez, M. and Möller, I(2005). Clinical and histopathological improvement of psoriasis with oral chondroitin sulfate: a serendipitous finding. *Dermatology online journal*, **11**(1).

Vishweshwar, P., McMahon, J.A., Bis, J.A. and Zaworotko, M.J(2006). Pharmaceutical co-crystals. *Journal of pharmaceutical sciences*, **95**(3), pp.499-516.

Wang, Y.J., Pan, M.H., Cheng, A.L., Lin, L.I., Ho, Y.S., Hsieh, C.Y. and Lin, J.K(1997). Stability of curcumin in buffer solutions and characterization of its degradation products. *Journal of pharmaceutical and biomedical analysis*, **15**(12), pp.1867-1876.

Wang, S.L., Lin, S.Y. and Wei, Y.S(2002). Transformation of metastable forms of acetaminophen studied by thermal Fourier transform infrared

(FT-IR) microspectroscopy. *Chemical and pharmaceutical bulletin*, **50**(2), pp.153-156.

Wang, L.F., Shen, S.S. and Lu, S.C(2003). Synthesis and characterization of chondroitin sulfate–methacrylate hydrogels. *Carbohydrate Polymers*, **52**(4), pp.389-396.

Wang, F.J. and Wang, C.H(2002). Effects of fabrication conditions on the characteristics of etanidazole spray-dried microspheres. *Journal of microencapsulation*, **19**(4), pp.495-510.

Wang, X., Shen, Q., Zhang, C., Jia, W., Han, L. and Yu, Q(2019). Chicken leg bone as a source of chondroitin sulfate. *Carbohydrate polymers*, **207**, pp.191-199.

Wasylaschuk, W.R., Harmon, P.A., Wagner, G., Harman, A.B., Templeton, A.C., Xu, H. and Reed, R.A(2007). Evaluation of hydroperoxides in common pharmaceutical excipients. Journal of pharmaceutical sciences, **96**(1), pp.106-116.

Wegiel, L.A., Zhao, Y., Mauer, L.J., Edgar, K.J. and Taylor, L.S(2014). Curcumin amorphous solid dispersions: the influence of intra and intermolecular bonding on physical stability. *Pharmaceutical development and technology*, **19**(8), pp.976-986.

Williams, N.A. and Polli, G.P(1984). The lyophilization of pharmaceuticals: a literature review. *PDA Journal of Pharmaceutical Science and Technology*, **38**(2), pp.48-60.

Williams, R.L., Adams, W.P., Poochikian, G., & Hauck, W.W. (2002).

Content uniformity and dose uniformity: Current approaches, statistical analyses, and presentation of an alternative approach, with special reference to oral inhalation and nasal drug products. *Pharmaceutical Research,* **19**, 359–366.

Wong, S.N., Hu, S., Ng, W.W., Xu, X., Lai, K.L., Lee, W.Y.T., Chow, A.H.L., Sun, C.C. and Chow, S.F (2018). Cocrystallization of curcumin with benzenediols and benzenetriols via rapid solvent removal. *Crystal Growth & Design*.

Wu, C.Y. and Benet, L.Z (2005). Predicting drug disposition via application of BCS: transport/absorption/elimination interplay and development of a biopharmaceutics drug disposition classification system. *Pharmaceutical research*, **22**(1), pp.11-23.

Wu, C.Y., Dihoru, L. and Cocks, A.C(2003). The flow of powder into simple and stepped dies. Powder Technology, **134**(1), pp.24-39

Wu, C.Y., Ruddy, O.M., Bentham, A.C., Hancock, B.C., Best, S.M. and Elliott, J.A(2005). Modelling the mechanical behaviour of pharmaceutical powders during compaction. Powder Technology, **152**(1), pp.107-117.

Wong, L.W. and Pilpel, N(1990). The effect of particle shape on the mechanical properties of powders. *International journal of pharmaceutics*, **59**(2), pp.145-154.

Xiong, S.L. and Jin, Z.Y(2007). The free radical-scavenging property of chondroitin sulfate from pig laryngeal cartilage in vitro. *Journal of food biochemistry*, **31**(1), pp.28-44.

York, P(1992) Crystal engineering and particle design for the powder compaction process. Drug Dev. Ind. Pharm., **18 pp** 677– 721.

Yuksel, N., Kanik, A.E., Baykara, T(2000). Comparison of in vitro dissolution profiles by ANOVA-based, model-depended and -independent methods. Int. J. Pharm. **209**, 57–67.

Zebib, B., Mouloungui, Z. and Noirot, V(2010). Stabilization of curcumin by complexation with divalent cations in glycerol/water system. Bioinorganic chemistry and applications,

Zhang, G.G., Law, D., Schmitt, E.A. and Qiu, Y(2004). Phase transformation considerations during process development and manufacture of solid oral dosage forms. *Advanced drug delivery reviews*, **56**(3), pp.371-390.

Zhao, Z., Liu, G., Lin, Q. and Jiang, Y (2018). Co-Crystal of Paracetamol and Trimethylglycine Prepared by a Supercritical CO2 Anti-Solvent Process. *Chemical Engineering & Technology*, **41**(6), pp.1122-1131.

Zhou, Z., Li, W., Sun, W.J., Lu, T., Tong, H.H., Sun, C.C. and Zheng, Y(2016). Resveratrol cocrystals with enhanced solubility and tabletability. *International journal of pharmaceutics*, **509**(1-2), pp.391-399.

ZIMMERMANN, B. and BARANOVIĆ, G(2011). Thermal analysis of paracetamol polymorphs by FT-IR spectroscopies. Journal of pharmaceutical and biomedical analysis, **54**(2), pp. 295-302.

Zou, H., Rowe, D.M. and Min, G(2001). Growth of p-and n-type bismuth telluride thin films by co-evaporation. *Journal of crystal growth*, **222**(1-2), pp.82-87.

Zhao, P., Liu, H., Deng, H., Xiao, L., Qin, C., Du, Y. and Shi, X(2014). A study of chitosan hydrogel with embedded mesoporous silica nanoparticles loaded by ibuprofen as a dual stimuli-responsive drug release system for surface coating of titanium implants. Colloids and Surfaces B: Biointerfaces, **123**, pp.657-663.

Zuurman, K., Riepma, K.A., Bolhuis, G.K., Vromans, H., & Lerk, C.F. (1994). The relationship between bulk density and compactibility of lactose granulations. *International Journal of Pharmaceutics,* **102**, 1–9.

APPENDIX

Paper in peer-reviewed international journal

Agbor Rose, Ayuk and Kaialy, W(2018). Improved tableting behaviour of paracetamol in the presence of polyvinylpyrrolidone additive: Effect of mixing conditions. *Particuology*.

Poster Presentations/ online conference

Waseem Kaialy and Rose Agbor, Ayuk. Effect of blending conditions on the tableting performance of paracetamol–polyvinylpyrrolidone mixture. *1st International Electronic Conference on Oral Drug Delivery.* 24th September 2016.

Agbor Rose, Ayuk and Waseem Kaialy, An investigation of the tableting properties of paracetmol−polyvinylpyrrolidone mixtures prepared using different mixing conditions. *UK PharmSci*, 5th–7th September **2017**, Hertfordshire, ***UK***

Agbor Rose, Ayuk and Waseem Kaialy. Engineering of paracetamol−polyvinylpyrrolidone mixtures with improved physico−mechanical properties. *UK PharmSci*, 7th September **2018**, Glasgow, ***UK***

Agbor Rose, Ayuk , Stephen Britland and Waseem Kaialy.
Influence of the preparation techniques on the physicomechanical properties of paracetamol−5nitroiphthalic acid cocrystal. *APV, 11th World meeting on Pharmaceutics and Biopharmaceutics*, March **2018, Granada *SPAIN***.

Supplementary materials (SM)

SM. 1. Water absorbed over the period of three months of commercial ibuprofen (IBU), and the mixtures (PA: IBU, 5:2 *w/w*) prepared Physical mixing (PM), compact milling (CPM); batch cooling crystallisation (BCC) ; Freeze drying (FD) and Milling (ML).

Products	**Initial weight(g) at 0 day**	**Final weight (g) after three months**
IBU	0.2985	0.2986
PM(PA−IBU)	0.3857	0.386
CPM(PA−IBU)	0.342	0.342
BCC(PA−IBU)	0.226	0.2338
DHS(PA−IBU)	0.1544	0.1545
FD(PA−IBU)	0.1139	0.114
ML(PA−IBU)	0.2293	0.2294

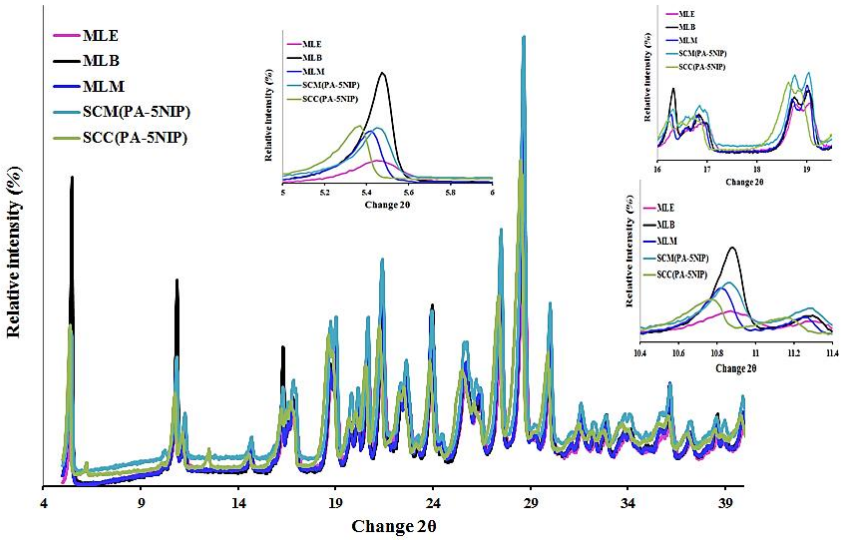

SM. 2. Powder X–ray diffraction of PA, 5NIP, physical mixing and PA–5NIP cocrystals prepared using slow cooling crystallisation and wet–milling and reduction in % of relative crystallinity in comparison to their specific peaks.

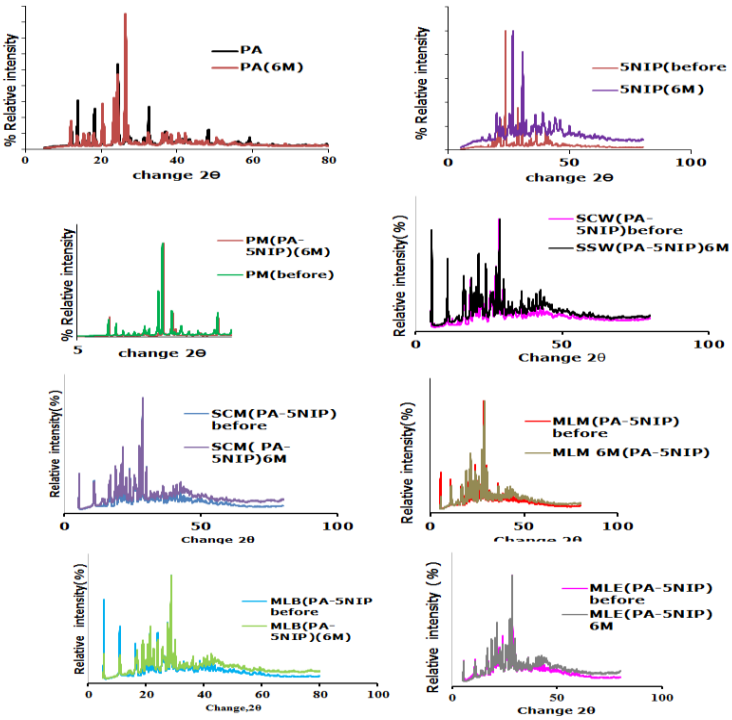

SM. 3. PXRD comparison plots showing, the stability of the cocrystals before and after six months (6M), exposed at high humidity temperature (40ºC, RH 75%).